Joana Manuela Torres Liberal

FRAGARIA VESCA LEAF AS A SOURCE OF BIOACTIVE PHYTOCHEMICALS - A FOCUS ON ELLAGITANNINS AND THEIR HUMAN MICROFLORA METABOLITES

Tese de doutoramento em Ciências Farmacêuticas, Especialidade de Biologia Celular Molecular,
orientada por Maria Teresa Pereira Marques Batista e Maria Teresa Teixeira Cruz Rosete
e apresentada à Faculdade de Farmácia da Universidade de Coimbra

Dezembro de 2015

· U C ·

UNIVERSIDADE DE COIMBRA

FRAGARIA VESCA LEAF AS A SOURCE OF BIOACTIVE PHYTOCHEMICALS - A FOCUS ON ELLAGITANNINS AND THEIR HUMAN MICROFLORA METABOLITES

Joana Manuela Torres Liberal

Universidade de Coimbra

2015

Capa:

Imagem elaborada por João Jesus.

FRAGARIA VESCA LEAF AS A SOURCE OF BIOACTIVE PHYTOCHEMICALS - A FOCUS ON ELLAGITANNINS AND THEIR HUMAN MICROFLORA METABOLITES

Joana Manuela Torres Liberal

Dissertação apresentada à Faculdade de Farmácia da Universidade de Coimbra para prestação de Provas de Doutoramento em Ciências Farmacêuticas, na Especialidade de Biologia Celular e Molecular.

Este trabalho foi realizado no Centro de Neurociências e Biologia Celular e na Faculdade de Farmácia da Universidade de Coimbra, sob orientação da Doutora Maria Teresa Batista e co-orientação da Doutora Maria Teresa Cruz, ao abrigo de uma bolsa de Doutoramento SFRH/BD/72918/2010 atribuída pela Fundação para a Ciência e Tecnologia.

Universidade de Coimbra

2015

Ao meu Avô Joaquim

AGRADECIMENTOS

Este espaço é dedicado a todos os que contribuíram para que esta dissertação fosse realizada. A todos eles expresso aqui o meu mais sincero agradecimento.

Às minhas orientadoras, Doutora Teresa Batista e Doutora Teresa Cruz, pela oportunidade de trabalhar com ambas dado que são para mim uma referência e inspiração no mundo da ciência. Por todo o apoio, incentivo e por todas as sugestões e discussões que levaram à produção deste trabalho. Pela confiança e pela liberdade de acção concedidas, as quais foram decisivas para o meu desenvolvimento científico e pessoal. E por último, e não menos importante, pela amizade, por todos os momentos extra-laboratório, pelas conversas e gargalhadas, e por estarem sempre disponíveis para mim.

A Carmen García-Rodríguez por haberme aceptado y recibido tan bien en el Instituto de Biología y Genética Molecular de la Universidad de Valladolid, por toda su amabilidad y ayuda. Muchas gracias también a Cris, Andrea, Patri, Maribel y Saray por su constante ayuda y buena disposición y por convertir mi paso por España en una experiencia tan agradable.

Aos Directores e Chefes de Grupo dos laboratórios onde desenvolvi este trabalho, por me terem proporcionado as condições necessárias à realização deste projecto.

À Doutora Anália, ao Doutor Henrique Girão, à Doutora Carla Marques e à Doutora Célia Gomes pelas sugestões e discussão deste trabalho, e pela disponibilidade, ajuda e simpatia ao longo desta etapa.

A todos os elementos da Universidade de Aveiro que colaboraram na realização dos ensaios de proteómica, ao Doutor Rui Vitorino, à Doutora Rosário Domingues e ao Doutor Pedro Domingues.

Aos elementos do laboratório de Farmacognosia, em particular àqueles que contribuíram para a obtenção e análise das amostras fitoquímicas, o Gustavo, a Tânia e o Doutor Artur Figueirinha, pela disponibilidade, ajuda e simpatia. Um agradecimento especial à Doutora Teresa Amaral pela disponibilidade e generosidade com que veio para o laboratório realizar e ensinar as técnicas de extracção e fraccionamento da planta usada neste estudo.

Aos meus colegas e sobretudo AMIGOS do laboratório,

À Ana Rufino, à Mónica, à Cátia, à Isabel, à Verinha, ao João Ferreira, à Madalena, à Joana, à Ana Silva, ao João Martins, ao Bruno, à Su e à Doutora Alexandrina. Obrigada pelo espirito de união, por toda ajuda e disponibilidade. Estou grata pelas nossas conversas mais sérias e pelas mais risonhas. Vocês fizeram com que este percurso custasse menos e fosse bem mais divertido. Obrigada por me fazerem sair do laboratório com um sorriso de orelha à orelha.

Não posso ainda deixar de agradecer aos meus antigos colegas de laboratório e que ainda hoje são bons amigos, a Áurea, a Célia, o Ermelindo, a Filipa, a Joana, o João e a Paula, pelos lanchinhos e jantares e por estarem sempre por perto, mesmo os que estão mais longe.

Aos meus amigos, em particular à Ana Lúcia que teve sempre uma enorme paciência para me ouvir, pela amizade incondicional e pelo apoio.

À minha família,

À Rita, ao Bé, ao Bruno, ao Hugo, à Tia Emília, à Bela, à Nela e a todos os outros que sempre me acompanharam e se interessaram por este meu percurso e que compreenderam as minhas ausências.

À minha querida Avó Maria, obrigada por me fazeres rir e chorar de comoção e por todas as velinhas que acendeste para iluminar o meu caminho.

Um agradecimento muito especial ao Nuno, que foi o meu grande apoio ao longo destes anos, partilhando as minhas alegrias e confortando-me nos momentos menos positivos. Obrigada por acreditares em mim, por aturares os meus caprichos e teimosia e por me dares força, ânimo e carinho. Contigo torna-se tudo mais simples!

Acima de tudo quero agradecer aos meus pais e à minha irmã. Vocês são a minha maior inspiração. Obrigada por estarem sempre presentes, por me incentivarem, por me ouvirem e por partilharem as minhas conquistas e derrotas. Sem vocês sei que não chegaria tão longe e este projecto também é vosso!

PUBLICAÇÕES

The results presented in this dissertation are published, were submitted or will be submitted for publication in peer-reviewed scientific journals, as follows:

Joana Liberal, Vera Francisco, Gustavo Costa, Artur Figueirinha, M. Teresa Amaral, Carla Marques, Henrique Girão, M. Celeste Lopes, M Teresa Cruz, M. Teresa Batista. (2014) *Bioactivity of Fragaria vesca leaves through inflammation, proteasome and autophagy modulation. Journal of Ethnopharmacology* 12/2014;158:1131-22.

Joana Liberal, Gustavo Costa, Anália Carmo, Rui Vitorino, Carla Marques, M. Rosário Domingues, Pedro Domingues, Ana C. Gonçalves, Raquel Alves, Ana Bela Sarmento-Ribeiro, Henrique Girão, M. Teresa Cruz, M. Teresa Batista. (2015) *Chemical characterization and cytotoxic potential of an ellagitannin-enriched fraction from Fragaria vesca leaves. Arabian Journal of Chemistry*. *In Press*.

Joana Liberal, Anália Carmo, Célia Gomes, M. Teresa Cruz, Maria Teresa Batista *In vitro antiproliferative activity of the ellagitannins metabolites, urolithins, on human tumor cell lines – emphasis on UMUC3 bladder cancer cells*. Submitted to *Molecular Nutrition & Food Research*

Joana Liberal, Anália Carmo, Célia Gomes, M. Teresa Cruz, Maria Teresa Batista *In vitro antiproliferative effects of urolithins on human osteosarcoma cells*. Manuscript in preparation.

Note: The results presented in this dissertation, included in Chapters 2-5, are formatted according to the style of the journal where the papers were published or submitted for publication, with minor modifications.

TABLE OF CONTENTS

FIGURES AND TABLE INDEX

FIGURE INDEX

TABLE INDEX

SUPPLEMENTARY FIGURE INDEX

SUPPLEMENTARY TABLE INDEX

ABBREVIATIONS

A549	Human lung adenocarcinoma epithelial cells
ABTS	2,2'-azino-bis-3-ethylbenzthiazoline-6-sulphonic acid
CAN	Acetonitrile
ANOVA	One-way analysis of variance
Apaf-1	Apoptotic protease activating factor
ATGs	Autophagy-related proteins
Bak	Bcl-2 antagonist killer 1
Bax	Bcl-2 associated X protein
Bcl 2	B-cell lymphoma protein 2
Bcl-xL	Bcl-2 related protein, long isoform
Bcl-xS	Bcl-2 related protein, short isoform
Bid	Bcl-2 interacting protein
BJ	Human skin fibroblasts
CCL2	Chemokine (C-C motif) ligand 2
Cdk	Cyclin dependent kinases
CMA	Chaperone-mediated autophagy
COX	Cyclooxygenase
DISC	Death-inducing signaling complex
DMEM	Dulbecco's modified eagle medium
DMSO	Dimethylsulfoxide
DPPH	1,1-diphenyl-2-picrylhydrazyl
DSS	Dextran sulfate sodium
E1	Ubiquitin activating enzyme
E2	Ubiquitin-conjugated enzyme
E3	Ubiquitin ligase
ECF	Enhanced chemifluorescence substrate
EDU	5-ethynyl-2'-deoxyuridine
EEF	Ellagitannin-enriched fraction
ERK	Extracellular signal-regulated kinase

FADD	Fas-associated death domain
FAK	Focal adhesion kinase
FAS	Fatty acid synthase
FasL	Fas ligand
FBS	Fetal bovine sérum
FITC	Fluorescein isothiocyanate
GSH	Glutathione
HBV	Hepatitis B virus
HepG2	Human hepatocellular carcinoma cells
HHDP	Hexahydroxydiphenoyl
HIV	Human immunodeficiency virus
HPLC	High-performance liquid chromatography
Hsp90	Heat shock protein 90
HSV	Herpes simplex viruses
IC_{50}	Half-maximal inhibitory concentration
IGFBP1	Insulin-like growth factor-binding protein 1
IKK	IκB Kinase
IL	Interleukin
INF-γ	Interferon-γ
iNOS	Inducible nitric oxide synthase
iTRAQ	Isobaric tag for relative and absolute quantitation
IκBα	Inhibitory κBα
JAK	Janus kinase
JNK	c-Jun N-terminal kinase
LC3	Microtubule-associated protein light chain 3
LPS	Lipopolysaccharide
MAPK	Mitogen activated protein kinase
MCF-7	Human breast carcinoma cells
MCP	Monocyte chemoattractant protein
MIC	Minimum inhibitory concentration
MMTS	S-methyl methanethiosulfonate

MNNG-HOS	Human osteosarcoma cells
mTOR	Mammalian target of rapamycin
MTT	3-[4,5-dimethylthiazol-2-yl]-2,5-diphenyl tetrazolium bromide
NFκB	Nuclear factor κB
NO	Nitric oxide
PAI-1	Plasminogen activator inhibitor-1
PARP	Poly (ADP-ribose) polymerase
PBS	Phosphate buffered saline
PGE2	Prostaglandin E2
PGG	Penta-*O*-galloyl-D-glucose
PI	Propidium iodide
PI3K	Phosphatidylinositide 3-kinase
PVDF	Polyvinylidene fluoride
RDA	Retro Diels-Alder
RIP	Receptor-interacting protein kinase
ROS	Reactive oxygen species
SDS	Sodium dodecyl sulphate-polyacrylamide gel electrophoresis
SEM	Standard error of the mean
SNAP	S-nitroso-N-acetylpenicillamine
SOD	Superoxide dismutase
STAT	Signal transducer and activator of transcription
Suc-LLVY-AMC	Suc-Leu-Leu-Val-Tyr-AMC
TCEP	Tris (2-carboxyethyl)phosphine
TEAB	Triethylammonium bicarbonate buffer
TFA	Trifluoroacetic acid
TLR	Toll-like receptor
TNF	Tumor necrosis factor
TRAIL	TNF-related apoptosis inducing ligand
UMUC3	Human bladder transitional carcinoma cells
UPS	Ubiquitin-proteasome system

RESUMO

Ao longo do tempo, os produtos naturais têm sido uma importante fonte de novas moléculas com atividade farmacológica. Em particular, das plantas têm sido isolados metabolitos secundários com propriedades biológicas, nomeadamente anti-inflamatória, anti-oxidante e anticancerígena. Estudos etnofarmacológicos referem que a folha da *Fragaria vesca* L., planta popularmente conhecida como morangueiro silvestre, tem sido utilizada no tratamento de diversas patologias. Contudo, existe muito pouca informação científica relativa aos mecanismos de ação molecular subjacentes ao seu efeito terapêutico.

Com o objetivo de validar os seus usos tradicionais e avaliar os mecanismos celulares e moleculares envolvidos nas atividades biológicas da *Fragaria vesca*, preparou-se um extrato hidroalcoólico a partir das suas folhas, e este foi quimicamente caracterizado relativamente ao seu perfil polifenólico por HPLC/PDA/ESI-MS^n. A análise fitoquímica permitiu identificar 20 polifenóis, entre os quais elagitaninos, proantocianidinas e conjugados glucoronados de conferol e quercetina. As propriedades anti-inflamatórias do extrato foram avaliadas numa linha celular de macrófagos de ratinho (Raw 264.7), observando-se uma inibição da produção de monóxido de azoto estimulada por lipopolissacarídeo, sendo que este efeito se deveu maioritariamente à atividade s*cavenger* do próprio extrato. Adicionalmente demonstrou-se que o extrato modula as vias proteolíticas da célula através da redução da atividade do proteassoma e modulação da autofagia, alvos celulares extremamente atrativos em estratégias terapêuticas anti-tumorais.

Assim, com o propósito de aquilatar os compostos responsáveis por estes efeitos biológicos procedeu-se ao fracionamento do extrato, sendo selecionada uma fração composta maioritariamente por elagitaninos. A fração foi analisada por HPLC/PDA/ESI-MS^n o que permitiu detectar 12 elagitaninos. A viabilidade da linha celular do carcinoma hepatocelular humano (HepG2) foi avaliada após tratamento com a fração e com o extrato hidroalcoólico, e as concentrações necessárias para inibir 50% da viabilidade celular (IC_{50}) foram determinadas. O IC_{50} da fração enriquecida em elagitaninos (113 µg/mL) foi aproximadamente 6 vezes inferior ao IC_{50} do extrato hidroalcoólico (690 µg/mL). O efeito da fração na proliferação celular e no ciclo celular foi igualmente alvo de estudo, observando-se que o tratamento diminuiu a proliferação celular através de uma resposta dependente da concentração e induziu uma acumulação de células em G2/M. Paralelamente, demonstrou-se que a fração induziu um bloqueio do fluxo autofágico responsável pela acumulação da proteína LC3-II, promoveu a acumulação de proteínas conjugadas com a ubiquitina, inibiu a atividade do tipo quimiotripsina da subunidade 26S do proteossoma e diminuiu a expressão de algumas subunidades do proteassoma, enfatizando uma inibição da degradação

proteolítica mediada pela via ubiquitina-proteossoma. Adicionalmente, a análise do proteoma das células com recurso ao método proteómico quantitativo (iTRAQ) permitiu identificar 914 proteínas, das quais 133 mostraram ser moduladas pela fração, com especial destaque para proteínas envolvidas em processos de metabolismo celular.

Recentemente, os alimentos que contêm elagitaninos têm suscitado considerável atenção na comunidade científica devido aos seus efeitos benéficos na saúde humana, sendo particularmente associados a potenciais efeitos quimioterapêuticos. Dada a baixa biodisponibilidade dos elagitaninos e sabendo-se que são metabolizados no trato intestinal em ácido elágico e posteriormente em urolitinas, hipotetiza-se que as suas propriedades benéficas sejam devidas ao efeito direto dos seus metabolitos. Tendo em conta as considerações acima explanadas, a atividade antiproliferativa dos principais metabolitos dos elagitaninos foram também alvo de estudo. Demonstrou-se que as urolitinas A, B e C diminuíram a viabilidade celular de cinco linhas tumorais humanas, apresentando um efeito dependente da concentração, e o precursor comum destas moléculas, o ácido elágico, revelou ser menos ativo que as urolitinas. Os resultados enfatizaram ainda diferenças claras entre os efeitos biológicos das urolitinas estudadas e, no geral, a urolitina A foi a molécula mais promissora. Na linha celular de cancro da bexiga (UMUC3), a urolitina A induziu a paragem do ciclo celular, aumentou a apoptose e modulou as vias de sinalização celular PI3K/Akt e MAPKs. Na linha celular humana de osteossarcoma (MNNG-HOS), a urolitina A teve um efeito semelhante, embora menos pronunciado, indicando que o efeito desta molécula não é dependente do tipo de célula. Os resultados permitiram ainda concluir que a urolitina B foi a molécula menos ativa em ambas as linhas celulares. Deste modo, considerando as diferenças estruturais das três urolitinas testadas, os resultados realçam a importância do número/posição dos grupos hidroxilo na atividade destas moléculas, fato extremamente relevante no desenho de moléculas bioativas baseadas nas urolitinas.

Em suma, estes resultados sugerem que a folha da *Fragaria vesca* poderá ser uma relevante fonte de moléculas com potencial terapêutico, principalmente tendo em conta os resultados notáveis na autofagia e no proteassoma. Suportando estes resultados, a fração enriquecida em elagitaninos demonstrou também inibir estes mecanismos proteolíticos bem como modular vários processos celulares e moleculares associados à carcinogénese. Por outro lado, este trabalho sustenta a importância do estudo dos metabolitos dos polifenóis, e em particular dos elagitaninos, encorajando fortemente estudos científicos focados no desenvolvimento de fármacos com ação quimiopreventiva/quimioterapêutica tendo por base estes metabolitos.

ABSTRACT

Natural products have been a rich source of novel lead molecules with pharmacological activity for drug discovery. Notably, plants have had a relevant role, being widely shown that many plant-derived compounds have anti-inflammatory, antioxidant and anticancer activities. The leaf of *Fragaria vesca* L., a plant commonly known as wild strawberry, has been used over the years by traditional medicine for the treatment of several diseases. However, scientific reports disclosing its molecular mechanisms of action are still lacking.

Therefore, to validate its traditional uses and to unveil the mechanisms involved in the activities previously reported, a hydroalcoholic extract from *Fragaria vesca* leaves was obtained. The phytochemical characterization was performed by HPLC-PDA-ESI/MS^n. Twenty compounds were tentatively identified, and among them ellagitannins, proanthocyanidins, and quercetin and kaempferol glucuronide derivatives were the main ones. Thereafter, using a mouse macrophage cell line (Raw 264.7), we observed that the extract inhibited the production of nitric oxide (NO) triggered by lipopolysaccharide, which was probably due to a direct scavenge of NO. The extract also affected the cellular proteolytic pathways, through the reduction of the proteasome activity and modulation of the autophagic machinery, mechanisms that are currently considered very attractive therapeutic targets in cancer treatment.

In order to identify the compounds responsible for these effects, the extract was further fractionated and an ellagitannin-enriched fraction (EEF) was selected. The analysis of EEF by HPLC-PDA-ESI/MS^n allowed the detection of 12 ellagitannins. The cell viability of both EEF and crude extract was determined after 24 h of cells treatment and the half-maximal inhibitory concentration (IC_{50}) was calculated. The IC_{50} of the EEF (113 μg/mL) was about 6 times lower than the IC_{50} of the crude extract (690 μg/mL). Furthermore, EEF induced cell cycle arrest at G2/M checkpoint and decreased cell proliferation in a dose-dependent way. This fraction also induced an accumulation of LC3-II protein through blockage of autophagic flux, and promoted the accumulation of ubiquitinated proteins, inhibited chymotrypsin-like activity of 26S proteasome and decreased the expression of several proteasome subunits, indicating an impairment of ubiquitin-proteasome system. Furthermore, to further unveil other putative molecular targets of EEF, an iTRAQ (isobaric tag for relative and absolute quantitation) based proteomics approach was performed. Several proteins (914) were identified, among which 133 proteins were significantly modulated, most of them related to metabolic processes.

Recently, ellagitannins-containing foods have gathered much attention due to their health benefits, namely their chemopreventive potential. Given the low bioavailability of those molecules

and their metabolization in the gastrointestinal tract into ellagic acid and consequently into urolithins, the systemic health benefits of their consumption may be a consequence of a direct effect of ellagitannins metabolites. Therefore, the antiproliferative effects of the main metabolites produced after ingestion of ellagitannins-containing foods, ellagic acid and urolithins A, B and C were investigated. The results indicate that urolithins A, B and C, decreased cell viability in a dose-dependent way in several human cancer cell lines and, in comparison with ellagic acid, their precursor, urolithins were much more active. Furthermore, clear differences among the compounds tested were shown, and, overall, urolithin A was the most promising molecule. In UMUC3 bladder cancer cells, urolithin A induced cell cycle arrest, increased apoptosis and modulated the intracellular PI3K/Akt and MAPKs signaling pathways. In human osteosarcoma cells (MNNG-HOS), although not so pronounced, the effects of urolithin A on cell death and cell cycle were similar, indicating that those effects are not cell type-specific. Furthermore, urolithin B was, in both cell lines, the less active molecule. Considering the structural differences between these three urolithins, the results highlight the significance of the number/position of hydroxyl groups for urolithins' activity, which constitutes valuable information in the design of urolithin-based molecules presenting potent bioactivity.

In conclusion, *Fragaria vesca* leaf is a source of molecules with therapeutic potential and with a notable effect on autophagy and proteasome. Furthermore, EEF markedly inhibited these proteolytic systems and modulated several cellular and molecular processes implicated in carcinogenesis. Moreover, this work generated important insights in the therapeutic value of ellagitannins metabolites, the urolithins, strongly supporting and encouraging further work on ellagitannins and urolithins in order to unveil their potential as chemopreventive/chemotherapeutic drugs.

Chapter 1

Introduction

1.1. USE OF NATURAL PRODUCTS AS THERAPEUTIC AGENTS

Natural products derive from natural sources such as plants, animals or microorganisms and have been used since ancient times for the treatment of many diseases in the form of traditional medicines, remedies, potions and oils. Plants have proven to be an extremely productive source of bioactive compounds and, more recently, many of these phytochemicals became chemical leads for several pharmaceuticals products.

Interestingly, the foundations of this knowledge were the trial and error tests that for hundreds of centuries gradually eliminated the harmful, worthless or less efficient plants. In the early 1800s, the development of new analytical and structural tools ushered in a new era for the study and use of natural products. Indeed, this led to the purification and chemical structure elucidation of many bioactive compounds that later allowed to synthetize them, rather than isolating them from natural sources. Classic examples of plant-derived compounds are morphine, codeine, digoxin, vincristine and paclitaxel.

Currently, natural products continue to be an important source of drugs and drug leads for the treatment of many diseases. In fact, Newman and Cragg (2012) reported that among all new drugs approved between 1981 and 2010, only 29% where totally synthetic in origin (Figure 1.1), which demonstrates the value of natural sources for the discovery of novel bioactive agents. Notably, and underlining the value of natural products research in medicine, Drs. William C. Campbell, Satoshi Ōmura and Youyou Tu were honored with the 2015 Nobel Prize in Physiology or Medicine for the discovery of novel natural products that became impactful therapies for infections by roundworm parasites (avermectins) and malaria (artemisinin)(Callaway and Cyranoski, 2015).

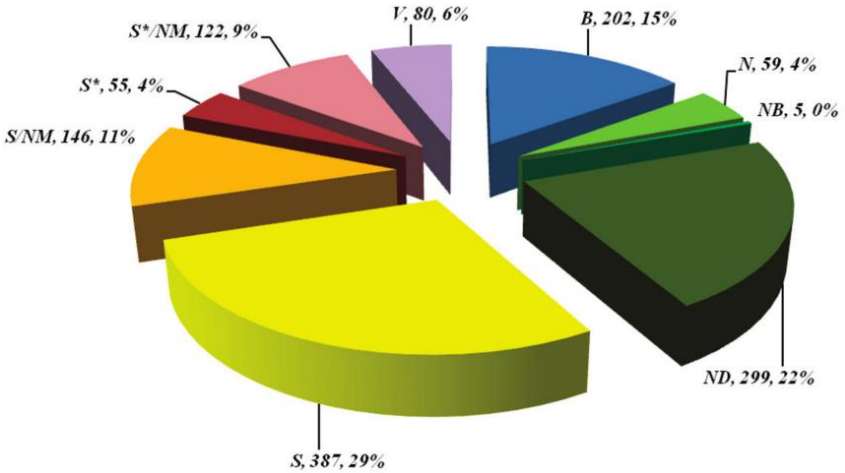

Figure 1.1 - New approved drugs (1981-2010). B – Biological (usually a large peptide or protein either isolated from an organism/cell line or produced by biotechnological means in a surrogate host); N - Natural product; NB - Natural product "Botanical"; NM - Natural product mimic; ND - Derived from a natural product, resulting usually from a semi-synthetic modification; S - Totally synthetic drug, often found by random screening/modification of an existing agent; S* - Made by total synthesis, but the pharmacophore is from a natural product; V - Vaccine. Adapted from Newman and Cragg (2012).

1.2. PLANTS SECONDARY METABOLITES

Plants synthesize a wide range of organic compounds that are traditionally referred as primary and secondary metabolites. The primary metabolism is found in all plants and is responsible for the synthesis of substances with an essential role in the plant growth and development, as carbohydrates, lipids, proteins and nucleic acids. The secondary metabolites are present in higher plants, are structurally diverse and participate in the interaction between the plant and its environment, for instance, in response to herbivore-induced damage or nutrient deprivation (Wink, 2010).

In the recent years research on the nutritional/medicinal properties of plant secondary metabolites has become very popular. In addition to the traditional uses of the plants, the isolation of their compounds and the study of associated biological activities increased the medicinal value of the phytochemicals. Based on their biosynthetic origin these chemicals are usually grouped in 3 major clusters: terpenoids, alkaloids and phenolic compounds (Harborne, 1999). This work will focus on phenolic phytochemicals.

1.2.1. PHENOLIC COMPOUNDS AND POLYPHENOLS

Phenolic compounds are characterized by the presence of one or more hydroxyl groups attached directly to an aromatic ring (Vermerris and Nicholson, 2007), while the term polyphenol should be applied to the compounds derived from the shikimate-derived phenylpropanoid and/or the polyketide pathways, with two or more phenolic rings and without nitrogen-based functional groups in their most basic structural expression (Quideau et al., 2011). The majority of polyphenols exists as glycosides with different sugar units and acylated sugars at different positions of the polyphenol skeletons (Tsao, 2010).

This group of natural products is highly diverse and contains several sub-groups. It has been classified in different ways, according to source of origin, biological function and chemical structure (Table 1.1).

The phenolic compounds originate from two metabolic pathways: the shikimate/phenylpropanoid pathway where, mainly phenylpropanoids are formed, or the polyketide pathway (also known as acetate/malonate pathway), which can produce simple phenols, or the combination of these two pathways that give rise to flavonoids and others monomeric and polymeric phenols (Figure 1.2) (Cheynier et al., 2013; Lattanzio, 2013).

Among the phenolic compounds, the chemical classes with relevance for this thesis will be the phenolic acids, flavonoids and tannins (with a special focus on hydrolysable tannins).

Table 1.1 - Main classes of polyphenols. Adapted from Santos-Buelga et al. (2012)

Structure	Class
C6	Simple phenols
C6 - C1	Hydroxybenzoic acids
C6 - C3	Hydroxycinnamic acids and derivatives
C6 - C3	Coumarins
C6 - C4	Naphtoquinones
C6 - C1 - C6	Xanthones
C6 - C2 - C6	Stilbenes
C6 - C2 - C6	Anthraquinones
C 6 - C3 - C6	Chalcones, aurones, dihydrochalcones
C 6 - C3 - C6	Flavonoids
(C6 - C3 - C6)n	Condensed tannins (proanthocyanidins)
$(C6 - C2)_2$	Lignans
(C6 - C3)n	Lignins
Oligomers or polymers	Hydrolysable tannins (gallotannins, ellagitannins)

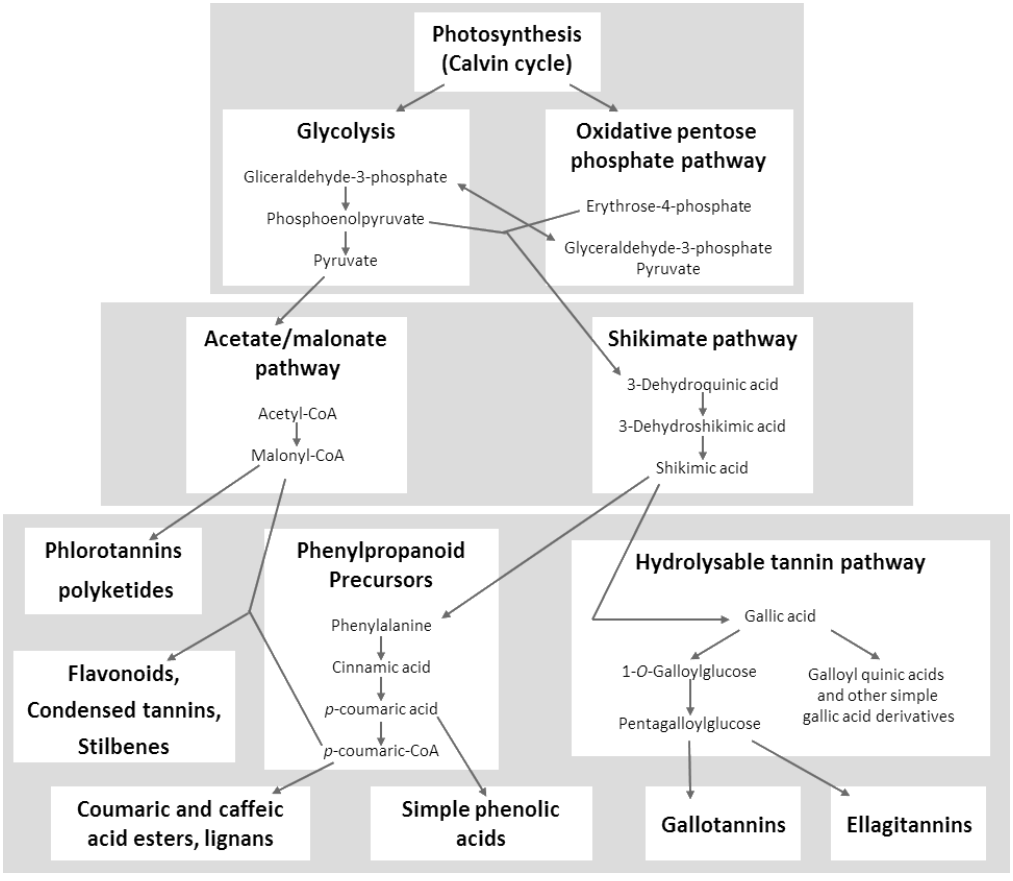

Figure 1.2 - Major polyphenolic biosynthetic pathways. Adapted from Salminen et al. (2012).

1.2.1.1. PHENOLIC ACIDS

Phenolic acids are composed by a benzene ring, a carboxylic group and one or more hydroxyl and/or methoxyl groups. These compounds could be divided in two classes: derivatives of benzoic acid (C_6-C_1) and derivatives of cinnamic acid (C_6-C_3) (Giada, 2013). The hydroxybenzoic acids, such as gallic acid and protocatechuic acid are found in certain foods and plants, such as red fruit. Among the cinnamic acids, caffeic *p*-coumaric, ferrulic and sinapic acids are the most abundant and are frequently found in plants as esters. For instance, chlorogenic acid is an ester of caffeic acid and quinic acid (Figure 1.3) (D'Archivio et al., 2007).

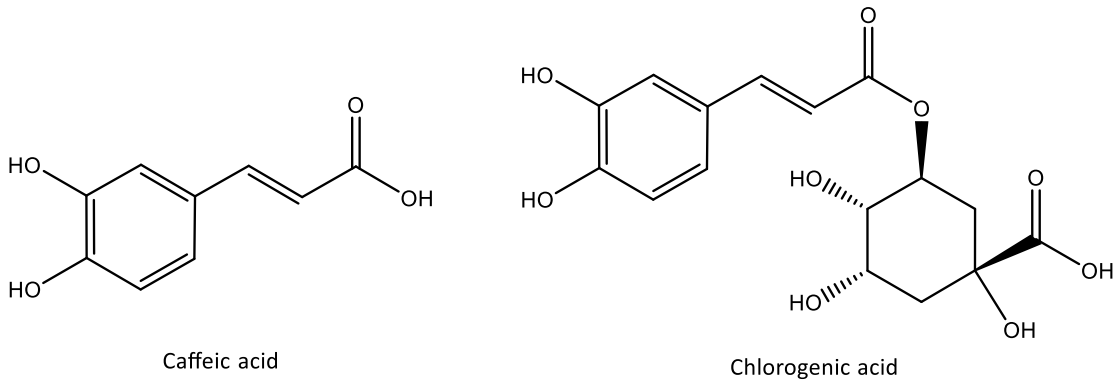

Figure 1.3 - Examples of phenolic acids.

1.2.1.2. FLAVONOIDS

Flavonoids are a large class of secondary metabolites that are broadly distributed in the plant kingdom, encompassing more than 10,000 structures (Mouradov and Spangenberg, 2014). These polyphenolic compounds comprise fifteen carbons, with two aromatic rings (A-ring and B-ring) joined by a three-carbon bridge (Figure 1.4). The central three-carbon chain may form a closed pyran ring (C-ring) (D'Archivio et al., 2007). Considering the hydroxylation pattern and the variations on C-ring, flavonoids can be further divided into the following main subclasses: flavonols, flavones, flavanones, isoflavones, anthocyanidins and flavanols. The basic structures of flavonoids are aglycones; however, most of these compounds exist naturally as glycosides (Tsao, 2010).

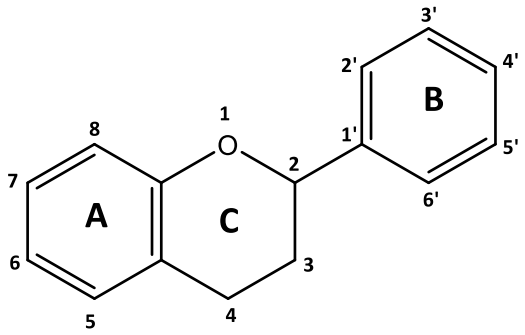

Figure 1.4 - Basic structure of flavonoids.

Flavonoids are an integral part of human diet, being present in fruits, vegetables and herbs. Furthermore, these molecules have received considerable attention because of their health benefits, namely as antioxidants (Heim et al., 2002), anti-inflammatory (Costa et al., 2012) and anticancer (Martinez-Perez et al., 2014) compounds.

1.2.1.3. TANNINS

Tannins are a group of polyphenols with a wide diversity in structure and with the ability to bind and precipitate proteins and alkaloids. Etymologically, the term tannin derives from the ancient Celtic word for oak and comes from the French word "tan", which refers to the powdered oak bark extracts used in the making of leather (Quideau et al., 2011). Based on their biochemical properties, tannins were typically defined, as water soluble phenolic compounds that are able to bind and precipitate proteins and other macromolecules, and that are known to have a molar mass between 300 and 3000 Da (Bate-Smith and Swain, 1962). However, this definition does not include all tannins, since molecules with a molar mass of up to 20000 Da were discovered. Hence, considering their molecular structures and their origin and role in plant life, Khanbabaee and van Ree (2001) defined this class as *polyphenolic secondary metabolites of higher plants, and are either galloyl esters and their derivatives, in which galloyl moieties or their derivatives are attached to a variety of polyol-, catechin- and triterpenoid cores (gallotannins, ellagitannins and complex tannins), or they are oligomeric and polymeric proanthocyanidins that can possess different interflavanyl coupling and substitution patterns (condensed tannins)*. Therefore, this definition covers the 4 subclasses of tannins: gallotannins and ellagitannins (hydrolysable tannins), complex tannins and condensed tannins (Figure 1.5). Tannins are generally found in wood, leaves, fruits and roots, and have a protective role against infections, insects or animal herbivory.

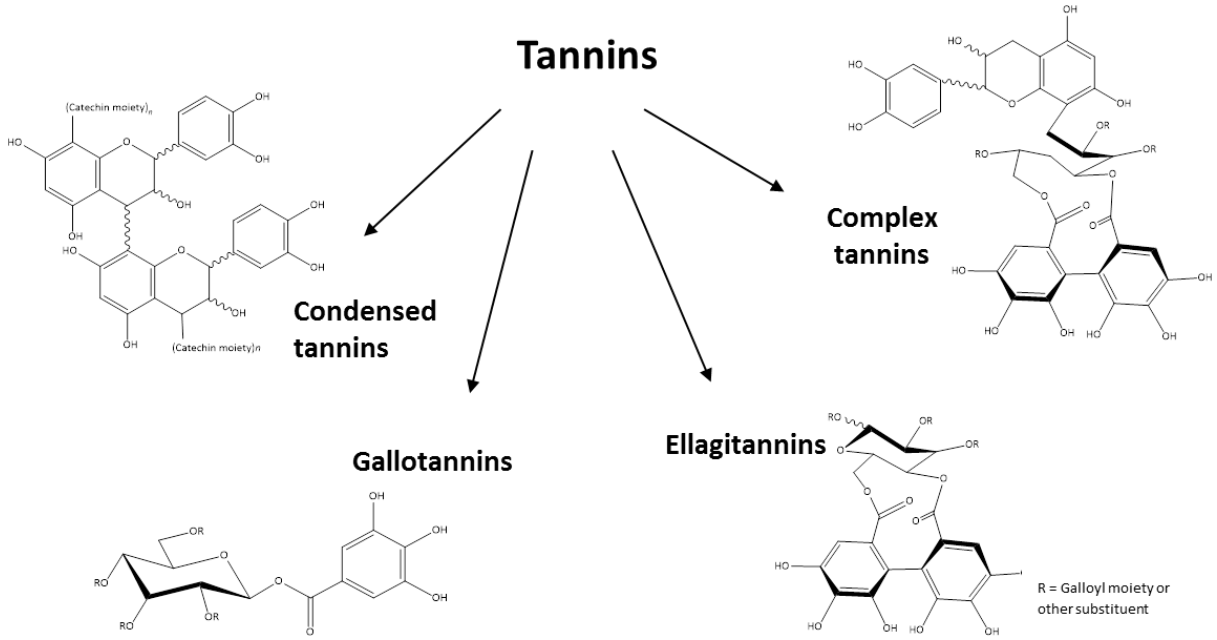

Figure 1.5 - Classification and structure of tannins. Adapted from Khanbabaee and van Ree (2001).

1.2.1.3.1. CONDENSED TANNINS

Condensed tannins or proanthocyanidins (Figure 1.5) are oligomeric or polymeric flavonoids, formed by linkage of C-4 of one flavan-3-ol unit with C-8 or C-6 of other flavan-3-ol unit that under hydrolysis with heating in acid yields anthocyanidins (Khanbabaee and van Ree, 2001). These compounds are found in berries, cereals, nuts, vegetables, chocolates and wines, and represent a large part of daily polyphenol ingestion from the diet (Gu et al., 2004). Furthermore, proanthocyanidins have a variety of health beneficial effects such as antioxidant and free radical scavenger (Maldonado et al., 2005), anticancer (Kresty et al., 2011) or anti-inflammatory (Tatsuno et al., 2012) properties.

1.2.1.3.2. COMPLEX TANNINS

Complex tannins (Figure 1.5) are tannins in which a flavan-3-ol unit is bound glycosidically to a gallotannin or an ellagitannin unit (Vermerris and Nicholson, 2007).

1.2.1.3.3. HYDROLYSABLE TANNINS

Hydrolysable tannins are esters of gallic acid and a polyol, usually glucose, but fructose, xylose and saccharose are also found (Serrano et al., 2009). As the name implies, these compounds are easily hydrolyzed to yield carboxylic acids such as gallic and ellagic acid (Cao et al., 2014).

The first step of hydrolysable tannins biosynthesis is the esterification of gallic acid and glucose to yield *β*-glucogallin (1-*O*-galloyl- β-D-glucose). Then, *β*-glucogallin, acting as receptor and as

principal donor of gallic acid, will be further esterified to form the 1,2,3,4,6-*penta*-*O*-*g*alloyl-*β*-D-*g*lucose (Figure 1.6). This molecule is found in many plant families and is considered the precursor of the majority of the hydrolysable tannins (Cunha and Batista, 2005).

1.2.1.3.3.1. GALLOTANNINS

Gallotannins (Figures 1.5 and 1.6) are the simplest hydrolysable tannins, consisting of gallic acid molecules that are bound to a central carbohydrate core (usually D-glucose) via ester bonds. Penta-*O*-galloyl-D-glucose (PGG) is a well-known example of this class of compounds (Figure 1.6).

The addition of further galloyl moieties to PGG originates more complex gallotannins that contain the characteristic *meta*-depside bonds between the gallic acid residues (Niemetz and Gross, 2005) and the degree of galloyl addition can reach up to as many as 10-12 galloyl units (Vermerris and Nicholson, 2007).

The distribution of gallotannins in nature is rather limited; these compounds were found in the leaves and galls of *Rhus* spp, fruit pods of *Caesalpina spinsosa* and galls of several oak species (Clifford and Scalbert, 2000).

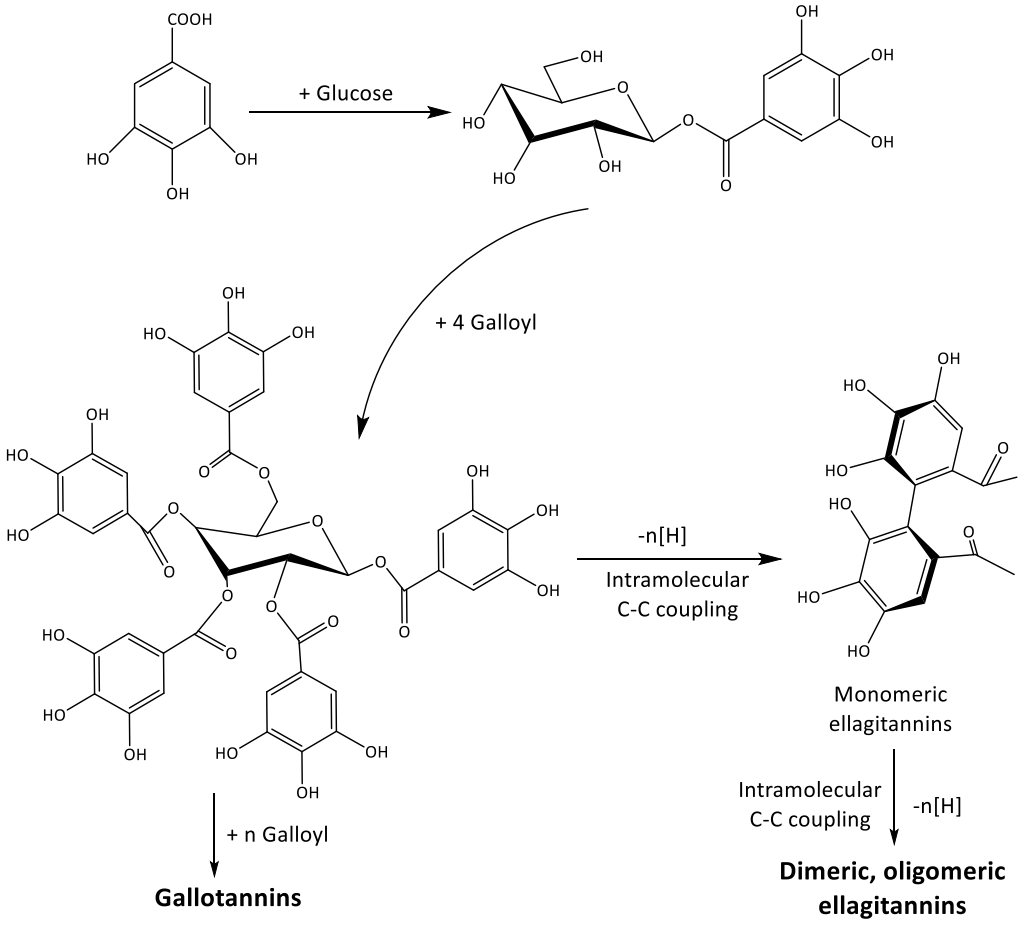

Figure 1.6 - Main steps of the biosynthesis of gallotannins and ellagitannins. Adapted from Gross (2009).

1.2.1.3.3.2. ELLAGITANNINS

Ellagitannins are structural diverse polyphenols derived of PGG (Figure 1.6) that contains adjacent galloyl groups linked with carbon-carbon (C-C) bonds to form an axially chiral hexahydroxydiphenoyl (HHDP) moiety (Figure 1.7), the typical feature of ellagitannins. These compounds can be cleaved upon hydrolysis, either enzymatically or with acid, from the glucose core and spontaneously undergo lactonization to form ellagic acid (Vermerris and Nicholson, 2007).

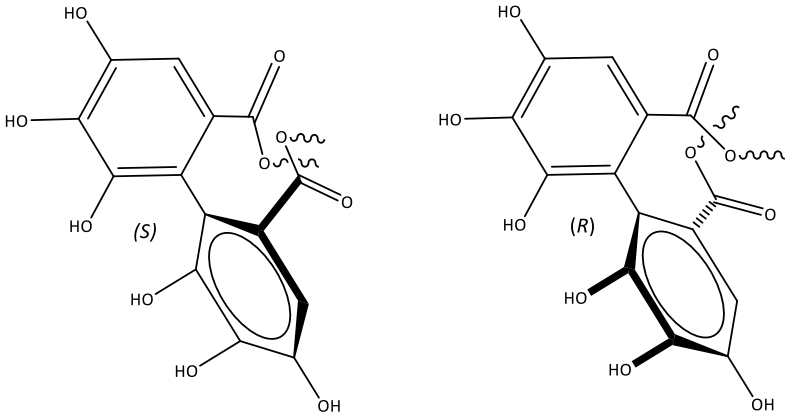

Figure 1.7 - HHDP unities with *S*- and *R*-configurations. Adapted from Vermerris and Nicholson (2007).

The wide structural variability of ellagitannins is mainly due to the different possibilities for the linkage of HHDP residues with the glucose moiety and also because these compounds tend to form high molecular oligomers.

The HHDP unit may be linked to the glucopyranose ring between 2,3-positions or between 4,6-positions, with the glucopyranose in the $^{4}C_{1}$ conformation (e.g. tellimagrandin I and II, and pedunculagin). Although, coupling across 1,6-; 1,3-; 3,6- and 2,4-positions in a less thermodynamic favored $^{1}C_{4}$ conformation are also known (e.g. geraniin) (Figure 1.8). In the first group the axially chiral HDDP unit almost exclusively adopts the *S*-configuration, whereas in the second one both *R*- and *S*-configurations are observed (Figure 1.7). In addition, there are also ellagitannins with an open-chain glucose that contain a 2,3-linked HHDP unit. These compounds are referred as *C*-glucosidic ellagitannins (e.g. vescalagin and castalagin) (Figure 1.9) (Quideau et al., 2010; Vermerris and Nicholson, 2007).

Figure 1.8 - Glucopyranose unities in the $^{4}C_{1}$ and $^{1}C_{4}$ conformations. Adapted from Vermerris and Nicholson (2007).

Monomeric unities of ellagitannins (Figure 1.10) can polymerize to form oligomeric and polymeric ellagitannins. Usually this reaction occurs between two galloyl groups (e.g. agrimoniin) or a galloyl group and a HHDP group (e.g. sanguiin H-6) by intermolecular oxidative coupling (C-C or C-O-C) (Figures 1.11 and 1.12) (Okuda et al., 2009).

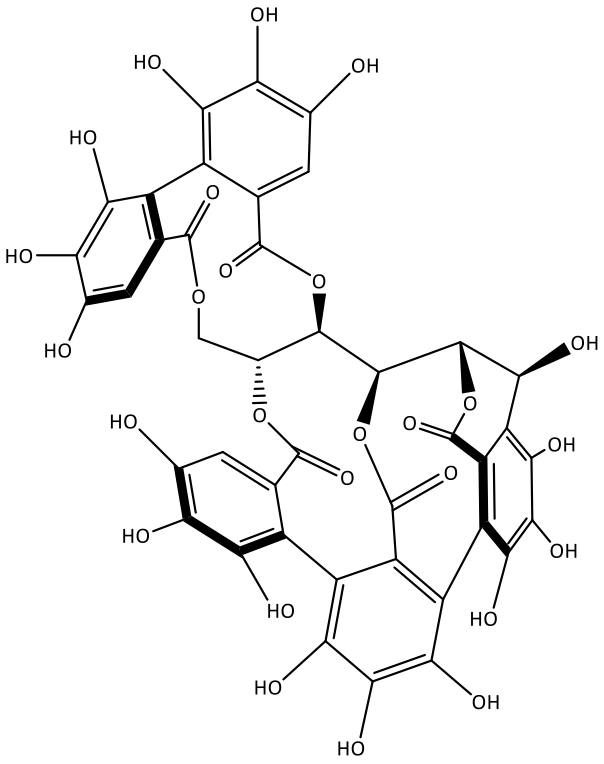

Figure 1.9 - Vescalagin, a C-glucosidic ellagitannin.

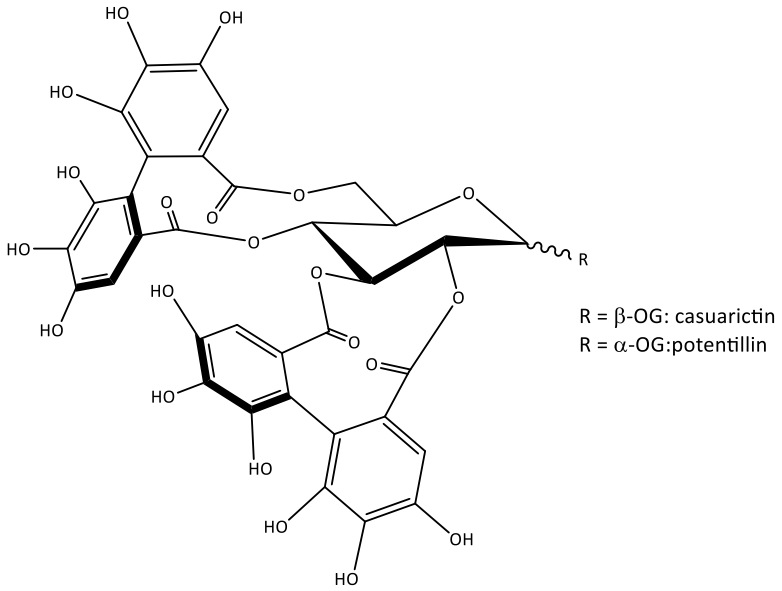

Figure 1.10 - Example of monomeric ellagitannins (casuarictin/potentillin). Adapted from (Pouységu et al., 2011)

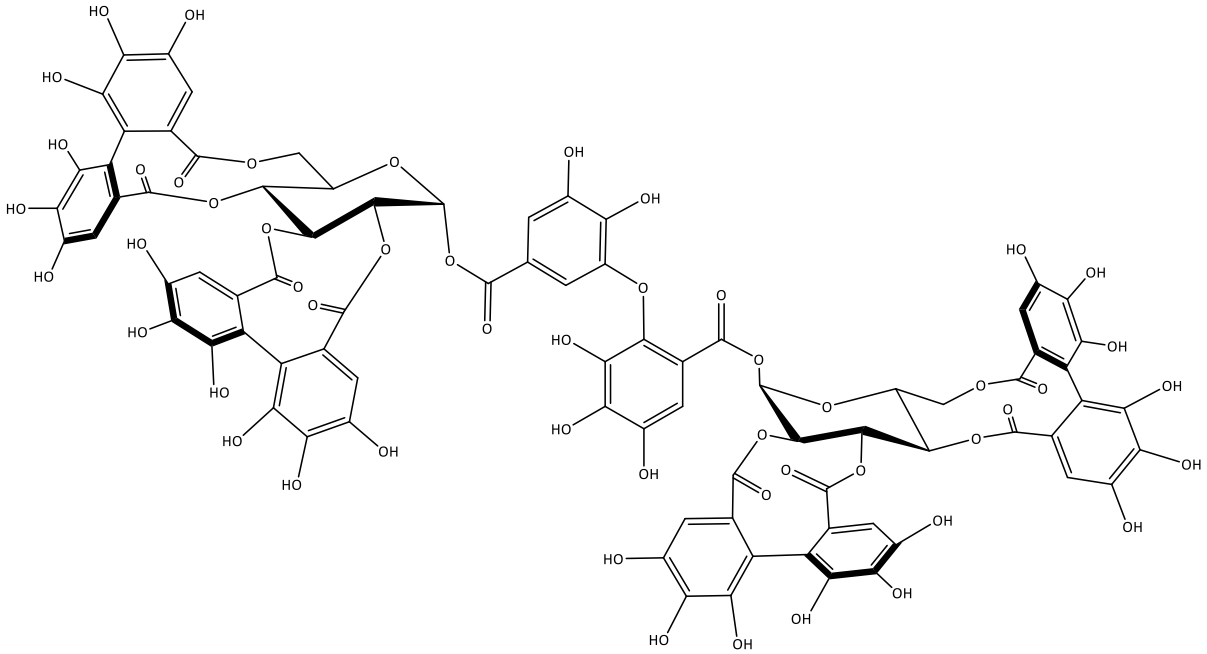

Figure 1.11 - Agrimoniin, a dimeric ellagitannin.

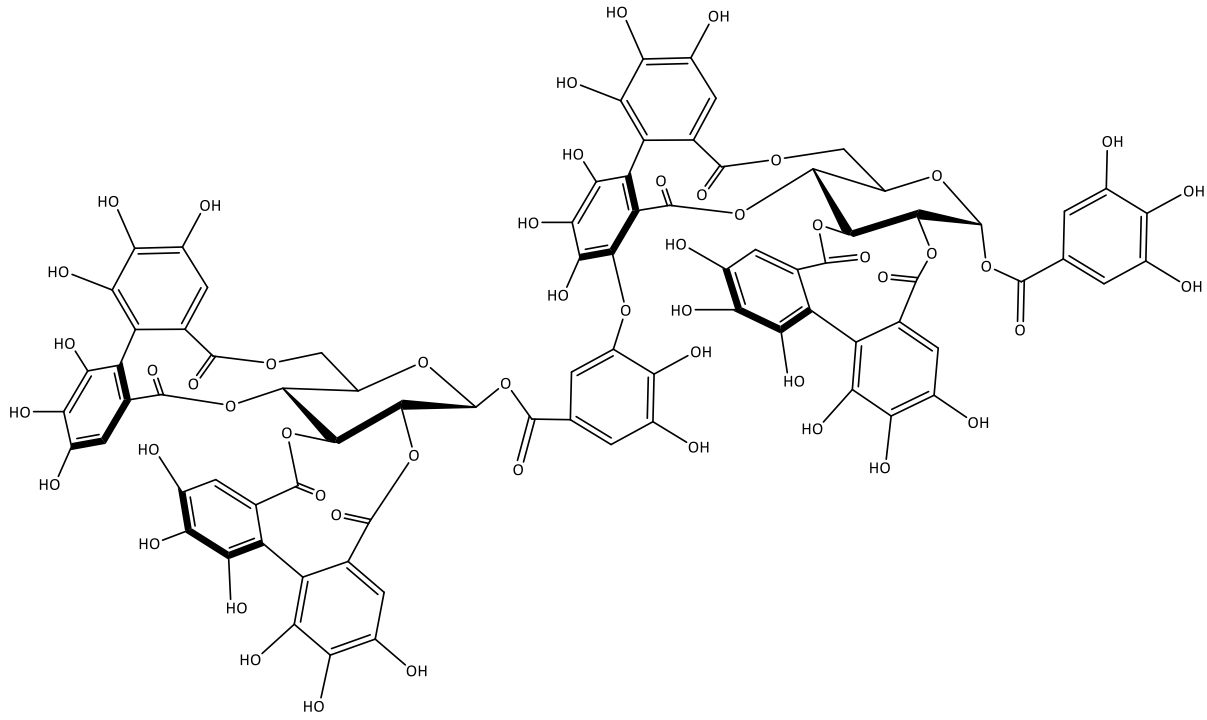

Figure 1.12 - Sanguiin H-6, a dimeric ellagitannin.

1.3. ELLAGITANNINS AND ITS COLONIC METABOLITES

1.3.1. SOURCES OF ELLAGITANNINS

Ellagitannins have a widespread distribution and their presence has been described in different plant tissues, namely leaves, roots, bark, wood, fruits and its husks, flowers and seeds. However, the distribution of ellagitannins is restricted to certain taxonomic branches, being specifically found in dicotyledonous angiosperms (Okuda et al., 1993). Quite recently, (Moilanen et al., 2015) screened the ellagitannins content of 82 Finnish plants and confirmed/identified some taxonomic families that were rich in ellagitannins, namely Onagraceae, Lyhtraceae, Geraniaceae, Elaeagnaceae, Fagaceae and Rosaceae (some species).

Ellagitannins are present in herbal preparations, foods and beverages. In fact, several ellagitannins are considered the principal active components of certain medicinal plants, including: agrimoniin (*Agrimonia pilosa*), camelliatannin A (*Camellia japonica*), casuarictin (*Liquidambar formosana*), chebulinic acid (*Terminalia chebula*), cornusiin A (*Cornus officinalis*), granatin A and B (*Punica granatum*), geraniin (*Geranium thunbergii*), and sanguiins H-6 and H-11 (*Sanguisorba officinalis* and *Rubus triphyllus*) (Okuda et al., 2009).

The major contributors of ellagitannins intake in Western diets are berries like strawberries, raspberries and blackberries (Aaby et al., 2007; Clifford and Scalbert, 2000; Koponen et al., 2007; Törrönen, 2009), and nuts including walnuts, pistachios, cashew nut, chestnuts, acorns and pecans (Anderson et al., 2001; Gonçalves et al., 2010; Malik et al., 2009). They are also abundant in pomegranates (Cerdá et al., 2006; Gil et al., 2000) and muscadine grapes (Törrönen, 2009). Furthermore, ellagitannins are also present in alcoholic beverages that have been aged in oak wood barrels, like wines (Clifford and Scalbert, 2000; Lee and Talcott, 2002) and whiskey (Glabasnia and Hofmann, 2006) (Table 1.2).

In an early review it was referred that the daily ellagitannin intake would probably not exceed the 5 mg/day (Radtke et al., 1998). As suggested by (Tomás-Barberan et al., 2009), this value is probably underestimated since several studies documented that the content of ellagitannins in various common foods can be pretty high, namely in pomegranate juice (> 1500 mg/L), walnuts (802 mg/50g) and raspberries (>50 mg/100g) (Table 1.2). Accordingly, a more recent study estimated that in northern Europe the daily intake of ellagitannins was higher (12 mg/day) and berries were the most important contributors (Ovaskainen et al., 2008).

Most of the studies reported in Table 1.2 are based in the quantification of ellagic acid after ellagitannin hydrolysis. However, it is important to notice that free ellagic acid is also naturally present in plants, particularly in fruits and nuts (Abe et al., 2012; Wada and Ou, 2002). Therefore, in

this kind of studies free ellagic acid must be measured before hydrolysis and compared to the value obtained after hydrolysis.

Table 1.2 - Ellagitannins and ellagic acid contents in various food products. Adapted from Larrosa et al. (2010a)

	Food	Content	Reference
Fresh fruits	Raspberries	263-330 mg/100 g f.w	Koponen et al. (2007)
		51-330 mg/100 g f.w	Törrönen (2009)
	Strawberries	77-85 mg/100 g f.w	Koponen et al. (2007)
		25 mg/100 g f.w	Aaby et al. (2007)
	Cloudberries	315 mg/100 g f.w	Koponen et al. (2007)
		56-360 mg/100 g f.w	Törrönen (2009)
	Blackberries	1.5-2 mg/ g d.w	Clifford and Scalbert (2000)
	Artic bramble	69-320 mg/100 g f.w	Törrönen (2009)
	Pomegranates	35-75 mg/100 g f.w arils	Gil et al. (2000)
	Muscadine grapes	36-91 mg/100 g f.w	Törrönen (2009)
Nuts	Walnut	802 mg/50g 8 nuts	Anderson et al. (2001)
	Pecan	20.96-86.2 mg/g EA	Malik et al. (2009)
	Chestnut	1.61-24.9 mg/Kg d.w EA	Gonçalves et al. (2010)
Processed fruits	Pomegranate juice	1500-1900 mg/L punicalagin	Gil et al. (2000)
		2020-2660 mg/L ETs and EA	Gil et al. (2000)
		5700 mg/L ETs and EA	Cerdá et al. (2006)
	Raspberry jam	76 mg/100 g f.w	Koponen et al. (2007)
	Strawberry jam	24 mg/100 g f.w	Koponen et al. (2007)
	Muscadine grape jam	8-24 mg/L	Lee and Talcott (2002)
Wines and Spirits	Oak-aged red wine	9.4 mg/L	Glabasnia and Hofmann (2006)
		50 mg/L	Clifford and Scalbert (2000)
	Muscadine grape wine	2-65 mg/L	Lee and Talcott (2002)
	Whiskey	1-2m g/L	Glabasnia and Hofmann (2006)
	Cognac	31-54 mg/L	Clifford and Scalbert (2000)

f.w. (fresh weight); d.w. (dried weight); EA (Ellagic acid); ETs (Ellagitannins)

1.3.2. BIOAVAILABILITY AND METABOLISM OF ELLAGITANNINS

The ellagitannins biodegradation after oral intake has been a topic of growing interest in recent years. Ellagitannins have characteristic structural features, namely the high molecular weight and polarity, which greatly decreases the bioavailability of these molecules. Therefore, the knowledge about absorption and metabolism of ellagitannins is of outmost importance, in order to unveil the health benefits of their consumption.

It is now well established that dietary ellagitannins are slowly hydrolyzed in the gastrointestinal tract, releasing ellagic acid (Seeram et al., 2004; Whitley et al., 2006). Then, the ellagic acid is metabolized into urolithins by gut microbiota (Cerdá et al., 2004; Espín et al., 2007).

Urolithins are a subfamily of metabolites generated by the opening and decarboxylation of ellagic acid lactone rings, followed by a sequential dehydroxylation that promotes the production of a series of hydroxylated dibenzopyranone derivatives. These molecules are further metabolized by phase I and II metabolism to facilitate their excretion (Larrosa et al., 2010b; Selma et al., 2014).

1.3.2.1. ELLAGITANNIN HYDROLYSIS INTO ELLAGIC ACID

Ellagitannins are not stable under basic and neutral conditions, leading to the release of ellagic acid due to the loss of an HHDP unit that undergoes lactonization and spontaneous rearrangement (Daniel et al., 1991). Therefore, after the addition of ellagitannins to the cell culture medium, in *in vitro* experiments, it was observed a conversion of ellagitannins into ellagic acid, leading some authors to attribute the cellular effects of the treatment to the presence and uptake of ellagic acid (Larrosa et al., 2006a, 2006b). However, this hydrolysis is gradual and the concentrations of ellagitannins in the medium depend not only on pH, but also on the matrix, or the constitution of the extract that contains the ellagitannins (Srubar-Vernon, 2014). Furthermore, several *in vivo* studies demonstrated that ellagitannins are degraded into ellagic acid in the upper gastrointestinal tract. A study conducted by González-Barrio et al. (2010), in which human volunteers who have undergone ileostomy consumed raspberries, documented that the recovery of ellagic acid in the ileum was 241% and the presence of ellagitannins drastically decreased, thus demonstrating that ellagitannins are partially degraded before reaching the ileum. Additionally, Seeram et al. (2004) investigated the presence of ellagic acid in the plasma of humans after ingestion of pomegranate juice. Ellagic acid was detected after 30 min and reached a maximum after 1 hour, suggesting that ellagic acid was absorbed directly from the stomach or from the proximal intestine.

1.3.2.2. ELLAGIC ACID METABOLIZATION INTO UROLITHINS

Ellagitannins were never identified in human bloodstream or urine even after consumption of relevant amounts of these compounds in foods. Moreover, also after ingestion of ellagitannins containing food, relatively low concentrations of ellagitannins and ellagic acid were found in colon and feces (Cerdá et al., 2003; González-Barrio et al., 2010) suggesting that microbial degradation is occurring during intestinal transit. Thus, it is now well established that ellagic acid and residual ellagitannins are metabolized to produce urolithins (Figure 1.13). Briefly, microbial enzymes catalyze the opening and descarboxylation of one of the lactone rings of ellagic acid. Then, the sequential dehydroxylation first produces urolithin M-5 (pentahydroxy-urolithin), followed by urolithin D or urolithin M-6 (tetrahydroxy-urolithins), urolithin C or urolithin M-7 (trihydroxy-urolithins) and urolithin A or isourolithin A (dihydroxy-urolithins). The final metabolite produced is the

monohydroxy-urolithin, urolithin B, that was mainly found in colon and feces (Garcia-Muñoz and Vaillant, 2014).

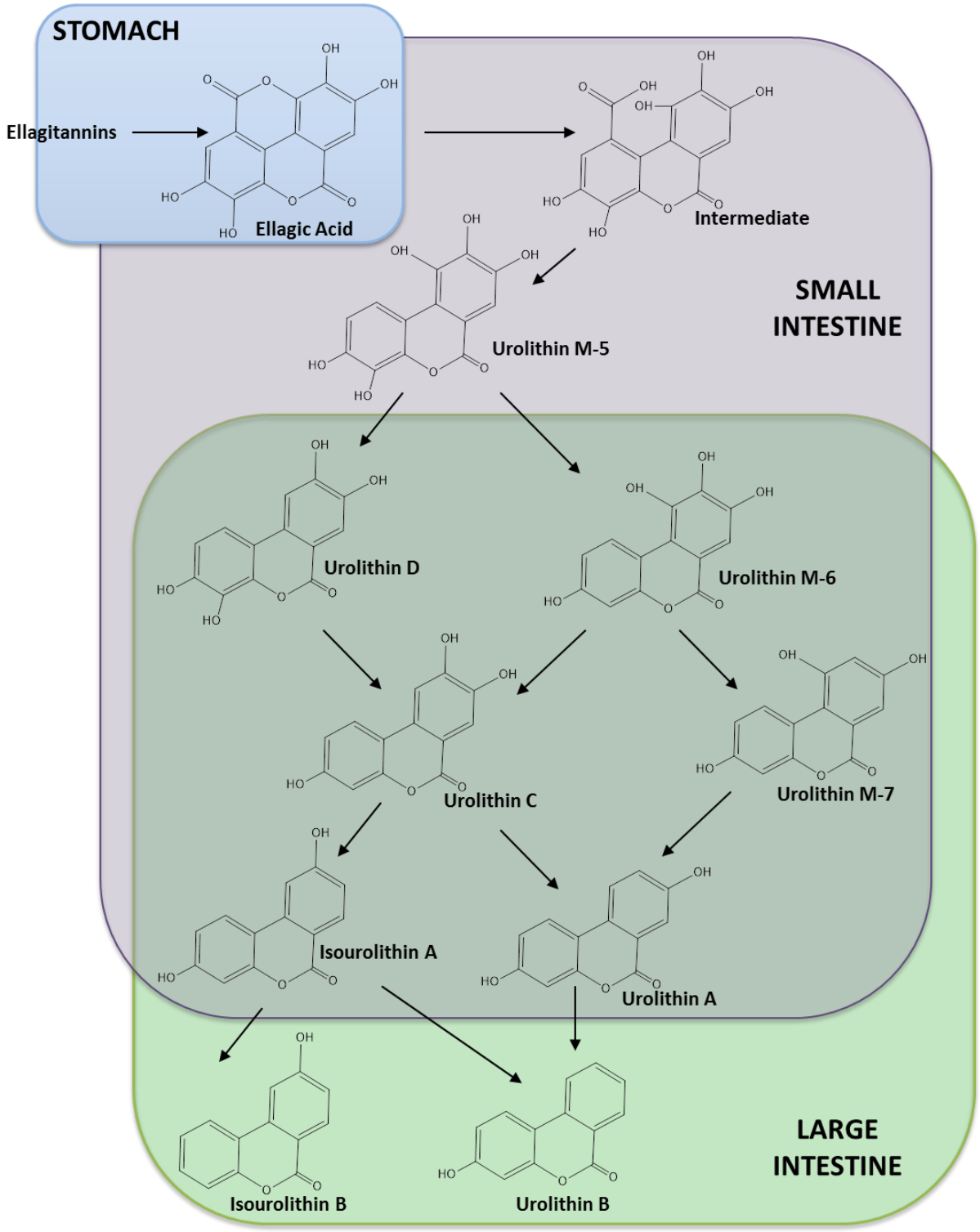

Figure 1.13 - Metabolism of ellagitannins and ellagic acid in the gastrointestinal tract. Adapted from Lipińska et al. (2014)**.**

The main urolithins identified in mammals are urolithins A and B (reviewed by (Espín et al., 2013)) and their progressive dehydroxylation was correlated to an increase in lipophilicity and intestinal absorption (Espín et al., 2007). There is, however, a great interindividual variability in the metabolites profile, both qualitatively and quantitatively, which was suggested to be dependent on the different gut microbiota composition in humans (Romo-Vaquero et al., 2015; Tomás-Barberán et al., 2014).

Ellagic acid and urolithins undergo phase I (hydroxylation) and phase II (methylation, glucuronidation and sulfation) metabolism in order to render more hydrophilic molecules that are required for their body elimination. Accordingly, urolithins were reported in the plasma mainly as glucuronides (Cerdá et al., 2004). However, this biotransformation may change the biological effects of these metabolites, often reducing the bioactivities in comparison to their aglycone (González-Sarrías et al., 2014).

(Espín et al., 2007) and colleagues, using Iberian pig as a model, evaluated the presence of ellagitannins metabolites in different tissues, such as liver, kidney, heart, brain, lung, and muscle, but no aglycone was detected. This study revealed the presence of large amounts of different conjugates of urolithins in the bile and low clearance of those molecules in the urine, which was indicative of enterohepatic circulation. In humans, urolithin metabolites were detected in prostate gland after the ingestion of pomegranate juice and walnuts (González-Sarrías et al., 2010). A similar finding was observed in mouse prostate (Seeram et al., 2007).

1.3.3. BIOLOGICAL AND PHARMACOLOGICAL PROPERTIES

Several biological activities and health-related properties have been reported either for ellagitannin-containing foods or for herbal preparations ellagitannins-enriched. However, and since ellagitannins have low bioavailability, considerable attention has been paid to their metabolites – ellagic acid and urolithins. All of these compounds have antioxidant, anti-inflammatory, anticancer and antimicrobial effects that will be explained in detail below.

1.3.3.1. ANTIOXIDANT ACTIVITY

Oxidative stress arises from the imbalance between the production of free radicals and the body's antioxidant defenses, and has been implicated in the pathogenesis of inflammatory, cardiovascular and neurodegenerative diseases (McCord, 2000). Under normal conditions, free radicals are produced continuously within the cells, being necessary for many physiological processes. The cells also own a competent detoxification system that consists of endogenous enzymatic free radical scavengers. However, under a pathological condition, reactive oxygen species

(ROS) are generated in high amounts and the body´s natural defenses do not efficiently scavenge them, causing damage in crucial macromolecules, thus leading to cell injury and homeostatic disruption.

Antioxidants can suppress the formation of free radicals, scavenge the active radicals to terminate free radical chain reactions, or they can recognize, degrade, and remove oxidatively modified proteins and prevent the accumulation of oxidized proteins (Lobo et al., 2010). Antioxidant capacity is a well-known bioactivity of ellagitannins. Many studies have highlighted the antioxidant properties of ellagitannins from strawberries (Aaby et al., 2007, 2005), raspberries and cloudberries (Kähkönen et al., 2012), pomegranates (Cerdá et al., 2004; Gil et al., 2000) and walnuts (Fukuda et al., 2003), among others. In fact, in chemical assays (e.g. 1,1-diphenyl-2-picrylhydrazyl; DPPH) the radical scavenging activity of ellagitannins was higher than that of their metabolic product, the ellagic acid (Fischer et al., 2011; Kähkönen et al., 2012). The strong antiradical activity conferred to ellagitannins has been correlated with the presence of a high number of hydroxyl groups (Gil et al., 2000; Hagerman et al., 1998).

Regarding urolithins, Cerdá et al. (2004) reported a lower antioxidant effect of urolithin A in comparison to its precursor punicalagin, with a 42- and 3500-fold lower activity in DPPH and 2,2'-azino-bis-3-ethylbenzthiazoline-6-sulphonic acid (ABTS) assays, respectively. Later, in a cell based assay that evaluated the intracellular generation of ROS, urolithins exhibited a significant antioxidant action that was correlated with the number of hydroxyl groups and with lipophilicity of the molecules. In this context, both urolithins C and D demonstrated higher antioxidant potency than their precursors, ellagic acid and punicalagin. Urolithin A exhibited 10-fold lower activity than the punicalagin; however, the calculated half-maximal inhibitory concentration (IC_{50}) (13.6 µM) for this molecule was within the range of urolithin A plasma concentrations (Bialonska et al., 2009). Similarly, Piwowarski et al. (2014a) demonstrated that urolithins (especially A and C) were very active in the direct scavenging of O_2•− and inhibited neutrophil oxidative burst, being both stronger than ascorbic acid. Furthermore, Qiu et al. (2013) documented that urolithins and ellagic acid decreased the levels of ROS and malondialdehyde (lipid peroxidation product), and increased the antioxidant enzyme superoxide dismutase (SOD) in bladder cells treated with H_2O_2. However in this study it was not observed a relation between the number of hydroxyls and the antioxidant activity. Interestingly, another study highlighted both antioxidant and pro-oxidant activities of ellagic acid and urolithins A and B, and demonstrated that their bioactivities are dependent on the assay system and experimental conditions (Kallio et al., 2013).

1.3.3.2. ANTIMICROBIAL ACTIVITY

The antimicrobial activity of some polyphenolic classes has been widely shown by the scientific literature and can be attributed both to the direct action against bacteria, virus and fungi and/or to the suppression of microbial virulence factors (Daglia, 2012).

In the last two decades *in vitro* antibacterial effects of ellagitannins and ellagitannin-containing foods has been studied. For instance, castalagin showed the ability to inhibit the growth of different strains of food-borne pathogenic bacteria (*Staphylococcus aureus*, *Salmonella* spp., *Escherichia coli* and *Vibrio* spp.) (Taguri et al., 2004), and tellimagrandins I and II, corilagin and pedunculagin showed to have minimum inhibitory concentrations (MICs) between of 6.25 to 12.5 µg/mL against four *Helicobacter pylori* strains (Funatogawa et al., 2004).

Little attention has been paid to urolithins that are produced by gut microbiota and hypothetically may modulate gut microbial population. Nevertheless, the ellagitannin metabolite urolithin A was shown to increase the growth of *Bifidobacterium*, *Lactobacillus* and *Clostridium* spp., and to decrease *Escherichia coli*, enterobacteria and total aerobic bacteria in the intestine of rats after chemically-induced inflammation (Larrosa et al., 2010b).

Furthermore, ellagitannins and ellagic acid exhibit antiviral activity against different virus. Several ellagitannins showed potent antiviral activities against herpes simplex viruses (HSV), type 1 and 2, namely eugenin (Kurokawa et al., 2001), casuarinin (Cheng et al., 2002), geraniin (Yang et al., 2007a) and hippomanin A (Yang et al., 2007b). Castalagin, vescalagin and grandinin displayed a strong inhibitory effect on the replication of acyclovir-resistant strains of HSV1 and HSV2 (Vilhelmova et al., 2011) with pronounced synergistic effects when used in combination with acyclovir (Vilhelmova-Ilieva et al., 2014). Furthermore, punicalagin and chebulagic acid targeted and inactivated HSV1 viral particles and prevented binding, penetration, cell-to-cell spread and secondary infection (Lin et al., 2011).

Ellagitannins also inhibited the replication of human immunodeficiency virus (HIV). Recently, (Bedoya et al., 2010) showed that an ellagitannin enriched fraction from *Tuberaria lignose* inhibited HIV infection in MT-2 infected lymphocytes, which appears to be mediated by CD4 down-regulation, the main receptor for HIV entry. Punicalin and 2-*O*-galloylpunicalin isolated from *Terminalia triflora* inhibited the activity of HIV1 reverse transcriptase, in a dose-dependent way (Martino et al., 2004). Geraniin, hyperin and ellagic acid present in *Geranium carolinianum*, a domestic plant grown in China, were the most active molecules against hepatitis B virus (HBV) (Li et al., 2008), corroborating a previous study demonstrating the potential of ellagic acid as anti-HBV (Shin et al., 2005).

Lastly, ellagitannins also showed antifungal activities against some yeast species. Casuarinin (Souza-Moreira et al., 2013) and punicalagin (Endo et al., 2010) inhibited *Candida albicans* growth.

Tellimagrandin II, isolated from *Ocotea odorifera* leaves, acted synergistically with the common antifungal drugs nystatin, amphotericin and fluconazole, against *Candida parapsilosis* strain (Yamaguchi et al., 2010).

1.3.3.3. ANTI-INFLAMMATORY ACTIVITY

Inflammation is a complex immunological response of the body to a specific pathogen or to an internal injury. If the inflammation persists over time it may contribute for the development and progress of several diseases, including rheumatoid arthritis (Goronzy and Weyand, 2009), asthma (Murdoch and Lloyd, 2010), inflammatory bowel diseases (O'Connor et al., 2010), cardiovascular diseases (Santos and Fonseca, 2009) and cancer (Mantovani, 2010). A variety of signaling pathways are involved in transducing the inflammatory response. The transcription factor nuclear factor κB (NF-κB) controls inflammatory gene expression. In non-stimulated cells, NFκB dimmers are retained in the cytoplasm through the association with the inhibitory protein IκBα. Inflammatory stimulus, including lipopolysaccharide (LPS), leads to the activation of a specific IκB kinase (IKK) that phosphorylates IκBα, which is then tagged for ubiquitination and degradation by proteasome. The liberated NFκB translocates into the nucleus modulating specific gene expression, such as inducible nitric oxide synthase (iNOS) and cyclooxygenase (COX) (Israël, 2010). The iNOS is one of the enzymes that catalyze the formation of nitric oxide (NO) through a series of redox reactions. NO is a bioactive free radical that has been implicated in many physiological functions (Gao, 2010), playing a critical role during inflammation and therefore constitutes a potential target for developing anti-inflammatory therapeutics (Hofseth, 2008).

Many plant polyphenols have anti-inflammatory properties, acting through different molecular mechanisms (reviewed in Costa et al., 2012). Ellagitannins, ellagic acid and their metabolites urolithins have also shown anti-inflammatory and immunomodulatory properties. Furthermore, ellagitannin-rich plant products are used in traditional medicine for internal treatment of different inflammatory-associated diseases (Table 1.3).

Several studies evidence the health promoting effect of fruits and juices containing ellagitannins. However, in order to evaluate the real effect of ellagitannins, the following sections will be focused in the health benefits of ellagitannins or ellagitannins enriched samples.

Table 1.3 - Traditional anti-inflammatory uses of plants rich in ellagitannins. Adapted from Piwowarski et al. (2014b).

Species	Family	Plant	Traditional use	Reference
***Filipendula ulmaria* (L.) *Maxim* (Ph. Eur.)**	Rosaceae	Herb	Rheumatism, infections, fever, respiratory tract and urogenital disorders	Sarić-Kundalić et al., 2011; Vogl et al., 2013
***Geranium pratense* L.**	Geraniaceae	Herb	Anti-inflammatory, jaundice, gastric disorders	Küpeli et al., 2007; Singh and Lal, 2008
***Geranium robertianum* L.**	Geraniaceae	Herb	Intermittent fever, inflammatory conditions of gallbladder and urogenital tract, sinus diseases	Menković et al., 2011
***Geum urbanum* L.**	Rosaceae	Root and rhizome	Rheumatism and gout, infections, fever, dysentery, gastro-enteritis, uterine disorders	Tiţă et al., 2009; Vogl et al., 2013
***Potentilla anserina* L.**	Rosaceae	Herb	Anti-inflammatory, renal and uterine disorders	Tiţă et al., 2009; Tomczyk and Latté, 2009
***Potentilla erecta* (L.) *Raeusch* (Ph. Eur.)**	Rosaceae	Rhizome	Dysentery, enterocolitis, respiratory tract disorders	Sarić-Kundalić et al., 2011; Tiţă et al., 2009; Tomczyk and Latté, 2009
***Quercus robur* L. (Ph. Eur.)**	Fagaceae	Bark	Anti-diabetic, anti-dysenteric, blood system and pulmonary disorders, renal and urinary bladder stones, analgesic	Neves et al., 2009; Sarić-Kundalić et al., 2011
***Rubus fruticosus* L.**	Rosaceae	Leaf	Bronchitis, urinary disorders, analgesic	Popović et al., 2012; Tiţă et al., 2009
***Rubus idaeus* L.**	Rosaceae	Leaf	Enterocolitis, bronchitis, prostate disorders, analgesic, cold, cough, fever	Popović et al., 2012; Sõukand and Kalle, 2013; Tiţă et al., 2009

1.3.3.3.1. *IN VITRO* STUDIES RELATED TO THE POTENTIAL ANTI-INFLAMMATORY BENEFITS OF ELLAGITANNINS AND ITS METABOLITES

In a mechanistic point of view several *in vitro* studies deeply explored putative molecular targets of ellagitannins, many of them using the LPS-activated RAW 264.7 macrophage cell line that is a well-established model of inflammation. Ishii et al. (1999) demonstrated that the ellagitannins casuarinin, casuarictin, pedunculagin and nobotannin B exhibited strong inhibitory activities towards NO production, with IC_{50} values between 2.0 and 5.1 mM and reduced protein levels of iNOS. Similarly, sanguiin H-6, isolated from *Sanguisorbae radix*, decreased the nitrite production and its inhibitory effect at a concentration of 25 mM was equal to that of aminoguanidine (iNOS inhibitor) at 50 mM. This study showed that the effect on nitrite production was probably due to a concomitant inhibition of the expression of iNOS mRNA and to the scavenging capacity of NO, as evaluated by using the NO donor, sodium nitroprusside (Yokozawa et al., 2002).

More recently, Schmid et al. (2012) reported that after stimulation of RAW 264.7 cells with LPS, a toll-like receptor (TLR)2 and TLR4 agonist, oenothein B inhibited iNOS mRNA and protein levels, via inhibition of TLR/NFκB-dependent inducible NO and cytokine synthesis independent from interferon-γ (INF-γ)/Janus kinase (JAK)/signal transducer and activator of transcription (STAT) pathways. Furthermore, punicalagin, a bioactive ellagitannin isolated from pomegranate, a fruit that is widely used for the treatment of several inflammatory-related diseases, decreased the LPS-induced production of NO, prostaglandin E2 (PGE2), interleukin (IL)-1β, IL-6, and tumor necrosis factor (TNF)-α. This ellagitannin also decreased the phosphorylation of IκBα, p65 and mitogen activated protein kinases (MAPKs), including p38, c-Jun N-terminal kinase (JNK), and extracellular signal-regulated kinase (ERK) (Xu et al., 2014). Moreover, Piwowarski et al. (2015) hypothesized that the main

urolithin metabolites in the gut, urolithins A, B, and C, elicited anti-inflammatory activity. Accordingly, these molecules decreased NO production via inhibition of the iNOS mRNA expression and consequently iNOS protein levels, as well as reduced the mRNA levels of IL-1β, TNF-α and IL-6. Moreover, urolithins, and mainly urolithin A, inhibited NFκB p65 nuclear translocation and p50 DNA-binding activity.

Other *in vitro* models have also been used to disclose the role of ellagitannins on inflammation and inflammatory-related diseases. For instance, in primary cultures of rat microglia stimulated with LPS, punicalagin reduced the production of TNF-α, IL-6 and PGE2, the phosphorylation of IKKα, IκBα and p65 and the activation of p38 and JNK MAPKs. Furthermore, punicalagin completely abolished IL-6 and TNF-α mRNA levels in LPS-stimulated organotypic hippocampal slices (Olajide et al., 2014). The potential of punicalagin for the prevention of intestinal chronic inflammation was also addressed. For that, human colon adenocarcinoma Caco-2 cells were pre-treated with punicalagin and then activated into a pro-inflammatory status evoked by cells treatment with LPS and a cocktail of cytokines (IL-1β, TNF-α and IFN-γ). After 24 hours of incubation, punicalagin decreased the mRNA levels of the pro-inflammatory markers IL-6 and monocyte chemoattractant protein (MCP)-1, while IL-8 transcription was unaffected. Furthermore, this ellagitannin also decreased the amount of these 3 proteins in the apical side that corresponds to the intestinal lumen. Interestingly, in a cell free assay, punicalagin lowered the levels of IL-6, IL-8 and MCP1, which indicates a direct molecular interaction (Hollebeeck et al., 2012). Regarding ellagitannins derivatives, the anti-inflammatory potential of urolithin A, urolithin B and ellagic acid was also evaluated in human colon fibroblasts. CCD18-Co cells were exposed to IL-1β plus TNF-α and fibroblasts migration and monocytes adhesion were determined. The mixture of metabolites at concentrations comparable to those found in the colon inhibited colon fibroblasts migration and monocytes adhesion to fibroblasts. It was also reported a decrease of the levels of PGE2, plasminogen activator inhibitor-1 (PAI-1) and IL-8 (Giménez-Bastida et al., 2012b).

Ellagitannins and their metabolites also show some relevant antiartherogenic, anti-thrombotic, and antiangiogenic activities in different cell models representative of vascular structure (reviewed in Larrosa et al., 2010a). Giménez-Bastida et al. (2012a) evaluated the vascular protective effects of urolithin A and its glucuronide derivative in human aortic endothelial cells exposed to TNF-α. The authors reported that urolithin A glucuronide inhibited monocyte adhesion and endothelial cell migration and down-regulated the levels of chemokine (C-C motif) ligand 2 (CCL2) and PAI-1. Urolithin A also inhibited endothelial cell migration but not monocyte adhesion and decreased the release of CCL2 and IL-8. The modulation of the intracellular signaling mechanisms implicated in inflammation by ellagitannins and urolithins are summarized in Figure 1.14.

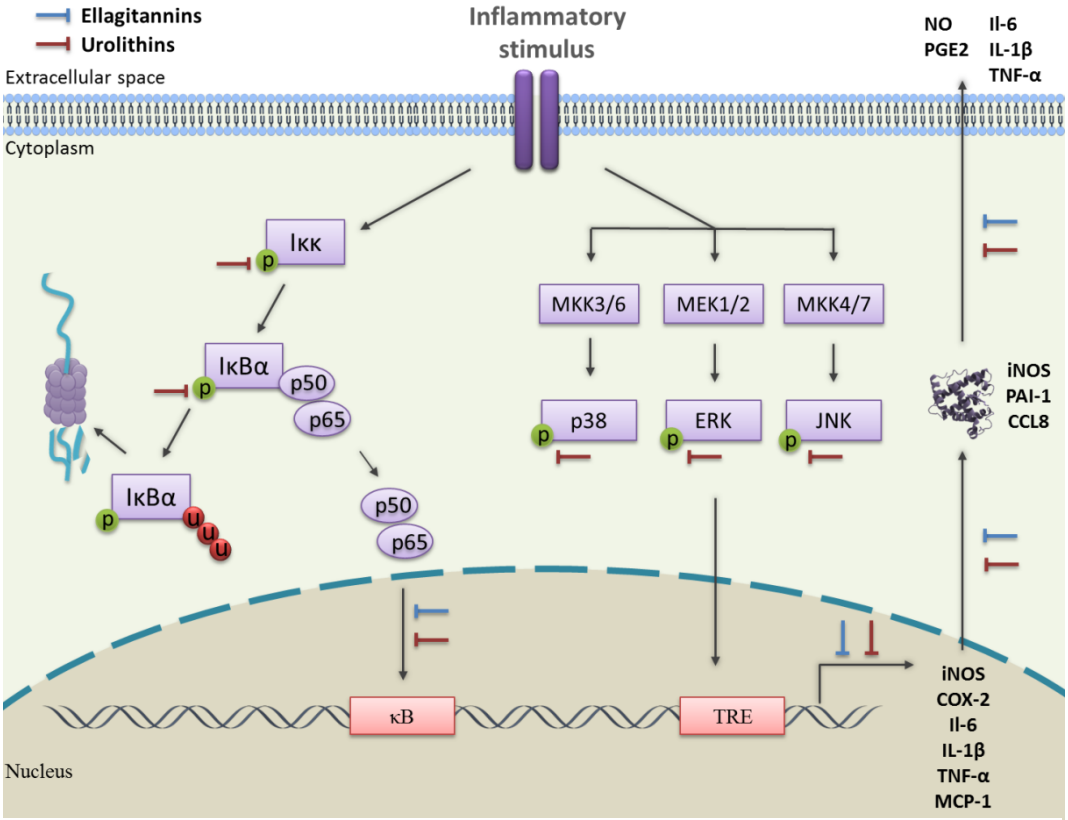

Figure 1.14 - Inflammatory intracellular signaling pathways modulated by ellagitannins and urolithins, according to the reported *in vitro* studies.

1.3.3.3.2. *IN VIVO* STUDIES RELATED TO THE POTENTIAL ANTI-INFLAMMATORY BENEFITS OF ELLAGITANNINS AND ITS METABOLITES

The anti-inflammatory activity of punicalagin and punicalin, isolated from *Terminalia catappa*, was tested in carrageenan-induced inflammation in the rat paw, a classical model of edema formation and hyperalgesia. Both ellagitannins reduced significantly the paw edema, but the treatment with larger doses of punicalin evidenced cell damage (Lin et al., 1999).

Al-Sayed and El-Naga (2015) investigated the gastroprotective activity of an ellagitannin-rich fraction obtained from *Eucalyptus citriodora* against ethanol-induced gastric ulceration in rats. Notably, pre-treatment with the fraction protected from gastric lesions in 99.6%. The investigators concluded that this effect was partially mediated by attenuating ethanol-induced oxidative stress, since the ellagitannin-rich fraction increased the depleted glutathione (GSH) and SOD levels. Furthermore, several inflammatory markers were evaluated and the fraction reduced IL-1β, TNF-α, 5-lipoxygenase and COX-2 levels. Corroborating those results, Sangiovanni et al. (2013) also reported that ellagitannins from blackberries and raspberries were able to protect the stomach against the gastric lesions caused by ethanol in rats. Pre-treatment with the fractions of blackberry and raspberry decreased Ulcer Index by 88% and 75% respectively and protected from the ethanol

induced oxidative stress in rats. Furthermore, in ellagitannins treated animals the secretion of the rat homologue of IL-8 decreased, which was associated to a decrease of NFκB nuclear translocation.

The anti-inflammatory properties of the ellagitannin metabolites, ellagic acid and urolithin A, were also investigated in rat/mice inflammatory bowel disease models. Marín et al. (2013) used mice models of dextran sulfate sodium (DSS)-induced chronic and acute colitis and supplemented animal diet with ellagic acid. In the acute model, ellagic acid slightly ameliorated several disease activity parameters (IL6, TNF-α and IFN-γ). In the chronic model of colitis, treatment with ellagic acid also downregulated some inflammatory mediators (COX-2 and iNOS), inhibited p38 phosphorylation, and NFκB and STAT3 signaling. Moreover, a study conducted by Larrosa et al. (2010b) evaluated the anti-inflammatory properties of urolithin A in a DSS-induced colitis rat model. The animals were fed with urolithin A for 25 days and this treatment reduced several inflammatory markers (iNOS, COX-2, prostaglandin E synthase and PGE2) in colonic mucosa, preserved the colonic architecture and modulated favorably the gut microbiota.

1.3.3.4. ANTICANCER RELATED EFFECTS OF ELLAGITANNINS

Carcinogenesis is a complex and multistep process, in which distinct molecular and cellular alterations are driven. In a simplistic view, carcinogenesis comprises three stages – initiation, promotion and progression. Initiation is a rapid and irreversible phase that consists of an initial uptake or exposure to a carcinogenic agent. This event may lead to DNA damage, which if not repaired originates genetic mutations. Promotion is an interruptible or reversible and long term process. In this stage abnormal cells persist, replicate and can originate a focus of preneoplastic cells. At last, in progression stage premalignant cells develop into tumors with invasive and metastatic potential (Surh, 2003). Several polyphenols have shown the capacity to block initiation of the carcinogenic process and to suppress promotion and progression of cancer (Figure 1.15) (Ramos, 2008; Surh, 2003). Their action can be ascribed to their antioxidant ability concomitantly to their capacity to interact with basic cellular function and to modulate cellular processes linked to carcinogenesis, including cell cycle, apoptosis, inflammation, angiogenesis and metastasis (Kampa et al., 2007).

There is a wealth of information arising from both *in vitro* and *in vivo* studies that highlight the potent anticancer properties of ellagitannins and their metabolites. Antioxidant properties can account for some of the therapeutic effects, but their role on other cellular mechanisms will be further described.

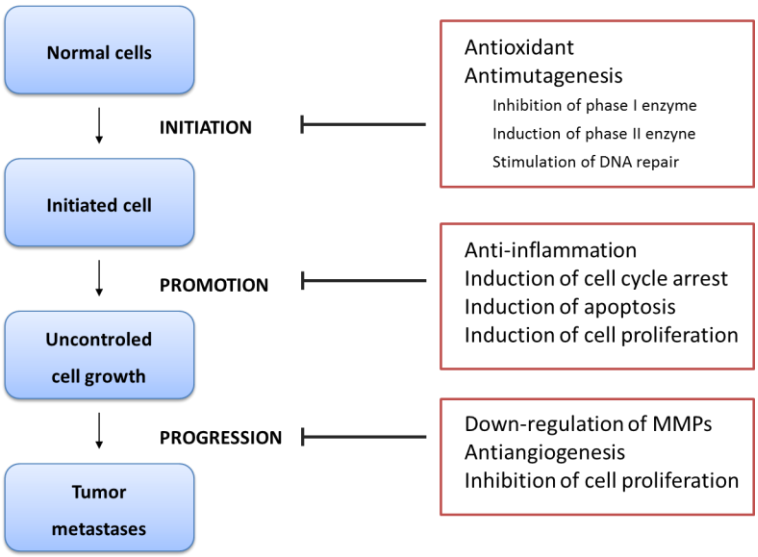

Figure 1.15 - Anticancer potential of polyphenols in carcinogenesis. Adapted from Dai and Mumper (2010).

1.3.3.4.1. CELL PROLIFERATION

Cancer cells are characterized by unbalanced control of cellular proliferation and an immortalized lifespan and, as such, any molecule capable of suppressing cancer cell proliferation may be valuable as a potential chemopreventive/chemotherapeutic agent (Feitelson et al., 2015). Several ellagitannins have shown ability to inhibit one or more pathways involved in cell proliferation, including cell cycle regulators, NFκB and MAPKs. Accordingly, the role of certain ellagitannins and their derivatives on these cellular and molecular targets will be described below.

1.3.3.4.1.1. CELL CYCLE

Defects in cell cycle checkpoints are associated with an increase of genetic instability and uncontrolled cell proliferation, which could lead to the development of the carcinogenesis process (Kastan and Bartek, 2004). Therefore, targeting cell cycle regulators could be an important strategy for cancer therapy and prevention.

Casuarinin, an ellagitannin isolated from the bark of *Terminalia arjuna*, blocked cell cycle at the G0/G1 phase in MCF-7 (human breast adenocarcinoma) and A549 (human non-small cell lung cancer) cells through p21 (Cip^1/Waf^1) upregulation (Kuo et al., 2005a, 2005b). The p21 protein is a cyclin-dependent kinase inhibitor that decreases the activity of cyclin dependent kinases (cdk)1 and cdk2 and blocks the transition from G1 phase into S phase, or from G2 phase into mitosis (Cmielová and Rezáčová, 2011). Likewise, the ellagitannin rugosin E arrested human breast cancer cells (MDA-MB-231) at G0/G1 phases and this effect was probably related to an decrease of cyclins D1, cyclin D2, cyclin E, cdk2, cdk4 and cdk6 and increase of p21 (Cip^1/Waf^1) levels (Kuo et al., 2007).

The ellagitannin geraniin also modulated cell cycle. Vassallo et al. (2013) demonstrated that this molecule was an inhibitor of the molecular chaperone heat shock protein 90 (Hsp90) and promoted an arrest at G2/M phases in HeLa (human cervical cancer cells) and Jurkat (human T lymphocyte cells) cell lines. Furthermore, in A549 cells, Li et al. (2013) verified that geraniin arrested cell cycle in the S phase.

The effect of an ellagitannin fraction from black raspberry seeds, ellagic acid and urolithins A and B on cell cycle was evaluated in HT-29 colon cancer cells. Interestingly, the different compounds affected differently cell cycle. Ellagitannins increased the number of cells in S and G2/M phases while ellagic acid slightly increased cells at S phase. Urolithins A and B promoted a cell cycle arrest at G2/M phase that was accompanied by the upregulation of p21 (Cho et al., 2015).

In Caco-2 cells treated with ellagic acid and its colonic metabolites, urolithins A and B modulated cell cycle distribution by increasing the cells at S and G2/M phases (González-Sarrías et al., 2009). Furthermore, urolithin A arrested cell cycle at G1 phase and concomitantly upregulated p21 in the LNCap (human prostate adenocarcinoma cells) cell line.

1.3.3.4.1.2. PI3K/AKT AND MAPK SIGNALING

The phosphatidylinositide 3-kinase (PI3K)/Akt and MAPK are intracellular signaling cascades that play a central role in growth, proliferation, survival, cell death and angiogenesis (Figure 1.16). Their activation modifies the expression and activity of target genes and transcription factors promoting a range of biologic responses. In tumor cells, some regulatory proteins of these cascades are overexpressed, which leads to their constitutive activation (De Luca et al., 2012).

The PI3K/Akt tightly regulates the balance between cell survival and apoptosis and became a promising target for cancer chemoprevention and therapy (Polivka and Janku, 2014). Studies addressing the effect of ellagitannins and their metabolites on this signaling cascade, in the context of cell proliferation inhibition, are scarce. A pomegranate extract (POMx) developed for use as a dietary ingredient standardized to ellagitannin content (37% punicalagins by HPLC) clearly decreased Akt phosphorylation at position Thr308 and Ser473 in LAPC4 prostate cancer cells. Treatment with POMx also decreased mammalian target of rapamycin (mTOR) phosphorylation at Ser2448 and slightly reduced at Ser2481 (Koyama et al., 2010). The mTOR is a downstream target of PI3K/Akt signaling and its regulation is frequently altered in many types of cancer. Punicalagin, the main ellagitannin of pomegranate inhibited TNFα-induced Akt activity in HT-29 colon cancer cells. Furthermore, ellagic acid also decreased PI3K/Akt activation *in vitro* (Shi et al., 2015; Umesalma et al., 2015) and *in vivo* (Umesalma and Sudhandiran, 2011; Zhao et al., 2013) models of carcinogenesis.

MAPKs are Ser/Thr kinases that convert extracellular stimuli into a wide range of cellular responses. Through a cascade of phosphorylations, the three most studied families of MAPKs in cancer, ERK, JNK and p38 kinases, are activated and regulate several cellular processes, such as cell proliferation, survival, apoptosis, cell migration, differentiation and inflammatory response (Figure 1.16) (Cargnello and Roux, 2011).

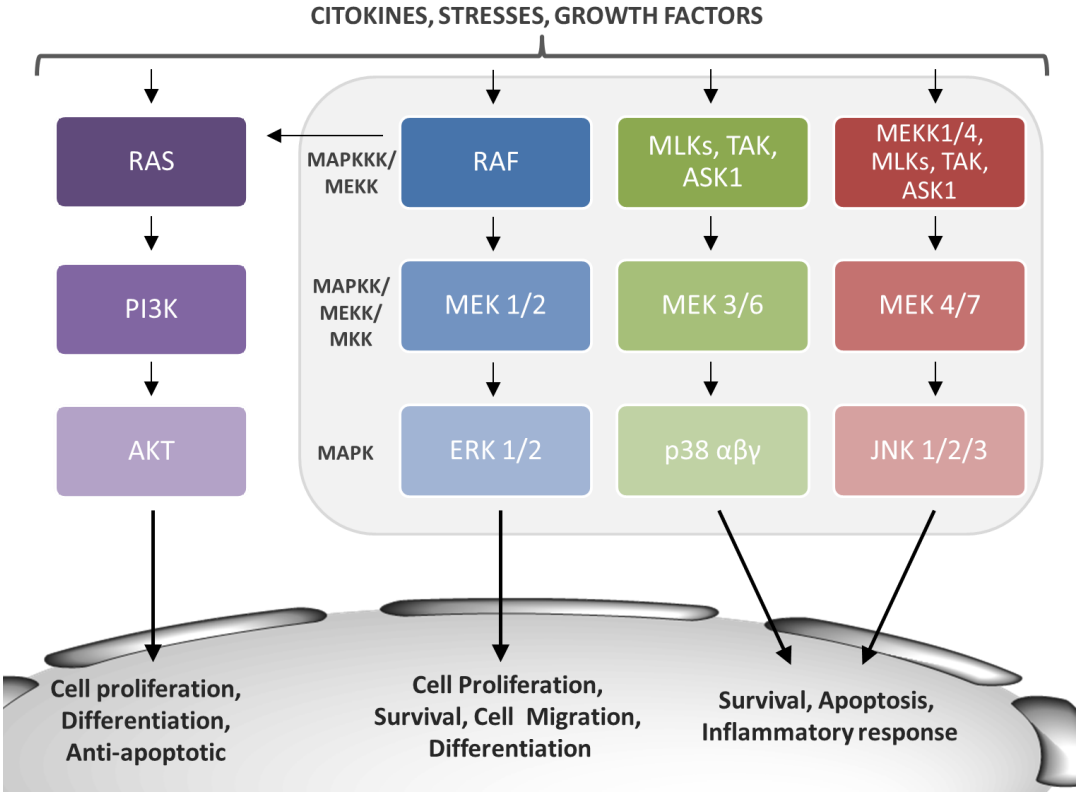

Figure 1.16 - Schematic representation of PI3K/Akt and MAPKs signaling pathways and downstream effects. Adapted from Xavier (2010).

As exposed above, considering an inflammatory context, casuarinin (Kwon et al., 2011), gerannin (Xiao et al., 2015) and punicalagin (Olajide et al., 2014; Xu et al., 2014) suppressed the activation of MAPKs in different types of cells. Furthermore, González-Sarrías et al. (2009) treated Caco-2 cells with ellagic acid (10 µM), urolithin A and B (40 µM) usually detected in the intestinal lumen after ellagitannins intake. The investigators demonstrated that these molecules changed the expression levels of several genes involved in the ERK1/2 signaling pathway. To confirm these results, the phosphorylation of ERK1/2 was evaluated and it was shown that a mixture of these three compounds inhibited the activation of this kinase. In T29 cells (bladder cancer cells), urolithins A and B increased the phosphorylation of p38 and decreased c-Jun phosphorylation and MEKK1 protein levels (Qiu et al., 2013). Accordingly, in a study performed in HepG2 cells (human hepatocellular

carcinoma), urolithin A also increased the phosphorylation of p38 and decreased the phosphorylation of c-Jun (Wang et al., 2015).

The NFκB transcription factor is also implicated in the regulation of cell proliferation and apoptosis, by promoting the expression of key genes that are implicated in these cellular functions. NFκB is activated in many cancers and contributes for the link between inflammation and carcinogenesis (Shen and Tergaonkar, 2009). Several ellagitannins that regulate NFκB signaling were described above, in the inflammation section.

1.3.3.4.2. CELL DEATH

Apoptosis is a type of programmed cell death that is characterized by cellular shrinkage, membrane bleeding and fragmentation into membrane bound apoptotic bodies, and nuclear fragmentation with chromatin condensation (Kerr et al., 1972). There are two major apoptotic signaling pathways: extrinsic and intrinsic pathways (Figure 1.17) that mutually converge through a cascade of proteolytic reactions involving the activation of caspases (Galluzzi et al., 2012). The intrinsic pathway is triggered by various intracellular stimuli, including DNA damage, growth factor deprivation, cytokine withdrawal and oxidative stress, which lead to permeabilization of mitochondrial outer membrane and the release of pro-apoptotic proteins, such as cytochrome *c*. In the cytoplasm, cytochrome *c*, apoptotic protease activating factor (Apaf-1) and procaspase-9 form a complex denominated apoptosome. Once caspase-9 is activated it cleaves and activates the effector caspases (caspase-3, 6 and 7)(de Bruin and Medema, 2008; Jin and El-Deiry, 2005).

The extrinsic pathway is initiated when extracellular ligands, such as Fas ligand (FasL), TNF-α or TNF-related apoptosis inducing ligand (TRAIL) bind to death receptors of the TNF receptor superfamily. This interaction is followed by the assembly of the death-inducing signaling complex (DISC), which consists of the Fas-associated death domain (FADD) protein and procaspase-8/10. The caspase is cleaved and activated, and therefore initiates a cascade of other caspases, leading to the activation of the downstream effector caspases (caspase-3, 6 and 7). Therefore, both pathways converge in the activation of the same effector caspases, which in turn cleave cytoskeletal and nuclear proteins, such as poly (ADP-ribose) polymerase (PARP) and lamin A (Jin and El-Deiry, 2005). Mitochondrial membrane permeabilization and activation of the extrinsic apoptotic pathway are regulated by a series of B-cell lymphoma protein (Bcl)-2 family members, such as the pro-apoptotic proteins Bcl-2 associated X protein (Bax), Bcl-2 antagonist killer 1 (Bak) and Bcl-2 interacting domain (Bid), and the anti-apoptotic proteins Bcl-2 and Bcl-2 related protein, long isoform (Bcl-xL) (Pradelli et al., 2010).

Tumor cells often have defects in these apoptosis-inducing pathways, which can lead to the expansion of neoplastic cells. Thus, these cells can acquire resistance to apoptosis through several strategies including the expression of anti-apoptotic proteins or the downregulation or mutation of pro-apoptotic proteins (Okada and Mak, 2004).

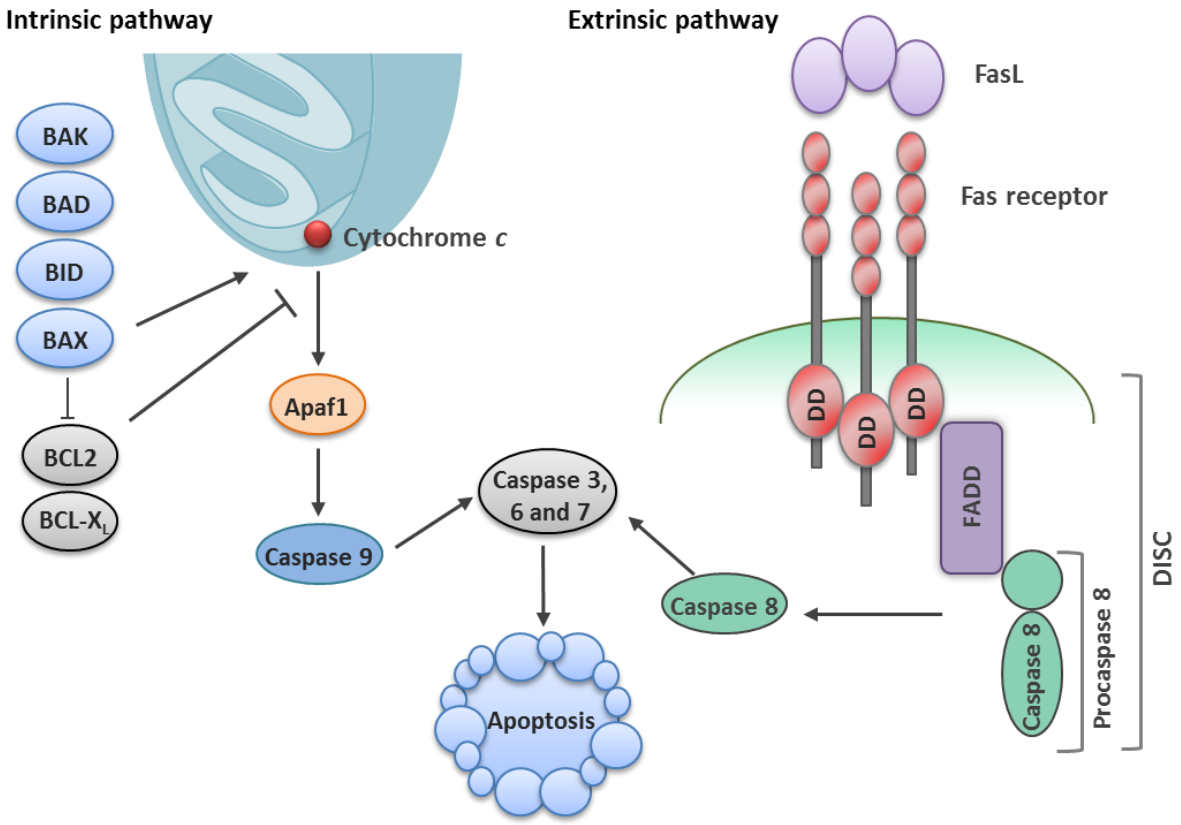

Figure 1.17 - Intrinsic (mitochondrial) and extrinsic (FAS) apoptotic pathways. Adapted from Fesik (2005)**.**

Ellagitannins and their metabolites have shown ability to induce apoptosis in different cell lines, modulating several molecular pathways and the expression of apoptotic regulators. For instance, the monomeric ellagitannin gerannin inhibited the proliferation of A549 cells, inhibited Bcl-2 expression and induced Bax expression to disintegrate the outer mitochondrial membrane causing cytochrome *c* release, which was associated to the activation of caspase-9 and caspase-3 cascades (Li et al., 2013). Furthermore, in human melanoma cells, gerannin induced caspase-3 activity, which leads to cleavage of focal adhesion kinase (FAK) and cell death. The FAK is a cytoplasmic tyrosine kinase located in the focal adhesion complex and plays an anti-apoptotic role in anchorage dependent cells (Sonoda et al., 2000). FAK has shown to be one of the critical factors protecting cells from apoptosis and is overexpressed in numerous tumor systems (Cance et al., 2000; Lightfoot et al., 2004). In addition, the induction of apoptosis was associated with the up-regulation of FasL expression, the activation of caspase-8, the cleavage of Bid, the release of cytochrome *c* for the

cytoplasm and the proteolytic cleavage of PARP (Lee et al., 2008). Rugosin E, an ellagitannin isolated from *Rosa rugosa*, increased apoptosis in the human breast cancer cell line MDA-MB-231. Treatment with rugosin E increased the pro-apoptic Bax, Bak, and Bcl-2 related protein, short isoform Bcl-xS protein levels and decreased the anti-apoptotic Bcl-2 and Bcl-xL proteins. Subsequently, rugosin E mediated the release of cytochrome *c* and activated the caspases 9 and 3 (Kuo et al., 2007). Larrosa et al. (2006b) studied the effect of punicalagin and ellagic acid in Caco-2 cells and demonstrated that both induced apoptosis via intrinsic pathway through Bcl-xL down-regulation, mitochondrial release of cytochrome *c* and activation of caspase 9 and 3. The investigators also showed that ellagic acid and punicalagin did not induce apoptosis in normal cells CCD-112CoN. Punicalagin was also shown to promote apoptosis in HT-29 colon cells (Seeram et al., 2005) and U87MG glioma cells (Wang et al., 2013).

Other examples of ellagitannins that modulate this type of programed cell death are cuphiin D1 (Wang et al., 2000), oenothein B, woodfordin C, woodfordin D (Sakagami et al., 2000), woodfordin I (Liu et al., 2004), 1-α-*O*-galloylpunicalagin, 2-*O*-galloylpunicalin, sanguiin H-4 (Chen et al., 2009), camelliin B (Wang et al., 2001) and casuarinin (Kuo et al., 2005a, 2005b).

More recently, Cho et al. (2015) showed that urolithins A and B induced apoptotic cell death in HT-29 cells through both extrinsic and intrinsic pathways, as suggested by the disruption of the mitochondrial membrane potential and activation of caspases 8 and 9. Accordingly, the authors also detected the activation of caspase 3 and cleavage of PARP. Corroborating these results, other studies demonstrated that urolithin A and B triggered apoptosis in prostate cancer cells LNCaP, which was correlated with a decrease in Bcl-2 levels (Sánchez-González et al., 2014) and with caspase 3 and 7 activation evoked by urolithin A (Sánchez-González et al., 2015).

In several studies, the induction of apoptosis by ellagitannins, ellagic acid and urolithins was accompanied by an increase of necrosis (Cho et al., 2015; Kasimsetty et al., 2010; Larrosa et al., 2006b). Necrosis is another form of cell death that occurs in both physiological and pathophysiological processes and, in contrast to apoptosis, provokes an inflammatory response in surrounding cells through the leakage of intracellular contents. The typically inflammatory response can stimulate an immune response towards potentially malignant cells and in this case, necrosis may contribute for the tumor regression. Conversely, during tumor development, the inflammation that occurs due to the excessive spontaneous necrosis, may stimulate the growth and aggressiveness of the tumor (de Bruin and Medema, 2008; Proskuryakov and Gabai, 2010).

Although initially reported as a nonregulated mechanism of death, some forms of necrosis are currently considered a consequence of the crosstalk between several biochemical and molecular events (Festjens et al., 2006), which gave rise to the concept of necroptosis or programed necrosis. Necroptosis was described to occur as a consequence of death receptor signaling and follows an

intracellular signaling cascade via receptor-interacting protein kinase (RIP)1/RIP3 complex (Linkermann and Green, 2014). This type of cell death was recently described (Degterev et al., 2005) and as far as we know the involvement of ellagitannins in this pathway was never addressed.

Moreover, several authors considered the existence of an autophagic cell death (Clarke and Puyal, 2012). However, the role of autophagy as an alternative cell death mechanism is still a controversial debated issue, since with some notable exceptions, autophagy appears to be associated with cellular death, rather than being itself a cell death mechanism (Das et al., 2012; S. Shen et al., 2012; Tait et al., 2014). The importance of autophagy, as well as of the other proteolytic system, the ubiquitin-proteasome system (UPS), in the context of carcinogenesis will be discussed below.

1.3.3.4.3. PROTEOLYTIC MECHANISMS AS NOVEL MOLECULAR EVENTS THAT CONTRIBUTE TO ANTICANCER ACTIVITY

The cellular homeostasis depends on the balance between biosynthesis and degradation of proteins. There are two main pathways for protein catabolism in eukaryotic cells: the UPS and the autophagy-lysosomal system. These processes are involved in the degradation of surplus, dysfunctional and damaged cellular components, ranging from soluble proteins to whole organelles (Korolchuk et al., 2010). Therefore, the dysregulation of these processes is implicated in a broad array of pathological conditions, including cancer (Driscoll and Chowdhury, 2012).

The protein degradation by UPS is a multistep process in which intracellular proteins, usually short-lived proteins, are targeted for destruction by the covalent attachment of homopolymers of a small, 76-amino acid long, highly conserved protein called ubiquitin. In short, ubiquitin is activated and conjugated with the target protein by three enzymes: E1 (ubiquitin activating enzyme), E2 (ubiquitin-conjugated enzyme) and E3 (ubiquitin ligase) (Hershko et al., 1983). The E3 enzymes endow the UPS with its high specificity, as they determine which substrate should be ubiquitinated and degraded in the proteasome (Bie and Ciechanover, 2011). The proteasome is a proteolytic complex present in both the nucleus and the cytosol, and is made up of three subunits: the barrel shaped 20S central complex and two 19S lid complexes. The 19S regulatory complex, through a process ATP-dependent, recognizes the ubiquitinated proteins and plays a role in their unfolding and translocation into the catalytic pore of 20S (Lam et al., 2002; Liu and Jacobson, 2013). The 20S subunit core has three catalytic activities, the trypsin, chymotrypsin and peptidyl-glutamyl peptide-hydrolyzing-like, which efficiently cleaves the proteins into smaller peptides (Figure 1.18) (Orlowski and Wilk, 2000). Due to the narrow size of the catalytic pore the proteins need to be partially unfolded to be degraded. Therefore, protein complexes or aggregates can only be digested if disassembled, making them poor proteasome substrates (Korolchuk et al., 2010).

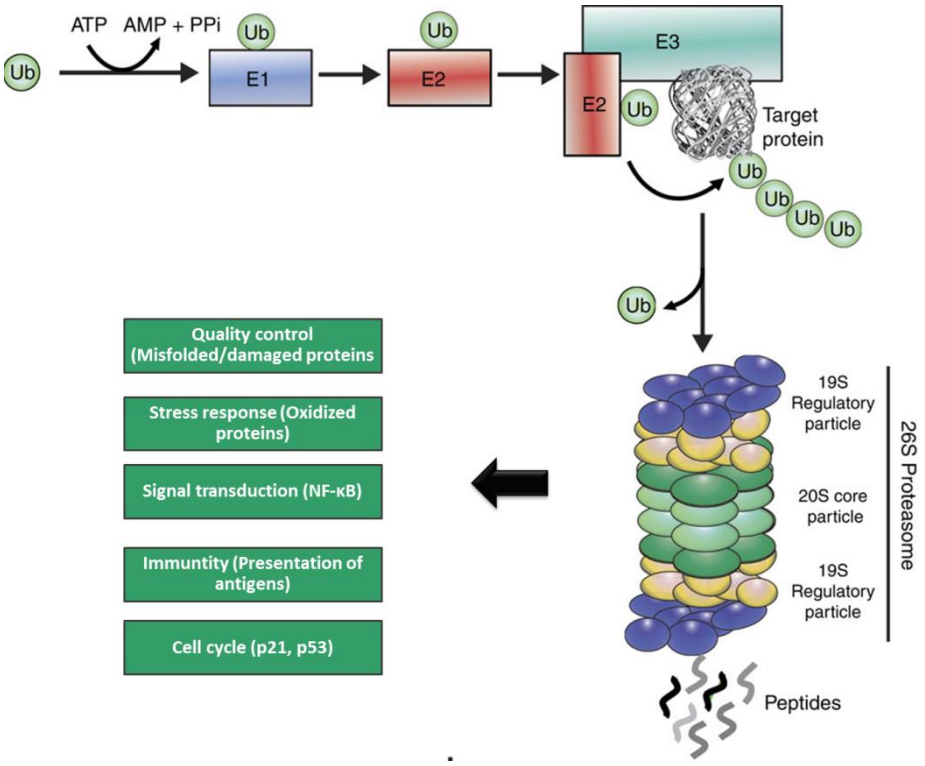

Figure 1.18 - Protein degradation by the ubiquitin–proteasome pathway. Adapted from Vilchez et al. (2014).

Autophagy-lysosomal pathway is the main system for degradation of long-lived proteins and bulk cytoplasmic components in the cell, including functional or misfolded soluble proteins, protein complexes, oligomers, aggregates and even cell organelles. There are three autophagic pathways depending on the delivery of the cargo to lysosomes: microautophagy, chaperone-mediated autophagy (CMA) and macroautophagy. In microautophagy, the lysosomal membrane invaginates to sequester regions of cytosol that are internalized into the lysosomal lumen (Li et al., 2012). CMA involves the direct translocation of cytosolic proteins into the lysosomal lumen through the coordinated action of cytosolic and lysosomal chaperones (Cuervo and Wong, 2014). Finally, the macroautophagy is the best characterized type of autophagy and has been broadly referred to as autophagy. Succinctly, macroautophagy is initiated by the formation and elongation of a double-layered membrane, the phagophore, that enwraps and sequesters portions of cytoplasm containing the proteins, leading to the formation of a microtubule-associated protein light chain 3 (LC3)-containing vacuoles (autophagosomes). The autophagosome fuses with a lysosome forming the autophagolysosome and its content is degraded by the acid hydrolases of the lysosome. Following the breakdown, the resulting macromolecules are released in the cytoplasm (Figure 1.19). This process is tightly regulated by specialized proteins such as autophagy-related proteins (ATGs), beclin-I (also known as Atg6) and mTOR (Mehrpour et al., 2010; Pattingre et al., 2008).

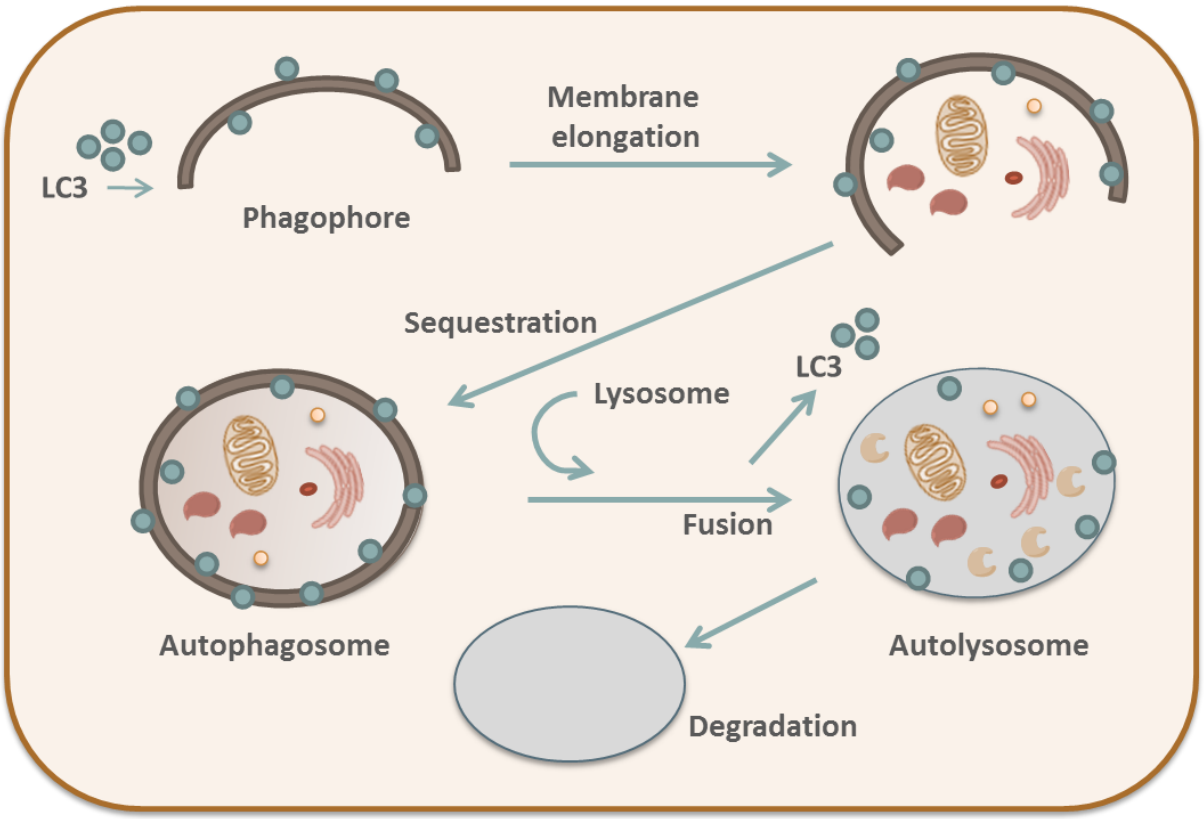

Figure 1.19 - Schematic model of autophagic process (macroautophagy). Adapted from Kondo et al. (2005).

An increasing number of studies suggests a crosstalk between these two degradation systems (Korolchuk et al., 2010). Indeed, various proteins are substrates of both clearance mechanisms and, under particular conditions, proteins that are usually degraded in the proteasome may be digested by autophagy and vice-versa (Fuertes et al., 2003a, 2003b). Additionally, ubiquitin, a tag once thought to be exclusive for UPS, confers selectivity to autophagy (Shaid et al., 2013). Some of the ubiquitin recognizing molecules, such as the signaling adaptor p62 (also known as sequestosome-1), can deliver ubiquitinated substrates to both autophagy and UPS (Geetha et al., 2008). Functional connections between these two systems may also exist at other levels. Experimental studies indicated that the impairment of UPS leads to an increase of autophagic function, which was thought to be a compensatory mechanism, allowing cells to reduce the levels of UPS substrates (Ding et al., 2007). Furthermore, impaired autophagy has also been shown to compromise the degradation of UPS substrates (Korolchuk et al., 2009).

In normal cells, UPS and autophagy are essential processes in the regulation of many cellular activities, including cell cycle, cell differentiation and apoptosis, and the malfunction in clearance of misfolded or aggregated proteins has been shown to underlie the pathogenesis of several diseases (Levine and Kroemer, 2008; Schmidt and Finley, 2014). Therefore, UPS and

autophagy have been considered highly attractive pharmacological targets for drug discovery and development.

Particularly in cancer, these mechanisms play pivotal roles in both chemoprevention and chemotherapeutics. Several proteasome substrates were recognized as key mediators in carcinogenesis, such as cyclins (W. Chen et al., 2004), tumor suppressor protein p53 (Li and Dou, 2000) and pro-apoptotic protein Bax (Li and Dou, 2000). Moreover, increased proteasome activity was present in several malignancies, including those of the colon (Loda et al., 1997) and leukemia (Kumatori et al., 1990). These facts lead to the design and development of proteasome inhibitors for cancer therapeutics. Accordingly, bortezomib, the first proteasome inhibitor approved by United States Food and Drug Administration (FDA), has been used for the treatment of multiple myeloma and has improved disease control and overall survival (Kouroukis et al., 2014). However, due to its side effects, mostly as neurotoxic and partial cell resistance, there is still a need to identify or design more specific and potent proteasome inhibitors (Brüning and Jückstock, 2015).

The relation between autophagy and cancer is very complex. Several studies support its double-faced function in cancer: tumor suppression or promotion. Under normal conditions, autophagy may function as a tumor suppressor, blocking cancer initiation and progression (Chen and White, 2011). Furthermore, it has been also suggested that hyperactivation of autophagy may lead to cell death, which is another way for tumor-cell elimination (Mathew et al., 2007). Paradoxically, under low-oxygen and low-nutrient conditions, autophagy promotes tumor survival, by supplying energy and the essential macromolecules to maintain tumorigenesis (Degenhardt et al., 2006). Consequently, the clinical use of autophagy inhibitors may be particularly important in tumors with a high metabolic demand (Ozpolat and Benbrook, 2015). Furthermore, due to a compensatory mechanism of autophagy after proteasome inhibition, another feasible approach in cancer treatment is to combine autophagy and proteasome inhibitors (Vogl et al., 2014). Thus, targeting both UPS and autophagy degradation may increase the susceptibility of oncogenic cells to proteasome inhibitors and selectively enhance cell death in cells with a high metabolic demand (Ding et al., 2009).

Plant-derived natural polyphenols have shown to modulate UPS and autophagic degradation. Regarding autophagy, most of the studies suggest a beneficial role of polyphenols consumption/treatment in order to increase autophagy, by preventing the age-related diseases closely associated to a decline of this clearance mechanism, or to induce “autophagic cell death” (Hasima and Ozpolat, 2014; Pallauf and Rimbach, 2013). Conversely, other studies reported that some polyphenols induce cancer cell death through autophagy inhibition (Gordon et al., 1995; Yang et al., 2012). Furthermore, it is well established that several polyphenols have the ability to inhibit the proteasome, which is intimately correlated with the activation of apoptotic cell death pathways (M. Shen et al., 2012). In this scenario, finding natural proteasome and autophagy inhibitors is a very

attractive therapeutic strategy, and their use separately, combined or in combination with traditional chemotherapeutic agents would be of utmost value for cancer treatment.

Regarding ellagitannins, there is very few information about the potential of these compounds to modulate the clearance mechanisms of the cell. Interestingly, Wang et al. (2013) showed that the ellagitannin punicalagin was able to induce autophagy in human glioma cells, while ellagic acid exerted anticancer effects through autophagy inhibition in ovarian cancer cells. Concerning UPS, from our knowledge ellagitannins were never reported as proteasome inhibitors, but their metabolite ellagic acid inhibited 26S proteasome activity (Chang et al., 2013), and its precursor PGG had potential anticancer effects through proteasome inhibition (Chen and Lin, 2004; Kuo et al., 2009). Giving the anticancer properties of ellagitannins and its metabolites it would be important to unveil their role as potential drugs to target these proteolytic mechanisms.

1.4. *FRAGARIA VESCA* L.

Fragaria vesca L. subsp. *vesca* (that will be referred in this work as *Fragaria vesca*) is commonly known as wild strawberry, woodland strawberry or European strawberry and in Portugal as *morangueiro*, *morangueiro-bravo* or *morangueiro-silvestre*.

The enchantment with wild strawberries dates back as far as 2200 years ago, at the ancient roman times, when the Roman poets Virgil and Ovid mentioned the strawberry in their verses, and accordingly with a mythological legend the strawberries were called tears of Venus, because when her love, Adonis, died, she shed copious tears that reaching on earth were converted into small red hearts, the strawberries. Even though the wild strawberry consumption dates more than two millennia only in 1300s, in France, the wild plants were transplanted to the garden, being reported that in 1368 the King Charles V had 1200 strawberry plants in the royal gardens of the Louvre, in Paris (Hummer et al., 2011).

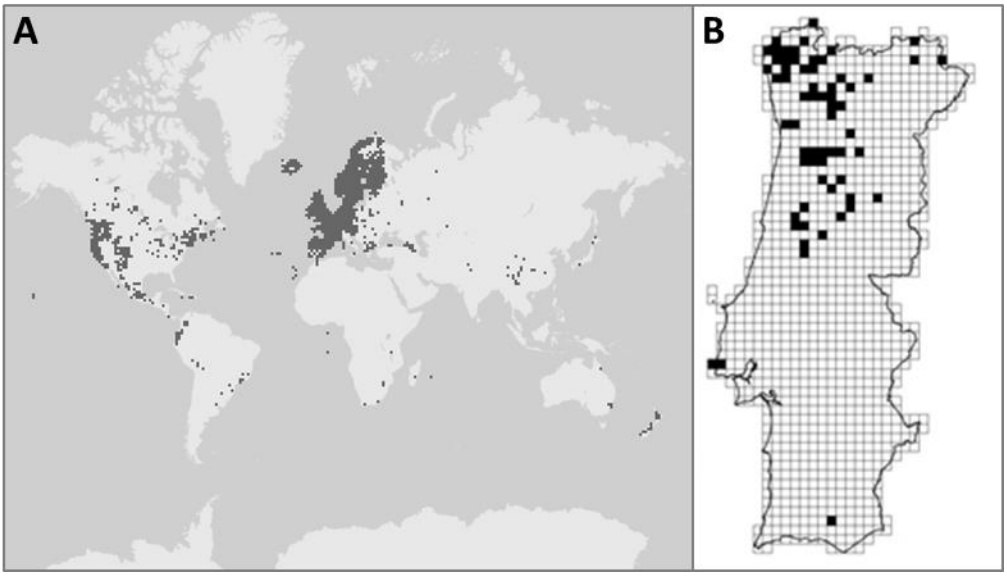

Figure 1.20 - Geographic distribution of *Fragaria vesca*. A) Worldwide geographic distribution. Adapted from GBIF Backbone Taxonomy (2013); B)Portugese geographic distribuition. Adapted from Almeida et al. (2015).

1.4.1. GEOGRAPHIC AND BOTANICAL CHARACTERIZATION

This plant occurs across the northern hemisphere, more specifically in Europe, North America and Asia, West of the Urals (Figure 1.20-A) (Hummer et al., 2011). It is an autochthonous plant of continental Portugal (North and Center) (Figure 1.20-B) and of the Portuguese archipelagos, Madeira and Azores (Figure 1.20) (Sequeira et al., 2011). *Fragaria vesca* grows spontaneously in grasslands or forests (usually deciduous), verges of roads, ravines and slopes ("Flora-On: Flora de Portugal Interactiva," 2014).

Fragaria vesca belongs to the family Rosaceae, subfamily Rosoideae, genus *Fragaria* L. and species *Fragaria vesca* L. The Swiss botanist C. Bauhin (Bauhin, 1623) was the first to summarize the genus *Fragaria* and after him, others botanists described this genus (Duchesne, 1766; Linnaeus, 1753, 1738). Presently, genus *Fragaria* comprises 20 wild species, three naturally occurring hybrid species and two cultivated hybrid species (Table 1.4)(Hummer et al., 2011). Most of the species are diploid with 14 chromosomes (2n = 2x = 14), but polyploid levels range from diploid to decaploid.

Table 1.4 - *Fragaria* species, ploydia and geographic distribution. Adapted from Hummer et al. (2011).

Ploidy	Species	Distribution Area
2x	*Fragaria bucharica* Losinsk	Western Himalayas
	Fragaria chinensis Losinsk	China
	Fragaria daltoniana J. Gay	Himalayas
	Fragaria iinumae Makino	Japan
	Fragaria mandshurica Staudt	North China
	Fragaria nilgerrensis Schlect.	Southeastern Asia
	Fragaria nipponica Makino	Japan
	Fragaria nubicola Lindl.	Himalayas
	Fragaria pentaphylla Losinsk	North China
	Fragaria vesca L.	Europe, Asia west of the Urals, disjunct in North America
	Fragaria viridis Duch.	Europe and Asia
	Fragaria x bifera Duch.	France, Germany
4x	*Fragaria corymbosa* Losinsk	Russian Far East/China
	Fragaria gracilis A. Los.	Northwestern China
	Fragaria moupinensis (French.) Card	Northern China
	Fragaria orientalis Losinsk	Russian Far East
	Fragaria tibeca Staudt & Dickoré	China
5x (9x)	*Fragaria X bringhurstii* Staudt	California
	Fragaria sp. Nov	China
6x	*Fragaria moschata* Duch.	Euro-Siberia
8x	*Fragaria chiloensis* (L.) Miller	Western N. America, Hawaii, Chile
	Fragaria virginiana Miller	North America
	Fragaria X ananassa Duch. ex Lamarck	Cultivated worldwide
	Fragaria X ananassa subsp. *Cuneifolia*	Northwester, N. America
10x	*Fragaria iturupensis* Staudt	Iturup Island, Kurile Island
	Fragaria virginiana subsp. platypetala Miller	Oregon, United States
	Fragaria X vescana R. Bauer & A. Bauer	Cultivated in Europe

Fragaria vesca, as the other *Fragaria* species, is spring-blooming, low-growing, insect-pollinated and has animal-dispersed fleshy fruits. The species from the genus *Fragaria* are herbaceous and perennials. *Fragaria vesca* (5-25 cm) has a horizontal or oblique rhizome that is covered by the remains of leaves and stipules from which arises epigeal stolons (or runners). When in contact with a moist substratum, the stolons generally take roots and form a sympodial network of stolons above the ground. The fertile stems, erect or ascending are usually higher than the leaves. The leaves are evergreen, trifoliate and with false rosettes. Flowers are hermaphrodites and actinomorphic, with five white and orbicular petals. The botanical fruits are dry achenes that are

embedded in a fleshy receptacle, the strawberry, which is technically considered an aggregate accessory fruit. When mature, the strawberry (10-17 mm) has an ovoid shape and an intense and bright red color (Figure 1.21) (Castroviejo, 1998; J.-S. Chen et al., 2004; Liston et al., 2014).

Figure 1.21 - *Fragaria vesca* L. A) Botanical Illustration adapted from Chaumeton et al. (1830); B) Photography adapted from Porto (2014).

1.4.2. MEDICINAL PROPERTIES OF *FRAGARIA VESCA*

Due to the natural appearance, intense taste and olfactory characteristics, wild strawberries are a highly appreciated product. Though primarily valued for their flavor, *Fragaria vesca* berries have also potential health properties, such as free-radical scavenger (Cheel et al., 2007), antioxidant (Scalzo et al., 2005), anticonvulsant (Patil et al., 2012) and anti-inflammatory (Kanodia et al., 2011) activities. The health benefits related to wild strawberries consumption could be associated with the presence of polyphenols. In fact, these fruits have higher polyphenolic content than *Fragaria* x *ananassa* and showed a strong DPPH scavenging. *Fragaria vesca* berries are also richer in sugars, citric and malic acids (Crespo et al., 2010; Doumett et al., 2011). These facts are particularly relevant because the consumption of *Fragaria* x *ananassa*, the most commercially diffused strawberry specie worldwide, may have a beneficial role on inflammation, cardiovascular diseases, oxidative stress, cancer, metabolic syndrome and neurodegeneration (reviewed in Giampieri et al., 2015, 2012)).

While the fruits are more appreciated for their taste, the leaves and the rhizomes of *Fragaria vesca* are valued for their medicinal properties. Several ethnopharmacological surveys reported the use of *Fragaria vesca*, but many of them did not discriminate the part of the plant that was used. The traditional preparations of non-edible parts of this plant are infusions and decoctions, both used internally and externally (Fleming, 2000). The dried rhizome is a popular household remedy and is mainly prepared by decoction. It has diuretic and astringent properties and has been used for several medicinal purposes, including as anti-dysenteric, antiseptic, detoxifying, emollient, dermatological protector, antirheumatic, and for the treatment of cough and hemorrhoids (Camejo-Rodrigues et al., 2003; Kanodia and Das, 2008; Lamari et al., 2007; Neves et al., 2009; Ozüdoğru et al., 2011; Savo et al., 2011). Furthermore, it was reported that the roots of *Fragaria vesca* are also rich in polyphenols namely proanthocyanidins, ellagitannins and flavonols, showing also a high antioxidant potential (Dias et al., 2015c).

The leaves are the most reported part of the *Fragaria vesca* plant, according to the ethnopharmacological surveys available. They are collected in the spring, preferentially harvested in the wild and air-dried in a shady place (Fleming, 2000). The leaves are traditionally prepared as infusion or decoction and their applications are very broad. These preparations have been used externally as a dermatological protector and for the treatment of skin diseases, including compresses for rashes or as a antiseptic, emollient and anti-inflammatory (Fleming, 2000; Kiselova et al., 2006; Neves et al., 2009; Sarić-Kundalić et al., 2010). It has also been applied in the treatment of stomatitis, pharyngitis, blepharitis and hemorrhoids, among other inflammatory related diseases of mucosal surfaces (Cabral et al., 2014; Jarić et al., 2007). The leaves are very popular as detox herbs, with diuretic, diaphoretic and cholagogue properties (Spiridonov, 2008; Zaurov et al., 2013). This herbal medicine is also used to treat respiratory ailments, including cough, catarrh and sore throats (Fleming, 2000; Popović et al., 2014; Zlatković et al., 2014), heart and circulatory pathologies by lowering blood pressure and heart rate and also for hematological diseases, namely anemia (Camejo-Rodrigues et al., 2003; Manolova, 2003; Spiridonov, 2008). One of the most described benefits of *Fragaria vesca* leaves is on gastrointestinal and liver diseases (Jarić et al., 2007; Kiselova et al., 2006; Menković et al., 2011), especially as antidiarrheal medicine, which is probably due to the presence of ellagitannins and its astringents properties (Cabral et al., 2014). This herb was used in the treatment of diabetes, renal stones, jaundice, arthritis and gout (Fleming, 2000; Spiridonov, 2008), being also reported its use on leukemia, and kidney and breast cancers (Patil, 2013; Spiridonov, 2008).

Even though *Fragaria vesca* leaf has been used for the treatment of several complaints, scientific reports validating its biologic effects are very scarce. Some scientific studies highlighted the high antioxidant potential of both aqueous and ethanolic extracts obtained from the leaves of *Fragaria vesca* (Buricova et al., 2011; Dias et al., 2015c; Kiselova et al., 2006) and this property was

correlated with their polyphenolic content (Batista and Amaral, 2000; Ivanov et al., 2015). A study performed by Mudnic et al. (2009) evaluated the cardiovascular effects of an aqueous extract of *Fragaria vesca.* This extract appeared to be an effective direct endothelium-dependent vasodilator and NO and cyclooxygenase products were critical mediators of this effect. Furthermore, the leaves of *Fragaria vesca* demonstrated to have antimicrobial properties (Borah et al., 2012) and the glycoconjugates isolated from them (essentially constituted of polyphenolic and polysaccharide components) owned anticoagulant activities (Pawlaczyk et al., 2013).

Moreover, as it happens in many plants, the phenolic content of the strawberry leaves may vary with the development stage and growing environmental conditions of the plant. Accordingly, it was demonstrated that the wild plants of *Fragaria vesca* have higher amounts of total phenolic compounds than the commercial (cultivated) ones (Dias et al., 2015c). The same investigation group showed that the infusion and decoction of *Fragaria vesca* leaves may also have a nutritional value, being a source of macro and micronutrients, namely tocoferols, vitamin B_9, mineral elements, soluble sugars and organic acids (Dias et al., 2015b).

From our knowledge there are no toxicology/safety studies regarding the use of these preparations. Indeed, individuals with allergy to strawberry should not take this herbal medicine (Fleming, 2000). Actually, its efficacy and safety is currently being evaluated by the European Medicines Agency.

Overall, the reported traditional uses, the high phenolic content along with the biological activities reported in both *in vitro* and *in chemico* studies point out *Fragaria vesca* leaf as a promising source of compounds with relevant pharmacological activity.

1.5. THESIS AIMS

Natural products and in particular, plant-derived compounds, are important sources of new drugs and drug leads for many diseases. Ethnopharmacological studies reported a widespread use of *Fragaria vesca* leaves namely for the treatment of dermatological, gastrointestinal, cardiovascular and urinary disorders. Polyphenols are phytoconstituents to which have been assigned biological properties related to its antioxidant and anti-inflammatory potential, which can be on basis of these diseases. Scientific reports validating the biologic effects of the *Fragaria vesca* leaves are scarce. As far as we know, until the beginning of this work there were no studies with a detailed characterization of the polyphenols of the leaves of this species. In a first approach, this work aimed to:

- disclose the bioactivity and the underlying action mechanisms of an extract from *Fragaria vesca* leaves, using a cell line of macrophages stimulated with LPS, in order to support its traditional uses;
- evaluate the effect of the extract in the two main intracellular protein degradation pathways in eukaryotic cells, UPS and autophagy, which dysregulation has been implicated in the pathogenesis of different diseases, including in cancer, thus constituting privileged targets for anticancer therapies;
- characterize the polyphenols through HPLC-PDA-ESI/MS^n.

Since *Fragaria vesca* leaves are especially rich in ellagitannins, which recently have been gathering much attention for their chemopreventive potential, other aims were to:

- evaluate the anticancer potential of an ellagitannin-enriched fraction (EEF) derived from *Fragaria vesca* leaves extract, on human hepatocellular carcinoma cells;
- elucidate the molecular mechanisms behind EEF bioactivity, with a special focus on autophagy and proteasome;
- disclose proteins differentially modulated by EEF based in a proteomic approach.

Given the low bioavailability of ellagitannins and their metabolization in the gastrointestinal tract into ellagic acid and consequently into urolithins, the systemic health benefits of their consumption may rely on a direct effect of ellagitannins metabolites. Therefore we also aimed to:

- evaluate the antiproliferative effect of ellagic acid and urolithins A, B and C in several human cell lines representative of different types of cancer;

- investigate the role of each compound in the mechanisms associated to cell proliferation, namely cell cycle, cell death and PI3K/Akt and MAPKs intracellular signaling pathways;
- establish a structure-activity relationship that may constitute valuable information in the design of urolithin derivatives presenting potent antiproliferative activity.

Altogether, this study aims to shed light in the medicinal properties of a traditional herbal medicine from *Fragaria vesca* leaves, identifying molecules with pharmacological activity and understanding their cellular mechanisms of action. Finally, the anticancer potential of urolithins was envisioned, constituting the starting point for their further exploitation in order to disclose fine-tuned effective therapeutic strategies against cancer.

Chapter 2

Bioactivity of *Fragaria vesca* leaves through inflammation, proteasome and autophagy modulation

Joana Liberal, Vera Francisco, Gustavo Costa, Artur Figueirinha, Maria Teresa Amaral, Carla Marques, Henrique Girão, Maria Celeste Lopes, Maria Teresa Cruz, Maria Teresa Batista

Journal of Ethnopharmacology 12/2014;158:1131-22

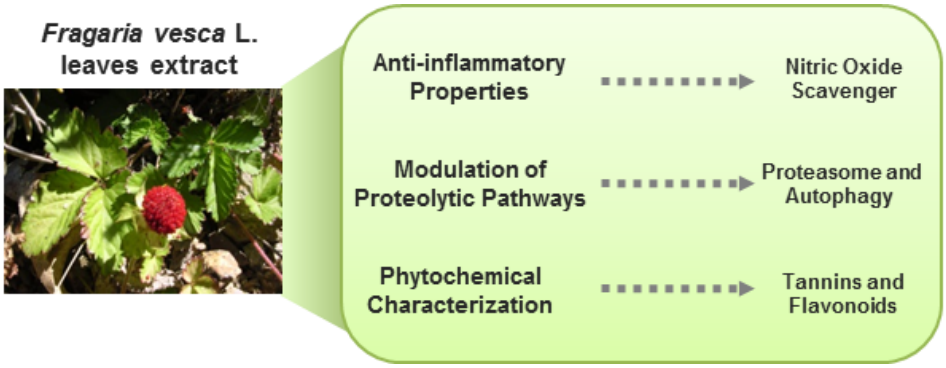

ABSTRACT

Ethnopharmacological relevance: *Fragaria vesca* leaves have been used in folk medicine for the treatment of several diseases, namely gastrointestinal, cardiovascular and urinary disorders, which could be related with the potential anti-inflammatory properties of the extract. This work aims to disclose the bioactivity and the underlying action mechanism of an extract from *Fragaria vesca* leaves in order to support its traditional uses.

Materials and Methods: A hydroalcoholic extract was prepared from *Fragaria vesca* leaves and its anti-inflammatory potential was evaluated through inhibition of nitric oxide production and expression of several pro-inflammatory proteins in lipopolysaccharide-triggered macrophages. Nitric oxide scavenger activity was also assessed using a standard nitric oxide donor. Since numerous inflammatory proteins are tightly regulated by ubiquitination and proteasomal degradation, the putative effect of the extract on these cellular proteolytic pathways was also disclosed. The phytochemical characterization was performed by HPLC-PDA-ESI/MSn and compared with an infusion prepared according to the traditional method.

Results: For non-cytotoxic concentrations (80 and 160 μg/mL) the extract inhibited nitrite production, probably due to a direct nitric oxide scavenging. Furthermore, inhibition of proteasome activity was verified, leading to the accumulation of ubiquitinated proteins. The extract also increased the conversion of the microtubule-associated protein light chain LC3-I to LC3-II, a marker of autophagy. Polyphenols, namely ellagitannins, proanthocyanidins, and quercetin and kaempferol glucuronide derivatives were identified in *Fragaria vesca* leaves extract. Most of the identified phenolic compounds matched with those found in traditional preparation, the infusion.

Conclusions: The extract has a direct nitric oxide scavenging activity giving support to the traditional use of this plant for the treatment of inflammatory disorders. Furthermore, the extract affects the proteolytic systems but its role in cancer treatment requires further studies.

Keywords

Fragaria vesca leaves; Polyphenols; Inflammation; Nitric Oxide scavenger; Ubiquitin-Proteasome system; Autophagy

2.1. INTRODUCTION

Natural products are important sources of new drugs and it has been widely shown that many plant-derived phytochemicals have considerable anti-inflammatory and anticancer effects (Newman and Cragg, 2012). Many plant polyphenols have anti-inflammatory properties, acting through different molecular mechanisms (Costa et al., 2012). For example, polyphenols can down-regulate inducible transcription factors that control inflammatory gene expression, such as nuclear factor κB (NFκB), a process that is tightly regulated by ubiquitination and proteasomal degradation (Liu and Chen, 2011). Importantly, some recent studies have also ascribed a role for natural compounds in the regulation of proteolytic pathways, including the proteasome activity (Bonfili et al., 2011; Milacic et al., 2008), and autophagy (Qian et al., 2011), which may constitute relevant findings for the development of new anticancer agents. Both the ubiquitin-proteasome system (UPS) and autophagy, constitute essential players of the cellular quality control systems, contributing for the removal of potentially toxic damaged, unfolded or obsolete proteins (Wong and Cuervo, 2010). Although initially described as two independent proteolytic pathways, recent studies have exquisitely shown that UPS and autophagy cross talk. Indeed, it has been established that the impairment of the UPS up-regulates autophagy (Du et al., 2009), whereas the blockage of autophagy compromises UPS degradation (Korolchuk et al., 2009). Thus, autophagy and the UPS are critical in the maintenance of cellular homeostasis, suggesting that their activities need to be carefully orchestrated.

Fragaria vesca L. (checked with www.theplantlist.org in 07-05-2014), commonly known as wild strawberry, is a perennial rosette plant, belonging to the genus *Fragaria* and Rosaceae family and is usually found in Europe, Asia West of the Urals and North America (Folta and Gardiner, 2009). Several health benefits have been attributed to *Fragaria vesca* berries, such as free-radical scavenger (Cheel et al., 2007), antioxidant (Scalzo et al., 2005) and anti-inflammatory (Kanodia et al., 2011) activities. Moreover, ethnobotanical studies reported a widespread use of the vegetative parts from wild growing *Fragaria vesca*. Particularly, the leaves are collected during the flowering season in the wild and are commonly prepared as infusion or decoction, being both administrated internally and externally (Fleming, 2000). Preparations of *Fragaria vesca* leaves have been used externally as antiseptic, emollient and dermatologic protector, as well as to treat inflammation of cutaneous and mucosal surfaces (Cunha et al., 2003; Neves et al., 2009). Internally, this herbal medicine has been used for respiratory system complaints, such as cough, catarrh and sore throats (Popović et al., 2014; Zlatković et al., 2014), cardiovascular diseases, including lowering of blood pressure and heart rate (Camejo-Rodrigues et al., 2003; Manolova, 2003), urinary ailments as the renal stones (Fleming, 2000), and as complementary treatment for diabetes (Spiridonov, 2008). It is also very popular in folk medicine in the treatment of gastrointestinal disorders, especially due to the astringent, antidiarrheic

and antidysenteric properties (Jarić et al., 2007; Kiselova et al., 2006; Sarić-Kundalić et al., 2010). Moreover, it was also reported the use of *Fragaria vesca* leaves to treat leukemia and kidney and breast cancers (Patil, 2013; Spiridonov, 2008). Thus, the etnopharmacological applications of *Fragaria vesca* are wide but most of these pathologies have in common a relevant inflammatory background. However, scientific reports validating the biologic properties of the leaves are still scarce. Previously we demonstrated a robust relationship between the strong antioxidant capacity of the *Fragaria vesca* leaves extract and the presence of polyphenols (Batista and Amaral, 2000). These evidences along with the reported traditional uses make *Fragaria vesca* leaf a potential source of bioactive compounds. Therefore, the aim of this work is to disclose the bioactivity of an extract obtained from *Fragaria vesca* leaves on inflammation and proteolysis and to characterize the phenolic compounds present in the preparation.

2.2. MATERIALS AND METHODS

2.2.1. PLANT MATERIAL

Wild plants (with flowers and fruits) of *Fragaria vesca* were sustainably collected from Granja de Figueira do Lorvão, Penacova, Portugal (May, 2011). The plant material was identified by Dr. Célia Cabral, plant taxonomist. A voucher specimen (ID-180611) was deposited at the Herbarium of Medicinal Plants, Faculty of Pharmacy, University of Coimbra.

2.2.2. EXTRACTS PREPARATION

The leaves were selected and dried in the dark, using an oven at 30 ºC, with air circulation. The dehydrated leaves were powdered, sieved and treated with dichloromethane (1:10, w/v - 2 times). The extraction was performed with ethanol absolute (2 times) and 50% aqueous ethanol (3 times) (1:10, w/v) at room temperature using an Ultra-Turrax homogenizer for 5 min at 8000–9500 rpm. After each extraction, the extracts were filtered under vacuum. The ethanol was removed using a rotary evaporator, and the aqueous extract was lyophilized and stored at -20 °C until the time for testing. A yield of 30% expressed in dry plant was obtained. The hydroalcoholic extract was solubilized in phosphate buffered saline (PBS) for *in vitro* biological assays.

The infusion is the most common herbal remedy from *Fragaria vesca* leaves reported in ethnobotanical studies. According with the recommendations of Physicians' Desk Reference for Herbal Medicines, the infusion was prepared by adding 4 gr of dried leaves to 150 mL of boiling water. Traditionally this preparation is taken several times a day (Fleming, 2000).

In order to compare the phenolic profile of the traditional preparation with the hydroalcoholic extract the infusion was prepared in a similar way. Therefore, the dried and chopped leaves were poured over boiled water (4 g: 150 mL, w/v) in a porcelain laboratory cup and left at room temperature for 15 min without additional heating. The infusion was filtrated and lyophilized. A yield of 23% expressed in dried plant was obtained.

2.2.3. CELL CULTURE

The mouse leukemic monocyte macrophage cell line, Raw 264.7, was kindly supplied by Dr. Otília Vieira (Center for Neurosciences and Cell Biology, University of Coimbra, Portugal) and cultured in Iscove's Modified Dulbecco's Eagle Medium containing 10% (v/v) non heat-inactivated fetal bovine serum (FBS), 100 U/mL penicillin, and 100 µg/mL streptomycin. The cells were maintained at 37 ºC and 5% CO_2/95% air in a humidifier incubator.

2.2.4. ASSESSMENT OF CELL VIABILITY

The cells ($3x10^5$ cells/well) were plated in 48-well plates for 12 hours and incubated with the hydroalcoholic extract 1 hour prior to stimulation with lipopolysaccharide (LPS) (1 µg/mL) for 24 hours. The viability of Raw 264.7 cells exposed to the extracts was measured using the 3-[4,5-dimethylthiazol-2-yl]-2,5-diphenyl tetrazolium bromide (MTT) assay. Briefly, MTT solution (5 mg/mL) prepared in PBS was added to the cells. The plates were incubated at 37 ºC for 15 min in a humidifier atmosphere of 95% air and 5% CO_2. Supernatants were removed and acidified isopropanol (0.004 *N* HCl in isopropanol) was added to adherent cells, in order to dissolve the dark blue crystals of formazan produced by metabolically active cells. Formazan was quantified by measuring the absorbance of the samples using an ELISA automatic microplate reader (SLT, Austria) at 570 nm, with a reference wavelength of 620 nm.

2.2.5. MEASUREMENT OF NITRITE PRODUCTION

Nitrite concentration in culture supernatants was measured using a colorimetric reaction with Griess reagent. The cells were plated and treated as described above. After 24 hours of LPS incubation, the cell-free supernatants were collected and diluted with equal volumes of Griess reagent (0.1% [w/v] N-(1-naphthyl)-ethylenediamine dihydrocloride and 1% [w/v] sulphanilamide containing 5% [w/v] H_3PO_4) in the dark. After 30 min, samples absorbance was registered in ELISA automatic microplate reader (SLT, Austria) at 550 nm. Nitrite concentration was established from a sodium nitrite standard curve and the culture medium was used as blank.

2.2.6. DETERMINATION OF NO SCAVENGING ACTIVITY

The NO scavenging activity of plant extracts were evaluated using S-nitroso-N-acetylpenicillamine (SNAP) as NO donor. *Fragaria vesca* hydroalcoholic extract (160 µg/mL) and SNAP (300 µM) were added to culture medium and maintained in a humidifier incubator at 37 ºC for 3 hours. The medium was collected and the levels of nitrite were determined by Griess reaction, as described above.

2.2.7. WESTERN BLOT ANALYSIS

Raw 264.7 macrophages ($12x10^5$ cells/well) were cultured in 12-well plates for 12 hours and further incubated alone with *Fragaria vesca* hydroalcoholic extract (160 µg/mL) or with LPS (1 µg/mL) for different time points, according to the proteins studied. Whole-cell lysates were obtained with RIPA buffer (50 mM Tris-HCl, pH 8.0, 1% Nonidet P-40, 150 mM NaCl, 0.5% sodium deoxycholate,

0.1% sodium dodecyl sulfate and 2 mM ethynediamine tetraacetic acid) supplemented with 1 mM dithiothreitol, protease and phosphatese inhibitor cocktails. Immediately, the cells were scraped, sonicated (four times for 4 s at 40 μm peak to peak) in Vibra Cell sonicator (Sonics & Materil INC.) and centrifuged at 12,000 rpm for 10 min at 4 °C to remove cell debris. The protein concentration of each sample was determined by the bicinchoninic acid protein assay. The lysates were denatured in sample buffer (0,125 mM Tris pH 6.8, 2% (w/v) sodium dodecyl sulphate, 100 mM dithiothreitol, 10% glycerol and bromophenol blue) and heated for 5 min at 95 ºC. In brief, equivalent amounts of proteins were separated by 4-10% (v/v) SDS-PAGE and transferred to PVDF membranes (Amersham Biosciences, Uppsala, Sweden). The membranes were incubated, overnight at 4 ºC, with the primary antibodies for: ciclo-oxigenase-2 (COX-2) (1:10000; Abcam, Cambridge, UK), inducible nitric oxide synthase (iNOS) (1:10,000; R&D Systems, Minneapolis, MN, USA), inhibitory kBα (IκBα), (1:1000; Cell Signaling Technologies, Danvers, USA), phospho-IκBα (p-IκBα) (1:1000; Cell Signaling Technologies, Danvers, USA), ubiquitin (1:500; provided by Dr. Fu Shang from Tufts University Boston, MA, USA) and microtubule-associated protein light chain 3 (LC3) (1:2000; Thermo Scientific, Rockford, IL, USA). The immunoreactive bands were visualized using the ECF substrate and the imaging system ThyphoonTM FLA 9000 (GE Healthcare). The bands densitometry was quantified using the Image Quant 5.0 software (Molecular Dynamics, Amersham Biosciences). The membranes were reprobed and tested for anti-actin antibody (1:20000; Millipore, Bedford, USA) to demonstrate that similar amounts of protein were loaded in the gels.

2.2.8. PROTEASOME CHYMOTRYPSIN-LIKE ACTIVITY

Raw 264.7 cells were suspended in 50 mM Tris–HCl buffer (pH 7.6) containing 1 mM ditiotreitol. Equal amounts of protein were incubated with the proteasome substrate (fluorogenic) Suc-Leu-Leu-Val-Tyr-AMC (Suc-LLVY-AMC). Enzymatic kinetic was measured with a temperature-controlled microplate fluorometric reader (37 °C). Excitation/emission wavelengths were 380/440 nm, and the results corresponding to 30 min, were analyzed.

2.2.9. HPLC-PDA-ESI/MS^n ANALYSIS

Polyphenols structural identification of *Fragaria vesca* leaves extracts was carried out on a Surveyor liquid chromatograph equipped with a PDA detector (Surveyor) and interfaced with a Finnigan LCQ Advantage Ion Max MS^n mass spectrometer (Thermo Fisher Scientific, Waltham, MA, USA) equipped with an API-ES ionization chamber. Separation occurred on a Spherisorb ODS-2 column (150 x 2.1 mm i.d.; particle size, 3 μm; Waters Corp., Milford, USA) and a Spherisorb ODS-2 guard cartridge (10 x 4.6 mm i.d.; particle size, 5 μm; Waters Corp., Milford, USA) at 25 ºC, using 1%

aqueous formic acid (v/v) (A) and methanol (B) as mobile phase. The gradient profile was 5–15% B (0–10 minutes), 15–25% B (10–15 minutes), 25–50% B (15–50 minutes), 50–80% B (50–60 minutes), 80–100% B (60–70 min) and an isocratic elution for 5 minutes, at a flow rate of 200 μL.min-1. The first detection was performed on a PDA detector in a wavelength range 200–450 nm, followed by a second detection in the mass spectrometer. Mass analyses were acquired in negative ion mode. The mass spectrometer was programmed to perform three consecutive scans: full mass (*m/z* 125–2000), MS^2 of the most abundant ion in the full mass and MS^3 of the most abundant ion in the MS^2. Source voltage was 4.7 kV and the capillary voltage and temperature were -7 V and 275 ºC, respectively. Nitrogen was used as sheath and auxiliary gas at 20 and 7 Finnigan arbitrary units, respectively. The normalized energy of collision was 49%, using helium as collision gas. Data treatment was carried out with XCALIBUR software (Thermo Scientific, Waltham, USA).

2.2.10. STATISTICAL ANALYSIS

The results are expressed as mean ± standard error of the mean (SEM). The data were analyzed using one-way analysis of variance (ANOVA), followed by Dunnett's post-hoc test or Student´s t-test. The differences between the means were considered significant for values of $p < 0.05$. The statistical analysis was performed using Prism 5.0 Software (GraphPad Software, San Diego, USA).

2.3. RESULTS AND DISCUSSION

2.3.1. EFFECT OF *FRAGARIA VESCA* LEAVES HYDROALCOHOLIC EXTRACT ON CELL VIABILITY, NO PRODUCTION AND NO SCAVENGING ACTIVITY

Fragaria vesca leaves has been used for the treatment of several inflammatory disorders (Fleming, 2000; Sarić-Kundalić et al., 2010). Hence, we studied the effect of the extract on NO production. NO, a bioactive free radical that has been implicated in many physiological functions, plays a critical role during inflammation and therefore constitutes a potential target for developing therapeutics for inflammatory diseases (Hofseth, 2008). Accordingly, it was evaluated the effect of non-cytotoxic concentrations (80 μg/mL and 160 μg/mL) of the extract (Figure 2.1-A) on NO production by macrophages, cultured in the presence or in the absence of LPS, a bacterial endotoxin known to easily induce NO production in macrophages. As expected, control cells (untreated) produced very low NO levels (0.35 ± 0.23 μM), while the culture medium of the cells treated with the inflammation inductor, LPS, for 24 hours showed an increase of NO content (28.64 ± 2.10 μM). Strikingly, in cells pre-treated with the plant extract, for both concentrations (160 μg/mL and 80 μg/mL), there was a significant decrease of nitrite production comparing to LPS treated cells (40% and 31% of inhibition, respectively). Cells incubation with the extract alone, in the absence of LPS, did not change the levels of nitrites when compared with control cells (Figure 2.1-B). Thus, the concentration that had the higher inhibitory effect (160 μg/mL) without cytotoxicity was selected to perform the succeeding experiments. To further elucidate the mechanism whereby the extract leads to a decreased production of nitrites, was investigated the NO scavenging capacity of the extract. Using SNAP as NO donor, *Fragaria vesca* extract promoted a significant decrease of nitrite content (23% of inhibition) in the culture medium (Figure 2.1-C). NO scavenging has protective effect for the cells, because excessive amounts of NO can react with superoxide radical (O2•−) to form peroxynitrite (ONOO−), a powerful oxidant with many harmful biological effects (Radi, 2013). The antioxidant properties of strawberry leaves were also previously observed in an extract from the leaves of garden strawberry, which retarded lipid oxidation from fish oil (Raudoniūtė et al., 2011). Another work using leaves of *Fragaria × ananassa* demonstrated that the extract has high antioxidant capacity being detected a linear correlation between phenolic content and oxygen radical absorbance capacity (Wang and Lin, 2000).

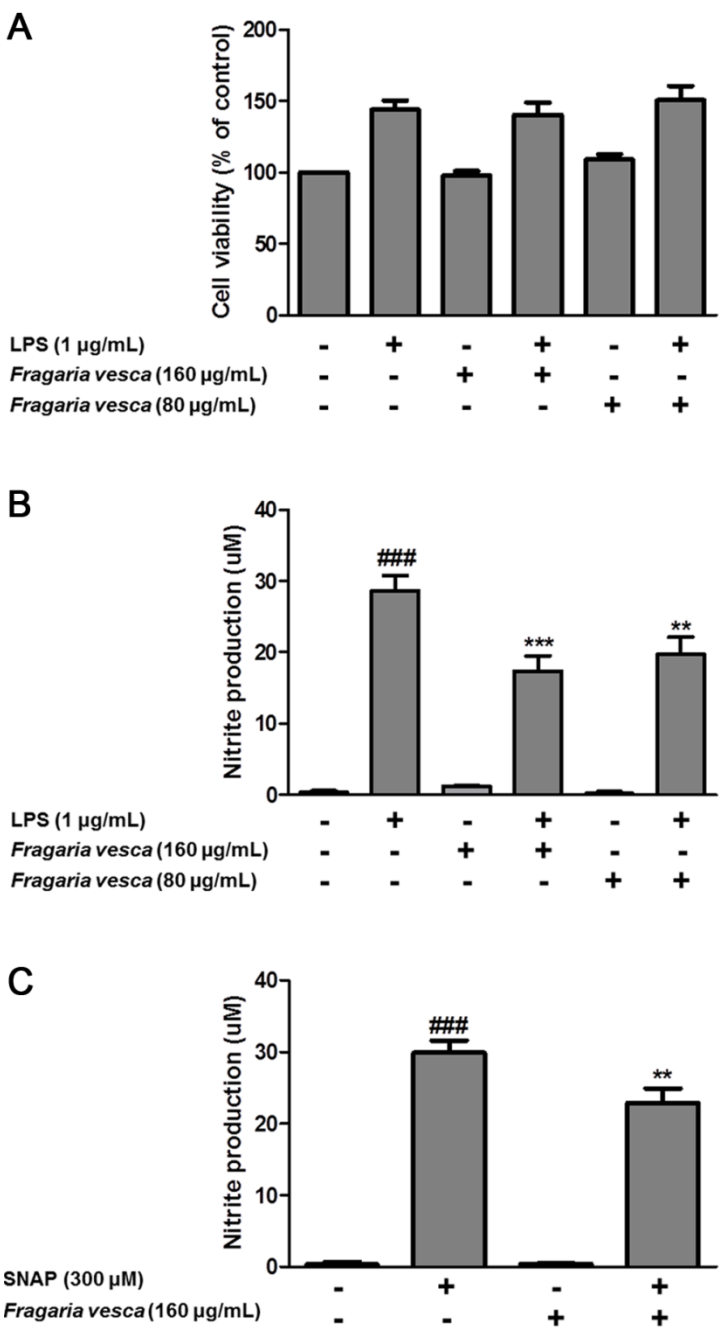

Figure 2.1 - *Fragaria vesca* leaves extract decreases nitrite production in macrophages stimulated with LPS and has NO scavenging activity. (A) Cell viability was assessed by the MTT reduction assay as described in 2.5. section. Groups treated only with the plant extract were compared with control group, while groups co-treated with LPS were compared with LPS alone. Data are presented as percentage of control (non-treated cells/medium); (B) Cells were pre-treated with plant extracts for 1 hour, followed by the addition of LPS (1µg/ml) for 24 hours. Cell culture supernatants were collected and nitrite concentration was measured by Griess reaction; (C) To evaluate the scavenging properties of the extract SNAP was used as NO donor. The mediums were collected after an incubation of 3 hours with SNAP and/or the extract and nitrite concentration was measured by the Griess reaction. Data represent the mean ± SEM from at least 3 independent experiments. ###p<0.001, significantly different from control; *** p<0.001 and **p<0.01, significantly different from LPS/SNAP, as determined by one-way ANOVA followed by Dunnet's post hoc test.

2.3.2. EFFECT OF *FRAGARIA VESCA* LEAVES HYDROALCOHOLIC EXTRACT ON INOS AND COX-2 PROTEIN EXPRESSION

The iNOS is responsible for the production of NO in response to inflammatory stimulus (Förstermann and Sessa, 2012). Thus, the inhibition of NO production in cells exposed to LPS and pre-treated with plant extract could be also due to a down-regulation of iNOS protein expression. By western blot, a significant iNOS increase in cells treated with LPS (299 ± 30% of control) was detected, however there were no differences between cells treated with LPS alone and cells co-treated with the extract (Figure 2.2). These results suggest that inhibition of NO production is not due to a decrease of iNOS expression. Macrophages release other pro-inflammatory mediators such as prostaglandin E_2 via the cyclooxygenase (COX) pathway during host-defense mechanism (Lee et al., 1992). COX has two main isoforms: COX-1 that is constitutively expressed in a wide variety of tissues; and COX-2 that is induced by inflammatory mediators such as LPS, interleukin-1 (IL-1) and tumor necrosis factor-alpha (TNF-α), in several cells and tissues (Rouzer and Marnett, 2009). COX-2 immunoreactivity was also visibly induced upon stimulation by LPS (Figure 2.2), however the pre-treatment with the extract did not inhibit LPS-induced COX-2 protein levels compared with LPS alone (1480 ± 499% of control).

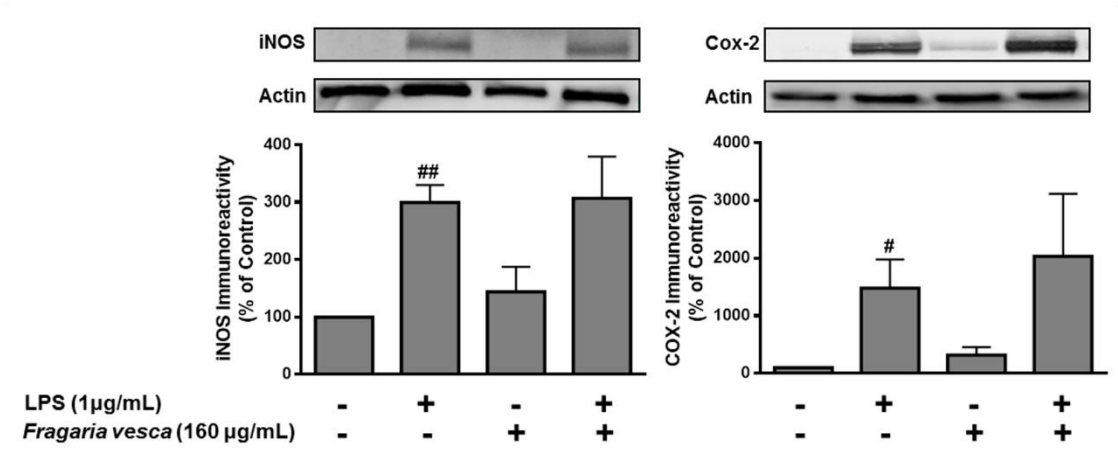

Figure 2.2 - *Fragaria vesca* leaves extract does not change iNOS and COX-2 protein content in Raw 264.7 macrophages. Cells were pre-incubated with plant extract for 1 hour and then were stimulated with LPS for 24 hours. Representative immunoblots are presented above the graphs; #p<0.05, ##p<0.01, significantly different from control, as determined by *one-way ANOVA followed by Dunnett's post hoc test.*

Evaluation of mRNA levels of iNOS and IL-1β (a pro-inflammatory cytokine that is secreted by macrophages activated by a number of pro-inflammatory stimuli, including LPS) was also performed; however the extract did not prevent the effect of LPS on mouse macrophages (Supplementary Figure 2.I). Taken together, the results obtained up to this point suggest that the anti-inflammatory effect of the extract relies on its NO scavenging property.

2.3.3. EFFECT OF *FRAGARIA VESCA* LEAVES HYDROALCOHOLIC EXTRACT ON NFKB PATHWAY

In several studies it has been shown that NFκB transcription factor enhances or represses the expression of genes implicated in inflammation, and their activation involves the phosphorylation of IκBα, which results in IκBα ubiquitination and degradation by the UPS (Skaug et al., 2009). As expected, in cells treated only with LPS (15 min) the protein levels of IκBα significantly decreased (29.62 ± 6.44% of control) while phosphorylated IκBα strongly increased (228.62 ± 18.25% of control), indicating that IκBα proteins are being phosphorylated and degraded by the proteasome. In cells co-treated with plant extracts, p-IκBα content increased (306.76 ± 16.01% of control) and even if were not statistically significant, the results suggest either an increase in the expression or a decrease in the degradation of IκBα (Figure 2.3).

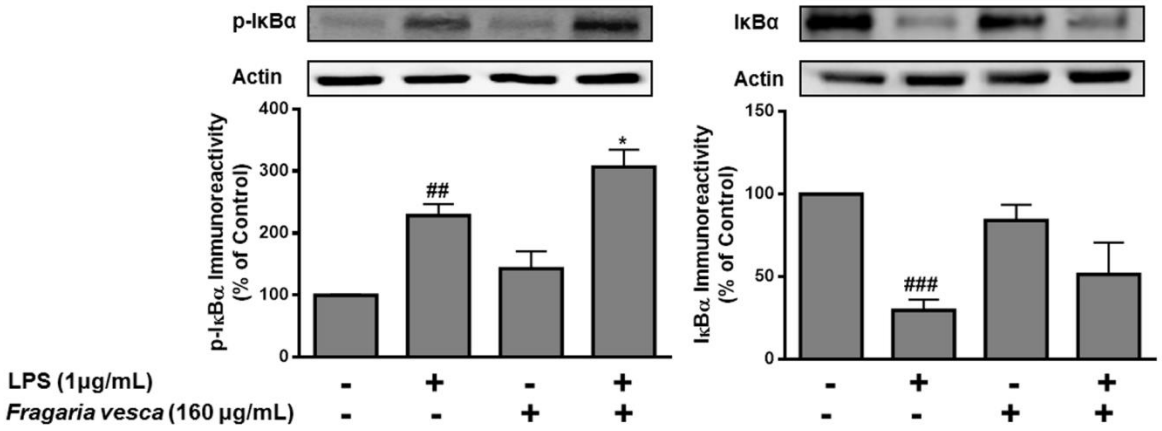

Figure 2.3 - Effect of *Fragaria vesca* leaves extract on LPS-activation of NFκB signaling. Cells were pre-incubated with plant extract for 1 hour and then were stimulated with LPS for 15 min. Data are presented as mean ± SEM of, at least, 3 independent experiments and are expressed as percentage of control. Representative immunoblots are presented above the graphs. ## p<0.01, ### p<0.001, significantly different from control; * p<0.05, significantly different from LPS as determined by *one-way ANOVA followed by Dunnett's post hoc test*.

2.3.4. EFFECT OF *FRAGARIA VESCA* LEAVES HYDROALCOHOLIC EXTRACT ON PROTEOLYTIC MECHANISMS

Since IκBα is a substrate of the proteasome, we hypothesized that an accumulation of IκBα in the cell could be consequence of the reduction of proteasome activity. To evaluate the effect of the extract in the proteasome activity the chymotrypsin-like activity of the proteasome was measured for 1, 3, 6, 12 and 24 hours after macrophages treatment with *Fragaria vesca* extract, and for all time points studied a decrease of the proteasome activity was observed (Figure 2.4-A). Since proteasome degradation of ubiquitinated substrates requires the removal of ubiquitin moieties from the proteins before their entrance into the proteasome catalytic core, a decrease in proteasome would lead to an

accumulation of polyubiquitinated proteins. Accordingly, an increase of ubiquitin conjugates after 24 hours of cells treatment with the plant extract was found (Figure2.4-B).

It is now well established the crosstalk between UPS and autophagy, suggesting a synchronized function between these proteolytic systems (Du et al., 2009). Recent studies also demonstrate that polyphenols consumption plays a role in autophagic process, most of them promoting an induction, which can be advantageous to prevent ageing diseases, like cancer and neurodegeneration (Pallauf and Rimbach, 2013). Therefore, we evaluated the conversion of LC3-I to LC3-II, which has been widely used as a hallmark of autophagy and a common experimental strategy to evaluate autophagic activity. LC3-I is a cytoplasmic protein, however upon autophagy induction it is conjugated with phosphatidylethanolamine in the autophagic membranes to form LC3-II, and this conversion is easily identified by the increased mobility on sodium dodecyl sulphate-polyacrylamide gel electrophoresis (SDS-PAGE). Curiously *Fragaria vesca* extract increased the conversion of LC3-I into LC3-II for all time points studied, with a more prominent effect after 6 hours (Fig. 4C), strongly suggesting that the extract is activating autophagy. However, this data has to be analyzed prudently. Indeed the increase in LC3-II may also be a consequence of an interruption of the autophagic flux (for example when the lysosomal proteases are inhibited or if the autophagosome-lysosome fusion is blocked). Therefore, at this stage, our data demonstrates, for the first time, that *Fragaria vesca* extract modulates autophagy, but the mechanism underlying such effect needs further clarification.

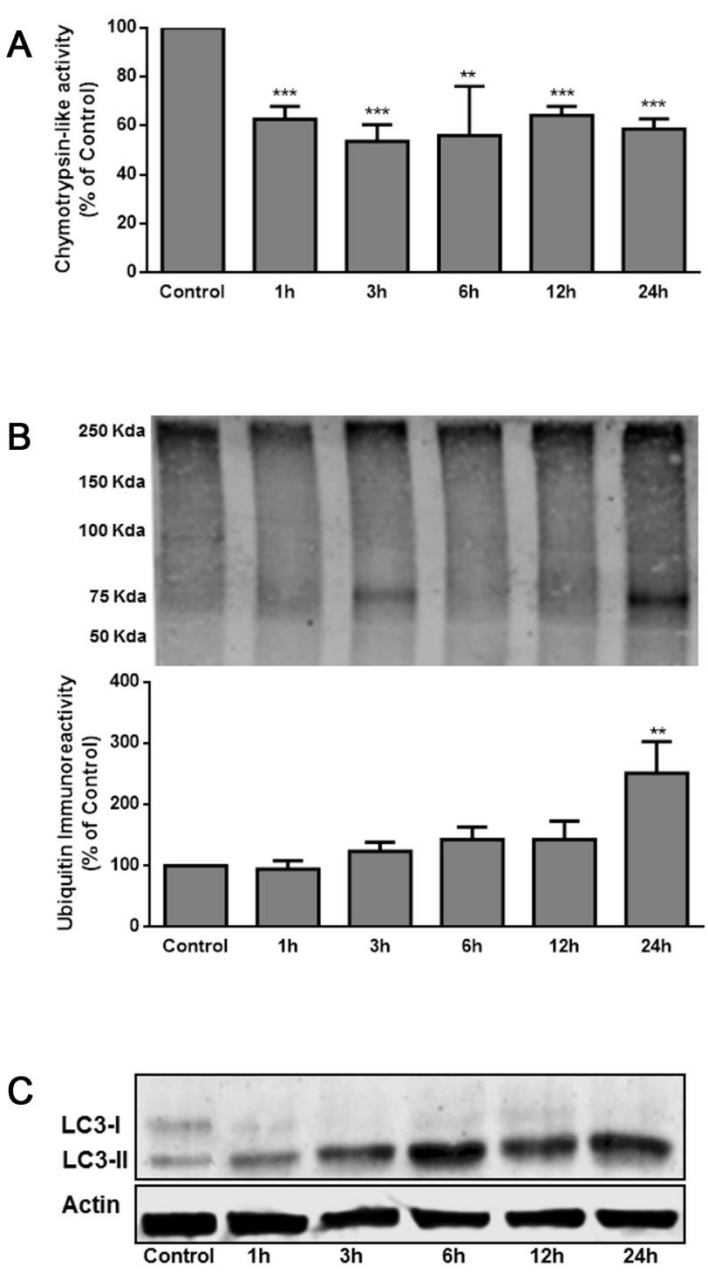

Figure 2.4 - *Fragaria vesca* leaves extract decreases proteasome activity, increases ubiquitin conjugates and increases the conversion of LC3-I into LC3-II. Cells were treated with plant extract for 1, 3, 6, 12 and 24 hours and it was evaluated the (A) chymotrypsin-like activity of the proteasome and (B) the ubiquitin conjugates by western blot using an antibody against ubiquitin; Data are presented as mean ± SEM of, at least, 3 independent experiments and are expressed as percentage of control. Representative immunoblots are presented above the graphs. ** p<0.01, ***p<0.001 significantly different from control as determined by *one-way ANOVA followed by Dunnett's post hoc test*. (C) Cells were treated with plant extract for 1, 3, 6, 12 and 24 hours and the blot was performed for a protein involved in autophagy, LC3. A representative immunoblot of three independent experiments is shown.

2.3.5. PHYTOCHEMICAL CHARACTERIZATION

HPLC-PDA phenolic profiles were recorded at 280 nm (Figure 2.5). The hydroalcoholic extract evidenced the presence of proanthocyanidins, flavonols, and ellagic acid and its derivatives (Figure 2.5-A). Twenty compounds were tentatively identified by HPLC-PDA-ESI/MS^n (Table 2.1).

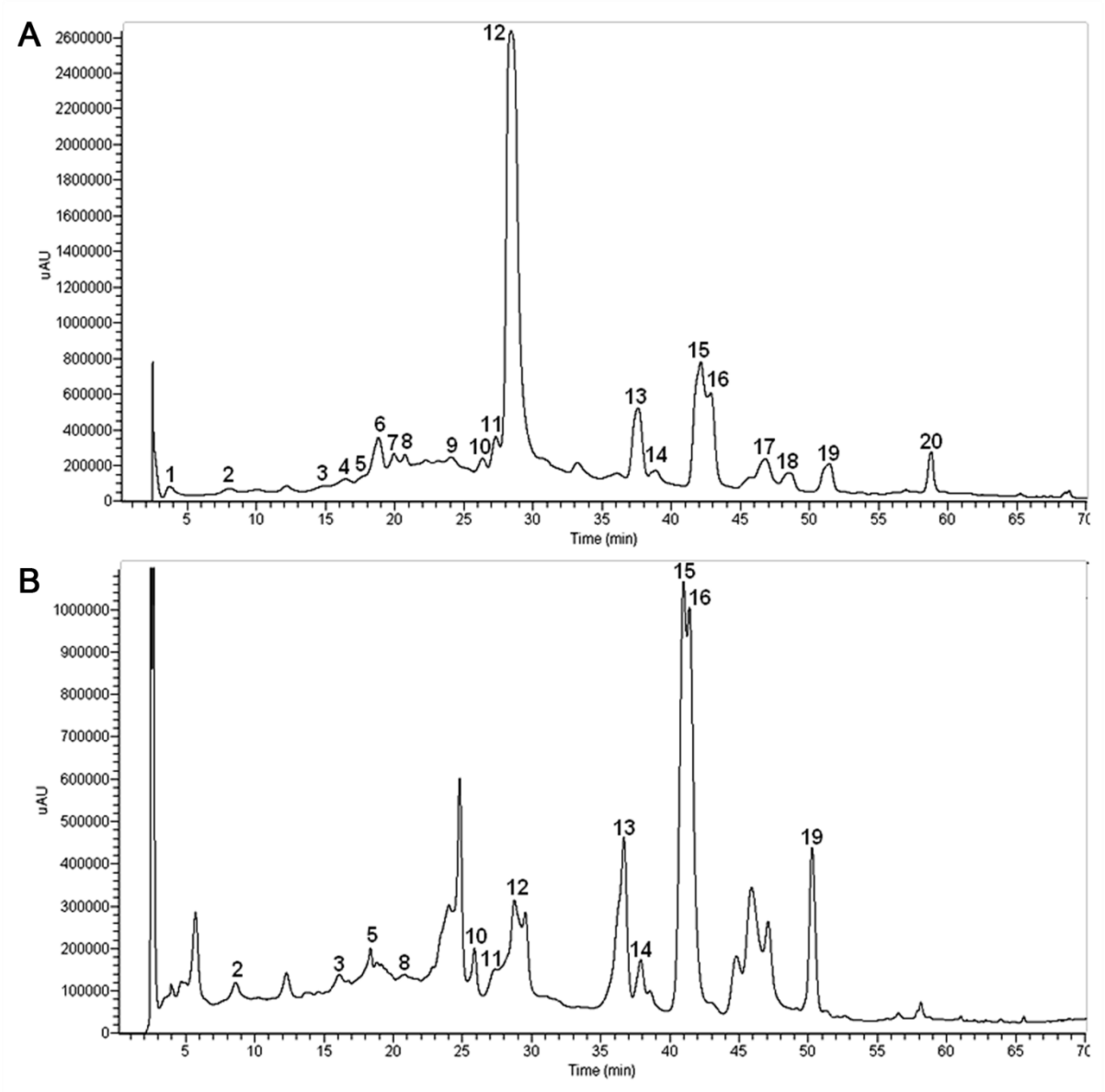

Figure 2.5 - HPLC polyphenolic profile of *Fragaria vesca* leaves extracts, recorded at 280 nm. The identification of the peaks is shown in Table 1. (A) Hydroalcoholic extract; (B) Infusion.

Table 2.1 - UV–vis and MS spectra, and identification of the compounds of *Fragaria vesca* leaves extracts.

Peak	*R*t (min)	λ_{max} (nm)	$[M-H]^-$ (*m/z*)	MS^2 *m/z*[1]	MS^3 *m/z*[1]	Compound tentatively identified
1	3.65	235, 247, 254(sh)	783	481, **301**, 275	**257**	Bis-HHDP-hexose
2	8.09	235, 248, 254(sh)	783	481, **301**, 275	247, **229**	Bis-HHDP-hexose
3	16.47	246, 278	577	451, **425**, 407, 289	**407**, 273	(Epi)catechin-(epi)catechin
4	18.82	245, 278	849	723, 696, 679, 561, **559**, 407	541, **433**, 407, 300, 280, 245	(Epi)catechin-(epi)catechin-(epi)afzelechin
5	19.10	246, 278	561	543, **435**, 425, 407, 289, 329	417, **329**, 273, 271, 219, 179, 175	(Epi)afzelechin-(epi)catechin
6	19.92	235, 247, 275(sh)	933	**451**	433, 408, 407, 395, 377, 328, 327, **301**	Castalagin/Vescalagin
7	20.75	272	833	707, 561, **543**, 434, 289	525, 436, 417, **407**, 309, 271, 255, 203	(Epi)catechin-(epi)afzelechin-(epi)afzelechin
8	22.11	236, 247, 272(sh)	933	631, **451**, 433, 301	405, **351**, 335, 307, 301, 285	Castalagin/Vescalagin
9	24.16	240, 246, 269(sh), 365(sh)	757	**595**, 461	461, 447, **301**	Ellagic acid derivative
10	26.35	247, 270(sh), 290(sh), 351	639	**463**, 301	343, **301**	Quercetin hexosyl-glucuronide
11	27.26	240, 247, 285(sh)	935	**633**, 301	597, **301**	Casuarictin/Potentillin
12	28.41	240, 250	1869	**1567**, 1265, 1103, 933, 915, 898, 897, 631	1265, 962, **935**, 933, 897, 633, 631, 613	Sanguiin H-6/Agrimoniin
13	37.58	255, 267sh, 295(sh), 353	623	459, **301**	273, 257, 229, **179**, 151	Quercetin glucuronyl-rhamnoside
14	38.89	247, 270(sh), 290(sh), 355	595	461, 447, **301**	**271**, 257	Ellagic acid derivative
15	42.16	240, 246(sh), 264, 295sh, 349	607	321, **285**	267, **257**, 241, 229, 213, 151	Kaempferol glucuronyl-rhamnoside
16	42.86	258, 295sh, 354	477	**301**	273, **179**, 151	Quercetin glucuronide
17	46.80	237, 253, 305(sh), 350(sh), 366	301	283, **257**, 229	-	Ellagic acid
18	48.55	246, 264, 295(sh), 346	461	**285**	267, **257**, 241, 229, 213	Kaempferol glucuronide
19	51.41	236, 249, 262 (sh), 290sh, 359 (sh), 375	461	446, **315**	**300**	Methyl ellagic acid rhamnoside
20	58.79	246, 266, 296(sh), 313	593	447, **285**	267, **257**, 229, 151	Kaempferol coumaroyl-hexoside

[1] The most abundant ions are shown in bold

Proanthocyanidins: Peaks **3**-**5** and **7** occur as minor polyphenols and showed UV absorption maxima and spectral profiles of flavan-3-ols. The molecular ions $[M-H]^-$ at *m/z* 561, 577, 833 and 849 correspond to (epi)afzelechin- and (epi)catechin-based proanthocyanidin dimers and trimers, respectively, MS^2 presenting signals with a typical fragmentation pattern of flavan-3-ol derivatives, according to Correia et al. (2007). Peaks **3** and **5** with $[M-H]^-$ at *m/z* 577 and 561 were identified as dimers differing 16 amu between them. These compounds exhibited, in MS^2, signals at *m/z* 425 (-152 from peak **3**, and -136 amu from peak **5**), which correspond to the Retro Diels-Alder (RDA) fission of flavan-3-ols with the B ring di- and mono-hydroxylated, respectively. To corroborate this hypothesis a fragment at *m/z* 407 (-170 and -154 amu for peaks **3** and **5**, respectively) was also observed, which matches the RDA fragmentation and a loss of water. Signal at *m/z* 289 (-288 and -272 amu) resulting of an interflavanic cleavage, suggests that an (epi)catechin unit exists in both compounds, however different units were lost. This fragmentation pattern has led to the identification of the (epi)catechin-(epi)catechin (peak **3**) and (epi)afzelechin-(epi)catechin (peak **5**). Peaks **4** and **7** presented $[M-H]^-$ at *m/z* 849 and 833, which differ 16 amu, the same difference being registered for main signals of their

fragmentation, at *m/z* 559 and 543, respectively, both resulting of a 290 amu lost, probably a (epi)catechin unit. MS^3 of those ions exhibited the fragment at *m/z* 407 ($[M-H-290-152]^-$ and ($[M-H-290-136]^-$), corresponding to the RDA fission of a di- and mono-hydroxylated B ring, for peak **4** and **7**, respectively. These data suggest that these compounds are trimmers, with two units of (epi)catechin and one of (epi)afzelechin (peak **4**) or one (epi)catechin and two (epi)afzelechin (peak **7**).

Flavonols: Six quercetin and kaempferol derivatives were detected (peaks **10**, **13**, **15**-**16**, **18**, **20**). These compounds were characterized on the basis of their UV spectra profiles and absorption maximum, at 352±1 nm for quercetin glycosides and 346±1 nm for kaempferol glycosides, and by MS spectra, aglycone fragments occurring at *m/z* 301 (quercetin) and 285 (kaempferol). Peak **10** had a molecular ion at *m/z* 639 with a MS/MS fragmentation ion at *m/z* 463 (-176 amu), corresponding to the loss of a glucuronyl group and a MS3 fragment of 301 (-162 amu), which matches the loss of a hexose residue. The spectral data are consistent with a quercetin hexosyl-glucuronide. Peak **13** exhibited a $[M-H]^-$ of 623, leading to MS^2 fragments of 301 (-322 amu) and 459 (-164 amu), which corresponds to the loss of glucuronyl-rhamnoside and rhamnoside residues, respectively. Hence, this compound was tentatively identified as quercetin glucuronyl-rhamnoside. Peak **16** presented a molecular ion of 447, which lead to a MS^2 spectrum with a fragment at *m/z* 301 (-176 amu), corresponding to the loss of a glucuronyl residue. The purposed structure for this compound is quercetin glucuronide. Peaks **15**, **18** and **20** were identified as kaempferol derivatives. Peak **15** showed a $[M-H]^-$ ion at *m/z* 607 and the loss of a glucuronyl-rhamnoside residue (-322 amu), having been characterized as kaempferol glucuronyl-rhamnoside. Peak **18** exhibited a molecular ion of 461, and a MS2 fragment at *m/z* 285 (-176 amu), corresponding to the loss of a glucuronyl residue. This compound was identified as kaempferol glucuronide. Peak **20** eluted later, showing that it was more lipophilic, and presented a UV spectrum characteristic of kaempferol *p*-coumaroyl glucosides, indicating that the sugar moiety on the flavonol was acylated with a hydroxycinnamic acid (most probably p-coumaric acid). The MS analysis showed ions at *m/z* 593 ($[M-H]^-$) and MS^2 fragments at *m/z* 447 (loss of a coumaroyl residue) and 285 (loss of a coumaroyl hexosyl residue). This peak was tentatively identified as kaempferol *p*-coumaroyl glucoside, previously reported in strawberries (Navindra P. Seeram et al., 2006).

Ellagic acid and derivatives: These compounds (peaks **1**-**2**, **6**, **8**-**9**, **11**-**12**, **14**, **17** and **19**) were identified on basis of their UV and MS spectra. In the mass spectra of most of these compounds, a signal at *m/z* 301 matches to that of ellagic acid. Peaks **1** and **2** presented characteristic mass spectra, with the molecular ion at 783, and MS^2 fragments at *m/z* 481 ($[M-H-302]^-$), 301, corresponding to ellagic acid residue, as a result of spontaneous lactonization of hexahydroxydiphenoyl (HHDP) fragment after cleavage and a characteristic fragment of this ellagic acid residue cleavage, at *m/z* 275 (Arapitsas et al., 2007). These peaks were both identified as bis-HHDP-glucose isomers

(pedunculagin) according to fragmentation pattern proposed by Simirgiotis et al. (2010) Peaks **6** and **8** showed a $[M-H]^-$ ion at *m/z* 933. Peak **8** exhibited a MS^2 fragments at *m/z* 451 from the cleavage of tri-galloyl unit and spontaneous lactonization, at *m/z* 631 from the loss of the HHDP group and at *m/z* 301 attributed to ellagic acid, such as the fragmentation pattern referred by Hager et al. (2008). Peak **6** showed a similar fragmentation profile as peak **8**, which is in accordance with previous findings described in the literature for this species (Del Bubba et al., 2012). Therefore, these compounds were identified as isomeric forms of castalagin/vescalagin. Peaks **9** and **14** showed $[M-H]^-$ ions at *m/z* 757 and 595, respectively, differing 162 amu between them. Both compounds have UV spectra profiles similar to peaks **6** and **8**, and one fragment at *m/z* 301, which matches with the presence of an ellagic acid unit. The major fragment at *m/z* 595 $[M-162]^-$ in MS^2 of peak **9** suggests the additional presence of a hexosyl group in this compound. Despite the fragmentation profile being common to two peaks, it has not been possible to establish their structure. Therefore peaks **9** and **14** were identified as ellagic acid derivatives, peak **9** probably containing more one hexosyl unit than peak **14**. Peak **11** showed a molecular ion at *m/z* 935 and MS^2 fragments at *m/z* 633(-302 amu) and 301 originated from lactonization of fragment 302. On the basis of this information and according to Hager et al. (2008) the compound was identified as casuarictin or potentillin (ellagitannin monomers). Peak **12**, which was the major compound of the extract, presented a mono charged molecular ion at *m/z* 1869, which originated, in MS^2 a fragment at *m/z* 1567 (-302 amu, a loss of an HHDP unit), 1265 (-302 amu, a further loss of HHDP), 1103 (-162, a loss of a glucosyl group), 933 (-170 amu, a loss of a gallic acid) and 631 (-302 amu, a loss of HHDP). The third order fragmentation pattern of fragment *m/z* 1567 originated a peak at *m/z* 935 resulting from the loss of galloyl-HHDP glucose moiety (Hager et al., 2008). On the basis of these fragmentation patterns and other results previously published, we may suggest that this compound is an isomeric form of sanguiin H-6/agrimoniin (Vrhovsek et al., 2012). The similar mass spectra fragments of these ellagitannins (Hanhineva et al., 2008), together with the absence of commercial available standards limit the identification of this peak. Peak **17** presented a retention time, and UV and MS spectra similar to that of ellagic acid reference. A molecular ion at *m/z* 301 and its fragments at *m/z* 283, 257 and 229 confirmed the identity of ellagic acid (Mullen et al., 2003). Peak **19** exhibited a molecular ion at *m/z* 461, and MS^2 fragments at *m/z* 315 (-146 amu) and 446 (-15 amu), which suggests the loss of a deoxyhexose and a methyl group, respectively. In the MS^3 the fragment at *m/z* 300 $[M-H-146-15]^-$, which possibly matches the ellagic acid molecule, suggests that the methyl group must be linked to the ellagic acid (Sun and Chen, 2012). The putative structure for this compound is methyl ellagic acid rhamnoside.

Ethnopharmacological studies report the use of *Fragaria vesca* infusion for the treatment of inflammation-related diseases and in this study, phytochemical analysis revealed that the

hydroalcoholic extract and the infusion have several compounds in common, predominantly the flavonoids (peaks **10**, **13**, **15**, **16** and **19**) (Figure 2.5). The antioxidant and anti-inflammatory properties of flavonoids are well-known (Kumar and Pandey, 2013; Reddy et al., 2014). As flavonoids may inhibit NO production through modulation of pro-inflammatory signaling pathways or by NO scavenging (Duarte et al., 2014), these compounds may be the responsible for the NO scavenging activity of the extract. Further work is required to evaluate the contribution of flavonoids on this effect.

Apart from the anti-inflammatory properties, ethnopharmacological studies also report the use of *Fragaria vesca* in cancer treatment. The impairment of UPS has been implicated in different diseases (Schwartz and Ciechanover, 2009), including cancer (Hoeller and Dikic, 2009) and inflammatory-related disorders (Wang and Maldonado, 2006). Some polyphenols have been referred as inhibitors of the chymotrypsin-like activity of proteasome, namely ester bond-containing polyphenols such as(-)-epigallocatechin-3-gallate (Nam et al., 2001) and pentagalloylglucose (Chen and Lin, 2004) and the flavonoids - quercetin and apigenin (Chen et al., 2005). Reinforcing the role of proteasome as a therapeutic target in oncology, recently the proteasome synthetic inhibitor, bortezomib, has been investigated for cancer therapy and was approved for clinical use in patients with multiple myeloma (Chen et al., 2011). However, natural proteasome inhibitors with similar pharmacological activity and with less toxicity are strongly desired.

2.4. CONCLUSIONS

This work evaluated the biological effects and polyphenol composition of a hydroalcoholic extract from *Fragaria vesca* leaves. The traditional preparation (the infusion) contained several polyphenols also identified in the hydroalcoholic extract, including the ellagitannin sanguiin H-6/agrimoniin isomer and glucuronide derivatives of quercetin and kaempferol.

In traditional medicine, *Fragaria vesca* leaves have been used in the treatment of pathologies with a strong inflammatory component. This study concludes that *Fragaria vesca* extract decreases NO levels, one of the most relevant mediators of the inflammatory response. However, we do not find changes in signaling molecules upstream iNOS expression, suggesting that the NO decrease was probably due to a direct scavenging effect. Additionally, ethnopharmacological reports also ascribe to *Fragaria vesca* leaves anticancer properties. These properties could be related to the effect of the extract on proteolytic mechanisms that are currently considered promising molecular targets in cancer therapy.

Herein we disclose the molecular action mechanism of *Fragaria vesca* leaves and provide evidences to understand its therapeutic effects, thus supporting the traditional use of this plant for the treatment of inflammatory disorders. Further experiments are required to evaluate the effect of the extract in the field of oncology, with special focus in the identification of the molecules responsible for proteolysis modulation, as well as the putative cellular mechanisms of action behind these effects.

ACKNOWLEDGMENTS

This research was supported by FEDER/COMPETE (FCOMP-01-0124-FEDER-011096) and FCT, through the projects PTDC/SAU-FCF/105429/2008, PEst-OE/SAU/UI0177/2011 and PEst-C/SAU/LA0001/2013-2014 and the Ph.D. fellowship SFRH/BD/72918/2010. We also acknowledge the Node CEF/UC integrated in the National Mass Spectrometry Network (RNEM) of Portugal, for MS analyses and Dr. Luis Rodrigues for kindly supplied the image of *Fragaria vesca* for the graphical abstract.

SUPPLEMENTARY DATA

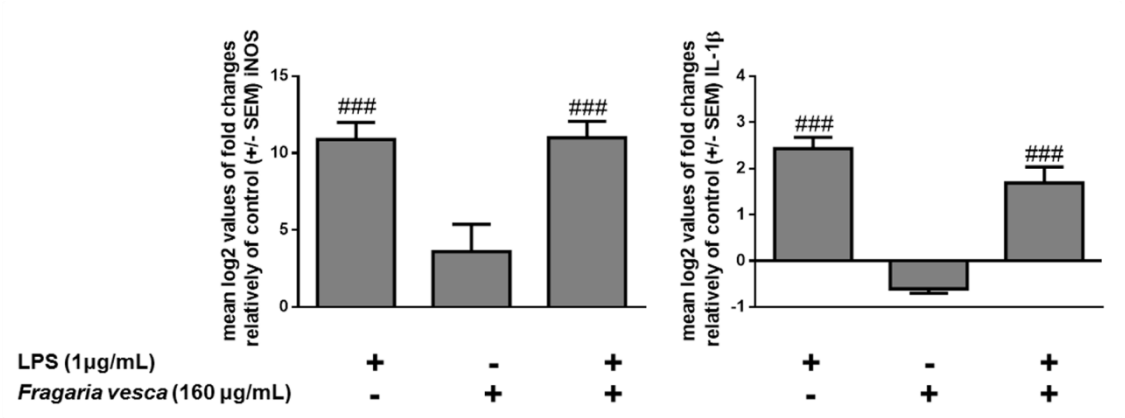

Supplementary Figure 2.I - *Fragaria vesca* leaves extract does not change iNOS and IL-1β mRNA levels in Raw 264.7 macrophages. Cells were treated with plant extract for 1 hour and then were stimulated with LPS for 6 hours. Data are presented as mean ± SEM of, at least, 3 independent experiments and are expressed as percentage of control. ###p<0.001, significantly different from control, as determined by one-way ANOVA followed by Dunnett's post hoc test.

Chapter 3

Chemical characterization and cytotoxic potential of an ellagitannin-enriched fraction from *Fragaria vesca* leaves

Joana Liberal, Gustavo Costa, Anália Carmo, Rui Vitorino, Carla Marques, Maria Rosário Domingues, Pedro Domingues, Ana Cristina Gonçalves, Raquel Alves, Ana Bela Sarmento-Ribeiro, Henrique Girão, Maria Teresa Cruz, Maria Teresa Batista

Arabian Journal of Chemistry

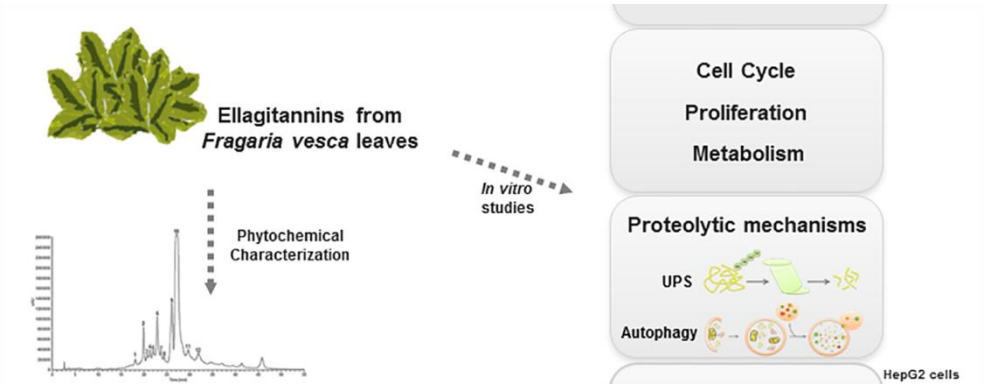

ABSTRACT

The hepatocellular carcinoma, a primary malignancy of the liver, has a very poor prognosis and a lower survival rate. Moreover, the inefficacy of conventional therapies emphasizes the importance of discovering new bioactive compounds. Several studies clearly state that plant-derived polyphenols, namely ellagitannins, have several health benefits. *Fragaria vesca* leaves contain high amounts of polyphenols, being especially rich in ellagitannins. Therefore, this study aimed to characterize an ellagitannin-enriched fraction (EEF) from *Fragaria vesca* leaves and to unveil the anticancer potential of this fraction on human hepatocellular carcinoma cells.

The analysis of EEF by HPLC-PDA-ESI/MS^n allowed the detection of 12 ellagitannins. The cell viability of both EEF and crude extract was determined after 24 h of cells treatment and the half-maximal inhibitory concentration (IC_{50}) was evaluated. The IC_{50} of the EEF (113 μg/mL) was about 6 times lower than the IC_{50} of the crude extract (690 μg/mL). Furthermore, EEF induced cell cycle arrest at G2/M checkpoint and decreased cell proliferation in a dose-dependent way. This fraction also induced an accumulation of LC3-II protein through blockage of autophagic flux, and inhibited chymotrypsin-like activity of 26S proteasome. These results showed, for the first time, that EEF from *Fragaria vesca* leaves inhibits both, autophagic and ubiquitin-proteasome system pathways, two main intracellular protein degradation systems that are targets for anticancer therapies. Additionally, a proteomic analysis allowed the identification of 914 proteins, among which 133 were modulated after cells treatment with EEF, most of them related to metabolic pathways. Overall, this study shows that the EEF from *Fragaria vesca* leaves decreased cell proliferation, inhibited the proteolytic mechanisms and modulated the metabolic pathways of the cell.

Additionally this study points out *Fragaria vesca* as a source of valuable molecules with anticancer potential, suggesting that ellagitannins, the polyphenols identified in this fraction, could be useful in the development of new fine-tuned therapeutic strategies against carcinogenesis.

Keywords

Cancer; HepG2; Proteolytic pathways; Proteome; Cell proliferation; Cell cycle

3.1. INTRODUCTION

Liver cancer is the sixth most frequent neoplasia and the third cause of cancer-related death worldwide (Center and Jemal, 2011). Hepatocellular carcinoma accounts for between 85% and 90% of primary liver cancers and generally occurs in patients with underlying chronic liver disease, especially with chronic hepatitis B virus (El-Serag and Rudolph, 2007). Hepatocellular carcinoma has a very poor prognosis because diagnosis is usually made at an advanced stage, when treatment options are limited and less effective (Lin et al., 2012). Therefore, the discovery of new bioactive molecules to overcome the inefficacy and the side effects of conventional therapies is still a hotspot of anticancer research.

Cancer cells are characterized by unbalanced control of cellular proliferation and an immortalized life span (Feitelson et al., 2015). Accordingly, any molecule capable of suppressing cancer cell proliferation may be valuable as a potential chemopreventive/chemotherapeutic agent. Several polyphenols have shown the capacity to block the initiation of the carcinogenic process and to suppress both promotion and progression of cancer (Ramos, 2008). Apart from the well-known antioxidant properties of polyphenols, their role on cell growth (Kampa et al., 2007), apoptosis (Fresco et al., 2010) and cell proliferation (Giovannini and Masella, 2012) is also well established, being those effects usually cell type- and dose-dependent.

Ellagitannins (hydrolysable tannins) are bioactive polyphenols composed by moieties of hexahydroxydiphenoyl (HHDP) esterified to a sugar, usually the glucose, that release ellagic acid upon hydrolysis (Aguilera-Carbo et al., 2008). They are distributed in the plant kingdom (Okuda et al., 1993) and are commonly found in herbal preparations (Quideau, 2009), fruits (Aaby et al., 2007) and beverages (Lee and Talcott, 2002). Multiple biological activities have been ascribed to ellagitannins, namely antioxidant, antiatherosclerotic, anti-inflammatory and antiviral (Ascacio-Valdes et al., 2011). Furthermore, there is a wealth of information indicating the potent anticancer activities of ellagitannins (Auzanneau et al., 2012; Sartippour et al., 2008). Accordingly, some ellagitannins were able to inhibit cell proliferation, which was in part due to their ability to arrest cell cycle (Cho et al., 2015; Vassallo et al., 2013). Additionally, these molecules have been shown to induce apoptotic cell death in different cell lines, modulating several molecular pathways and the expression of apoptotic regulators (Li et al., 2013; Wang et al., 2013).

Fragaria vesca L., commonly known as wild strawberry, is an herbaceous perennial plant that is primarily valued for its fruits, the strawberries. However, the leaf has a great pharmacological potential considering traditional uses (Camejo-Rodrigues et al., 2003; Neves et al., 2009) and the presence of high amounts of bioactive compounds (Buricova et al., 2011; Ivanov et al., 2015). In fact, our group previously demonstrated that a crude extract obtained from *Fragaria vesca* L. was

enriched in polyphenols, namely ellagitannins, proanthocyanidins, and quercetin and kaempferol glucuronide derivatives, being ellagitannins the main phenolic compounds. In addition, we proved that this extract modulated the activity of the proteolytic mechanisms of the cells, the ubiquitin-proteasome system (UPS) and autophagy-lysosomal system (Liberal et al., 2014). These processes are responsible for the degradation of dysfunctional and damaged cellular components and their dysregulation is implicated in wide a range of pathological conditions (Vilchez et al., 2014). Moreover, given their association with the carcinogenic process, these proteolytic pathways constitute privileged targets for anticancer therapies (Driscoll and Chowdhury, 2012).

In this study, we aimed to obtain an ellagitannin-enriched fraction (EEF) from the crude extract previously reported and to further explore the molecular mechanisms behind EEF bioactivity. Briefly, the polyphenols of this fraction were characterized and its cytotoxic effect on human hepatocellular carcinoma cells (HepG2) was evaluated. Then, we investigated the effect of EEF on cell proliferation, cell cycle and cell death, as well as its effect in the proteolytic mechanisms. Furthermore, a proteomic based approach was used to disclose differentially expressed proteins following cell treatment with this fraction, evaluating the main cellular processes modulated by EEF.

3.2. MATERIAL AND METHODS

3.2.1. MATERIALS

Fetal calf serum was obtained from GIBCO (Paisley, UK). Protease and phosphatase inhibitor cocktail tablets were acquired from Roche (Basel, Switzerland). Polyvinylidene fluoride (PVDF) membranes were obtained from Millipore Iberica (Madrid, Spain) and acrylamide from BioRad (Hercules, CA, USA) The following antibodies were used: anti-ubiquitin, clone P4D1 (Biolegend, San Diego, CA, USA), anti-microtubule-associated protein light chain 3 (LC3) (Cell Signaling Technologies, Danvers, MA, USA), anti-insulin-like growth factor-binding protein 1 (IGFBP1) (Abcam, Cambridge, UK), anti-fatty acid synthase (FAS) (Cell Signaling Technologies, Danvers, MA, USA) and anti-β-tubulin antibody (Sigma Chemical Corporation, St. Louis, MO, USA). Enhanced chemifluorescence (ECF) substrate, anti-mouse and anti-rabbit alkaline phosphatase-conjugated secondary antibodies were purchased from GE Healthcare (Chalfont St. Giles, UK). Suc-Leu-Leu-Val-Tyr-AMC (Suc-LLVY-AMC) was from Enzo Life Sciences (Farmingdale, NY, USA). Click-iT® EdU Alexa Fluor® 488 Flow Cytometry Assay Kit was obtained from Molecular Probes, Invitrogen (Eugene, OR, USA) and propidium iodide (PI) with RNase solution and annexin V-fluorescein isothiocyanate (FITC)/PI from Immunostep (Salamanca, Spain). All other reagents were acquired from Sigma Chemical Corporation (St. Louis, MO, USA) and Merck (Darmstadt, Germany).

3.2.2. PLANT MATERIAL

Fragaria vesca wild plants (with flowers and fruits) were sustainably collected from Granja de Figueira do Lorvão, Penacova, Portugal (May, 2011). A voucher specimen (ID-180611) was deposited at the Herbarium of Medicinal Plants, Faculty of Pharmacy, University of Coimbra.

The leaves were separated from stems, flowers and fruits and dried in a drying oven during 24 h, at 30 ºC with forced air circulation. They were powdered and sieved before extraction.

3.2.3. EXTRACT FRACTIONATION

A hydroalcoholic extract from *Fragaria vesca* leaves was prepared as previously described (Liberal et al., 2014). Briefly the dry and powdered leaves were treated with dichloromethane (2 times) and the extraction was performed with ethanol (2 times) and 50% aqueous ethanol (3 times) at room temperature using an Ultra-Turrax homogenizer for 5 min at 8000–9500 rpm. The ethanol and hydroalcoholic extracts were combined and concentrated on a rotatory evaporator to a small volume and lyophilized. This extract was stored at -20 °C until the time for testing.

The lyophilized extract (3 g) was recovered with 50% aqueous methanol and fractionated by gel chromatography on a Sephadex® LH-20 (Sigma-Aldrich) column (25 cm × 5 cm) by elution successively with 50% (2 L) and 75% aqueous methanol (2.5 L) and 70% aqueous acetone (1 L).

All the fractionation process was monitored by high-performance liquid chromatography (HPLC) providing 8 major fractions: F1 (174 mL; phenolic acids), F2 (320 mL; phenolic acids and flavonoids;), F3 (710 mL; flavonoids), F4 (1198 mL; gallotannins and ellagic acid), F5 (704 mL; proanthocyanidins and ellagic acid), F6 (1087 mL; proanthocyanidins and ellagic acid), F7 (383 mL; proanthocyanidins) and F8 (946 mL; ellagitannins). The polyphenol-rich fractions were then taken to dryness under reduced pressure on a rotatory evaporator, at 40 ºC, lyophilized and weighted in sterilized and humidity-controlled conditions.

Since ellagitannins were one of the main phenolic compounds of the hydroalcoholic extract, an EEF was selected to evaluate the effect of these polyphenols in the hepatocellular carcinoma cell line. Ellagitannins were only identified in this fraction, which was obtained with 70% aqueous acetone (yield of 14% of 100 g of the *Fragaria vesca* extract). The yields of the remaining fractions were the following: F1 – 48%, F2 – 19%, F3 – 8%, F4 – 3%, F5 – 3%, F6 – 3% and F7 – 1%.

3.2.4. HPLC-PDA-ESI/MS^N ANALYSIS

Polyphenols structural identification of EEF was carried out on a Surveyor liquid chromatograph equipped with a PDA detector (Surveyor) and interfaced with a Finnigan LCQ Advantage Ion Max MS^n mass spectrometer (Thermo Fisher Scientific) equipped with an API-ES ionization chamber. Separation occurred on a Spherisorb ODS-2 column (150 x 2.1 mm i.d.; particle size, 3 μm; Waters Corp.) and a Spherisorb ODS-2 guard cartridge (10 x 4.6 mm i.d.; particle size, 5 μm; Waters Corp.) at 25 ºC, using 2% aqueous formic acid (v/v) (A) and methanol (B) as mobile phase. The gradient profile was 5–15% B (0–10 min), 15–25% B (10–15 min), 25–50% B (15–50 min), 50–80% B (50–60 min), 80–100% B (60–70 min) and an isocratic elution for 5 min, at a flow rate of 200 μL.min^{-1}. The first detection was performed on PDA detector in a wavelength range 200–450 nm, followed by a second detection in the mass spectrometer. Mass spectra were acquired in negative ion mode. The mass spectrometer was programmed to perform four consecutive scans: full mass (*m/z* 125–2000), MS^2 of the most abundant ion in the full mass, MS^3 of the most abundant ion in the MS^2 and MS^4 of the most abundant ion in the MS^3. Source voltage was 4.7 kV and the capillary voltage and temperature were -7 V and 275 ºC, respectively. Nitrogen was used as sheath and auxiliary gas at 20 and 7 Finnigan arbitrary units, respectively. The normalized energy of collision was 49%, using helium as collision gas. Data treatment was carried out with XCALIBUR software (Thermo Scientific).

3.2.5. CELL CULTURE

Human hepatic carcinoma cell line (HepG2 - ATCC HB-8065) was kindly supplied by Professor Conceição Pedroso Lima (Center for Neurosciences and Cell Biology, University of Coimbra, Portugal) and cultured in Dulbecco's Modified Eagle Medium (DMEM) containing 10% (v/v) heat-inactivated fetal bovine serum, 100 U/mL penicillin, and 100 μg/mL streptomycin. Cells were maintained at 37 ºC and 5% CO_2 in a humidified incubator.

3.2.6. ASSESSMENT OF CELL VIABILITY

The effect of EEF on cell viability/metabolic activity was evaluated by resazurin assay (O'Brien et al., 2000). Cells ($8x10^4$ cells/well) were plated in 96-well plates, in duplicates, for 12 h and incubated with serial concentrations of EEF for 24 h. Resazurin (50 μM) was added to the cells 1 h before recording fluorescence. Absorbance was recorder at 570 nm, with a reference wavelength of 620 nm, using a standard spectrophotometer (SLT, Austria). In this assay, metabolic active cells reduce resazurin (blue dye) into resorufin (pink colored); therefore, their number correlates with the magnitude of dye reduction. Cell viability was evaluated based on a comparison with untreated cells. The half-maximal inhibitory concentration (IC_{50}) represents the EEF concentration required to inhibit 50% of cell viability and was determined by nonlinear regression.

3.2.7. CELL PROLIFERATION, CELL CYCLE AND CELL DEATH ANALYSIS

Cells ($6.4x10^5$) were plated in 12-well plates. HepG2 proliferation was assessed by incorporation of 5-ethynyl-2'-deoxyuridine (EdU), a thymidine analog that is incorporated into DNA of dividing cells during S phase. Cells were treated with different concentrations of EEF for 24 h and EdU (10 μM) was added 3 h before cell fixation with 70% aqueous ethanol. Click-iT® EdU Alexa Fluor® 488 Flow Cytometry Assay Kit was performed according to the manufacturer's instructions (Molecular Probes, Invitrogen).

Cell cycle distribution was analyzed after 24 and 48 h of EEF addition. Cells were harvested by trypsinization, washed twice and fixed with 70% ice-cold aqueous ethanol overnight and then incubated with PI with RNase solution for 15 min at room temperature before analysis. After cells incubation for 24 h with EEF, apoptosis was detected using an annexin V-fluorescein isothiocyanate (FITC)/PI double staining, as described by the supplier (Immunostep).

All the flow cytometry measurements were performed on a Becton Dickinson FACSCalibur cytometer using the Cellquest software (BD Biosciences). PI histogram modeling was performed in ModFit LT software (Verity Software House). The flow cytometer was calibrated with fluorescent standard microbeads (CaliBRITE Beads; BD Biosciences) for accurate instrument setting.

3.2.8. MORPHOLOGICAL ANALYSIS WITH MAY-GRÜNWALD-GIEMSA AND HOECHST 33258

After 24 h of EEF treatment cells were trypsinized, resuspended in 30 μl of FBS and placed on a slide for microscopic analysis. The cells were stained for 3 min with May–Grünwald solution (0.3% v/v in methanol, then diluted in distilled water at 1:1 (v/v) ratio) and finally incubated during 15 min with Giemsa solution (0.75% w/v in glycerol/methanol 1:1) previously diluted in distilled water (8x). Cells were rinsed with distilled water and then left to dry at room temperature. Cell morphology was analyzed by light microscopy using an Olympus BX51TF microscope (Olympus Co. Ltd.)

For nuclear Hoechst-33258 staining cells were plated in 8-well chambered slides. After 24 h of treatment with EEF, cells were washed with PBS and fixed with 4% paraformaldehyde for 10 min, washed with PBS and incubated with 5 μg/mL Hoechst 33258 for 5 min at room temperature. Nuclear morphology was visualized under a fluorescence microscope (Leica DM4000B, Leica Microsystems).

3.2.9. WESTERN BLOT ANALYSIS

Protein samples preparation, quantification and western blot were performed as previously described (Liberal et al., 2014). The antibodies were used in the following concentrations: anti-ubiquitin, clone P4D1 (1:2000), anti-LC3 (1:1000), anti-IGFBP1 (1:1000), anti-FAS (1:1000), anti-β-tubulin (1:20,000), and anti-mouse and anti-rabbit alkaline phosphatase-conjugated secondary antibodies (1:20,000).

3.2.10. PROTEASOME CHYMOTRYPSIN-LIKE ACTIVITY

HepG2 cells were lysed in 50 mM Tris–HCl buffer (pH 7.6) containing 1 mM dithiothreitol and 2 mM of adenosine triphosphate (ATP). Equal amounts of protein were incubated with the proteasome substrate (fluorogenic) Suc-Leu-Leu-Val-Tyr-AMC (Suc-LLVY-AMC). Enzymatic kinetic was measured, during 30 min, in a temperature-controlled microplate fluorometric reader (37 °C), with excitation/emission wavelengths of 380/440 nm. The proteasome inhibitor MG132 was used as a positive control for proteasome activity inhibition.

3.2.11. ISOBARIC TAG FOR RELATIVE AND ABSOLUTE QUANTITATION (ITRAQ)-BASED PROTEOMICS LABELING

Cells were plated, allowed to stabilize for 12 h and incubated with EEF concentration corresponding to IC_{50} (113 μg/mL) for 24 h. Cells were harvested and resuspended in HEPES-EDTA buffer (50 mM HEPES, 1mM EDTA, pH 7.4). Then, the samples were sonicated (3 times for 5 s at 30 μm peak to peak) in a Vibra Cell sonicator (Sonics & Materials, Inc.) and centrifuged at 14,000 rpm for 10 min at 4 °C to remove cell debris. The supernatant was collected and protein concentration was assessed by bicinchoninic acid assay. For iTRAQ-based quantitative proteomic analysis, 100 μg of protein of each sample was prepared. The proteins were precipitated with 6 volumes of cold acetone at −20°C overnight and centrifuged for 30 min at 14,000 g. Then, pellets were resuspended with triethylammonium bicarbonate buffer (TEAB) (0.1 M, pH 8.5) and 2% SDS to achieve a final concentration of 0.05%. Samples were then reduced with 50 mM tris (2-carboxyethyl)phosphine (TCEP) for 1 h at 37 ºC. Following this, samples were alkylated with 10 mM S-methyl methanethiosulfonate (MMTS) (Sigma-Aldrich) for 10 min at room temperature with agitation. Trypsin was added to each sample and the digestion was performed for 18 h at 37 ºC. Digested sample peptides were subsequently labeled with the iTRAQ® reagent - 8plex (ABSciex) following the protocol provided by the manufacturer. Labels were reconstituted in 60% isopropanol, added to each sample peptides and incubated for 2 h at room temperature with agitation. The reaction was stopped by adding water and acidified with formic acid (0.1% final concentration). Labeled samples were then combined and dried in SpeedVac.

Labelled peptides were separated from an adapted multidimensional liquid chromatography approach, as described by Vitorino et al., 2012 based on high pH for the first dimension peptide chromatography with a C18 reverse phase HPLC column and acidic pH for the second one. Thus, sample loading was performed at 200 μL/min with buffers (A) 2% ammonium hydroxide and 0.014% formic acid in water, pH 10 and (B) 2% ammonium hydroxide and 90% acetonitrile (ACN) in water, pH 10. After 5 min of sample loading and washing, peptide fractionation was performed with linear gradient to 70% B over 85 min. Sixty fractions were collected, dried in a SpeedVac and resuspended in 5% ACN and 0.1% trifluoroacetic acid (TFA). Collected fractions were then separated by LC. Peptides were loaded onto a C18 pre-column (5 mm particle size, 5 mm; Dionex) connected to an RP column PepMap100 C18 (150 mm_75 mm i.d., 3 mm particle size). The flow-rate was set at 300 nl/min. The mobile phases A and B were 2% ACN and 0.05% TFA in water, and 90% ACN with 0.045% TFA in water, respectively. The gradient started at 10 min and ramped to 60% B till 50 min and 100% B at 55 min and retained at 100% B till 65 min. The separation was monitored at 214 nm using a UV detector (Dionex/LC Packings). Using the micro-collector Probot (Dionex/LC Packings) and, after a lag time of 15 min, peptides eluting from the capillary column were mixed with a continuous flow of

alpha-CHCA matrix solution (in internal standard Glu-Fib) and were directly deposited onto the LC-MALDI plates. The spectra were generated and processed with 4800 MALDI-TOF/TOF. Protein identification based on MS/MS data was performed with ProteinPilot™ software (v.4.0, ABSciex) using Paragon search method. SwissProt from *homo sapiens* (release date 06022013) was used as protein database. Default search parameters used were as follows: trypsin as the digestion enzyme, carbamidomethyl modification on cysteine residue and iTRAQ 8-plex. Bias correction was applied and proteins were identified with a confidence level of 95%. Proteins were found to be differentially expressed when $p<0.05$ (FDR-corrected).

3.2.12. STATISTICAL ANALYSIS

The results are expressed as mean ± standard error of the mean (SEM). Data were analyzed using one-way analysis of variance (ANOVA), followed by *Dunnett's post-hoc test*. The differences between the means were considered significant for values of $p<0.05$. The statistical analysis was performed using Prism 5.0 Software (GraphPad Software).

3.3. RESULTS AND DISCUSSION

3.3.1. PHYTOCHEMICAL CHARACTERIZATION OF EEF

HPLC-PDA phenolic profile was recorded at 280 nm (Figure 3.1) and 12 compounds were tentatively identified by HPLC-PDA-ESI/MS^n as ellagitannins (Table 3.1), based on their characteristic UV and MS spectra. All these compounds exhibit a characteristic UV spectrum with maximum absorbance below 270 nm such as those referred by Arapitsas et al. (2012). Almost all compounds presented a maximum at 248-257 nm with a slight shoulder between 280 and 284 nm, a characteristic UV spectral profile that has been referred as a slope (Hanhineva et al., 2008).

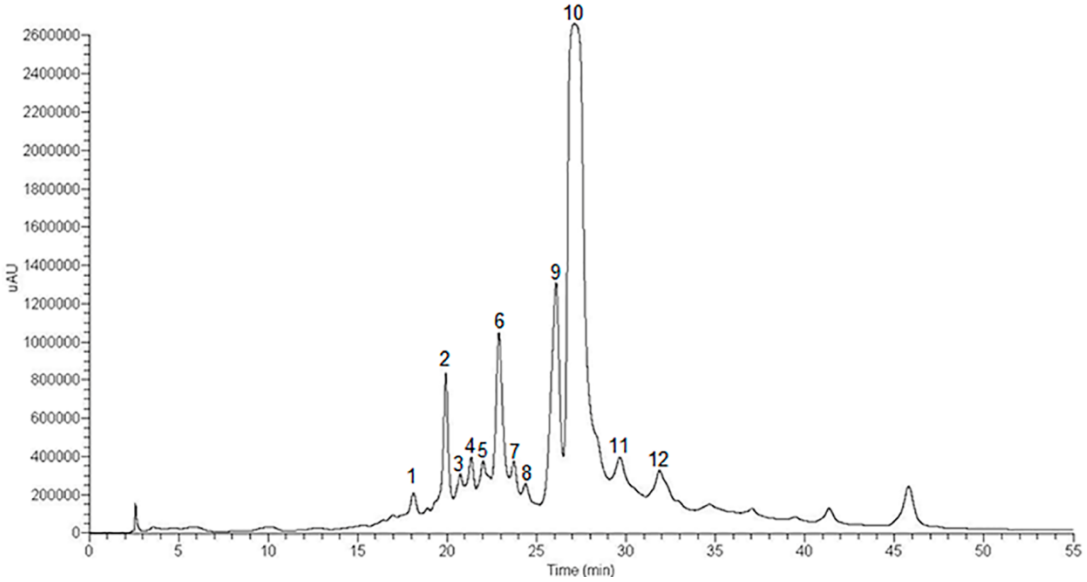

Figure 3.1 - HPLC polyphenolic profile of EEF recorded at 280 nm. The identification of the peaks is shown in Table 3-1.

Table 3.1 - Structural elucidation of ellagitannins of an enriched fraction obtained from *Fragaria vesca* leaf.

Peak	*R*t (min)	λ_{max} (nm)	MW	$[M-H]^-$ (*m/z*)	MS^2	MS^3 *m/z*[a]	MS^4	Compound tentatively identified
1	18.12	250, 282sh	966	965	**783**	481, **301**, 275	-	Unknown ellagitannin
2	19.92	255, 283sh	1568	783[b]	1265, 935, 915, 897, **633**, 613, 301	**301**	-	Sanguiin H-10 isomer
3	20.75	250, 283sh	934	933	631, **451**, 301	433, 407, **405**, 327, 283	-	Castalagin/vescalagin isomer
4	21.35	251, 283sh	1104	1103	1059, **935**, 915, 897, 782	**633**, 301	**301**	Sanguiin H-2 isomer
5	21.97	250, 283sh	934	933	631, **451**	434, 407, **405**, 351, 301, 283	348, **377**	Castalagin/Vescalagin isomer
6	22.89	257, 282sh	1568	1567	**1265**, 963, 935, 915, 897, 783, 633, 613	1097, 963, **935**, 897, 783, 613	633, **301**	Sanguiin H-10 isomer
7	23.72	250, 282sh	1104	1103	**1059**, 935, 757	**935**, 897, 757, 633, 613	898, 877, **633**	Sanguiin H-2 isomer
8	24.37	248, 282sh	936	935	**633**, 301	463, **301**	-	Casuarictin/Potentillin isomer
9	26.07	257, 282sh	936	935	**633**, 301	463, **301**	-	Casuarictin/Potentillin isomer
10	27.12	258, 284sh	1870	1869	1567, 1265, 1085, **935**, 963, 897, 633	898, **633**, 465, 301	**301**, 275	Sanguiin H-6/Agrimoniin/ Lambertianin A isomer
11	29.64	252, 280sh, 370	1118	1117	**935**, 897, 633	**633**, 301	481, **301**	Unknown ellagitannin
12	31.87	250, 284sh	2020	1009[b]	1717, 1567, 1235, **1085**, 1065, 935, 897, 783, 451	**897**	-	Unknown ellagitannin

[a] The most abundant ions are shown in bold;

[b] Doubly charged ion $[M-2H]^{2-}$

Particular fragmentation patterns are described as follows: Peak **1** showed a $[M-H]^-$ ion at *m/z* 965 and the fragmentation originated a third order ion that matches with ellagic acid (*m/z* 301). Hanhineva et al. (2008) found similar molecules on stamens of *Fragaria ananassa* flowers, however the ellagitannin structure was not elucidated yet (Supplementary Figure 3.I).

Peaks **2** and **6** were identified as sanguiin H-10 isomers. Peak **2** presented a $[M-2H]^{2-}$ at *m/z* 783 and peak **6** evidenced a $[M-H]^-$ ion at *m/z* 1567, giving a molecular mass of 1568. The fragmentation patterns were slightly different. Peak **2** originated a most intense MS^2 ion at *m/z* 633 (corresponding to one galloyl-HHDP-glucose unit) and MS^3 ion at *m/z* 301 (loss of galloyl-glucose residue), whereas peak **6** displayed a main MS^2 ion at *m/z* 1265 (loss of HHDP unit), MS^3 ion at *m/z* 935 (loss of galloyl-glucose residue), and MS^4 ions at *m/z* 633 (loss of other HHDP unit) and 301 (HHDP unit, corresponding to a loss of HHDP-galloyl-glucose) (Mullen et al., 2003).

Peaks **3** and **5** evidenced a $[M-H]^-$ ion at *m/z* 933, MS^2 fragments at *m/z* 451 from the cleavage of tri-galloyl unit and spontaneous lactonization, 631 from the loss of HHDP unit and 301 which corresponds to ellagic acid residue. These compounds were tentatively identified as isomers of vescalagin/castalagin (Simirgiotis and Schmeda-Hirschmann, 2010).

Peaks **4** and **7** were identified, according to Kool et al. (2010), as sanguiin H-2 and presented a mono charged molecular ion at *m/z* 1103. The fragmentation pattern of peak **4** and **7** was similar in MS^2, however the most intense fragments differed, showing a fragment at m/z 935 (-44 and -124 amu, a loss of CO_2 and trihydroxybenzene) and 1059 (-44 amu, a loss of CO_2), respectively. In MS^3, the parent MS^2 ion at m/z 935 (peak **4**) produced ions at m/z 633 (- 302 amu, a loss of HHDP) and 301 (- 302 and -332 amu, a loss of HHDP and of galloyl-glucosyl moieties respectively), while the parent MS^2 ion of peak **7**, at m/z 1059, gave a main fragment at m/z 935 (-124 amu, loss of trihydroxybenzene) and the ions at 897 (-162 amu, a loss of glucosyl moiety) and 633 (-44, -124 and -302 amu, a loss of CO_2,trihydroxybenzene and HHDP moieties).

Peaks **8** and **9** were identified as the isomeric forms of casuarictin or potentillin and presented a molecular ion at *m/z* 935 and MS^2 main fragments at *m/z* 633 (-302 amu) corresponding to one galloyl-HHDP-glucose unit and the ion at *m/z* 301 originated from lactonization of fragment 302 (Hanhineva et al., 2008). In the MS^3 the fragments at m/z 463 and 301 suggest the successive loss of the galloyl and galloylglucose residues.

Peak **10** is the major compound of this fraction and was also the main component of the crude extract. It showed a $[M-H]^-$ ion at *m/z* 1869 and MS^2 ions at m/z 1567 (loss of an HHDP unit), 1265 (loss of bis-HHDP), 1085 (loss of bis-HHDP-glucose) and 935, the main fragment, corresponding to one galloyl-bis-glucose unit. This fragmentation matched with sanguiin H-6/agrimoniin/lambertianin A isomers, previously identified in the leaves of *Fragaria* species (Simirgiotis and Schmeda-Hirschmann, 2010). The third and fourth orders of fragmentation pattern

confirmed the identification as evidenced, respectively by ions at *m/z* 633 (935-302 amu, loss of HHDP unit) and 301 (633-332, loss of galloyl-glucose residue).

Peak **11** displayed a $[M-H]^-$ ion at m/z 1117, giving a molecular mass of 1118. The structure of this molecule was not fully elucidated. However, the fragmentation pattern is consistent with an ellagitannin as evidenced by the main MS^2 ion at *m/z* 935 (corresponding to a galloyl-bis-HHDP-glucose), MS^3 ion at *m/z* 633 (loss of HHDP) and MS^4 at *m/z* 301 (loss of galloyl-glucose residue) (Supplementary Figure 3.II).

Peak **12** presented a $[M-2H]^{2-}$ at *m/z* 1009, giving a molecular mass of 2020 Da, and MS^2 fragments at *m/z* 1717, 1567, 1235, 1085, 1065, 935, 897, 783 and 451 (Supplementary Figure 3.III). An ellagitannin with the same molecular mass and a similar fragmentation pattern was also previously reported in *Fragaria* spp. (Gasperotti et al., 2013).

Several ellagitannins identified in the EEF were also previously disclosed in strawberries (Gasperotti et al., 2013; Simirgiotis and Schmeda-Hirschmann, 2010; Vrhovsek et al., 2012) - fruits well-known for their anticarcinogenic, antioxidant and genoprotective properties (reviewed in (Giampieri et al., 2012). The major peak of the fraction, identified as sanguiin H-6, agrimoniin or lambertianin A isomer, was also the major compound of the crude extract. Although there are still few studies with the isolated molecules, the anticancer activities of these proposed compounds were previously addressed in other cells. For example, it was demonstrated that agrimoniin induces apoptosis in human gastric cancer cells (SGC-7901) (Wang and Jin, 2011) and sanguiin-H6 isolated from blackberry seed extracts protects the DNA of human lymphocytes (Gođevac et al., 2011). These results suggest the importance of the ellagitannins as anticancer natural molecules.

3.3.2. EFFECT OF *FRAGARIA VESCA* LEAVES CRUDE EXTRACT AND EEF ON CELL VIABILITY

Once identified the compounds present in the EEF we proceeded to evaluate the biologic effects of this fraction on HepG2 cells. We started to determinate the IC_{50} for cell viability of both, the EEF and the crude extract of *Fragaria vesca* leaves. Resazurin reduction colorimetric assay was used to assess the cell viability after 24 h of treatment with increasing concentrations of the extract and fraction (up to 10,000 μg/mL). In order to determine cell sensitivity to treatments, data points of the dose-response curves were fitted with a sigmoid function for the calculation of the IC_{50} values. Data showed that both treatments reduce cell viability in a dose-dependent manner as represented in Figure 3.2-A. In fact, the IC_{50} of EEF was 6 times lower (113 ± 1 μg/mL) than the IC_{50} of the crude extract (690 ± 1 μg/mL), suggesting that ellagitannins could be responsible for the cytostatic/cytotoxic effect of the extract. Based on the high effect of the fraction relatively to the extract, all the subsequent experiments were performed only with EEF.

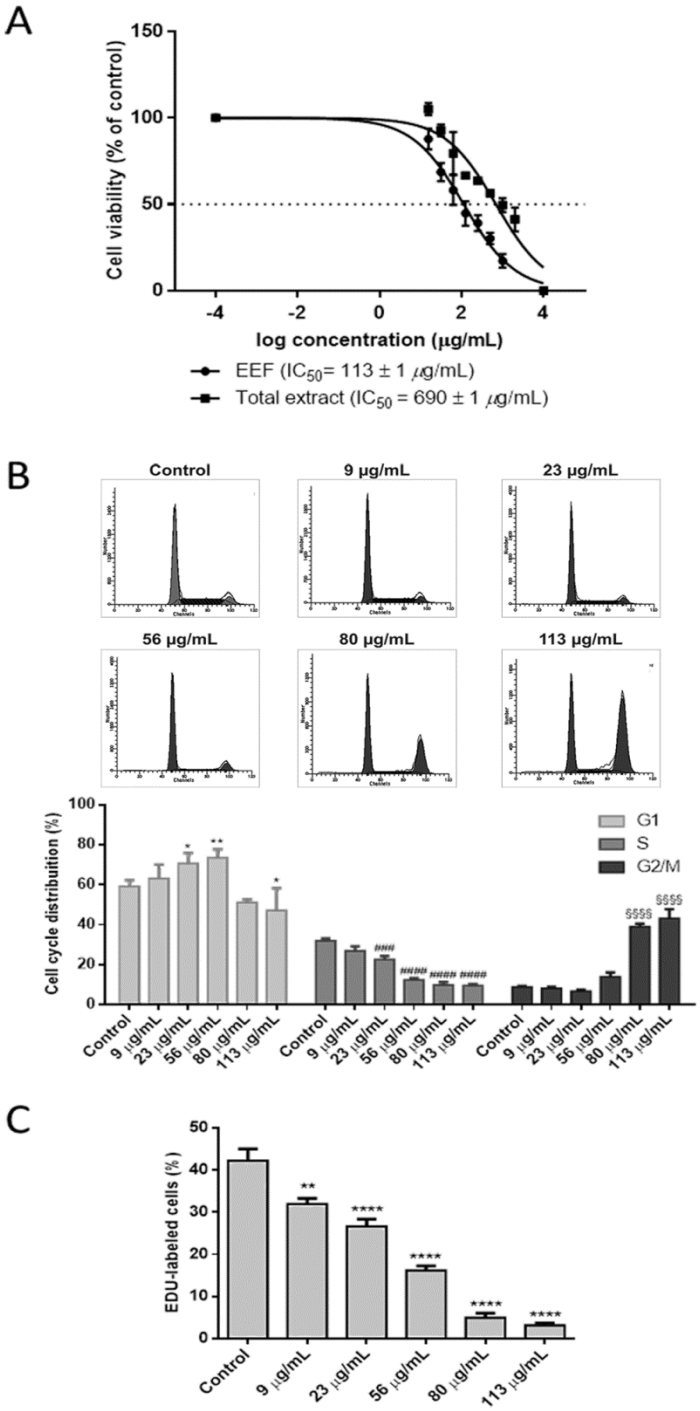

Figure 3.2 - Effect of EEF on HepG2 viability, cell cycle and cell proliferation.A) Evaluation of cell viability after incubation with different concentrations of the extract or EEF for 24 h. Data-points correspond to the mean ± standard deviation of at least three independent assays performed in duplicate. The IC_{50} values were fitted to a sigmoidal function from the dose-response curves. B) Cell cycle distribution of cells treated with different concentrations of EEF for 24 h. Data are expressed as percentage of PI-positive cells and are given as the means ± SEM of at least three independent experiments. C) EdU incorporation after the treatment with different concentrations of EEF. Data represent the mean ± SEM percentage of EdU-labelled cells from three independent experiments (* p<0.05, ** p<0.01, ***p<0.001, ****p<0.0001 when compared to control; the symbols *, #, $, * were used for G1, S, G2/M and EdU, respectively).

Since ellagitannins yield ellagic acid on neutral and alkaline conditions (Daniel et al., 1991; Ross et al., 2007) it would be conceivable that ellagitannins hydrolysis could occur in the culture medium, thus generating ellagic acid that could be responsible for the antiproliferative effect of EEF. However, the absence of any effect on cell viability after cells treatment with concentrations up to 250 μg/mL of ellagic acid (data not shown) led us to suggest that cytotoxic effects could be ascribed to ellagitannins.

3.3.3. CELL CYCLE AND CELL PROLIFERATION AFTER TREATMENT WITH EEF

Defects in cell cycle checkpoints are associated with an uncontrolled cellular proliferation and, as such, targeting cell cycle could be an important strategy for cancer therapy. To further investigate alterations in the cell cycle of HepG2 cells exposed to EEF we used flow cytometry.

Cells were incubated with different concentrations of EEF during 24 h (IC_{50} = 113 μg/mL; IC_{45} = 80 μg/mL; IC_{40} = 56 μg/mL; IC_{25} = 23 μg/mL; IC_{15} = 9 μg/mL) and subsequently analyzed for the distribution of G0/G1, S and G2/M phases. EEF was able to interfere with cell cycle distribution, being the effect dependent on the concentrations used. In fact, higher concentrations of the EEF clearly induced an increase in cells in the G2/M phase whereas lower doses promoted a significant increase in cells in G1 when compared to control cells (Figure 3.2-B). Since tumor cells commonly adapt to toxic insults and recover over time we further evaluated whether EEF effects are sustained over time. For that, cells were treated with the same concentrations of EEF for 48 h and a markedly G2/M cell cycle arrest was disclosed for the three higher concentrations tested (Supplementary Figure 3.IV). We may therefore point out that the inhibition of cell proliferation by EEF occurs, at least in part, through cell cycle arrest in G2/M phases.

We further evaluated HepG2 cell proliferation by the incorporation of EdU, determined by flow cytometry, after 24 h of EEF treatment. The results presented in Figure 3.2-C show that the incorporation of EdU is decreased for all the concentrations studied in a dose-dependent way, thus confirming and supporting the previous described effects on cell cycle.

As far as we know, the effect of the ellagitannins herein tentatively identified on cell cycle was never addressed. However, others ellagitannins were reported to modulate cell cycle distribution and cell cycle regulators, such as casuarinin (Kuo et al., 2005a, 2005b) and geraniin (Vassallo et al., 2013).

3.3.4. APOPTOSIS/NECROSIS DETECTION IN EEF-TREATED CELLS

In order to evaluate cell death and to discriminate between apoptosis and necrosis triggered by the EEF treatment, cells were incubated with different concentrations of EEF for 24 h and then stained with annexin V-FITC/PI. The two higher concentrations of EEF promoted an increase in necrotic cells (annexin V-negative/PI-positive cells). This increase was accompanied by a rise, although not statistically significant, of annexin V-positive/PI-positive cells that correspond to late apoptotic/necrotic cells (Figure 3.3-A). To further clarify the mechanism of cell death, changes in cell morphology were evaluated through May-Grunwald-Giemsa staining. Cells treated with EEF for 24 h showed both features of necrosis (swelling, loss of membrane integrity) and apoptosis (membrane bleeding and cell shrinkage), with a predominance of a necrotic cell death (Figure 3.3-B). Furthermore, nuclear morphology of HepG2 cells was assessed with Hoechst 33258. The results indicated that most of the nuclei are similar to those of control. Nevertheless, larger nuclei that could be related to necrotic cell death were occasionally observed (Figure 3.3-C).

Previous studies indicated that ellagitannins induce apoptotic cell death in *in vitro* and *in vivo* models (Li et al., 2013; Wang et al., 2014). Therefore, it was expected that cells end up dying by apoptosis. However, we did not detect an increase in apoptotic cells, neither through the analysis with PI, nor with annexin V/PI experiment and although the May-Grunwald-Giemsa staining allowed the visualization of apoptotic cells, necrosis was clearly the predominant mechanism of cell death. Accordingly, several studies demonstrated that the induction of apoptotic cell death evoked by ellagitannins was accompanied by an increase of necrosis (Cho et al., 2015; Kasimsetty et al., 2010). Importantly, while initially described as a nonregulated mechanism of death, necrosis is currently considered a consequence of the crosstalk between several biochemical and molecular events (Festjens et al., 2006). Necrosis occurs in both physiological and pathophysiological processes and in contrast to apoptosis, typically promotes an inflammatory response, which may contribute for the tumor regression. On the other hand, during tumor development, the inflammation due to the excessive spontaneous necrosis may stimulate the growth and aggressiveness of the tumor (Proskuryakov and Gabai, 2010).

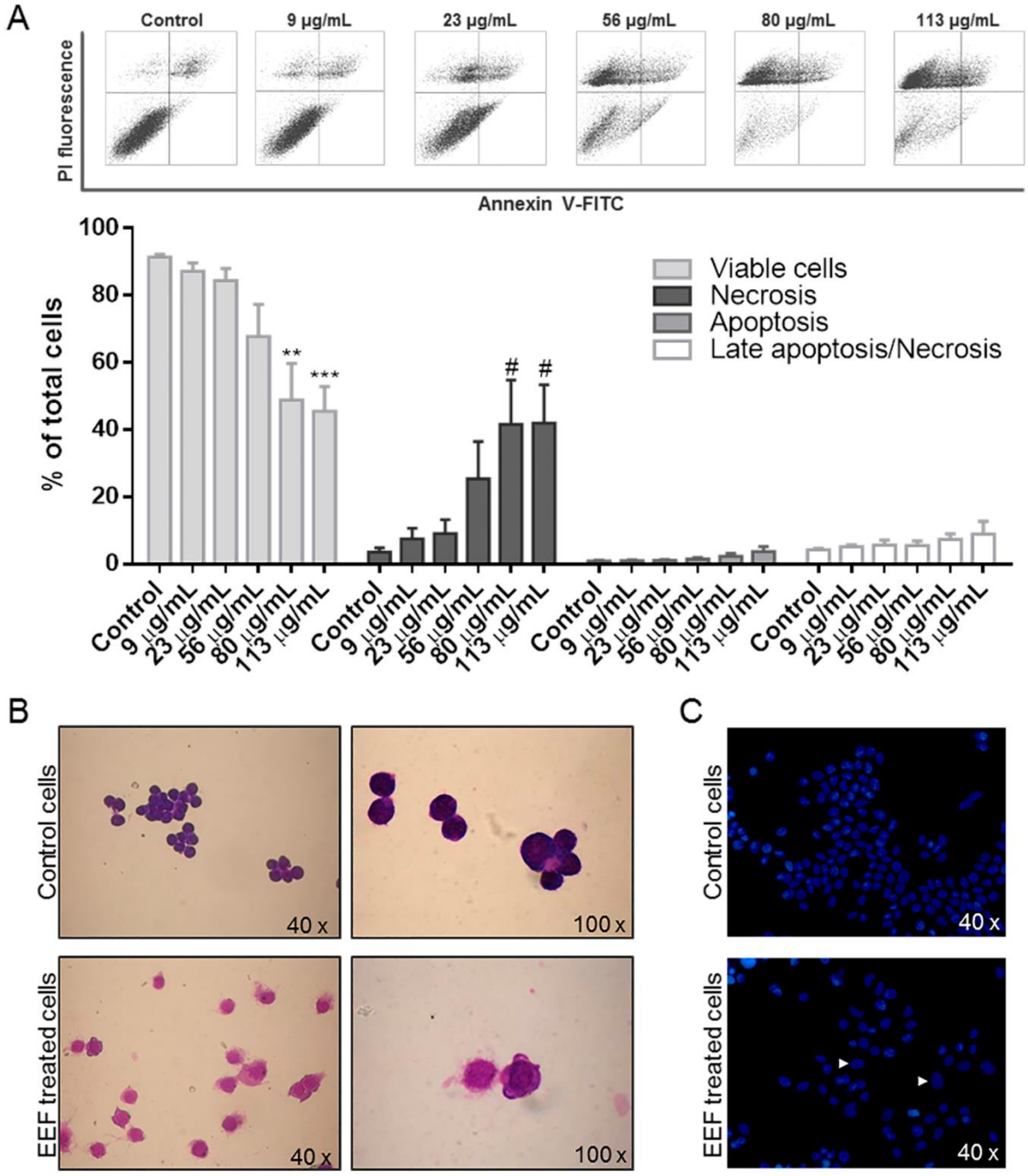

Figure 3.3 - Detection of Apoptosis/Necrosis after EEF treatment. Cells were incubated with different concentrations of EEF for 24 h. A) Annexin V-FITC/PI labelling was detected by FACSCalibur flow cytometer. The populations of early apoptotic cells (annexin V-positive/PI negative), late apoptotic cells (annexin V positive/PI positive), necrotic cells (annexin V negative/PI positive) and viable cells (annexin V negative/PI negative) were evaluated as a percentage of total cells and are given as the means ± SEM of at least three independent experiments (* $p<0.05$, ** $p<0.01$, *** $p<0.001$ when compared to control; the symbols * and # were used for viable and necrotic cells respectively). B) Evaluation of the morphology of cells stained with May-Grunwald-Giemsa and observed under light microscopy. Cells were visualized at 40x and 100x magnification; C) Evaluation of the nuclear morphology of cells stained with Hoechst 33258 and visualized under fluorescent microscopy at 40x magnification. Arrowheads show nuclear swelling.

3.3.5. EEF EFFECT ON THE CELLULAR PROTEOLYTIC MECHANISMS

Our previous data established that *Fragaria vesca* leaves crude extract modulates chymotrypsin-like activity of proteasome and autophagy (Liberal et al., 2014). Consequently, in this work we sought to evaluate whether the EEF displays similar bioactivity.

Cells were treated with different concentrations of EEF and the proteasome inhibitor MG132 was used as control. EEF significantly decreased chymotrypsin-like activity of the 26S proteasome after 6 and 24 h of treatment in a dose-dependent way (Figure 3.4-A and 3.4-B, respectively). A decrease in proteasome degradation would lead to an accumulation of polyubiquitinated proteins. Accordingly, for the highest EEF concentrations tested during 24 h, an accumulation of ubiquitinated proteins was disclosed, suggesting an impairment of proteasome degradation (Figure 3.4-C and 3.4-D), thus corroborating the previous results.

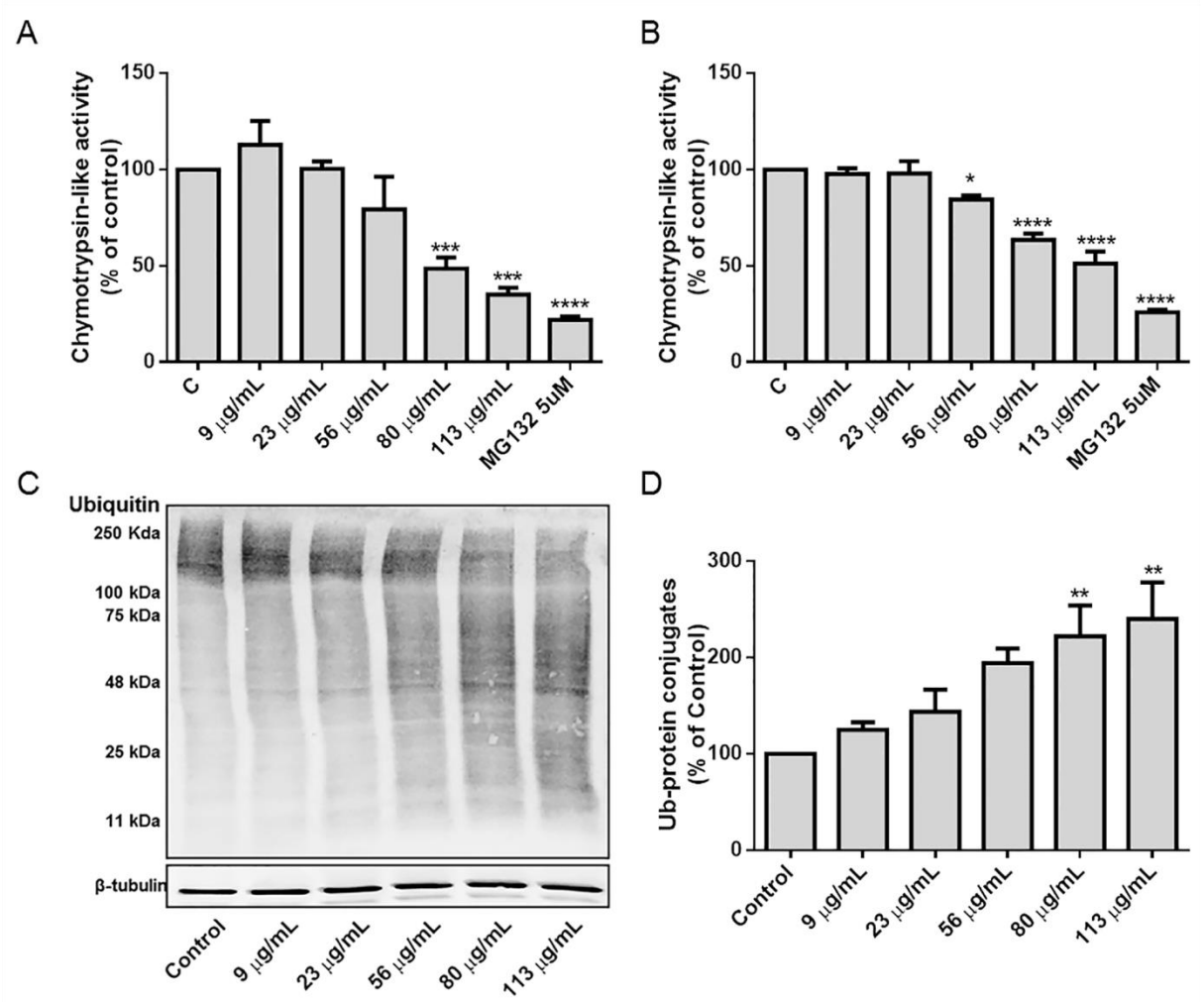

Figure 3.4 - Effect of EEF on ubiquitin-proteasome system. Chymotrypsin-like activity of the 26S proteasome of cells treated with the EEF for 6 (A) and 24 (B) Data are presented as mean ± SEM of, at least, 3 independent experiments and are expressed as percentage of control; Ubiquitinated proteins after incubation with EEF for 24 h were evaluated by western blot using an antibody against ubiquitin (P4D1). A representative immunoblot (C) and densitometric quantification of the whole lanes are presented (D). Data are presented as mean ± SEM of 4 independent experiments and are expressed as percentage of control (* p<0.05, ** p<0.01, ***p<0.001, **** p<0.0001 when compared to control).

To evaluate whether EEF affects macroautophagy, we evaluated the levels of LC3-II after 6 h of treatment. The conjugation of LC3-I with phosphatidylethanolamine in the autophagic membranes leads to the formation of LC3-II, which is usually used as a measure of autophagosomes number and, at a certain point, constitutes a reliable marker of autophagic activity. However, besides the increase in autophagosomes formation, the increased amounts of LC3-II may also reflect the blockage of autophagosomes fusion with the lysosome (Klionsky et al., 2012), thus leading to an accumulation of these structures. Our data clearly demonstrate that EEF increased the expression of LC3-II in a dose-dependent way (Figure 3.5) but, to further clarify the molecular mechanism behind autophagy modulation by EEF, we used chloroquine to measure the autophagic flux. Chloroquine is an inhibitor of autophagy that raises the lysosomal pH leading to the blockage of the fusion between autophagosomes and lysosomes and to the inhibition of lysosomal enzymes, thus decreasing protein degradation (Klionsky et al., 2012). As expected, cells treated with chloroquine elicited an accumulation of LC3-II. If the EEF was able to increase basal autophagy, cells co-incubated with chloroquine should present higher levels of LC3-II than cells treated with chloroquine alone. However, data show that the levels of LC3-II of cells treated with chloroquine or co-treated with EEF were similar (Figure 3.5), suggesting that the effect of EEF on autophagy relies on the inhibition of autophagosomes degradation. Still, the mechanism underlying such effects needs further clarification, in order to understand how EEF impairs the autophagic clearance.

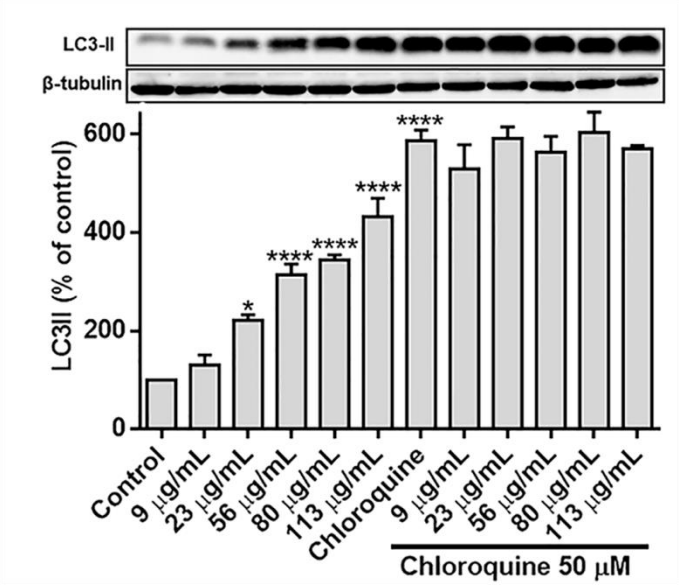

Figure 3.5 - Effect of EEF on autophagy. Cells were treated with EEF alone or co-treated with chloroquine. A representative immunoblot is shown above the graph. Data are presented as mean ± SEM of, at least, 3 independent experiments and are expressed as percentage of control (* p<0.01, **** p<0.0001 when compared to control).

Recent studies demonstrated that polyphenols have a dual effect on autophagy, acting as either activators or inhibitors and it is widely accepted that an up-regulation of autophagy is beneficial in preventing ageing and age-related diseases (Pallauf and Rimbach, 2013). However, given the dependence of tumor cells on autophagy for their growth, the activation of this proteolytic pathway can promote the survival of cancer cells (Degenhardt et al., 2006). Accordingly, the inhibition of autophagy or the combination of autophagy inhibitors with anticancer agents has been proposed as a therapeutic strategy in cancer therapy (Amaravadi, 2009).

Regarding ellagitannins, there is very few information about the potential of these compounds to modulate the clearance mechanisms of the cells. To the best of our knowledge ellagitannins have not been reported as proteasome inhibitors, although their precursor, pentagalloylglucose, demonstrated anticancer effects through proteasome inhibition (Kuo et al., 2009) and ellagic acid was shown to inhibit 26S proteasome activity (Chang et al., 2013). Additionally, ellagic acid inhibited autophagy in ovarian cancer cells (Chung et al., 2013), while the ellagitannin punicalagin was able to induce autophagy in human glioma cells (Wang et al., 2013).

3.3.6. IDENTIFICATION OF DIFFERENTIALLY EXPRESSED PROTEINS IN EEF-TREATED HEPG2 CELLS

To further unveil other molecular targets of EEF, we evaluated changes induced by EEF in the proteome of HepG2 cells. For this purpose, we performed a comparative proteomics study using iTRAQ in cells incubated in the presence or absence of EEF (113 μg/mL for 24 h). Overall, this approach allowed the identification of 914 proteins, being 133 differentially expressed in EEF-treated cells (Figure 3.6) (Supplementary Table I). Looking at the biological processes and according to PANTHER classification system, those proteins are involved in metabolic pathways (39.5%), in cellular (18.4%) and developmental (7.9%) processes and also in cellular component organization or biogenesis (12.3%) (Figure 3.7-A).

A protein interaction network was generated with Cytoscape (ClueGO plugin), allowing the identification of proteins and biological processes which are either up- or down-regulated by EEF (Figure 3.7-B). The major clusters of interacting proteins are related to the regulation of translational elongation, *de novo* post translational protein folding and several metabolic processes, as NADPH regeneration and glycolysis. It was also observed a down-regulation of several proteasome subunits, namely proteasome subunits alpha type-1 and -4, beta type -4 and 26S protease regulatory subunit 4, which are implicated in the regulation of cellular amine metabolic process, thus corroborating the inhibition of proteasome function, previously detected (Figure 3.7-B). The most significant cluster - cell metabolism, mainly covers the protein, nuclease-containing compound, carbohydrate and lipid metabolic processes. It is well established that cancer cells have altered metabolism, enabling its

rapid proliferation and continuous growth (DeBerardinis et al., 2008). Hence, drugs that perturb cancer cell metabolism may open a perspective in cancer treatment.

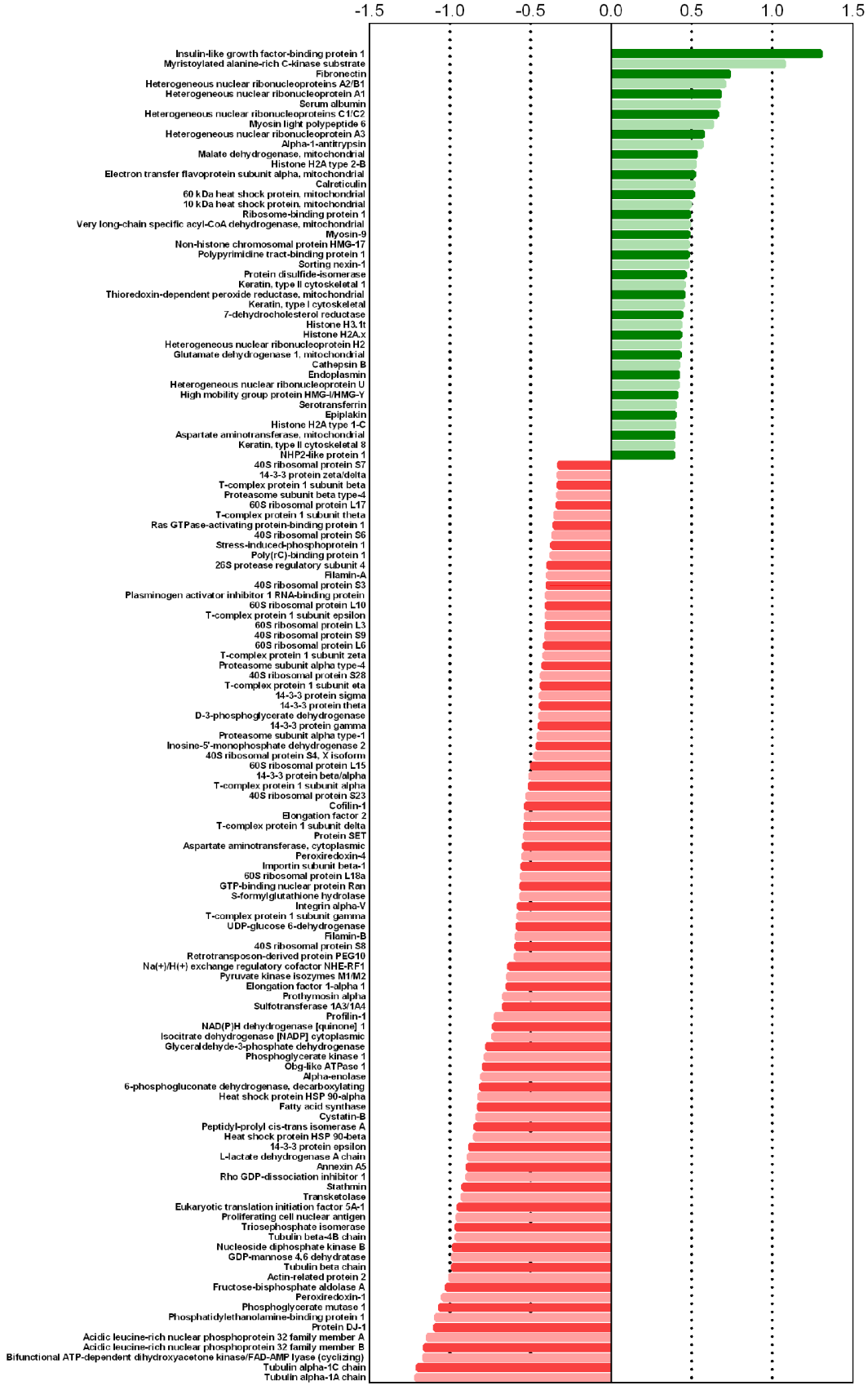

Figure 3.6 - Log ratio comparison of the relative intensity for the significantly regulated proteins (EEF/Control).

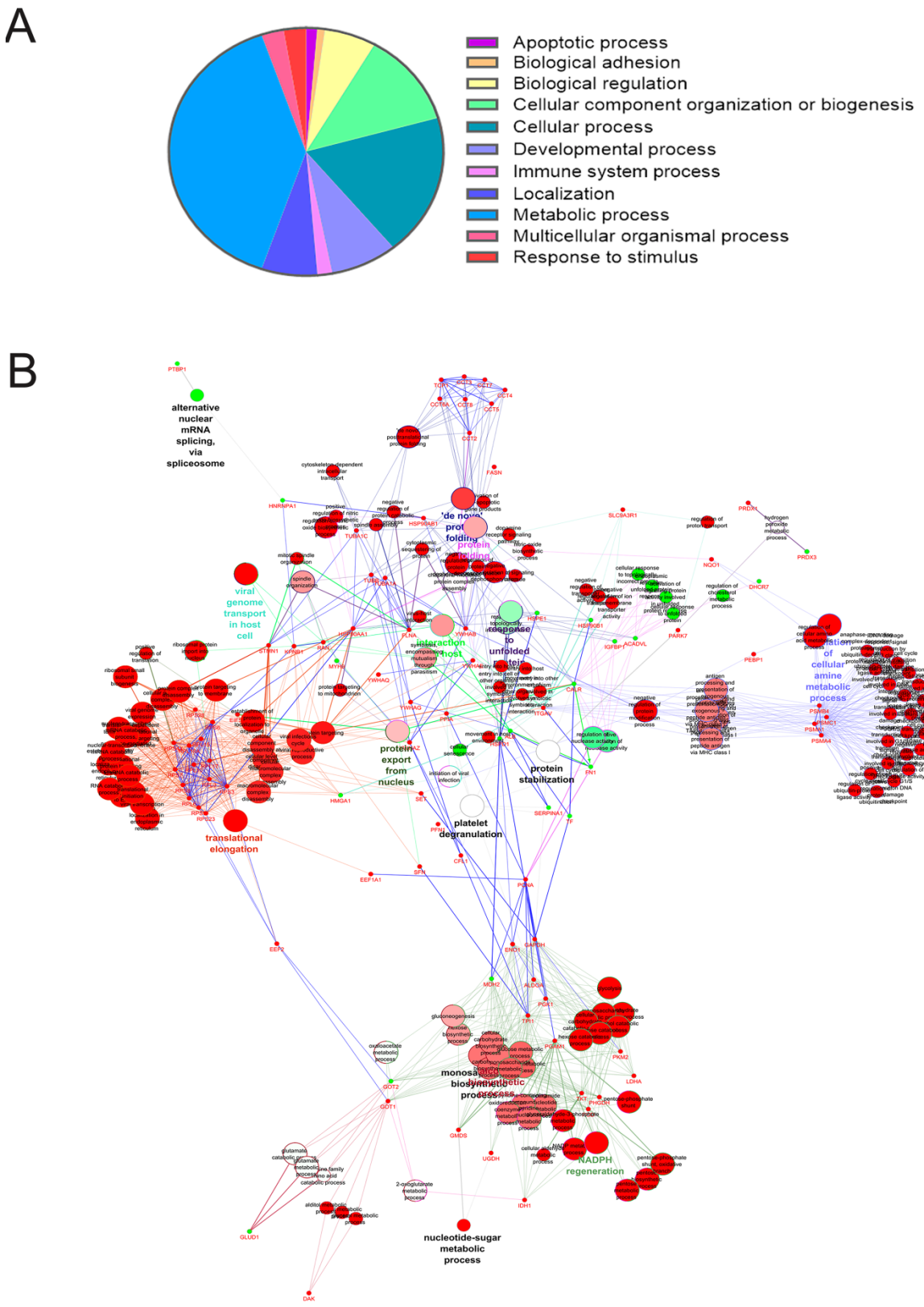

Figure 3.7 - Effect of EEF on HepG2 proteome. A) Distribution of differentially regulated proteins according to biological processes based on gene ontology annotation, after cells treatment with EEF; B) Protein-protein interaction network generated with Cytoscape. Green nodes represent upregulated proteins while red nodes demonstrate downregulated proteins after 24 h of treatment with EEF.

Two of the most differently expressed proteins (FAS and IGFBP1) were chosen to validate the iTRAQ experiment by western blot. Besides the concentration used in proteomic experiments, lower concentrations were also tested in order to check whether the effects are dose-dependent. The results confirmed that EEF decreased FAS (Figure 3.8-A) and increased IGFBP1 (Figure 3.8-B), being those effects dependent on EEF concentration. IGFBPs interact with insulin-growth factors (IGF) I-II limiting their bioavailability. Since increased levels of insulin and IGF have been linked to cancer progression (Yu, 2000), *Fragaria vesca* leaves and particularly its EEF may be an important source of molecules able to disturb cancer cells metabolism and therefore represent an attractive therapeutic strategy for cancer. Increased fatty acid biosynthesis is also characteristic of cancer cells. FAS is a key enzyme for *de novo* fatty acid synthesis, catalyzing the conversion of acetyl-CoA and malonyl-CoA to palmitic acid. It was reported that enhanced FAS expression and activity confer both growth and survival advantages in human tumors, including the hepatocellular carcinoma (Hao et al., 2014), being considered a metabolic oncogene. Moreover, several FAS inhibitors have shown antitumor activity, such as cerulenin (Pizer et al., 1996), the plant derived polyphenol curcumin (Fan et al., 2014) and epigallocatechin gallate (Brusselmans et al., 2003). In this work, we showed that EEF decreases FAS protein expression in a hepatocellular carcinoma cell line. Accordingly, Liu et al. (2009) reported that several ellagitannins were strong inhibitors of FAS activity. Taken together, ellagitannins might be potential anticancer molecules through the inhibition of FAS expression and activity**.**

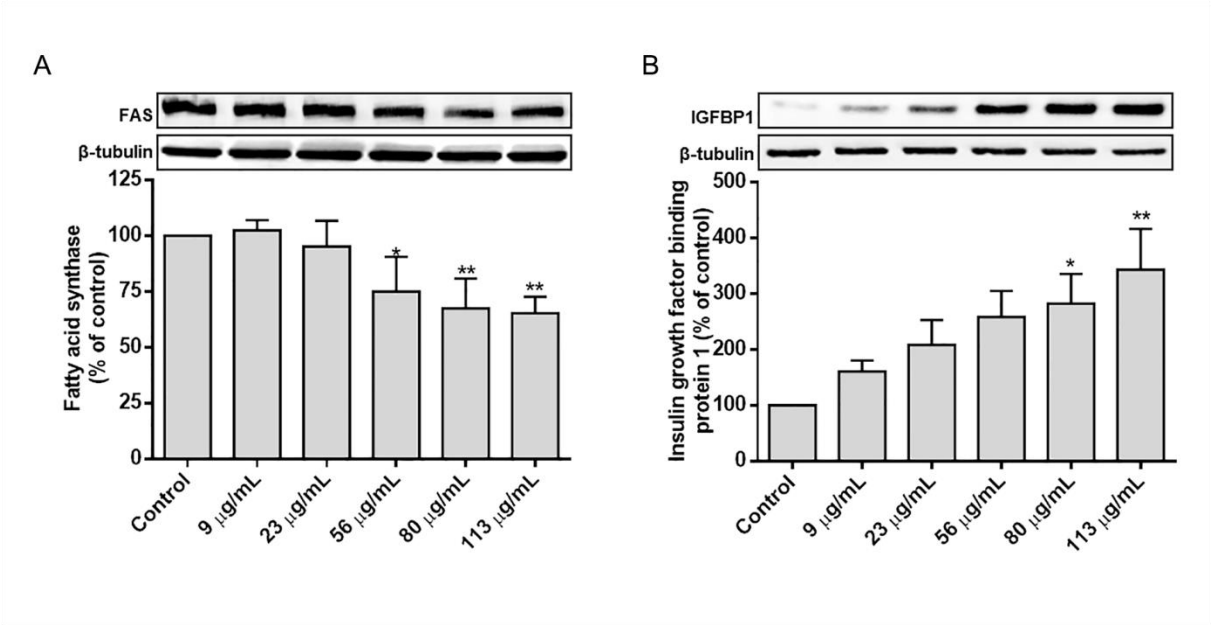

Figure 3.8 - Effect of EEF on FAS and IGFBP1 protein levels. HepG2 cells were incubated with different concentrations of EEF fraction for 24 h and FAS (A) and IGFBP1 (B) protein levels were evaluated by western blot. Data are presented as mean ± SEM of, at least, 3 independent experiments and are expressed as percentage of control (* $p<0.05$, ** $p<0.01$ when compared to control). Representative immunoblots are presented above the graphs.

3.4. CONCLUSION

The potential of polyphenols for cancer therapeutics has gained increased attention in the last years. Particularly, ellagitannins have been indicated as antiproliferative, antiangiogenic and pro-apoptotic compounds. In this study the phenolic characterization of an ellagitannin- enriched fraction from *Fragaria vesca* leaves was performed. This fraction was more active than the crude extract in inhibiting HepG2 cell viability. Additionally, EEF also decreased cell proliferation, and induced the cell cycle arrest in G2/M. Our previous results strongly suggested that autophagy was modulated by the crude extract of *Fragaria vesca* leaves. Herein, we demonstrated that EEF impairs autophagic flux, possibly leading to the cytoplasmic accumulation of autophagosomes that are not efficiently degraded. Along with the inhibition of autophagy, EEF also promoted the accumulation of ubiquitinated proteins, inhibited chymotrypsin-like activity of 26S proteasome and decreased the expression of several proteasome subunits, indicating an impairment of UPS degradation. Furthermore, the proteomic analysis allowed the identification of differentially expressed proteins from several functional clusters, primarily affecting metabolic processes.

Overall, several cellular and molecular targets of EEF, and most probably of ellagitannins, were unveiled, suggesting that these compounds could be potential therapeutic agents against hepatocellular carcinoma. However, future studies should be considered in order to dissect the effect of EEF isolated compounds and also to investigate the synergism between ellagitannins and conventional chemotherapeutic agents.

ACKNOWLEDGMENTS

We acknowledge FEDER/COMPETE (FCOMP-01-0124-FEDER-011096), Fundação para a Ciência e a Tecnologia - Portugal, European Union and QREN for funding the projects PTDC/SAU-FCF/105429/2008, PEst-C/SAU/LA0001/2013-2014, PEst-C/QUI/UI0062/2013, the Ph.D. fellowship SFRH/BD/72918/2010 and the QOPNA research unit (project PEst-C/QUI/UI0062/2013; FCOMP-01-0124-FEDER-037296). We also thank the Portuguese National Mass Spectrometry Network (RNEM, REDE/1504/REM/2005) for MS analyses obtained in Nodes CEF/Universidade de Coimbra and Universidade de Aveiro.

SUPPLEMENTARY DATA

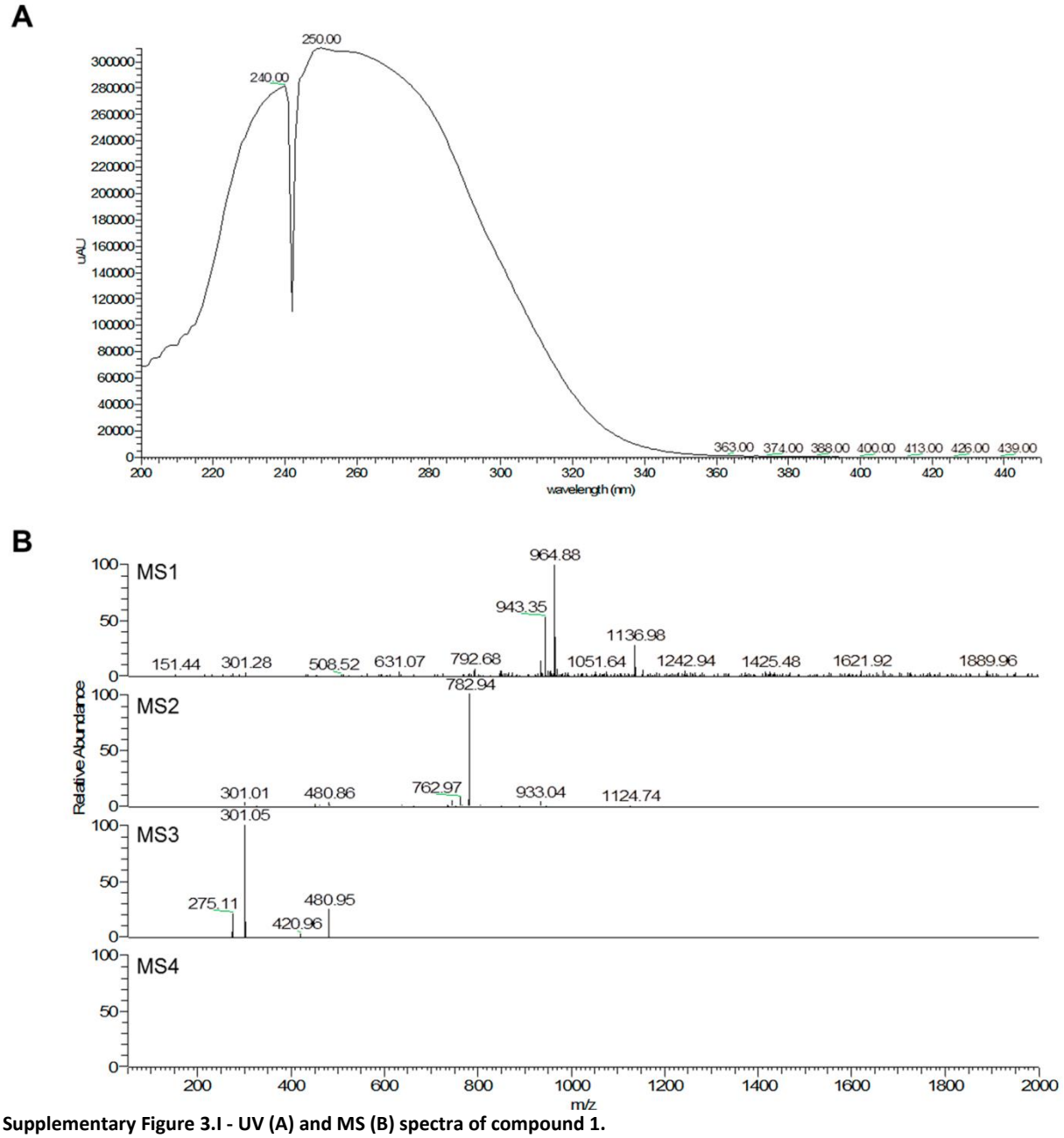

Supplementary Figure 3.I - UV (A) and MS (B) spectra of compound 1.

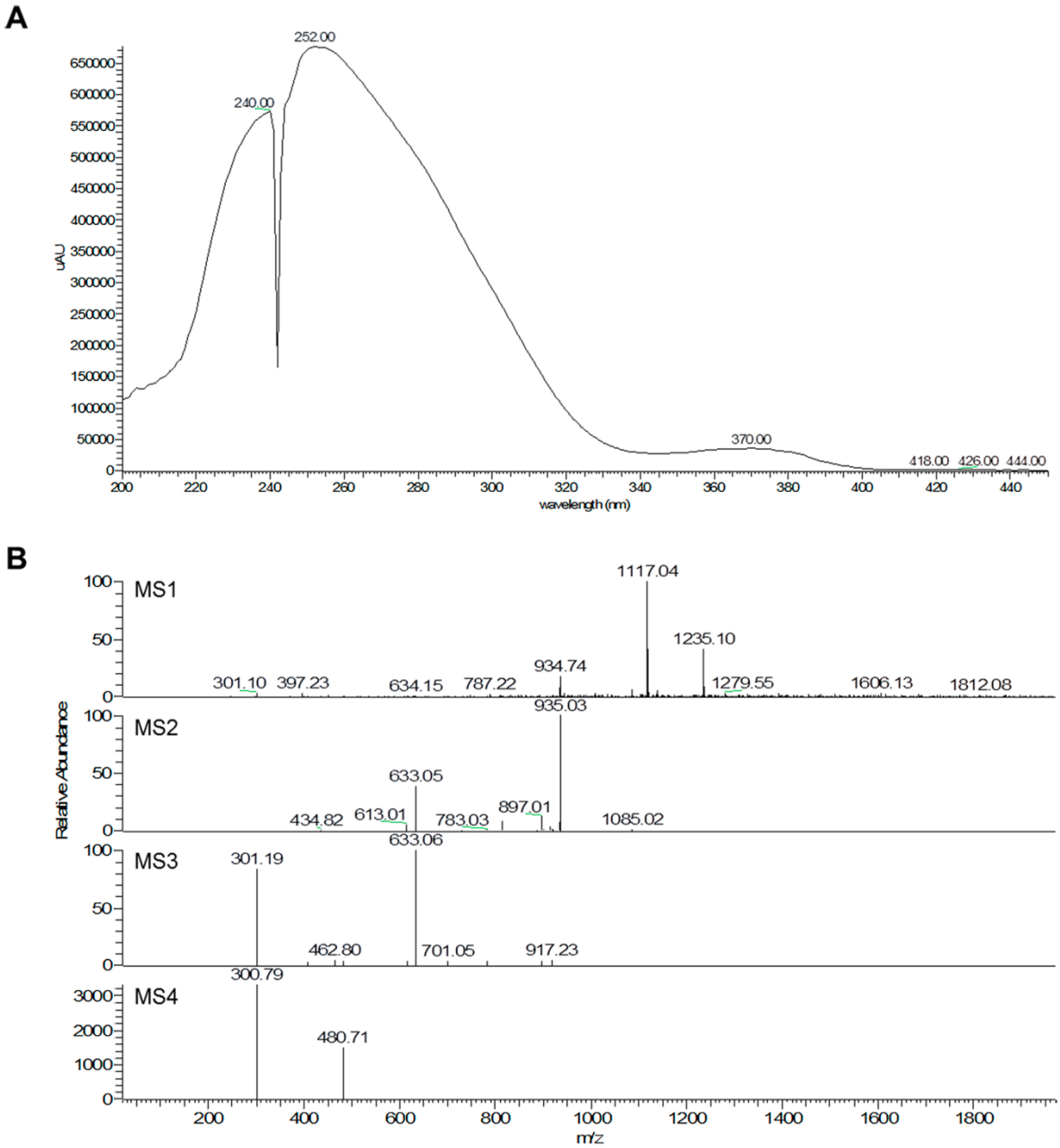

Supplementary Figure 3.II - UV (A) and MS (B) spectra of compound 11.

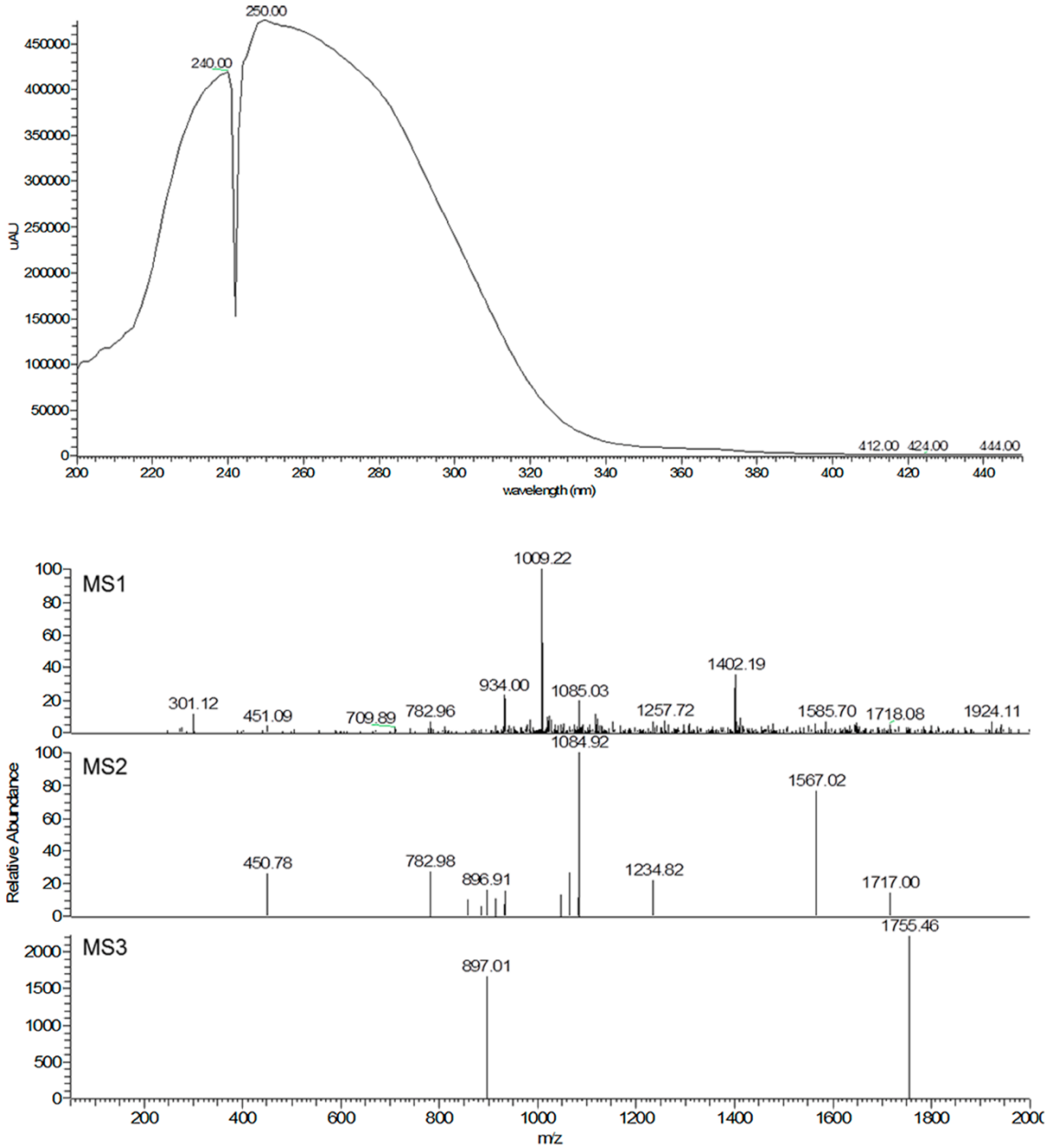

Supplementary Figure 3.III - UV (A) and MS (B) spectra of compound 12.

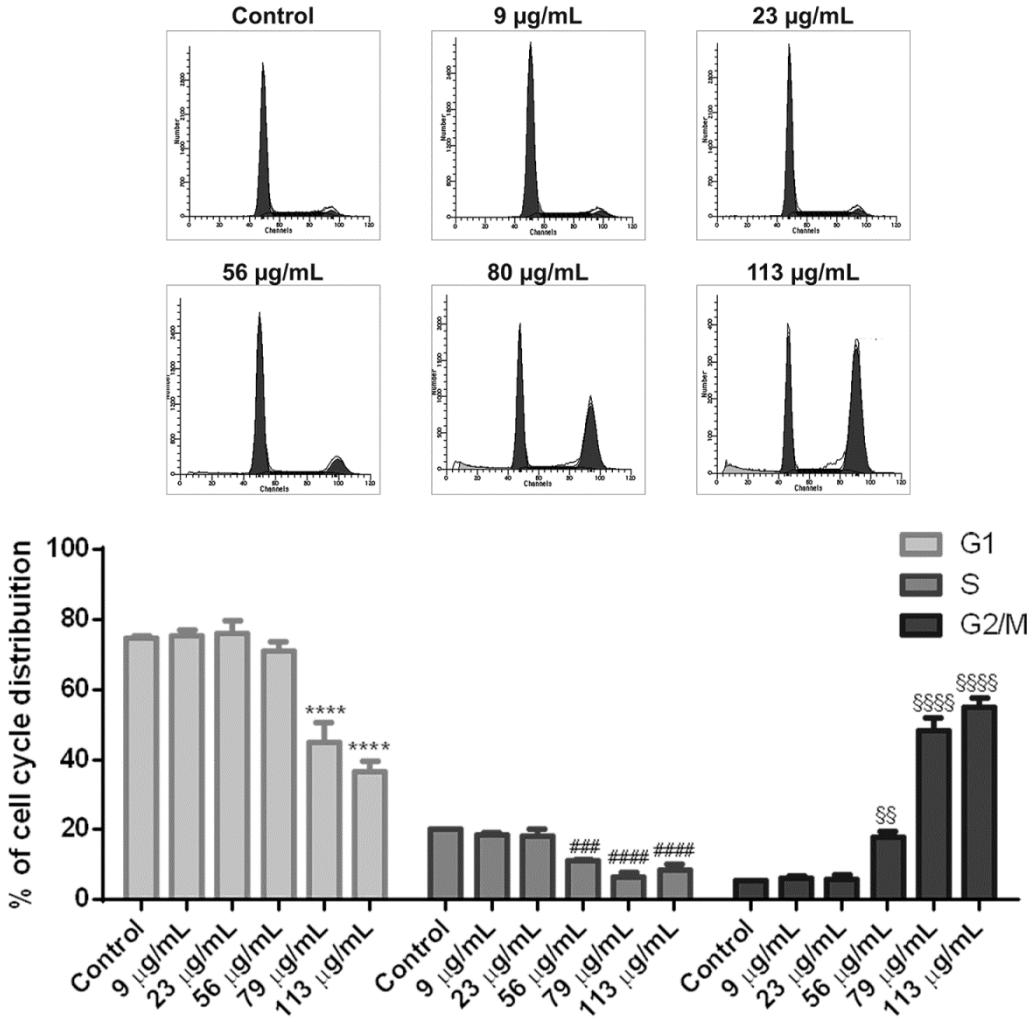

Supplementary Figure 3.IV - Effect of 48 h of EEF treatment on HepG2 cell cycle. Data are expressed as percentage of PI-positive cells and are given as the means ± SEM of at least three independent experiments (** p<0.01, ***p<0.001, * ***p<0.0001 when compared to control; the symbols *, #, $ were used for G1, S, G2/M, respectively).

Supplementary Table 3.I - List of all proteins identified in HepG2 cells.

Protein name	Accession	Mass	Ratio	Hit	Score
10 kDa heat shock protein, mitochondrial	CH10_HUMAN	14575	1,403474903	33	526
116 kDa U5 small nuclear ribonucleoprotein component	U5S1_HUMAN	127619	-	40,2	96
14-3-3 protein beta/alpha	1433B_HUMAN	34453	0,707920792	69,1	327
14-3-3 protein epsilon	1433E_HUMAN	34935	0,544927536	69,5	216
14-3-3 protein gamma	1433G_HUMAN	33761	0,735384615	69,3	270
14-3-3 protein sigma	1433S_HUMAN	33232	0,739255014	69,6	179
14-3-3 protein theta	1433T_HUMAN	33831	0,739255014	69,4	235
14-3-3 protein zeta/delta	1433Z_HUMAN	34116	0,79787234	69,2	305
2',3'-cyclic-nucleotide 3'-phosphodiesterase	CN37_HUMAN	59717	-	664	33
2,4-dienoyl-CoA reductase, mitochondrial	DECR_HUMAN	43954	-	532	45
26S protease regulatory subunit 10B	PRS10_HUMAN	53575	-	521	47
26S protease regulatory subunit 4	PRS4_HUMAN	63147	0,763358779	493,1	50
26S protease regulatory subunit 6A	PRS6A_HUMAN	60428	-	549	44
26S protease regulatory subunit 7	PRS7_HUMAN	58642	-	284	91
26S protease regulatory subunit 8	PRS8_HUMAN	55940	-	493,2	45
26S proteasome non-ATPase regulatory subunit 1	PSMD1_HUMAN	127367	-	705	30
26S proteasome non-ATPase regulatory subunit 13	PSD13_HUMAN	50219	-	755	26
26S proteasome non-ATPase regulatory subunit 2	PSMD2_HUMAN	115954	-	160	168
26S proteasome non-ATPase regulatory subunit 4	PSMD4_HUMAN	48316	-	673	33
26S proteasome non-ATPase regulatory subunit 6	PSMD6_HUMAN	53716	-	559	43
28S ribosomal protein S2, mitochondrial	RT02_HUMAN	36574	-	802	22
28S ribosomal protein S23, mitochondrial	RT23_HUMAN	26016	-	457	54
28S ribosomal protein S28, mitochondrial	RT28_HUMAN	25089	-	551	44
28S ribosomal protein S7, mitochondrial	RT07_HUMAN	35721	-	834	19
28S ribosomal protein S9, mitochondrial	RT09_HUMAN	55845	-	773	24
2-oxoglutarate dehydrogenase, mitochondrial	ODO1_HUMAN	131376	-	678	32
39S ribosomal protein L14, mitochondrial	RM14_HUMAN	19588	-	703	30
39S ribosomal protein L19, mitochondrial	RM19_HUMAN	40206	-	340	76
39S ribosomal protein L38, mitochondrial	RM38_HUMAN	48523	-	508	48
39S ribosomal protein L4, mitochondrial	RM04_HUMAN	39156	-	305	85
39S ribosomal protein L41, mitochondrial	RM41_HUMAN	19023	-	756	26
39S ribosomal protein L44, mitochondrial	RM44_HUMAN	44204	-	290	89
39S ribosomal protein L49, mitochondrial	RM49_HUMAN	21924	-	341	76
3-ketoacyl-CoA thiolase, peroxisomal	THIK_HUMAN	50348	-	596	39
3-mercaptopyruvate sulfurtransferase	THTM_HUMAN	36504	-	327	79
40S ribosomal protein S10	RS10_HUMAN	23145	0,857908847	90	263
40S ribosomal protein S11	RS11_HUMAN	25112	0,804674457	515	47
40S ribosomal protein S12	RS12_HUMAN	19677	0,807073955	287	90
40S ribosomal protein S13	RS13_HUMAN	22992	0,842696629	188	135
40S ribosomal protein S14	RS14_HUMAN	20217	-	246	107
40S ribosomal protein S15	RS15_HUMAN	22201	-	817	20
40S ribosomal protein S15a	RS15A_HUMAN	18480	-	433	57
40S ribosomal protein S16	RS16_HUMAN	21607	0,805031447	187	135
40S ribosomal protein S17-like	RS17L_HUMAN	19799	-	362	70
40S ribosomal protein S18	RS18_HUMAN	22879	-	112	225
40S ribosomal protein S19	RS19_HUMAN	20918	0,830564784	118	216
40S ribosomal protein S2	RS2_HUMAN	38910	0,858995138	338	77
40S ribosomal protein S20	RS20_HUMAN	17623	-	307	84
40S ribosomal protein S21	RS21_HUMAN	11235	-	618	38
40S ribosomal protein S23	RS23_HUMAN	22186	0,69771529	215	120
40S ribosomal protein S25	RS25_HUMAN	22251	-	445	55
40S ribosomal protein S28	RS28_HUMAN	9053	0,741935484	91	261
40S ribosomal protein S29	RS29_HUMAN	8193	-	524	47
40S ribosomal protein S3	RS3_HUMAN	33060	0,761609907	142	182
40S ribosomal protein S30	RS30_HUMAN	10903	-	593	40
40S ribosomal protein S3a	RS3A_HUMAN	41790	0,90060241	50	405
40S ribosomal protein S4, X isoform	RS4X_HUMAN	38097	0,721568627	152,1	171

Protein name	Accession	Mass	Ratio	Hit	Score
40S ribosomal protein S4, Y isoform 1	RS4Y1_HUMAN	37651	-	152,2	116
40S ribosomal protein S5	RS5_HUMAN	28034	-	333	77
40S ribosomal protein S6	RS6_HUMAN	39919	0,779661017	225	115
40S ribosomal protein S7	RS7_HUMAN	29718	0,799007444	174	149
40S ribosomal protein S8	RS8_HUMAN	33925	0,665016502	296	87
40S ribosomal protein S9	RS9_HUMAN	28662	0,755639098	203	126
40S ribosomal protein SA	RSSA_HUMAN	36484	-	44	443
45 kDa calcium-binding protein	CAB45_HUMAN	48777	-	744	27
4F2 cell-surface antigen heavy chain	4F2_HUMAN	77078	-	314	83
5'-3' exoribonuclease 2	XRN2_HUMAN	125549	-	239	111
5'-nucleotidase domain-containing protein 2	NT5D2_HUMAN	67372	-	655	34
60 kDa heat shock protein, mitochondrial	CH60_HUMAN	77443	1,422735346	4	1645
60S acidic ribosomal protein P0	RLA0_HUMAN	40336	-	399	63
60S acidic ribosomal protein P1	RLA1_HUMAN	13940	0,927480916	421	59
60S acidic ribosomal protein P2	RLA2_HUMAN	15004	-	336	77
60S ribosomal protein L10	RL10_HUMAN	31889	0,75862069	259	101
60S ribosomal protein L10a	RL10A_HUMAN	34550	-	505	48
60S ribosomal protein L11	RL11_HUMAN	25411	-	785	23
60S ribosomal protein L12	RL12_HUMAN	22675	-	581	40
60S ribosomal protein L13	RL13_HUMAN	32156	0,838495575	113	224
60S ribosomal protein L13a	RL13A_HUMAN	32384	0,991596639	499	49
60S ribosomal protein L14	RL14_HUMAN	34977	-	309	84
60S ribosomal protein L15	RL15_HUMAN	29607	0,711340206	210	122
60S ribosomal protein L17	RL17_HUMAN	29293	0,794871795	448	55
60S ribosomal protein L18	RL18_HUMAN	27705	-	171	152
60S ribosomal protein L18a	RL18A_HUMAN	26225	0,681547619	588	40
60S ribosomal protein L19	RL19_HUMAN	33490	-	207	123
60S ribosomal protein L21	RL21_HUMAN	26158	-	638	36
60S ribosomal protein L22	RL22_HUMAN	20862	1,016194332	81	282
60S ribosomal protein L23	RL23_HUMAN	19723	-	592	40
60S ribosomal protein L23a	RL23A_HUMAN	27115	0,890196078	480	52
60S ribosomal protein L24	RL24_HUMAN	26286	-	430	57
60S ribosomal protein L26	RL26_HUMAN	24853	0,822147651	244	107
60S ribosomal protein L27	RL27_HUMAN	23089	-	737	27
60S ribosomal protein L27a	RL27A_HUMAN	22635	-	424	58
60S ribosomal protein L28	RL28_HUMAN	20301	-	835	19
60S ribosomal protein L29	RL29_HUMAN	27780	-	294	88
60S ribosomal protein L3	RL3_HUMAN	63419	0,757425743	232	113
60S ribosomal protein L30	RL30_HUMAN	17339	-	686	32
60S ribosomal protein L31	RL31_HUMAN	19625	0,954248366	444	56
60S ribosomal protein L34	RL34_HUMAN	18456	0,802631579	720	29
60S ribosomal protein L35	RL35_HUMAN	22756	0,943342776	625	37
60S ribosomal protein L35a	RL35A_HUMAN	16180	-	722	28
60S ribosomal protein L38	RL38_HUMAN	13384	-	579	41
60S ribosomal protein L4	RL4_HUMAN	65311	-	159	168
60S ribosomal protein L5	RL5_HUMAN	45292	0,906976744	238	111
60S ribosomal protein L6	RL6_HUMAN	48831	0,75255102	176	146
60S ribosomal protein L7	RL7_HUMAN	39854	0,832460733	170	155
60S ribosomal protein L7a	RL7A_HUMAN	42145	0,846666667	277	94
60S ribosomal protein L8	RL8_HUMAN	36221	-	199	129
6-phosphofructokinase, liver type	K6PL_HUMAN	96524	-	414	60
6-phosphogluconate dehydrogenase, decarboxylating	6PGD_HUMAN	64057	0,571428571	146	176
78 kDa glucose-regulated protein	GRP78_HUMAN	91149	1,279816514	2,1	2360
7-dehydrocholesterol reductase	DHCR7_HUMAN	60234	1,351648352	439	56
Acetyl-CoA acetyltransferase, cytosolic	THIC_HUMAN	48017	-	830	19
Acetyl-CoA acetyltransferase, mitochondrial	THIL_HUMAN	54601	-	80	283
Acidic leucine-rich nuclear phosphoprotein 32 family member A	AN32A_HUMAN	33740	0,455026455	346,1	75
Acidic leucine-rich nuclear phosphoprotein 32 family member B	AN32B_HUMAN	34246	0,449197861	346,2	36
Aconitate hydratase, mitochondrial	ACON_HUMAN	102407	-	240	109

Protein name	Accession	Mass	Ratio	Hit	Score
Actin, alpha cardiac muscle 1	ACTC_HUMAN	48076	1,169230769	1,2	1918
Actin, cytoplasmic 1	ACTB_HUMAN	47794	1,174603175	1,1	2848
Actin-related protein 2	ARP2_HUMAN	52642	0,5	1,4	65
Actin-related protein 2/3 complex subunit 3	ARPC3_HUMAN	26313	-	604	39
Actin-related protein 3	ARP3_HUMAN	54642	-	489	50
Activated RNA polymerase II transcriptional coactivator p15	TCP4_HUMAN	20471	-	702	30
Activator of 90 kDa heat shock protein ATPase homolog 1	AHSA1_HUMAN	46768	-	316	82
Activin receptor type-1B	ACV1B_HUMAN	64071	-	808	21
Acylamino-acid-releasing enzyme	ACPH_HUMAN	89995	-	379	67
Acyl-coenzyme A thioesterase 1	ACOT1_HUMAN	52028	1,031746032	140	184
Adenine phosphoribosyltransferase	APT_HUMAN	22333	-	367	70
Adenosylhomocysteinase	SAHH_HUMAN	56811	-	64	346
Adenylate kinase 2, mitochondrial	KAD2_HUMAN	32545	1,080357143	217	118
Adenylate kinase isoenzyme 4, mitochondrial	KAD4_HUMAN	29815	1,138461538	233	113
Adipocyte plasma membrane-associated protein	APMAP_HUMAN	51622	-	482	52
ADP/ATP translocase 3	ADT3_HUMAN	39842	-	253	102
ADP-ribosylation factor 3	ARF3_HUMAN	24847	-	763	25
ADP-sugar pyrophosphatase	NUDT5_HUMAN	29180	-	609	38
AFG3-like protein 2	AFG32_HUMAN	107693	-	658	34
Aflatoxin B1 aldehyde reductase member 2	ARK72_HUMAN	43823	-	777	24
Agmatinase, mitochondrial	SPEB_HUMAN	40678	1,063829787	403	63
Alanine aminotransferase 2	ALAT2_HUMAN	66993	-	520	47
Alanine--tRNA ligase, cytoplasmic	SYAC_HUMAN	127125	-	467	53
Aldehyde dehydrogenase X, mitochondrial	AL1B1_HUMAN	66905	-	181	141
Aldehyde dehydrogenase, mitochondrial	ALDH2_HUMAN	65472	-	103,1	235
Aldo-keto reductase family 1 member C1	AK1C1_HUMAN	44979	-	204	125
Alpha-1-antitrypsin	A1AT_HUMAN	57354	1,477941176	273	96
Alpha-2-HS-glycoprotein	FETUA_HUMAN	44471	-	469	53
Alpha-2-macroglobulin	A2MG_HUMAN	190566	-	605	39
Alpha-2-macroglobulin receptor-associated protein	AMRP_HUMAN	52088	-	446	55
Alpha-actinin-1	ACTN1_HUMAN	119724	-	30,2	291
Alpha-actinin-4	ACTN4_HUMAN	122737	1,100334448	30,1	572
Alpha-aminoadipic semialdehyde dehydrogenase	AL7A1_HUMAN	67880	-	317	82
Alpha-enolase	ENOA_HUMAN	59003	0,573913043	8	1231
Alpha-fetoprotein	FETA_HUMAN	81714	1,264637002	380	67
Aminoacylase-1	ACY1_HUMAN	50723	-	687	32
Aminopeptidase N	AMPN_HUMAN	123464	-	793	23
Amyloid-like protein 2	APLP2_HUMAN	99981	-	408	62
Ankyrin repeat domain-containing protein 35	ANR35_HUMAN	128151	-	601	39
Annexin A11	ANX11_HUMAN	61960	-	428	57
Annexin A3	ANXA3_HUMAN	44566	-	271	96
Annexin A4	ANXA4_HUMAN	42857	-	111	226
Annexin A5	ANXA5_HUMAN	42911	0,539735099	61	354
Annexin A6	ANXA6_HUMAN	91948	-	303	86
Annexin A7	ANXA7_HUMAN	57269	-	281	92
AP-1 complex subunit beta-1	AP1B1_HUMAN	123735	-	633	37
AP-1 complex subunit sigma-1A	AP1S1_HUMAN	23284	-	460	54
AP-2 complex subunit alpha-2	AP2A2_HUMAN	119714	-	728	28
Apolipoprotein A-I	APOA1_HUMAN	37756	-	818	20
Apolipoprotein E	APOE_HUMAN	40391	-	401	63
Apoptosis regulator BAX	BAX_HUMAN	24213	-	494	50
Apoptosis-inducing factor 2	AIFM2_HUMAN	46890	-	757	26
Apoptotic chromatin condensation inducer in the nucleus	ACINU_HUMAN	181279	-	353	73
Arginine--tRNA ligase, cytoplasmic	SYRC_HUMAN	92366	-	789	23
Asialoglycoprotein receptor 1	ASGR1_HUMAN	37424	-	436	56
Aspartate aminotransferase, cytoplasmic	AATC_HUMAN	52911	0,687272727	286	91
Aspartate aminotransferase, mitochondrial	AATM_HUMAN	56613	1,308300395	70	315
Aspartate--tRNA ligase, cytoplasmic	SYDC_HUMAN	66226	0,853125	423	58
Ataxin-2-like protein	ATX2L_HUMAN	126993	-	845	17

Protein name	Accession	Mass	Ratio	Hit	Score
ATP synthase subunit alpha, mitochondrial	ATPA_HUMAN	69144	1,197612732	26	676
ATP synthase subunit beta, mitochondrial	ATPB_HUMAN	63826	1,205607477	16	869
ATP synthase subunit d, mitochondrial	ATP5H_HUMAN	24868	-	667	33
ATP synthase subunit delta, mitochondrial	ATPD_HUMAN	19000	-	224	115
ATP synthase subunit e, mitochondrial	ATP5I_HUMAN	10362	-	500	49
ATP synthase subunit f, mitochondrial	ATPK_HUMAN	14257	1,125	552	43
ATP synthase subunit gamma, mitochondrial	ATPG_HUMAN	41189	-	572	41
ATP synthase subunit O, mitochondrial	ATPO_HUMAN	29043	-	491	50
ATP synthase-coupling factor 6, mitochondrial	ATP5J_HUMAN	15926	-	368	69
ATPase family AAA domain-containing protein 3A	ATD3A_HUMAN	82580	-	740	27
ATPase inhibitor, mitochondrial	ATIF1_HUMAN	15588	-	635	36
ATP-binding cassette sub-family F member 1	ABCF1_HUMAN	126895	-	610	38
ATP-citrate synthase	ACLY_HUMAN	142969	-	779	24
ATP-dependent RNA helicase A	DHX9_HUMAN	160947	1	32	528
ATP-dependent RNA helicase DDX3X	DDX3X_HUMAN	83237	0,940092166	84,3	203
ATP-dependent RNA helicase DDX42	DDX42_HUMAN	122989	-	443	56
ATP-dependent RNA helicase DDX50	DDX50_HUMAN	100158	-	71,2	128
Basic leucine zipper and W2 domain-containing protein 1	BZW1_HUMAN	61398	-	651	34
Basigin	BASI_HUMAN	47650	-	200	129
Bcl-2-associated transcription factor 1	BCLF1_HUMAN	134350	-	746	27
Beta-1-syntrophin	SNTB1_HUMAN	68368	-	514	47
Beta-catenin-like protein 1	CTBL1_HUMAN	76388	-	574	41
Beta-hexosaminidase subunit alpha	HEXA_HUMAN	66748	-	813	20
Bifunctional ATP-dependent dihydroxyacetone kinase/FAD-AMP lyase (cyclizing)	DHAK_HUMAN	67732	0,447228312	114	223
Bifunctional glutamate/proline--tRNA ligase	SYEP_HUMAN	215810	-	220	117
Bifunctional methylenetetrahydrofolate dehydrogenase/cyclohydrolase, mitochondrial	MTDC_HUMAN	44868	-	509	48
Bifunctional purine biosynthesis protein PURH	PUR9_HUMAN	76135	-	117	218
BolA-like protein 1	BOLA1_HUMAN	15497	-	848	16
BolA-like protein 2	BOLA2_HUMAN	11935	-	458	54
C-1-tetrahydrofolate synthase, cytoplasmic	C1TC_HUMAN	120660	-	412	60
Calmodulin	CALM_HUMAN	19565	-	133	192
Calnexin	CALX_HUMAN	84561	1,291566265	382	67
Calreticulin	CALR_HUMAN	61193	1,425474255	94	259
Calumenin	CALU_HUMAN	46210	1,172413793	157	169
cAMP-dependent protein kinase type II-beta regulatory subunit	KAP3_HUMAN	53270	-	836	18
Carcinoembryonic antigen-related cell adhesion molecule 1	CEAM1_HUMAN	63609	-	700	31
Casein kinase II subunit beta	CSK2B_HUMAN	27968	-	713	29
Catalase	CATA_HUMAN	69149	-	804	22
Catenin alpha-1	CTNA1_HUMAN	122824	-	293	88
Catenin beta-1	CTNB1_HUMAN	93656	-	280	93
Catenin delta-1	CTND1_HUMAN	124835	-	533	45
Cathepsin B	CATB_HUMAN	42664	1,336206897	258	101
Cathepsin D	CATD_HUMAN	51825	1,266094421	291	89
CDKN2AIP N-terminal-like protein	C2AIL_HUMAN	15317	-	568	42
Cell division cycle 5-like protein	CDC5L_HUMAN	115922	-	776	24
Chloride intracellular channel protein 1	CLIC1_HUMAN	32686	-	585	40
Chloride intracellular channel protein 4	CLIC4_HUMAN	36663	-	483	52
Chromobox protein homolog 3	CBX3_HUMAN	28708	-	721	29
Chromodomain-helicase-DNA-binding protein 8	CHD8_HUMAN	342357	-	815	20
Citrate synthase, mitochondrial	CISY_HUMAN	59893	1,044444444	123	202
Citron Rho-interacting kinase	CTRO_HUMAN	277829	-	645	35
Clathrin heavy chain 1	CLH1_HUMAN	221000	-	137	185
Clathrin light chain A	CLCA_HUMAN	31015	0,964285714	504	49
Cleavage and polyadenylation specificity factor subunit 5	CPSF5_HUMAN	30774	-	708	30
Cleavage stimulation factor subunit 2	CSTF2_HUMAN	65179	-	617	38
Coatomer subunit alpha	COPA_HUMAN	163811	0,846590909	391	65
Coatomer subunit beta'	COPB2_HUMAN	119458	-	573	41
Cocaine esterase	EST2_HUMAN	67851	-	580	40

Protein name	Accession	Mass	Ratio	Hit	Score
Cofilin-1	COF1_HUMAN	26400	0,693679092	163	166
Coiled-coil domain-containing protein 124	CC124_HUMAN	34033	-	569	41
Coiled-coil-helix-coiled-coil-helix domain-containing protein 2, mitochondrial	CHCH2_HUMAN	16720	-	697	31
Cold shock domain-containing protein E1	CSDE1_HUMAN	107385	-	803	22
Cold-inducible RNA-binding protein	CIRBP_HUMAN	20766	-	501	49
Complement C3	CO3_HUMAN	221709	-	183	140
Complement component 1 Q subcomponent-binding protein, mitochondrial	C1QBP_HUMAN	36514	-	661	33
COP9 signalosome complex subunit 7b	CSN7B_HUMAN	35688	-	843	17
Copine-1	CPNE1_HUMAN	66322	-	780	24
Coproporphyrinogen-III oxidase, mitochondrial	HEM6_HUMAN	57117	-	487	51
Core histone macro-H2A.1	H2AY_HUMAN	54499	-	205	124
Coronin-1C	COR1C_HUMAN	64471	-	347	75
Coxsackievirus and adenovirus receptor	CXAR_HUMAN	48826	-	541	44
Creatine kinase B-type	KCRB_HUMAN	49310	-	677	32
C-terminal-binding protein 1	CTBP1_HUMAN	52069	-	748	26
CUB and sushi domain-containing protein 2	CSMD2_HUMAN	408391	-	823	20
Cystatin-B	CYTB_HUMAN	14175	0,562700965	684	32
Cystatin-C	CYTC_HUMAN	18223	-	308	84
Cysteine desulfurase, mitochondrial	NFS1_HUMAN	57161	-	696	31
Cysteine-rich protein 1	CRIP1_HUMAN	11873	-	750	26
Cytochrome b5	CYB5_HUMAN	18058	-	120	209
Cytochrome b-c1 complex subunit 2, mitochondrial	QCR2_HUMAN	56018	-	324	80
Cytochrome b-c1 complex subunit 8	QCR8_HUMAN	11421	-	798	22
Cytochrome c	CYC_HUMAN	17521	-	442	56
Cytochrome c oxidase subunit 2	COX2_HUMAN	27069	-	704	30
Cytochrome c oxidase subunit 4 isoform 1, mitochondrial	COX41_HUMAN	25952	-	261	100
Cytochrome c oxidase subunit 5B, mitochondrial	COX5B_HUMAN	15816	-	544	44
Cytochrome c oxidase subunit 6C	COX6C_HUMAN	11209	-	831	19
Cytoplasmic dynein 1 intermediate chain 2	DC1I2_HUMAN	83885	-	426	57
Cytoskeleton-associated protein 4	CKAP4_HUMAN	78455	1,214788732	105	233
Cytosol aminopeptidase	AMPL_HUMAN	67386	-	321	81
Cytosolic acyl coenzyme A thioester hydrolase	BACH_HUMAN	48766	-	778	24
D-3-phosphoglycerate dehydrogenase	SERA_HUMAN	64828	0,736585366	279	94
DAZ-associated protein 1	DAZP1_HUMAN	49136	-	400	63
DBIRD complex subunit KIAA1967	K1967_HUMAN	116831	-	627	37
DBIRD complex subunit ZNF326	ZN326_HUMAN	77781	-	801	22
D-dopachrome decarboxylase	DOPD_HUMAN	14225	-	450	55
Dehydrogenase/reductase SDR family member 2	DHRS2_HUMAN	31680	1,104615385	107	232
Delta(24)-sterol reductase	DHC24_HUMAN	69797	-	172	151
Delta(3,5)-Delta(2,4)-dienoyl-CoA isomerase, mitochondrial	ECH1_HUMAN	41269	1,180451128	56	373
Delta-1-pyrroline-5-carboxylate dehydrogenase, mitochondrial	AL4A1_HUMAN	72936	1,247272727	62	353
Delta-1-pyrroline-5-carboxylate synthase	P5CS_HUMAN	99112	1,277486911	59	363
DENN domain-containing protein 4B	DEN4B_HUMAN	175607	-	847	16
Deoxyuridine 5'-triphosphate nucleotidohydrolase, mitochondrial	DUT_HUMAN	30197	-	799	22
Desmoplakin	DESP_HUMAN	406099	1,005882353	180	141
Developmentally-regulated GTP-binding protein 1	DRG1_HUMAN	52077	-	598	39
Diablo homolog, mitochondrial	DBLOH_HUMAN	31373	-	631	37
Dihydrolipoyl dehydrogenase, mitochondrial	DLDH_HUMAN	66007	-	393	65
Dihydrolipoyllysine-residue succinyltransferase component of 2-oxoglutarate dehydrogenase complex, mitochondrial	ODO2_HUMAN	57242	1,291457286	178	142
Dihydropyrimidinase-related protein 2	DPYL2_HUMAN	72293	-	710	30
Dimethyladenosine transferase 1, mitochondrial	TFB1M_HUMAN	47123	-	639	36
Dipeptidyl peptidase 1	CATC_HUMAN	59730	-	409	62
DNA fragmentation factor subunit alpha	DFFA_HUMAN	42584	-	718	29
DNA replication licensing factor MCM2	MCM2_HUMAN	115217	-	736	27
DNA topoisomerase 1	TOP1_HUMAN	131737	-	495	50
DNA-(apurinic or apyrimidinic site) lyase	APEX1_HUMAN	44658	-	416	59
DNA-binding protein A	DBPA_HUMAN	44629	0,93040293	257,1	102
DNA-dependent protein kinase catalytic subunit	PRKDC_HUMAN	553053	1,06870229	78	287
DnaJ homolog subfamily A member 1	DNJA1_HUMAN	56095	-	490	50

Protein name	Accession	Mass	Ratio	Hit	Score
DnaJ homolog subfamily A member 3, mitochondrial	DNJA3_HUMAN	62798	-	473	53
DnaJ homolog subfamily B member 11	DJB11_HUMAN	48398	-	530	46
DnaJ homolog subfamily C member 8	DNJC8_HUMAN	40775	-	599	39
Dolichol-phosphate mannosyltransferase	DPM1_HUMAN	35396	-	760	25
Dolichyl-diphosphooligosaccharide--protein glycosyltransferase 48 kDa subunit	OST48_HUMAN	57461	-	245	107
Dolichyl-diphosphooligosaccharide--protein glycosyltransferase subunit 1	RPN1_HUMAN	80999	-	58	369
Dolichyl-diphosphooligosaccharide--protein glycosyltransferase subunit 2	RPN2_HUMAN	78367	1,028776978	674	33
Dolichyl-diphosphooligosaccharide--protein glycosyltransferase subunit STT3A	STT3A_HUMAN	89299	-	292	89
Dolichyl-diphosphooligosaccharide--protein glycosyltransferase subunit STT3B	STT3B_HUMAN	106999	-	434	57
Double-stranded RNA-binding protein Staufen homolog 1	STAU1_HUMAN	78353	-	266	98
Double-stranded RNA-specific adenosine deaminase	DSRAD_HUMAN	163359	-	398	64
Drebrin	DREB_HUMAN	78382	-	837	18
Dynein light chain roadblock-type 1	DLRB1_HUMAN	13348	-	471	53
E3 ubiquitin-protein ligase UHRF1	UHRF1_HUMAN	105576	-	806	21
Echinoderm microtubule-associated protein-like 4	EMAL4_HUMAN	129230	-	230	114
ELAV-like protein 1	ELAV1_HUMAN	41849	1,004784689	150	171
Electron transfer flavoprotein subunit alpha, mitochondrial	ETFA_HUMAN	43271	1,428571429	96	252
Electron transfer flavoprotein subunit beta	ETFB_HUMAN	35735	1,186206897	144	181
Elongation factor 1-alpha 1	EF1A1_HUMAN	64711	0,640569395	46	424
Elongation factor 1-beta	EF1B_HUMAN	31745	0,908256881	299	86
Elongation factor 1-delta	EF1D_HUMAN	37491	-	141	183
Elongation factor 1-gamma	EF1G_HUMAN	60126	0,916666667	128	198
Elongation factor 2	EF2_HUMAN	115355	0,692307692	40,1	478
Elongation factor G, mitochondrial	EFGM_HUMAN	98933	-	749	26
Elongation factor Tu, mitochondrial	EFTU_HUMAN	58941	1,118589744	36	498
Emerin	EMD_HUMAN	31105	-	365	70
Endoplasmic reticulum resident protein 29	ERP29_HUMAN	37493	1,037037037	175	147
Endoplasmin	ENPL_HUMAN	116444	1,334916865	6,2	1281
Endothelial differentiation-related factor 1	EDF1_HUMAN	22747	-	730	28
Enhancer of rudimentary homolog	ERH_HUMAN	14685	-	827	19
Enoyl-CoA delta isomerase 1, mitochondrial	ECI1_HUMAN	36750	-	682	32
Enoyl-CoA delta isomerase 2, mitochondrial	ECI2_HUMAN	53900	-	733	28
Enoyl-CoA hydratase, mitochondrial	ECHM_HUMAN	38972	1,073732719	86	267
Epiplakin	EPIPL_HUMAN	595130	1,315151515	73,1	305
Erlin-1	ERLN1_HUMAN	48636	-	221	116
ERO1-like protein alpha	ERO1A_HUMAN	63484	-	550	44
ES1 protein homolog, mitochondrial	ES1_HUMAN	33628	-	510	48
Espin	ESPN_HUMAN	103235	-	800	22
Estradiol 17-beta-dehydrogenase 2	DHB2_HUMAN	50971	-	650	35
Ethanolamine-phosphate cytidylyltransferase	PCY2_HUMAN	50196	-	385	67
Ethylmalonyl-CoA decarboxylase	ECHD1_HUMAN	41282	-	819	20
Eukaryotic initiation factor 4A-I	IF4A1_HUMAN	52513	-	132,1	194
Eukaryotic initiation factor 4A-III	IF4A3_HUMAN	54142	1,114035088	132,2	146
Eukaryotic peptide chain release factor subunit 1	ERF1_HUMAN	60560	-	531	46
Eukaryotic translation elongation factor 1 epsilon-1	MCA3_HUMAN	23753	-	498	49
Eukaryotic translation initiation factor 1A, X-chromosomal	IF1AX_HUMAN	21622	-	644	35
Eukaryotic translation initiation factor 2 subunit 1	IF2A_HUMAN	42782	-	850	16
Eukaryotic translation initiation factor 2 subunit 2	IF2B_HUMAN	52966	-	519	47
Eukaryotic translation initiation factor 3 subunit A	EIF3A_HUMAN	192934	-	394	65
Eukaryotic translation initiation factor 3 subunit B	EIF3B_HUMAN	108851	-	608	38
Eukaryotic translation initiation factor 3 subunit C	EIF3C_HUMAN	128702	-	464	54
Eukaryotic translation initiation factor 3 subunit G	EIF3G_HUMAN	44715	-	415	60
Eukaryotic translation initiation factor 3 subunit K	EIF3K_HUMAN	28998	-	603	39
Eukaryotic translation initiation factor 3 subunit L	EIF3L_HUMAN	78244	-	358	71
Eukaryotic translation initiation factor 4 gamma 1	IF4G1_HUMAN	204890	-	805	22
Eukaryotic translation initiation factor 4 gamma 2	IF4G2_HUMAN	124808	0,834782609	462	54
Eukaryotic translation initiation factor 4B	IF4B_HUMAN	81279	-	275	95
Eukaryotic translation initiation factor 4H	IF4H_HUMAN	31019	-	459	54
Eukaryotic translation initiation factor 5A-1	IF5A1_HUMAN	21080	0,518987342	274	96

Protein name	Accession	Mass	Ratio	Hit	Score
Eukaryotic translation initiation factor 5B	IF2P_HUMAN	194715	-	699	31
Exosome component 10	EXOSX_HUMAN	123887	-	742	27
Exportin-2	XPO2_HUMAN	128294	-	304	86
Extended synaptotagmin-1	ESYT1_HUMAN	139207	-	486	51
Ezrin	EZRI_HUMAN	86405	1,006711409	131,1	195
FACT complex subunit SPT16	SP16H_HUMAN	152693	-	577	41
FACT complex subunit SSRP1	SSRP1_HUMAN	104448	-	413	60
F-actin-capping protein subunit alpha-2	CAZA2_HUMAN	39621	-	334	77
F-actin-capping protein subunit beta	CAPZB_HUMAN	37719	0,815217391	692	31
Far upstream element-binding protein 1	FUBP1_HUMAN	76340	0,966824645	68,2	193
Far upstream element-binding protein 2	FUBP2_HUMAN	82805	1,063063063	68,1	333
Far upstream element-binding protein 3	FUBP3_HUMAN	69207	-	68,3	91
Farnesyl pyrophosphate synthase	FPPS_HUMAN	55241	-	688	32
Fatty acid synthase	FAS_HUMAN	299416	0,565868263	23	713
Fibronectin	FINC_HUMAN	286492	1,661654135	125	200
Filamin-A	FLNA_HUMAN	329541	0,76284585	53,1	387
Filamin-B	FLNB_HUMAN	330922	0,665480427	53,2	157
Fragile X mental retardation syndrome-related protein 2	FXR2_HUMAN	82696	-	784	24
Frataxin, mitochondrial	FRDA_HUMAN	27380	-	567	42
Fructose-bisphosphate aldolase A	ALDOA_HUMAN	47609	0,493307839	11	1026
Fumarate hydratase, mitochondrial	FUMH_HUMAN	64641	-	265	98
Galectin-1	LEG1_HUMAN	17444	-	528	46
Galectin-3	LEG3_HUMAN	28874	-	229	114
Galectin-3-binding protein	LG3BP_HUMAN	71373	-	330	78
GDP-mannose 4,6 dehydratase	GMDS_HUMAN	50137	0,506459948	546	44
Glucose-6-phosphate 1-dehydrogenase	G6PD_HUMAN	68345	-	255	103
Glucose-6-phosphate isomerase	G6PI_HUMAN	74059	-	226	115
Glucosidase 2 subunit beta	GLU2B_HUMAN	69731	1,209150327	106	232
Glutamate dehydrogenase 1, mitochondrial	DHE3_HUMAN	71702	1,344444444	9	1146
Glutamine--fructose-6-phosphate aminotransferase [isomerizing] 1	GFPT1_HUMAN	92750	-	477	52
Glutamine--tRNA ligase	SYQ_HUMAN	102041	-	364	70
Glutaredoxin-related protein 5, mitochondrial	GLRX5_HUMAN	19964	-	311	83
Glutathione reductase, mitochondrial	GSHR_HUMAN	66868	-	235	113
Glutathione S-transferase omega-1	GSTO1_HUMAN	34849	-	370	69
Glutathione synthetase	GSHB_HUMAN	59349	-	441	56
Glyceraldehyde-3-phosphate dehydrogenase	G3P_HUMAN	44244	0,586872587	17	809
Glycine dehydrogenase [decarboxylating], mitochondrial	GCSP_HUMAN	127259	-	356	72
Glycylpeptide N-tetradecanoyltransferase 1	NMT1_HUMAN	69546	-	662	33
Glypican-3	GPC3_HUMAN	76167	1,135391924	297	87
GMP synthase [glutamine-hydrolyzing]	GUAA_HUMAN	91573	-	752	26
Golgi apparatus protein 1	GSLG1_HUMAN	160929	-	587	40
Golgi resident protein GCP60	GCP60_HUMAN	69986	-	222	116
G-rich sequence factor 1	GRSF1_HUMAN	60089	-	668	33
Growth/differentiation factor 6	GDF6_HUMAN	56105	-	792	23
GrpE protein homolog 1, mitochondrial	GRPE1_HUMAN	31869	-	392	65
GTP:AMP phosphotransferase, mitochondrial	KAD3_HUMAN	30721	-	619	38
GTP-binding nuclear protein Ran	RAN_HUMAN	30188	0,67953668	243	107
GTP-binding protein SAR1a	SAR1A_HUMAN	26307	-	689	32
Guanine nucleotide-binding protein subunit beta-2-like 1	GBLP_HUMAN	40530	0,934579439	237	111
H/ACA ribonucleoprotein complex subunit 4	DKC1_HUMAN	76803	-	715	29
Heat shock 70 kDa protein 1A/1B	HSP71_HUMAN	85524	0,929347826	2,4	521
Heat shock 70 kDa protein 4	HSP74_HUMAN	119216	-	206	124
Heat shock cognate 71 kDa protein	HSP7C_HUMAN	87586	0,867276888	2,3	1225
Heat shock protein 105 kDa	HS105_HUMAN	121444	-	302	86
Heat shock protein 75 kDa, mitochondrial	TRAP1_HUMAN	93749	1,157575758	52	395
Heat shock protein HSP 90-alpha	HS90A_HUMAN	109247	0,567669173	6,3	1179
Heat shock protein HSP 90-beta	HS90B_HUMAN	106332	0,556701031	6,1	1529
Hematological and neurological expressed 1-like protein	HN1L_HUMAN	24310	-	425	58
Hemoglobin subunit alpha	HBA_HUMAN	18898	-	774	24

Protein name	Accession	Mass	Ratio	Hit	Score
Hepatoma-derived growth factor	HDGF_HUMAN	35290	-	724	28
Heterochromatin protein 1-binding protein 3	HP1B3_HUMAN	85506	-	345	75
Heterogeneous nuclear ribonucleoprotein A/B	ROAA_HUMAN	45329	-	219	117
Heterogeneous nuclear ribonucleoprotein A0	ROA0_HUMAN	36602	-	121	209
Heterogeneous nuclear ribonucleoprotein A1	ROA1_HUMAN	44503	1,598290598	5,2	1532
Heterogeneous nuclear ribonucleoprotein A3	ROA3_HUMAN	46263	1,48427673	27	669
Heterogeneous nuclear ribonucleoprotein D0	HNRPD_HUMAN	48449	1,286324786	179,1	142
Heterogeneous nuclear ribonucleoprotein D-like	HNRDL_HUMAN	55231	1,081799591	179,2	64
Heterogeneous nuclear ribonucleoprotein F	HNRPF_HUMAN	50814	1,176470588	21,3	440
Heterogeneous nuclear ribonucleoprotein H	HNRH1_HUMAN	54370	1,260204082	21,1	759
Heterogeneous nuclear ribonucleoprotein H2	HNRH2_HUMAN	54404	1,345489443	21,2	498
Heterogeneous nuclear ribonucleoprotein H3	HNRH3_HUMAN	39641	1,179566563	99	246
Heterogeneous nuclear ribonucleoprotein K	HNRPK_HUMAN	57941	1,071428571	38	484
Heterogeneous nuclear ribonucleoprotein L	HNRPL_HUMAN	73219	1,211991435	189	135
Heterogeneous nuclear ribonucleoprotein M	HNRPM_HUMAN	89937	1,049450549	20	769
Heterogeneous nuclear ribonucleoprotein Q	HNRPQ_HUMAN	83857	1,085858586	57,2	141
Heterogeneous nuclear ribonucleoprotein R	HNRPR_HUMAN	84588	1,21025641	57,1	371
Heterogeneous nuclear ribonucleoprotein U	HNRPU_HUMAN	112127	1,331983806	37	492
Heterogeneous nuclear ribonucleoprotein U-like protein 1	HNRL1_HUMAN	106935	-	455	55
Heterogeneous nuclear ribonucleoprotein U-like protein 2	HNRL2_HUMAN	99654	-	331	78
Heterogeneous nuclear ribonucleoproteins A2/B1	ROA2_HUMAN	43491	1,628620102	5,1	1623
Heterogeneous nuclear ribonucleoproteins C1/C2	HNRPC_HUMAN	42776	1,578457447	256	102
Hexokinase-2	HXK2_HUMAN	119349	0,879310345	479	52
High mobility group protein B2	HMGB2_HUMAN	36491	-	797	23
High mobility group protein HMG-I/HMG-Y	HMGA1_HUMAN	16841	1,323873122	328	79
High mobility group protein HMGI-C	HMGA2_HUMAN	16084	-	223	115
Histidine triad nucleotide-binding protein 1	HINT1_HUMAN	16835	-	357	71
Histidine triad nucleotide-binding protein 2, mitochondrial	HINT2_HUMAN	19585	-	582	40
Histidine--tRNA ligase, cytoplasmic	SYHC_HUMAN	70759	-	747	27
Histone deacetylase 2	HDAC2_HUMAN	67801	-	781	24
Histone H1.0	H10_HUMAN	38190	-	319	81
Histone H1.2	H12_HUMAN	39604	1,074010327	34,2	516
Histone H1.4	H14_HUMAN	41017	1,157608696	34,1	519
Histone H1.5	H15_HUMAN	42644	1,103585657	34,3	94
Histone H1x	H1X_HUMAN	35250	-	548	44
Histone H2A type 1-C	H2A1C_HUMAN	18356	1,313868613	47,1	424
Histone H2A type 2-B	H2A2B_HUMAN	18246	1,434931507	47,4	197
Histone H2A.V	H2AV_HUMAN	18064	1,139664804	47,3	220
Histone H2A.x	H2AX_HUMAN	19394	1,346863469	47,2	287
Histone H2B type 1-C/E/F/G/I	H2B1C_HUMAN	20286	1,208722741	28,2	610
Histone H2B type 2-E	H2B2E_HUMAN	20300	1,22	28,1	632
Histone H3.1t	H31T_HUMAN	19757	1,347619048	101	239
Histone H4	H4_HUMAN	15011	1,231974922	10	1079
Histone-binding protein RBBP4	RBBP4_HUMAN	54927	-	525	46
Homeobox protein SIX5	SIX5_HUMAN	79687	-	840	18
Hsp90 co-chaperone Cdc37	CDC37_HUMAN	57217	-	488	50
Hydroxysteroid dehydrogenase-like protein 2	HSDL2_HUMAN	57838	-	612	38
Hypoxia up-regulated protein 1	HYOU1_HUMAN	134994	1,09771987	147	175
Importin subunit alpha-2	IMA2_HUMAN	66648	-	268	97
Importin subunit beta-1	IMB1_HUMAN	110493	0,682432432	192	134
Inorganic pyrophosphatase	IPYR_HUMAN	41461	-	503	49
Inosine-5'-monophosphate dehydrogenase 2	IMDH2_HUMAN	67329	0,728	344	75
Insulin-like growth factor 2 mRNA-binding protein 1	IF2B1_HUMAN	78043	0,935582822	43,1	446
Insulin-like growth factor 2 mRNA-binding protein 2	IF2B2_HUMAN	78857	-	759	25
Insulin-like growth factor 2 mRNA-binding protein 3	IF2B3_HUMAN	78267	-	43,2	211
Insulin-like growth factor-binding protein 1	IBP1_HUMAN	30927	2,462140992	247	106
Integrin alpha-V	ITAV_HUMAN	131783	0,673076923	783	24
Inter-alpha-trypsin inhibitor heavy chain H2	ITIH2_HUMAN	126474	-	485	51
Intercellular adhesion molecule 1	ICAM1_HUMAN	65090	-	547	44

Protein name	Accession	Mass	Ratio	Hit	Score
Interferon-inducible double stranded RNA-dependent protein kinase activator A	PRKRA_HUMAN	41683	-	653	34
Interleukin enhancer-binding factor 2	ILF2_HUMAN	48511	-	269	97
Interleukin enhancer-binding factor 3	ILF3_HUMAN	115357	1,141630901	74	304
Isocitrate dehydrogenase [NAD] subunit beta, mitochondrial	IDH3B_HUMAN	50066	-	366	70
Isocitrate dehydrogenase [NADP] cytoplasmic	IDHC_HUMAN	58189	0,602836879	75,1	301
Isocitrate dehydrogenase [NADP], mitochondrial	IDHP_HUMAN	62132	-	75,2	92
Isoleucine--tRNA ligase, cytoplasmic	SYIC_HUMAN	169959	0,892857143	248	106
Isoleucine--tRNA ligase, mitochondrial	SYIM_HUMAN	135622	-	378	68
Keratin, type I cytoskeletal 10	K1C10_HUMAN	66093	-	14,3	23
Keratin, type I cytoskeletal 18	K1C18_HUMAN	54721	1,28685259	14,1	931
Keratin, type I cytoskeletal 19	K1C19_HUMAN	48642	1,362204724	14,2	860
Keratin, type II cytoskeletal 1	K2C1_HUMAN	74821	1,367088608	136	189
Keratin, type II cytoskeletal 8	K2C8_HUMAN	63710	1,307692308	3,1	1727
KH domain-containing, RNA-binding, signal transduction-associated protein 1	KHDR1_HUMAN	55802	1,059259259	456	54
Kinesin-1 heavy chain	KINH_HUMAN	139733	-	824	19
Lactoylglutathione lyase	LGUL_HUMAN	26544	-	714	29
Ladinin-1	LAD1_HUMAN	71090	-	709	30
Lamina-associated polypeptide 2, isoforms beta/gamma	LAP2B_HUMAN	62199	-	637	34
Lamin-B receptor	LBR_HUMAN	81609	-	288	90
Lamin-B1	LMNB1_HUMAN	78536	0,926829268	25,2	180
Lamin-B2	LMNB2_HUMAN	79816	-	25,3	157
Laminin subunit beta-1	LAMB1_HUMAN	224070	-	406	62
Laminin subunit gamma-1	LAMC1_HUMAN	202433	-	447	55
Lanosterol 14-alpha demethylase	CP51A_HUMAN	66808	-	727	28
LDLR chaperone MESD	MESD_HUMAN	34882	-	754	26
Leucine-rich PPR motif-containing protein, mitochondrial	LPPRC_HUMAN	189138	1,022624434	29	579
Leucine-rich repeat-containing protein 47	LRC47_HUMAN	74081	-	375	68
Leucine-rich repeat-containing protein 59	LRC59_HUMAN	46469	-	767	24
Leucine--tRNA ligase, cytoplasmic	SYLC_HUMAN	168450	-	769	24
LIM and SH3 domain protein 1	LASP1_HUMAN	36391	-	228	115
LIM domain only protein 7	LMO7_HUMAN	229385	-	786	23
L-lactate dehydrogenase A chain	LDHA_HUMAN	45487	0,542094456	76	297
Long-chain-fatty-acid--CoA ligase 3	ACSL3_HUMAN	98621	-	529	46
Long-chain-fatty-acid--CoA ligase 4	ACSL4_HUMAN	98910	-	241	109
Long-chain-fatty-acid--CoA ligase 5	ACSL5_HUMAN	90848	-	820	20
Lupus La protein	LA_HUMAN	65669	-	841	17
Lysine-specific demethylase 2B	KDM2B_HUMAN	185676	-	832	19
Lysine-specific histone demethylase 1A	KDM1A_HUMAN	108663	-	732	28
Lysine--tRNA ligase	SYK_HUMAN	82911	-	735	27
Lysosomal alpha-glucosidase	LYAG_HUMAN	110124	-	306	84
Lysosome-associated membrane glycoprotein 1	LAMP1_HUMAN	50634	-	348	74
Lysozyme C	LYSC_HUMAN	18656	-	481	52
Malate dehydrogenase, cytoplasmic	MDHC_HUMAN	46138	-	169	155
Malate dehydrogenase, mitochondrial	MDHM_HUMAN	43694	1,440318302	65	340
Malectin	MLEC_HUMAN	37689	-	461	54
MARCKS-related protein	MRP_HUMAN	25297	1,116207951	359	71
Matrin-3	MATR3_HUMAN	114947	1,228571429	85	273
Membrane-associated progesterone receptor component 1	PGRC1_HUMAN	25612	-	272	96
Membrane-associated progesterone receptor component 2	PGRC2_HUMAN	27758	-	517	47
Methionine aminopeptidase 2	AMPM2_HUMAN	66547	-	669	33
Methionine--tRNA ligase, cytoplasmic	SYMC_HUMAN	115350	-	622	37
Methylcrotonoyl-CoA carboxylase beta chain, mitochondrial	MCCB_HUMAN	70116	-	381	67
Methylmalonate-semialdehyde dehydrogenase [acylating], mitochondrial	MMSA_HUMAN	68450	-	263	99
Microsomal triglyceride transfer protein large subunit	MTP_HUMAN	120583	-	695	31
Microtubule-associated protein RP/EB family member 1	MARE1_HUMAN	36977	-	395	64
Mitochondrial import inner membrane translocase subunit TIM44	TIM44_HUMAN	64100	-	685	32
Mitochondrial import receptor subunit TOM22 homolog	TOM22_HUMAN	17337	-	706	30
Mitochondrial-processing peptidase subunit alpha	MPPA_HUMAN	64908	-	683	32
Mitochondrial-processing peptidase subunit beta	MPPB_HUMAN	60416	-	791	23

Protein name	Accession	Mass	Ratio	Hit	Score
Mitogen-activated protein kinase kinase kinase kinase 4	M4K4_HUMAN	165133	-	666	33
Monocarboxylate transporter 4	MOT4_HUMAN	54608	1,170568562	542	44
Monofunctional C1-tetrahydrofolate synthase, mitochondrial	C1TM_HUMAN	123368	-	583	40
Multifunctional protein ADE2	PUR6_HUMAN	58001	-	208	123
Myosin light polypeptide 6	MYL6_HUMAN	19961	1,546137339	79	285
Myosin regulatory light chain 12A	ML12A_HUMAN	24345	-	575	41
Myosin-10	MYH10_HUMAN	288786	0,987261146	216	119
Myosin-9	MYH9_HUMAN	289666	1,395348837	127	198
Myristoylated alanine-rich C-kinase substrate	MARCS_HUMAN	40358	2,104821803	377	68
Na(+)/H(+) exchange regulatory cofactor NHE-RF1	NHRF1_HUMAN	45841	0,645631068	173	151
N-acetylglucosamine-6-sulfatase	GNS_HUMAN	70560	-	561	42
N-acetyltransferase 10	NAT10_HUMAN	138168	-	343	76
NAD(P)H dehydrogenase [quinone] 1	NQO1_HUMAN	38453	0,604203152	124	200
NADH dehydrogenase [ubiquinone] 1 alpha subcomplex subunit 2	NDUA2_HUMAN	13044	-	656	34
NADH dehydrogenase [ubiquinone] 1 beta subcomplex subunit 9	NDUB9_HUMAN	26380	-	738	27
NADH dehydrogenase [ubiquinone] flavoprotein 1, mitochondrial	NDUV1_HUMAN	58694	-	641	36
NADH dehydrogenase [ubiquinone] flavoprotein 2, mitochondrial	NDUV2_HUMAN	32546	-	719	29
NADH dehydrogenase [ubiquinone] iron-sulfur protein 2, mitochondrial	NDUS2_HUMAN	59508	-	734	27
NADH dehydrogenase [ubiquinone] iron-sulfur protein 3, mitochondrial	NDUS3_HUMAN	34177	-	418	59
NADH-cytochrome b5 reductase 3	NB5R3_HUMAN	39384	-	313	83
NADPH:adrenodoxin oxidoreductase, mitochondrial	ADRO_HUMAN	59583	-	252	103
NADPH--cytochrome P450 reductase	NCPR_HUMAN	87897	1,257425743	168	155
Nascent polypeptide-associated complex subunit alpha	NACA_HUMAN	28541	-	227	115
NEDD8	NEDD8_HUMAN	12108	-	717	29
Neuron navigator 1	NAV1_HUMAN	244023	-	839	18
Neurotensin receptor type 1	NTR1_HUMAN	49879	-	795	23
Neutral alpha-glucosidase AB	GANAB_HUMAN	115324	1,028037383	155	171
Neutral amino acid transporter B(0)	AAAT_HUMAN	60821	-	796	23
NHP2-like protein 1	NH2L1_HUMAN	17511	1,306451613	186	139
Nicalin	NCLN_HUMAN	69627	-	725	28
Nicotinamide mononucleotide adenylyltransferase 1	NMNA1_HUMAN	40126	-	828	19
Nicotinate-nucleotide pyrophosphorylase [carboxylating]	NADC_HUMAN	34781	-	474	52
Non-histone chromosomal protein HMG-17	HMGN2_HUMAN	16384	1,392931393	298	86
Non-POU domain-containing octamer-binding protein	NONO_HUMAN	62715	1,04778157	42,1	469
NSFL1 cofactor p47	NSF1C_HUMAN	46024	-	126	199
Nuclear migration protein nudC	NUDC_HUMAN	48866	-	476	52
Nuclear pore complex protein Nup93	NUP93_HUMAN	105598	-	821	20
Nuclear receptor coactivator 5	NCOA5_HUMAN	70060	-	846	17
Nuclease-sensitive element-binding protein 1	YBOX1_HUMAN	41074	1,01497006	257,2	83
Nucleobindin-1	NUCB1_HUMAN	62972	-	634	37
Nucleolar and coiled-body phosphoprotein 1	NOLC1_HUMAN	107631	-	468	53
Nucleolar GTP-binding protein 1	NOG1_HUMAN	95212	-	856	14
Nucleolar protein 56	NOP56_HUMAN	86086	-	138	185
Nucleolar protein 58	NOP58_HUMAN	81748	1,149659864	342	76
Nucleolar protein 7	NOL7_HUMAN	39447	-	535	45
Nucleolar RNA helicase 2	DDX21_HUMAN	115277	1,02	71,1	314
Nucleolar transcription factor 1	UBF1_HUMAN	121596	-	502	49
Nucleolin	NUCL_HUMAN	104251	1,181003584	13	965
Nucleolysin TIA-1 isoform p40	TIA1_HUMAN	49020	-	794	23
Nucleophosmin	NPM_HUMAN	42898	1,246376812	39	482
Nucleoprotein TPR	TPR_HUMAN	320975	0,970930233	194	132
Nucleoside diphosphate kinase B	NDKB_HUMAN	21546	0,508130081	130	195
Nucleosome assembly protein 1-like 4	NP1L4_HUMAN	52836	-	218	118
Obg-like ATPase 1	OLA1_HUMAN	58405	0,578616352	404	62
Olfactory receptor 52N2	O52N2_HUMAN	39566	-	855	14
Ornithine aminotransferase, mitochondrial	OAT_HUMAN	57326	-	198	131
Palmitoyl-protein thioesterase 1	PPT1_HUMAN	39647	-	295	88
Paraspeckle component 1	PSPC1_HUMAN	66311	-	538	45
Parathymosin	PTMS_HUMAN	15782	-	283	92

Protein name	Accession	Mass	Ratio	Hit	Score
PDZ and LIM domain protein 1	PDLI1_HUMAN	43046	-	161	167
Peptidyl-prolyl cis-trans isomerase A	PPIA_HUMAN	22564	0,558746736	54	381
Peptidyl-prolyl cis-trans isomerase B	PPIB_HUMAN	31941	1,283536585	51	402
Peptidyl-prolyl cis-trans isomerase FKBP10	FKB10_HUMAN	70288	-	739	27
Peptidyl-prolyl cis-trans isomerase FKBP1A	FKB1A_HUMAN	14681	-	213	121
Peptidyl-prolyl cis-trans isomerase FKBP2	FKBP2_HUMAN	19594	-	623	37
Peptidyl-prolyl cis-trans isomerase FKBP3	FKBP3_HUMAN	36113	-	516	47
Peroxiredoxin-1	PRDX1_HUMAN	28180	0,48540146	41,1	472
Peroxiredoxin-2	PRDX2_HUMAN	26441	-	41,2	224
Peroxiredoxin-4	PRDX4_HUMAN	34780	0,685446009	41,3	180
Peroxiredoxin-6	PRDX6_HUMAN	30799	-	211	121
Peroxisomal sarcosine oxidase	SOX_HUMAN	49818	-	354	72
Pescadillo homolog	PESC_HUMAN	85300	0,944954128	417	59
PHD finger-like domain-containing protein 5A	PHF5A_HUMAN	16352	-	716	29
Phenylalanine--tRNA ligase alpha subunit	SYFA_HUMAN	66349	-	437	56
Phenylalanine--tRNA ligase beta subunit	SYFB_HUMAN	80371	-	410	61
Phosphate carrier protein, mitochondrial	MPCP_HUMAN	47978	1,140939597	282	92
Phosphatidylethanolamine-binding protein 1	PEBP1_HUMAN	25911	0,470588235	276	95
Phosphoacetylglucosamine mutase	AGM1_HUMAN	71070	-	743	27
Phosphoenolpyruvate carboxykinase [GTP], mitochondrial	PCKGM_HUMAN	77986	0,984293194	162	166
Phosphoglucomutase-1	PGM1_HUMAN	72666	-	422	58
Phosphoglycerate kinase 1	PGK1_HUMAN	57667	0,582677165	95	257
Phosphoglycerate mutase 1	PGAM1_HUMAN	34566	0,479289941	129	196
Phosphoserine aminotransferase	SERC_HUMAN	48915	-	646	35
Plasminogen activator inhibitor 1 RNA-binding protein	PAIRB_HUMAN	55890	0,758853288	88	265
Platelet-activating factor acetylhydrolase IB subunit gamma	PA1B3_HUMAN	27848	-	652	34
Plectin	PLEC_HUMAN	606605	1,018867925	73,2	75
Poly [ADP-ribose] polymerase 1	PARP1_HUMAN	151646	1,165289256	108	228
Poly(rC)-binding protein 1	PCBP1_HUMAN	42037	0,774590164	82,1	281
Poly(rC)-binding protein 2	PCBP2_HUMAN	44031	0,832653061	82,2	248
Poly(U)-binding-splicing factor PUF60	PUF60_HUMAN	69876	-	675	32
Polyadenylate-binding protein 1	PABP1_HUMAN	83402	-	87	266
Polypyrimidine tract-binding protein 1	PTBP1_HUMAN	67529	1,392473118	329	79
Polyribonucleotide nucleotidyltransferase 1, mitochondrial	PNPT1_HUMAN	100803	-	853	15
Porimin	PORIM_HUMAN	24256	-	564	42
POTE ankyrin domain family member E	POTEE_HUMAN	148056	0,980263158	1,3	1655
Prefoldin subunit 1	PFD1_HUMAN	19069	-	586	40
Prefoldin subunit 2	PFD2_HUMAN	21201	-	553	43
Prelamin-A/C	LMNA_HUMAN	86567	1,152173913	25,1	695
Pre-mRNA 3'-end-processing factor FIP1	FIP1_HUMAN	76221	-	254	103
Pre-mRNA-processing factor 6	PRP6_HUMAN	128761	-	351	73
Pre-mRNA-processing-splicing factor 8	PRP8_HUMAN	319970	-	363	70
Pre-mRNA-splicing factor 38A	PR38A_HUMAN	45059	-	647	35
pre-rRNA processing protein FTSJ3	RRMJ3_HUMAN	122965	-	396	64
Presequence protease, mitochondrial	PREP_HUMAN	137153	-	497	49
Probable ATP-dependent RNA helicase DDX17	DDX17_HUMAN	89957	1,095588235	84,2	274
Probable ATP-dependent RNA helicase DDX23	DDX23_HUMAN	121990	-	782	24
Probable ATP-dependent RNA helicase DDX27	DDX27_HUMAN	116245	-	540	44
Probable ATP-dependent RNA helicase DDX5	DDX5_HUMAN	79752	0,970238095	84,1	277
Probable rRNA-processing protein EBP2	EBP2_HUMAN	48520	-	629	37
Probable serine carboxypeptidase CPVL	CPVL_HUMAN	62647	-	680	32
Procollagen-lysine,2-oxoglutarate 5-dioxygenase 1	PLOD1_HUMAN	94753	-	325	80
Procollagen-lysine,2-oxoglutarate 5-dioxygenase 2	PLOD2_HUMAN	100754	-	139	184
Procollagen-lysine,2-oxoglutarate 5-dioxygenase 3	PLOD3_HUMAN	92641	-	770	24
Profilin-1	PROF1_HUMAN	18391	0,608455882	49	419
Programmed cell death protein 5	PDCD5_HUMAN	17927	-	300	86
Prohibitin	PHB_HUMAN	33741	1,114649682	92	261
Prohibitin-2	PHB2_HUMAN	39360	1,166666667	262	100
Proliferating cell nuclear antigen	PCNA_HUMAN	33922	0,516042781	193	133

Protein name	Accession	Mass	Ratio	Hit	Score
Proliferation-associated protein 2G4	PA2G4_HUMAN	56840	-	332	78
Prolyl 4-hydroxylase subunit alpha-1	P4HA1_HUMAN	74700	-	536	45
Prostaglandin E synthase 3	TEBP_HUMAN	22640	-	534	45
Proteasome activator complex subunit 2	PSME2_HUMAN	34381	-	640	36
Proteasome activator complex subunit 3	PSME3_HUMAN	36180	-	387	66
Proteasome subunit alpha type-1	PSA1_HUMAN	33492	0,73089701	165	161
Proteasome subunit alpha type-2	PSA2_HUMAN	30445	0,839805825	369	69
Proteasome subunit alpha type-3	PSA3_HUMAN	34195	0,986206897	562	42
Proteasome subunit alpha type-4	PSA4_HUMAN	37679	0,748031496	320	81
Proteasome subunit alpha type-5	PSA5_HUMAN	30653	-	578	41
Proteasome subunit alpha type-6	PSA6_HUMAN	33466	-	389	66
Proteasome subunit alpha type-7-like	PSA7L_HUMAN	36117	-	606	39
Proteasome subunit beta type-1	PSB1_HUMAN	30731	0,899497487	134	191
Proteasome subunit beta type-4	PSB4_HUMAN	31011	0,796052632	249	106
Proteasome subunit beta type-6	PSB6_HUMAN	26862	-	465	54
Protein AMBP	AMBP_HUMAN	44754	-	584	40
Protein BUD31 homolog	BUD31_HUMAN	22160	-	768	24
Protein canopy homolog 2	CNPY2_HUMAN	23681	-	451	55
Protein CutA	CUTA_HUMAN	21234	-	492	50
Protein DEK	DEK_HUMAN	63334	-	556	43
Protein disulfide-isomerase	PDIA1_HUMAN	71683	1,373695198	15,1	877
Protein disulfide-isomerase A3	PDIA3_HUMAN	71653	1,266558966	12	967
Protein disulfide-isomerase A4	PDIA4_HUMAN	92965	1,206060606	31	553
Protein disulfide-isomerase A6	PDIA6_HUMAN	57217	1,272321429	22	735
Protein DJ-1	PARK7_HUMAN	25050	0,469061876	122	204
Protein dpy-30 homolog	DPY30_HUMAN	13676	-	787	23
Protein ERGIC-53	LMAN1_HUMAN	66943	-	854	15
Protein ETHE1, mitochondrial	ETHE1_HUMAN	29680	-	518	47
Protein HEXIM1	HEXI1_HUMAN	47899	-	526	46
Protein NipSnap homolog 1	NIPS1_HUMAN	38765	-	326	80
Protein phosphatase 1G	PPM1G_HUMAN	70186	-	745	27
Protein RCC2	RCC2_HUMAN	66392	-	764	24
Protein Red	RED_HUMAN	85944	-	844	17
Protein S100-A6	S10A6_HUMAN	13215	-	616	38
Protein SET	SET_HUMAN	40770	0,689981096	145	180
Protein transport protein Sec31A	SC31A_HUMAN	153009	-	545	44
Protein transport protein Sec61 subunit gamma	SC61G_HUMAN	9866	-	852	15
Protein YIPF5	YIPF5_HUMAN	29796	-	771	24
Protein-L-isoaspartate(D-aspartate) O-methyltransferase	PIMT_HUMAN	29792	-	615	38
Prothrombin	THRB_HUMAN	79118	-	663	33
Prothymosin alpha	PTMA_HUMAN	14934	0,630508475	234	113
Puratrophin-1	PKHG4_HUMAN	140150	-	822	20
Puromycin-sensitive aminopeptidase	PSA_HUMAN	120855	-	470	53
Putative 40S ribosomal protein S26-like 1	RS26L_HUMAN	16949	-	420	59
Putative 60S ribosomal protein L39-like 5	R39L5_HUMAN	9969	-	614	38
Putative ATP-dependent Clp protease proteolytic subunit, mitochondrial	CLPP_HUMAN	33203	-	758	25
Putative pre-mRNA-splicing factor ATP-dependent RNA helicase DHX15	DHX15_HUMAN	105477	1,024096386	270	96
Putative RNA-binding protein 3	RBM3_HUMAN	18377	0,986547085	167	156
Putative ubiquitin-conjugating enzyme E2 N-like	UE2NL_HUMAN	20712	-	523	47
Putative uncharacterized protein C17orf82	CQ082_HUMAN	26595	0,982565041	807	21
Pyrroline-5-carboxylate reductase 1, mitochondrial	P5CR1_HUMAN	38815	-	151	171
Pyruvate carboxylase, mitochondrial	PYC_HUMAN	146891	1,166037736	156	170
Pyruvate dehydrogenase E1 component subunit alpha, somatic form, mitochondrial	ODPA_HUMAN	50569	-	788	23
Pyruvate dehydrogenase E1 component subunit beta, mitochondrial	ODPB_HUMAN	45292	-	594	40
Pyruvate kinase isozymes M1/M2	KPYM_HUMAN	69460	0,641025641	55	377
Quinone oxidoreductase	QOR_HUMAN	42485	-	496	49
Rab GDP dissociation inhibitor beta	GDIB_HUMAN	62191	-	195	131
Radixin	RADI_HUMAN	89207	-	131,2	95
Ran-specific GTPase-activating protein	RANG_HUMAN	31205	-	729	28

Protein name	Accession	Mass	Ratio	Hit	Score
Ras GTPase-activating protein-binding protein 1	G3BP1_HUMAN	58216	0,783669141	312	83
Ras GTPase-activating protein-binding protein 2	G3BP2_HUMAN	61085	-	624	37
Ras-related protein Rab-10	RAB10_HUMAN	29219	-	429	57
Ras-related protein Rab-11A	RB11A_HUMAN	28333	-	352	73
Ras-related protein Rab-1A	RAB1A_HUMAN	28139	1,121212121	264	99
Ras-related protein Rab-5B	RAB5B_HUMAN	28255	-	576	41
Ras-related protein Rab-6A	RAB6A_HUMAN	27837	-	527	46
Ras-related protein Rab-7a	RAB7A_HUMAN	28951	-	212	121
Ras-related protein Rap-1b-like protein	RP1BL_HUMAN	25171	-	707	30
Regulation of nuclear pre-mRNA domain-containing protein 1B	RPR1B_HUMAN	46003	-	613	38
Reticulocalbin-1	RCN1_HUMAN	47384	-	384	67
Reticulocalbin-2	RCN2_HUMAN	42634	-	323	80
Reticulon-4	RTN4_HUMAN	155709	-	563	42
Retinal dehydrogenase 1	AL1A1_HUMAN	66691	-	103,2	169
Retinol dehydrogenase 11	RDH11_HUMAN	40839	-	712	30
Retrotransposon-derived protein PEG10	PEG10_HUMAN	86510	0,663265306	182	140
Rho GDP-dissociation inhibitor 1	GDIR1_HUMAN	29277	0,539215686	166	160
Ribonuclease inhibitor	RINI_HUMAN	55113	-	672	33
Ribosomal protein S6 kinase alpha-3	KS6A3_HUMAN	100110	-	812	21
Ribosomal RNA small subunit methyltransferase NEP1	NEP1_HUMAN	32179	-	315	82
Ribosome biogenesis protein BOP1	BOP1_HUMAN	91791	-	826	19
Ribosome-binding protein 1	RRBP1_HUMAN	207746	1,399217221	7	1458
RNA binding protein fox-1 homolog 3	RFOX3_HUMAN	36894	-	851	15
RNA polymerase II-associated factor 1 homolog	PAF1_HUMAN	70891	-	694	31
RNA-binding motif protein, X chromosome	RBMX_HUMAN	46565	-	143	182
RNA-binding protein 14	RBM14_HUMAN	75533	1,107594937	148	172
RNA-binding protein 25	RBM25_HUMAN	126894	-	335	77
RNA-binding protein 39	RBM39_HUMAN	70598	-	373	69
RNA-binding protein 4	RBM4_HUMAN	45460	-	310	83
RNA-binding protein 47	RBM47_HUMAN	73184	-	761	25
RNA-binding protein 8A	RBM8A_HUMAN	23831	-	657	34
RNA-binding protein EWS	EWS_HUMAN	74216	-	676	32
RNA-binding protein FUS	FUS_HUMAN	57957	-	654	34
RNA-binding protein Raly	RALY_HUMAN	39440	-	484	51
RNA-binding protein with serine-rich domain 1	RNPS1_HUMAN	43314	1,040856031	250	105
rRNA 2'-O-methyltransferase fibrillarin	FBRL_HUMAN	39848	0,875722543	209	122
RuvB-like 2	RUVB2_HUMAN	59642	-	388	66
S-adenosylmethionine synthase isoform type-1	METK1_HUMAN	50617	-	339	76
SAP domain-containing ribonucleoprotein	SARNP_HUMAN	31870	1,13986014	440	56
Sarcoplasmic/endoplasmic reticulum calcium ATPase 2	AT2A2_HUMAN	132326	-	621	38
Sepiapterin reductase	SPRE_HUMAN	32594	-	814	20
Serine hydroxymethyltransferase, mitochondrial	GLYM_HUMAN	62954	1,086694762	60	358
Serine palmitoyltransferase 1	SPTC1_HUMAN	62141	-	648	35
Serine/arginine repetitive matrix protein 1	SRRM1_HUMAN	133607	-	762	25
Serine/arginine repetitive matrix protein 2	SRRM2_HUMAN	339289	-	660	34
Serine/arginine-rich splicing factor 1	SRSF1_HUMAN	30466	1,155737705	185	140
Serine/arginine-rich splicing factor 10	SRS10_HUMAN	37974	-	260	101
Serine/arginine-rich splicing factor 2	SRSF2_HUMAN	29416	0,971153846	236	112
Serine/arginine-rich splicing factor 3	SRSF3_HUMAN	21143	-	149,2	165
Serine/arginine-rich splicing factor 5	SRSF5_HUMAN	36721	-	679	32
Serine/arginine-rich splicing factor 6	SRSF6_HUMAN	47777	1,278481013	201	128
Serine/arginine-rich splicing factor 7	SRSF7_HUMAN	29784	-	149,1	172
Serine/arginine-rich splicing factor 9	SRSF9_HUMAN	28264	-	322	81
Serine/threonine-protein kinase PRP4 homolog	PRP4B_HUMAN	156158	-	670	33
Serine/threonine-protein phosphatase 2A 65 kDa regulatory subunit A alpha isoform	2AAA_HUMAN	75306	-	765	24
Serine/threonine-protein phosphatase 4 catalytic subunit	PP4C_HUMAN	39012	-	811	21
Serine/threonine-protein phosphatase PP1-alpha catalytic subunit	PP1A_HUMAN	44485	-	602	39
Serine/threonine-protein phosphatase PP1-gamma catalytic subunit	PP1G_HUMAN	44261	-	595	40
Serine--tRNA ligase, mitochondrial	SYSM_HUMAN	63113	-	591	40

Protein name	Accession	Mass	Ratio	Hit	Score
Serotransferrin	TRFE_HUMAN	94962	1,316176471	89	265
Serpin H1	SERPH_HUMAN	57058	-	643	36
Serrate RNA effector molecule homolog	SRRT_HUMAN	121899	-	431	57
Serum albumin	ALBU_HUMAN	87878	1,589108911	135	190
Serum paraoxonase/arylesterase 2	PON2_HUMAN	45152	-	566	42
S-formylglutathione hydrolase	ESTD_HUMAN	38439	0,678571429	511	47
Short/branched chain specific acyl-CoA dehydrogenase, mitochondrial	ACDSB_HUMAN	56581	-	659	34
Sialic acid synthase	SIAS_HUMAN	50016	-	350	73
Sialidase-1	NEUR1_HUMAN	49089	-	671	33
Signal peptidase complex subunit 3	SPCS3_HUMAN	23951	-	829	19
Signal recognition particle 14 kDa protein	SRP14_HUMAN	20949	-	386	67
Signal recognition particle 9 kDa protein	SRP09_HUMAN	13147	-	555	43
Single-stranded DNA-binding protein, mitochondrial	SSBP_HUMAN	19987	-	438	56
Small nuclear ribonucleoprotein F	RUXF_HUMAN	11544	-	371	69
Small nuclear ribonucleoprotein Sm D1	SMD1_HUMAN	16620	-	355	72
Small nuclear ribonucleoprotein Sm D2	SMD2_HUMAN	18994	1,224652087	512	47
Small nuclear ribonucleoprotein Sm D3	SMD3_HUMAN	17254	-	374	69
Small ubiquitin-related modifier 2	SUMO2_HUMAN	13602	-	507	48
SNW domain-containing protein 1	SNW1_HUMAN	77884	-	630	37
Sodium/potassium/calcium exchanger 5	NCKX5_HUMAN	60024	-	849	16
Sodium/potassium-transporting ATPase subunit alpha-1	AT1A1_HUMAN	130164	1,015	98	250
Solute carrier family 2, facilitated glucose transporter member 1	GTR1_HUMAN	59220	-	191,2	86
Solute carrier family 2, facilitated glucose transporter member 3	GTR3_HUMAN	59061	0,858369099	191,1	135
Sorting nexin-1	SNX1_HUMAN	72114	1,390625	723	28
Sorting nexin-3	SNX3_HUMAN	22097	-	751	26
SPATS2-like protein	SPS2L_HUMAN	79943	-	600	39
Spectrin alpha chain, non-erythrocytic 1	SPTN1_HUMAN	344901	1,130136986	35	517
Spectrin beta chain, non-erythrocytic 1	SPTB2_HUMAN	329196	1,132947977	24	710
Spermidine synthase	SPEE_HUMAN	38366	-	731	28
Spliceosome RNA helicase DDX39B	DX39B_HUMAN	58086	-	190	135
Splicing factor 1	SF01_HUMAN	76804	-	432	57
Splicing factor 3A subunit 1	SF3A1_HUMAN	107083	-	681	32
Splicing factor 3A subunit 2	SF3A2_HUMAN	56221	-	665	33
Splicing factor 3B subunit 1	SF3B1_HUMAN	171596	1,120418848	557	43
Splicing factor 3B subunit 2	SF3B2_HUMAN	126022	-	452	55
Splicing factor 3B subunit 3	SF3B3_HUMAN	151615	1,004032258	301	86
Splicing factor U2AF 35 kDa subunit	U2AF1_HUMAN	31201	-	402	63
Splicing factor, proline- and glutamine-rich	SFPQ_HUMAN	86445	-	42,2	405
Squalene synthase	FDFT_HUMAN	55081	-	753	26
SRA stem-loop-interacting RNA-binding protein, mitochondrial	SLIRP_HUMAN	14471	-	289	89
Staphylococcal nuclease domain-containing protein 1	SND1_HUMAN	119882	0,908629442	63	349
Stathmin	STMN1_HUMAN	24593	0,529816514	72	310
Stomatin-like protein 2	STML2_HUMAN	43986	-	632	37
Stress-70 protein, mitochondrial	GRP75_HUMAN	89758	1,21369863	2,2	1548
Stress-induced-phosphoprotein 1	STIP1_HUMAN	82069	0,776119403	435	56
Structural maintenance of chromosomes protein 1A	SMC1A_HUMAN	190904	-	397	64
Succinate dehydrogenase [ubiquinone] iron-sulfur subunit, mitochondrial	DHSB_HUMAN	39518	-	810	21
Succinate-semialdehyde dehydrogenase, mitochondrial	SSDH_HUMAN	66000	-	318	81
Succinyl-CoA ligase [ADP/GDP-forming] subunit alpha, mitochondrial	SUCA_HUMAN	42919	-	628	37
Succinyl-CoA ligase [GDP-forming] subunit beta, mitochondrial	SUCB2_HUMAN	57433	-	543	44
Sulfotransferase 1A3/1A4	ST1A3_HUMAN	40562	0,630136986	202	127
Superkiller viralicidic activity 2-like 2	SK2L2_HUMAN	144804	-	411	60
Superoxide dismutase [Mn], mitochondrial	SODM_HUMAN	29574	-	472	53
Surfeit locus protein 4	SURF4_HUMAN	34024	-	360	71
Syndecan-4	SDC4_HUMAN	25279	-	642	36
Talin-1	TLN1_HUMAN	319185	-	251	104
TAR DNA-binding protein 43	TADBP_HUMAN	51100	-	372	69
TATA-binding protein-associated factor 2N	RBP56_HUMAN	66965	-	607	39
T-complex protein 1 subunit alpha	TCPA_HUMAN	72778	0,704347826	231	114

Protein name	Accession	Mass	Ratio	Hit	Score
T-complex protein 1 subunit beta	TCPB_HUMAN	69012	0,797413793	100	241
T-complex protein 1 subunit delta	TCPD_HUMAN	70056	0,69047619	196	131
T-complex protein 1 subunit epsilon	TCPE_HUMAN	73018	0,757763975	390	66
T-complex protein 1 subunit eta	TCPH_HUMAN	72106	0,741935484	184	140
T-complex protein 1 subunit gamma	TCPG_HUMAN	71751	0,671586716	153	171
T-complex protein 1 subunit theta	TCPQ_HUMAN	72359	0,785714286	102	235
T-complex protein 1 subunit zeta	TCPZ_HUMAN	71981	0,750798722	154	171
Tether containing UBX domain for GLUT4	ASPC1_HUMAN	68055	-	809	21
Thimet oligopeptidase	THOP1_HUMAN	90653	-	453	55
Thioredoxin domain-containing protein 12	TXD12_HUMAN	23452	-	560	43
Thioredoxin domain-containing protein 17	TXD17_HUMAN	17278	-	337	77
Thioredoxin domain-containing protein 5	TXND5_HUMAN	55812	1,247030879	15,2	121
Thioredoxin-dependent peroxide reductase, mitochondrial	PRDX3_HUMAN	31934	1,366336634	77	297
Thioredoxin-like protein 1	TXNL1_HUMAN	38011	-	701	30
Thiosulfate sulfurtransferase	THTR_HUMAN	37971	-	475	52
THO complex subunit 4	THOC4_HUMAN	30522	-	116	220
Thymidylate kinase	KTHY_HUMAN	28976	-	463	54
Thymosin beta-10	TYB10_HUMAN	7760	-	570	41
Thyroid hormone receptor-associated protein 3	TR150_HUMAN	139326	-	267	98
Tight junction protein ZO-2	ZO2_HUMAN	154258	-	571	41
Trafficking protein particle complex subunit 3	TPPC3_HUMAN	23303	-	772	24
Transcription elongation factor A protein 3	TCEA3_HUMAN	51723	-	691	31
Transcription factor A, mitochondrial	TFAM_HUMAN	38813	-	626	37
Transcription intermediary factor 1-beta	TIF1B_HUMAN	101574	-	158	169
Transferrin receptor protein 1	TFR1_HUMAN	100332	1,25	97	251
Transformer-2 protein homolog alpha	TRA2A_HUMAN	34799	-	698	31
Transformer-2 protein homolog beta	TRA2B_HUMAN	36079	-	565	42
Transforming protein RhoA	RHOA_HUMAN	27230	-	558	43
Transgelin	TAGL_HUMAN	28072	-	466	54
Transitional endoplasmic reticulum ATPase	TERA_HUMAN	103868	0,901785714	45	430
Transketolase	TKT_HUMAN	80916	0,528037383	177	143
Translin	TSN_HUMAN	30730	-	711	30
Translocon-associated protein subunit alpha	SSRA_HUMAN	35866	-	833	19
Translocon-associated protein subunit delta	SSRD_HUMAN	20812	-	214	120
Translocon-associated protein subunit gamma	SSRG_HUMAN	26543	-	164	164
Transmembrane protein 205	TM205_HUMAN	23009	-	589	40
Transmembrane protein 97	TMM97_HUMAN	25093	-	726	28
Trifunctional enzyme subunit alpha, mitochondrial	ECHA_HUMAN	104850	1,073643411	115	220
Trifunctional enzyme subunit beta, mitochondrial	ECHB_HUMAN	62213	0,981578947	119	209
Triosephosphate isomerase	TPIS_HUMAN	37160	0,514734774	66	338
tRNA (cytosine(34)-C(5))-methyltransferase	NSUN2_HUMAN	104060	-	537	45
tRNA methyltransferase 112 homolog	TR112_HUMAN	15407	-	383	67
tRNA-splicing ligase RtcB homolog	RTCB_HUMAN	65214	-	405	62
Tropomyosin alpha-1 chain	TPM1_HUMAN	44553	0,896551724	109,3	132
Tropomyosin alpha-3 chain	TPM3_HUMAN	44663	0,915789474	109,2	146
Tropomyosin alpha-4 chain	TPM4_HUMAN	36414	0,898876404	109,1	228
Trypsin-1	TRY1_HUMAN	31104	0,942455243	278	94
Tubulin alpha-1A chain	TBA1A_HUMAN	56188	0,433009709	19,2	776
Tubulin alpha-1C chain	TBA1C_HUMAN	55948	0,435212661	19,1	779
Tubulin beta chain	TBB5_HUMAN	54506	0,50623053	18,1	801
Tubulin beta-4B chain	TBB4B_HUMAN	54666	0,514382403	18,2	661
Tubulin beta-6 chain	TBB6_HUMAN	54388	0,827004219	18,3	310
Tubulin-specific chaperone A	TBCA_HUMAN	17410	-	506	48
Tumor necrosis factor receptor superfamily member 6B	TNF6B_HUMAN	33571	-	842	17
Twinfilin-1	TWF1_HUMAN	48775	-	649	35
Tyrosine--tRNA ligase, cytoplasmic	SYYC_HUMAN	77967	-	620	38
U1 small nuclear ribonucleoprotein 70 kDa	RU17_HUMAN	58523	-	407	62
U1 small nuclear ribonucleoprotein A	SNRPA_HUMAN	38256	-	554	43
U3 small nucleolar ribonucleoprotein protein IMP3	IMP3_HUMAN	24574	-	690	32

Protein name	Accession	Mass	Ratio	Hit	Score
U3 small nucleolar RNA-interacting protein 2	U3IP2_HUMAN	60935	-	790	23
U4/U6.U5 tri-snRNP-associated protein 2	SNUT2_HUMAN	79333	-	775	24
U5 small nuclear ribonucleoprotein 200 kDa helicase	U520_HUMAN	286333	-	741	27
Ubiquinone biosynthesis protein COQ9, mitochondrial	COQ9_HUMAN	38529	-	693	31
Ubiquitin carboxyl-terminal hydrolase 5	UBP5_HUMAN	111544	-	838	18
Ubiquitin thioesterase OTUB1	OTUB1_HUMAN	36740	-	825	19
Ubiquitin-40S ribosomal protein S27a	RS27A_HUMAN	25863	1,256410256	67	336
Ubiquitin-conjugating enzyme E2 variant 1	UB2V1_HUMAN	19526	-	590	38
Ubiquitin-like modifier-activating enzyme 1	UBA1_HUMAN	134201	-	104	234
UDP-glucose 6-dehydrogenase	UGDH_HUMAN	66245	0,66875	48	421
UDP-glucose:glycoprotein glucosyltransferase 1	UGGG1_HUMAN	208411	-	376	68
Uncharacterized protein C1orf173	CA173_HUMAN	204868	-	816	20
Unconventional myosin-Ib	MYO1B_HUMAN	165060	-	427	57
Vacuolar protein sorting-associated protein 35	VPS35_HUMAN	105947	-	197	131
Valacyclovir hydrolase	BPHL_HUMAN	39214	-	766	24
Valine--tRNA ligase	SYVC_HUMAN	158031	-	349	74
Very long-chain specific acyl-CoA dehydrogenase, mitochondrial	ACADV_HUMAN	82818	1,397163121	242	107
Very-long-chain (3R)-3-hydroxyacyl-[acyl-carrier protein] dehydratase 3	HACD3_HUMAN	49824	-	611	38
Vesicle-associated membrane protein 3	VAMP3_HUMAN	13736	-	285	91
Vesicle-associated membrane protein-associated protein A	VAPA_HUMAN	35176	-	636	36
Vesicle-trafficking protein SEC22b	SC22B_HUMAN	28836	-	539	44
Vigilin	VIGLN_HUMAN	174831	-	110	227
Villin-1	VILI_HUMAN	110889	0,837320574	83	278
Voltage-dependent anion-selective channel protein 1	VDAC1_HUMAN	38663	-	449	55
Voltage-dependent anion-selective channel protein 2	VDAC2_HUMAN	38847	-	522	47
Voltage-dependent anion-selective channel protein 3	VDAC3_HUMAN	39157	-	478	52
WD repeat-containing protein 1	WDR1_HUMAN	78624	-	454	55
X-ray repair cross-complementing protein 5	XRCC5_HUMAN	102121	0,936	513	47
X-ray repair cross-complementing protein 6	XRCC6_HUMAN	88051	-	93	260
Zinc finger CCCH domain-containing protein 15	ZC3HF_HUMAN	67433	-	597	39
Zinc finger protein 207	ZN207_HUMAN	58626	-	361	70
Zinc transporter ZIP4	S39A4_HUMAN	70782	-	419	59

Chapter 4

In vitro antiproliferative activity of the ellagitannins metabolites, urolithins, on human tumor cell lines – emphasis on UMUC3 bladder cancer cells

Joana Liberal, Anália Carmo, Célia Gomes, Maria Teresa Cruz, Maria Teresa Batista

Submitted to *Molecular Nutrition & Food Research*

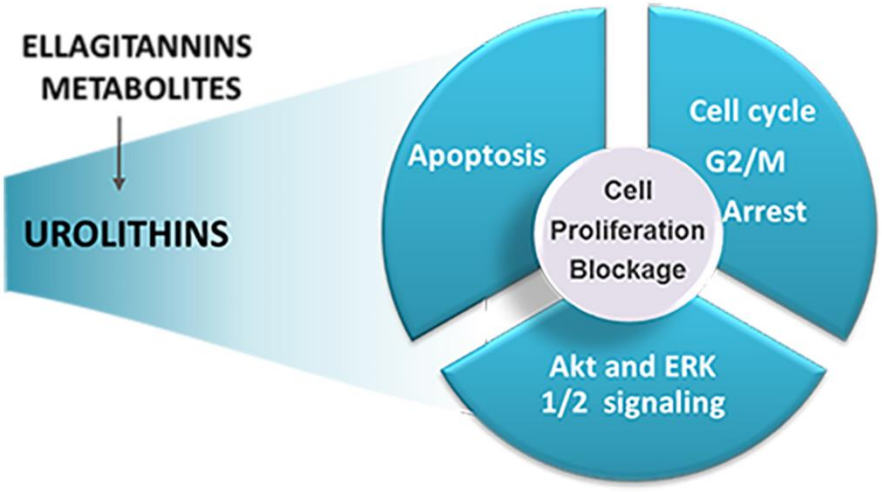

ABSTRACT

Scope

Ellagitannins-containing foods have been gathering attention for their health benefits, namely as chemopreventive molecules. However, the low bioavailability of ellagitannins and their extensive metabolization in the gastrointestinal tract into ellagic acid and urolithins, suggest that the systemic health benefits of ellagitannins consumption would rely on a direct effect of their metabolites. To gain new insights in the role of urolithins as novel drugs for cancer therapy, this work focused on the antiproliferative effects of urolithins in different tumour cells.

Methods and results

The results showed that urolithins A, B and C, decreased cell viability in a dose-dependent way, and in comparison with ellagic acid, urolithins were much more active. However, the sensitivity to urolithins was quite different among the panel of cell lines studied and the human bladder cancer cells (UMUC3) were the most susceptible. Furthermore, in UMUC3, urolithin A was the most active molecule, promoting cell cycle arrest at G2/M checkpoint and increasing apoptotic cell death. In addition, this molecule was also able to inhibit PI3K/Akt and MAPK signalling.

Conclusions

The present data emphasizes the chemopreventive/chemotherapeutic potential of the ellagitannins metabolites, urolithins, highlighting the stronger effect of urolithin A and the potential to target transitional bladder cancer.

Keywords

Apoptosis; Cell cycle; Cell proliferation; Intracellular signaling pathways; UMUC3

4.1. INTRODUCTION

The discovery of efficient and safe anticancer molecules from natural products is still a current demand in medical research. Among such compounds, ellagitannins that are found in some fruits and nuts such as pomegranates, strawberries and walnuts, emerge as promising leads. Ellagitannins are a subclass of hydrolysable tannins that comprise one or more hexahydroxydiphenic acid unities esterified to a polyol (usually α-D-glucopyranose) (Niemetz and Gross, 2005). The therapeutic significance of this group of polyphenols, namely as anticancer, antioxidant and anti-inflammatory compounds has been demonstrated *in vitro* and *in vivo* (Ascacio-Valdes et al., 2011; Liberal et al., 2015).

It has been established that dietary ellagitannins are partially hydrolyzed in the upper gastrointestinal tract into ellagic acid, which is also poorly absorbed (Seeram et al., 2004; Whitley et al., 2006) and, as a consequence, ellagic acid is metabolized by gut microbiota into urolithins (Cerdá et al., 2004; Espín et al., 2007). Urolithins are a subfamily of metabolites generated by the opening and decarboxylation of ellagic acid lactone rings, followed by a sequential dehydroxylation that promotes the production of a series of hydroxylated dibenzopyranones derivatives (Larrosa et al., 2010b; Selma et al., 2014). Importantly, after ellagitannins intake, urolithins or its conjugates (mainly glucuronides) were found in plasma at micromolar concentrations (Cerdá et al., 2004; Seeram et al., 2008) and were also identified in human tissues, namely prostate gland (González-Sarrías et al., 2010) and colon (Nuñez-Sánchez et al., 2014). Although the concentration of urolithins in plasma, urine and feces varies considerably between individuals, which is probably related with different gut microbiota composition (Bialonska et al., 2010; Cerdá et al., 2004; González-Barrio et al., 2010; Larrosa et al., 2010b), urolithin A (3,8-dihydroxy-6H-dibenzopyran-6-one) and its monohydroxylated analog, urolithin B, were the main ones reported in different mammals, including humans (Cerdá et al., 2004; Espín et al., 2007; González-Barrio et al., 2011). Urolithins remain in the body for long periods of time due to enterohepatic recirculation and are found in urine up to 4 days after consumption of ellagitannin-containing foods (Cerdá et al., 2004; Navindra P Seeram et al., 2006). Considering these evidences and the very low bioavailability of ellagitannins, urolithins have been proposed to be responsible for the biological activity and the systemic health effects related to the intake of ellagitannins.

Corroborating these observations, several studies highlight the antioxidant (Ishimoto et al., 2011), the estrogenic and/or anti-estrogenic activities (Larrosa et al., 2006a) and the anti-inflammatory properties (Larrosa et al., 2010b) of urolithins. Furthermore, *in vitro* chemopreventive and chemotherapeutic effects were also recently ascribed to urolithins and their derivatives (Kasimsetty et al., 2009; Qiu et al., 2013; Seeram et al., 2007; Vicinanza et al., 2013), although the

knowledge of the urolithins action mechanisms remain scarce. Therefore, to gain new insights in the putative role of urolithins as novel drugs for cancer therapy we proposed to investigate the antiproliferative effects of the urolithins most produced in humans, urolithins A and B, and its trihydroxylated precursor, urolithin C (Figure 4.1) in different tumour cell lines. The role of each compound in the mechanisms associated with cell proliferation, namely in cell cycle and cell death, as well as its effects on phosphatidylinositol 3-kinase (PI3K)/Akt and mitogen–activated protein kinases (MAPKs) intracellular signaling pathways were also unveiled. Additionally, this work aimed to establish a structure-activity relationship, which may constitute valuable information in the design of urolithins derivatives presenting potent antiproliferative activity.

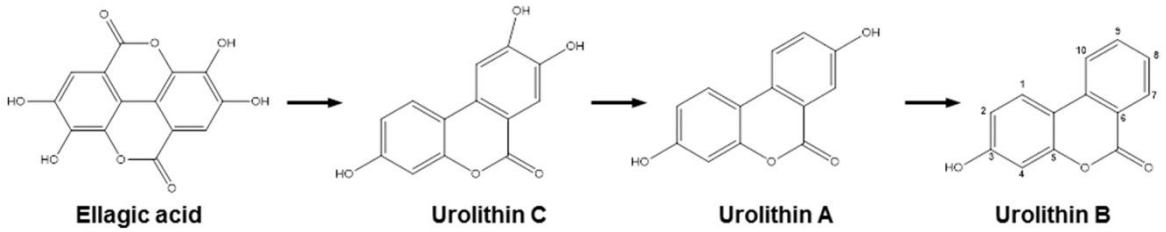

Figure 4.1 - Chemical structures of ellagic acid and urolithins

4.2. MATERIALS AND METHODS

4.2.1. CHEMICALS

DMEM, RPMI-1640, resazurin sodium salt, trypan blue, penicillin, streptomycin, β-tubulin antibody and ellagic acid were obtained from Sigma–Aldrich Química (St. Louis, MO, USA). Fetal bovine serum was from Gibco (Paisley, UK). Propidium iodide (PI), RNAse solution and annexin V-flourescein isothiocyanate (FITC)/PI double staining kit were purchased from Immunostep (Salamanca, Spain). Protease and phosphatase inhibitor cocktails were from Roche (Mannheim, Germany). Polyvinylidene difluoride (PVDF) membranes were obtained from Millipore Corp. (Bedford, MA, USA) and polyacrylamide from BioRad (Hercules, CA, USA). Alkaline phosphatase-conjugated secondary antibodies and enhanced chemifluorescence substrate (ECF) were purchased from GE Healthcare (Chalfont St. Giles, UK). Phospho (p-) extracellular signal-regulated protein kinases 1 and 2 (Erk1/2; Thr202/Tyr204), stress activated protein kinase/c-Jun amino terminal kinase (SAPK/JNK; Thr183/Tyr185), p38 MAPK (Thr180/Tyr182) and Akt (Ser473) antibodies were obtained from Cell Signaling Technology (Danvers, MA, USA).

Urolithins A (3,8-dyhydroxy-urolithin; 98.3% purity), B (3-hydroxy-urolithin; 99.4% purity) and C (3,8,9-dyhydroxy-urolithin; 98.3% purity) (Figure 4.1) were acquired from Dalton Pharma Services (Toronto, Canada). Urolithins were diluted in DMSO and stored at -20 ºC, and ellagic acid was diluted in 1 M NaOH, as described by the supplier.

4.2.2. CELL CULTURE

HepG2 (human hepatocellular carcinoma; ATCC® HB-8065™) cells were cultured in DMEM with 1 g/L of glucose, A549 (human lung adenocarcinoma epithelial cells; ATCC® CCL-185™), MCF-7 (human breast carcinoma; ATCC® HTB-22™) and BJ (human skin fibroblasts derived from normal foreskin; ATCC® CRL-2522™) cells in DMEM with 5 g/L of glucose, and UMUC3 (human bladder transitional carcinoma; ATCC® CRL-1749™) in RPMI-1640 medium with L-Glutamine. All mediums contained 10% (v/v) heat-inactivated fetal bovine serum, 100 U/mL penicillin, and 100 μg/mL streptomycin. Cells were maintained at 37 ºC and 5% CO_2 in a humidifier incubator.

4.2.3. ASSESSMENT OF CELL VIABILITY

Cell viability/metabolic activity was determined by resazurin assay (O'Brien et al., 2000). Resazurin (blue) is reduced into resorufin (pink) by metabolically active cells; therefore the magnitude of dye reduction is correlated with the number of viable cells. Cells were plated in 48-well plates for 12 h, the medium was carefully removed and cells were treated with serial concentrations

of urolithins A, B and C (from 0.25 to 200 µM) and ellagic acid (from 0.5 to 75 µM) for 48 h. Similarly, sequential concentrations of DMSO and NaOH, respectively, were used as controls. Resazurin (50 μM) was added to the cells 1 h before fluorescence recording. Since BJ cells have a lower metabolic activity the incubation with resazurin was performed during 4 h. Absorbance was read using a standard spectrophotometer (SLT, Austria) at 570 nm, with a reference wavelength of 620 nm. Treated cells were compared with the respective controls and the IC_{50} value was determined by nonlinear regression, representing the concentration required to inhibit 50% of cell viability.

4.2.4. CELL CYCLE AND CELL DEATH ANALYSIS

UMUC3 cells were plated in 12-well plates and analyzed after 24 and 48 h of treatment with the urolithins A (23.92 µM), B (41.8 µM) and C (16.28 µM). In order to investigate cell cycle distribution, cells were trypsinized, washed twice with phosphate-buffered saline (PBS) and fixed overnight with ice-cold 70% aqueous ethanol. Cells were then incubated with PI in RNase solution for 15 min at room temperature and analyzed by flow cytometry.

Apoptosis was evaluated using an annexin V-fluorescein FITC/PI double staining kit as described by the supplier. Briefly, UMUC3 cells were harvested by trypsinization, washed with PBS, incubated with annexin V and PI and analysed by flow cytometry.

The results were obtained on a Becton Dickinson FACSCalibur cytometer using the Cellquest software (BD Biosciences). PI histogram modelling was performed in ModFit LT software (Verity Software House). For accurate instrument setting, the flow cytometer was calibrated with fluorescent standard microbeads (CaliBRITE Beads; BD Biosciences).

4.2.5. TRYPAN BLUE EXCLUSION ASSAY

After 48 h of each treatment, cells were trypsinized and suspended in cell culture medium. A sample of this suspension was diluted with the same volume of trypan blue dye and cells were immediately counted using a Neubauer's hemocytometer. Control cells were incubated with the same volume of DMSO available in urolithin-treated cells.

4.2.6. PREPARATION OF UMUC3 CELLS EXTRACTS

UMUC3 were cultured in 24-well plates for 12 h and further incubated with urolithins A, B and C at different time points, accordingly to the proteins studied. Whole-cell lysates were obtained with RIPA buffer (50 mM Tris-HCl, pH 8.0, 1% Nonidet P-40, 150 mM NaCl, 0.5% sodium deoxycholate, 0.1% sodium dodecyl sulfate and 2 mM ethylenediaminetetraacetic acid) supplemented with 1 mM dithiothreitol, protease and phosphatase inhibitor cocktails tablets. Cells

were scraped and centrifuged at 12,000 rpm for 10 min at 4 °C to remove cell debris. The supernatant was collected and stored at -80 ºC until use.

4.2.7. WESTERN BLOT ANALYSIS

The protein concentration of cell lysates was determined by the bicinchoninic acid protein assay. Samples were denatured in sample buffer (0.125 mM Tris pH 6.8, 2% (w/v) sodium dodecyl sulphate, 100 mM dithiothreitol, 10% glycerol and bromophenol blue) and heated for 5 min at 95 ºC. Briefly, equal amounts of proteins were separated by 4-10% (v/v) SDS-PAGE and transferred to PVDF membranes. The membranes were incubated, overnight at 4 ºC, with the primary antibodies for phosphorylated proteins Erk1/2, SAPK/JNK and p38 MAPKs and Akt (1:1000) and with anti-rabbit or anti-mouse alkaline phosphatase-linked IgG secondary antibody for 1 h at room temperature. The bands were visualized using the ECF substrate and the imaging system TyphoonTM FLA 9000 (GE Healthcare). The bands densitometry was quantified using the Image Quant 6.0 software (Molecular Dynamics, Amersham Biosciences). The membranes were reprobed for *β*-tubulin antibody (1:20000) to demonstrate that similar amounts of protein were loaded in gels.

4.2.8. STATISTICAL ANALYSIS

Data are expressed as mean ± SEM. Statistical significance was determined using one-way analysis of variance (ANOVA), followed by *Dunnett's post-hoc test*. The statistical analysis was performed using Prism 5.0 Software (GraphPad Software). Differences were considered significant for $p < 0.05$.

4.3. RESULTS AND DISCUSSION

4.3.1. EFFECT OF UROLITHINS AND ELLAGIC ACID ON CELL VIABILITY

In this study, we intended to identify the most potent antiproliferative ellagitannins' metabolites, evaluate the sensitivity of several tumor cell lines to urolithins A, B and C, as well as to investigate the selective effect of these urolithins in cancer cells. Resazurin reduction colorimetric assay was used to assess the cell viability of urolithins and ellagic acid treated cells. Human tumor cell lines (UMUC3, A549, HepG2 and MCF-7) and non-tumor cells (BJ) were treated with increasing concentrations of those compounds for 48 h. For urolithins, data points of the dose-response curves were fitted with a sigmoid function for the calculation of the IC_{50} values that were further used in subsequent studies. Data showed that urolithins A, B and C reduced cell viability in a dose dependent manner (Figure 4.2). Overall, and taking to account the curves and the IC_{50} values, urolithins A and C were the most active samples presenting the lowest IC_{50} values for the tumor cell lines tested (Table 1). The effect of urolithins was also dependent on the cell type, being the UMUC3 and A549 the most sensitive cell lines to treatment with the urolithins. Importantly, the highest IC_{50} values of urolithins were observed in the non-tumor BJ cells and urolithin A showed about 5 times less toxicity on normal fibroblasts than the other urolithins. All together these results suggest that urolithins, and particularly urolithin A, exhibited a preferential cytotoxicity against human tumor cell lines.

Regarding ellagic acid treatment, it was not possible to determine the IC_{50} using a sigmoidal curve fitting since no dose-response effects were observed within the range of tested drug concentrations, in any of the cell lines. The upper concentration tested (75 μM) was superior to the mean IC_{50} values found for urolithins A and C in tumor cell lines and exerted marginal effects on the viability of almost cells lines, suggesting that ellagic acid had no significant cytotoxic activity in these cells.

From our knowledge this is the first report analyzing the effect of urolithins in A549, UMUC3 and BJ cell lines. Our results are in agreement with those obtained by Kallio et al. (2013) in HepG2 cells, demonstrating that urolithins A and B, but not ellagic acid, decreases liver cells viability, and that urolithin A is more active than urolithin B. Moreover, our data show that urolithin C was the most active molecule in HepG2 cells, since it presented the lowest IC_{50} value. Furthermore, among the tumor cell lines tested, the MCF-7 cells were the most resistant to urolithins treatment. However, the urolithins were still able to decrease MCF-7 cells viability and again, urolithin C, presented the lowest IC_{50}. Accordingly, previous studies in MCF-7 cells indicated that, urolithins A and B are able to bind estrogenic receptors exhibiting estrogenic and antiestrogenic activities (Larrosa et al., 2006a), and to inhibit aromatase activity (Adams et al., 2010), events that may be critical for breast cancer chemoprevention.

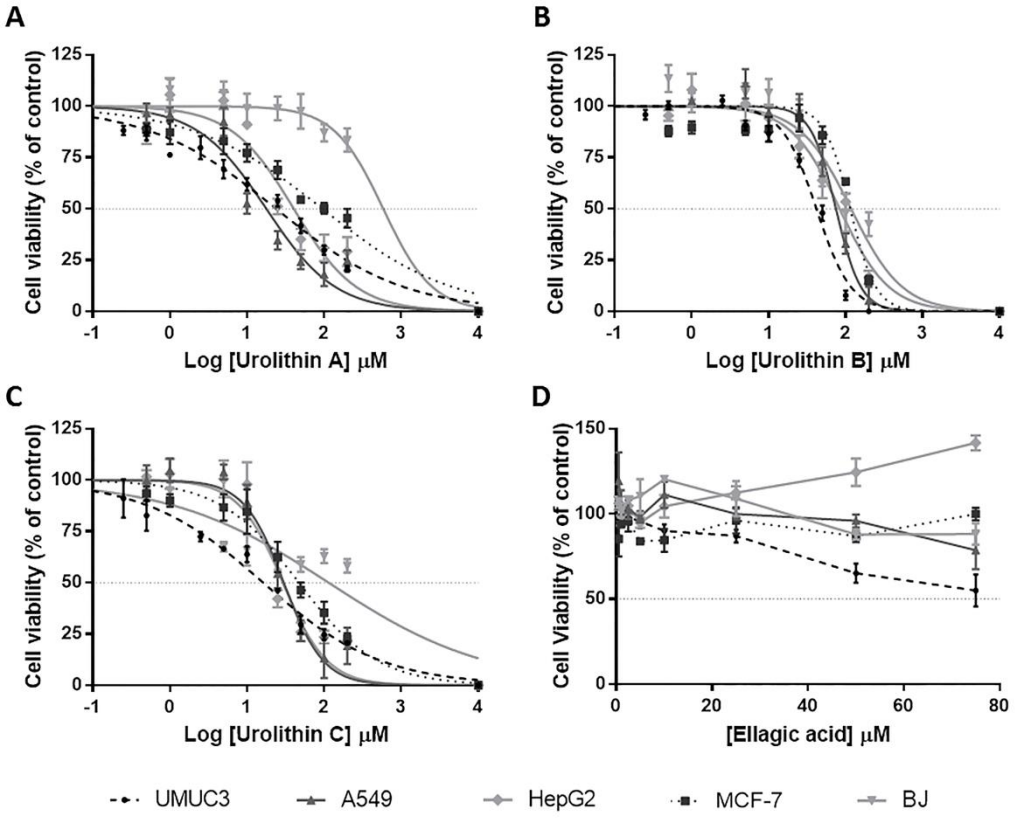

Figure 4.2 - Dose-response effect of urolithins and ellagic acid on cell viability in different cell lines. Cells were treated with different concentrations of urolithin A (A), urolithin B (B), urolithin C (C) and ellagic acid (D) for 48 h. Data-points correspond to the mean ± SEM of at least three independent assays. For urolithins, dose-response curves were fitted to a sigmoidal function to calculate the mean IC_{50} values.

Table 4.1 - IC_{50} values and confidence intervals (CI) of urolithins A, B and C in different cell lines

	Urolithin A (μM)		Urolithin B (μM)		Urolithin C (μM)	
	IC_{50}	95% CI	IC_{50}	95% CI	IC_{50}	95% CI
UMUC3	23.92	[19.64 - 29.14]	41.8	[37.74 - 46.29]	16.28	[12.55 - 21.11]
MCF-7	95.56	[69.62 - 131.2]	114.9	[101.0 - 130.6]	47.25	[36.99 - 60.35]
A549	17.81	[13.63 - 23.42]	74.83	[65.97 - 84.89]	30.09	[24.21 - 37.39]
HepG2	40.53	[30.73 - 53.46]	83.72	[67.87 - 103.3]	29.29	[22.98 - 37.32]
BJ	586	[215.8 - 1591]	117.8	[89.86 - 154.4]	114.9	[63.51 - 208.0]

Overall, we considered that the UMUC3 cell line was the most susceptible to these molecules since the IC_{50} values for all the urolithins tested were lower than 50 μM (urolithin A - 23.92 μM; urolithin B - 41.8 μM; urolithin C -16.28 μM). Based on these data, the UMUC3 cells were used in subsequent experiments. Furthermore, since ellagic acid was the less active molecule and its IC_{50} was not able to be calculated we did not perform additional experiments with this compound.

4.3.2. EFFECT OF UROLITHINS ON CELL CYCLE

Defects in cell cycle checkpoints are associated with an increase of genetic instability and uncontrolled cell proliferation, which could lead to the development of the carcinogenic process. Several bladder transitional carcinoma cell lines, including UMUC3 cells, have defective cell cycle checkpoint functions (Doherty et al., 2003). Therefore, targeting cell cycle machinery would lead to the inhibition of cell proliferation and induction of apoptotic cell death, thus presenting potential value in identifying novel therapies to circumvent disease progression.

Hence, the effect of the urolithins on the cell cycle of UMUC3 cells was evaluated. Cells were treated with urolithin A, B and C at the corresponding IC_{50} values for 24 or 48 h and analyzed for the distribution of G0/G1, S and G2/M phases by flow cytometry. Urolithin A, at both time periods, clearly decreased the number of cells at G0/G1 stage. However, its effect was more pronounced after 24 h since there was a reduction of 30.0% in the percentage of cells in G0/G1 as compared to control cells, whereas after 48 h of incubation the percentage of cells in G0/G1 suffered a reduction of 21.6% as compared to that observed in control. This decrease in the percentage of cells in G0/G1 was accompanied by a significant rise of the percentage of cells in G2/M. In fact, in cells incubated for 24 h with urolithin A, the percentage of cells in G2/M increased 26.1% as compared to that in control cells. However, in cells incubated with urolithin A for 48 h, the percentage of cells in the G2/M increased 13.1% as compared to control. These results seem to indicate that urolithin A induces a cell cycle arrest in G2/M which is more evident at 24 h of incubation (Figure 4.3). Accordingly, cell cycle arrest at G2/M phase was also previously reported in colon and prostate cell lines treated with urolithin A (Cho et al., 2015; González-Sarrías et al., 2014; Kasimsetty et al., 2010; Vicinanza et al., 2013). Several key proteins are involved in controlling G2/M checkpoint. A study performed by Vicinanza et al. (2013) demonstrated that urolithin A changed cell cycle distribution, increased cdc 2 kinase phosphorylation at tyrosin-15 and induced an accumulation of cyclin B1, suggesting an inactivation of the cyclin B1/cdc2 kinase complex that is a known regulator of the G2/M transition.

Our data also showed that urolithin C decreased the percentage of cells in the G0/G1 phase although less pronounced than the decrease observed for urolithin A. In fact, after 24 h of incubation with urolithin C the percentage of cells in G0/G1 decreased 10% as compared to control cells (Figure

4.3-A). However, this reduction was not sustained after 48 h of incubation with urolithin C (Figure 4.3-B). Therefore, our data showed that unlike urolithin A, there was not a cell cycle arrest with urolithin C.

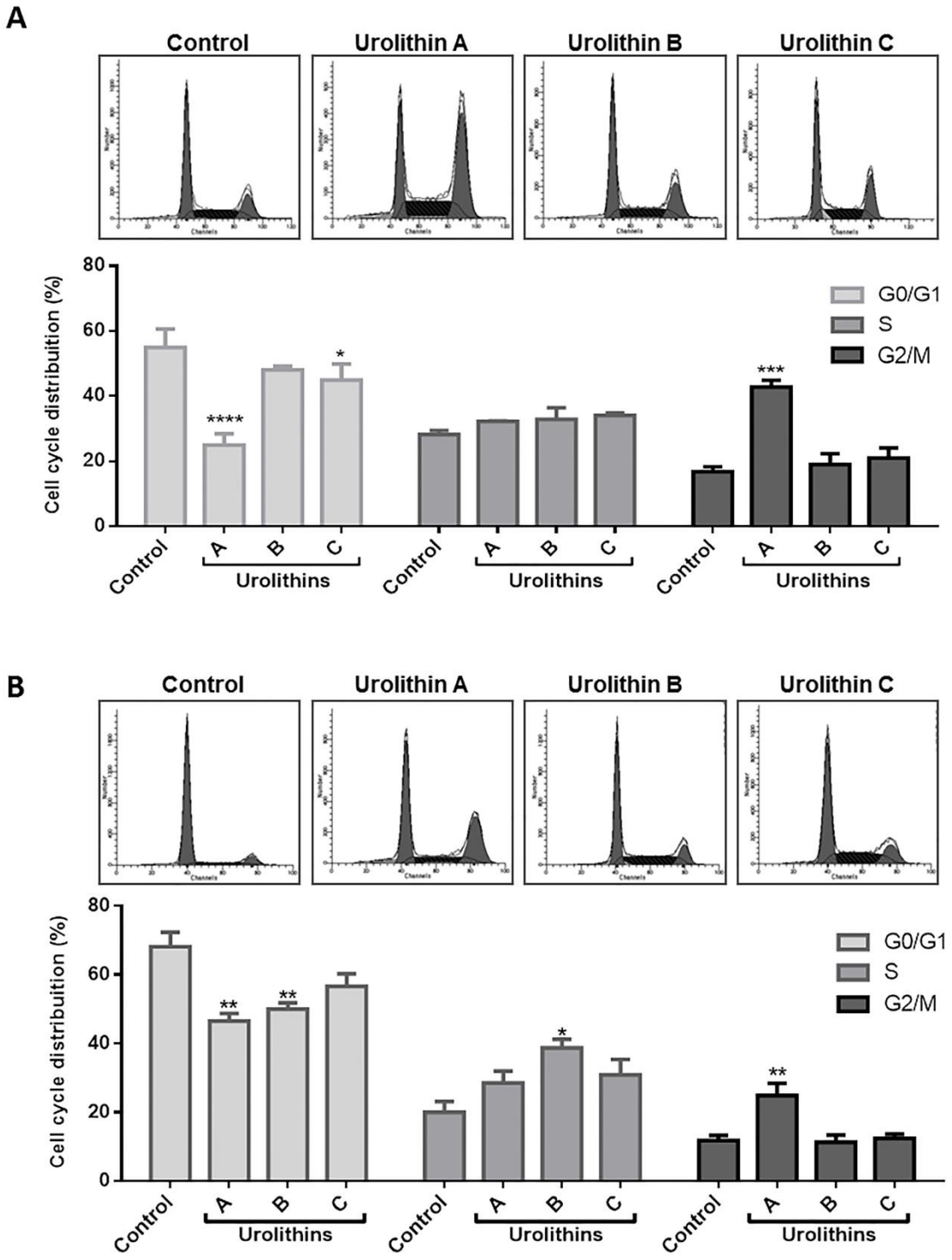

Figure 4.3 - Effects of urolithins on cell cycle progression in UMUC3 cells. Cells were incubated with urolithins A, B and C for 24 (A) and 48 (B) h and then assayed for cell cycle analysis by flow cytometry with PI. Data are expressed as percentage of PI-positive cells and were given as the means ± SEM of at least three independent experiments. * p<0.05, ** p<0.01, ***p<0.001, ****p<0.0001 when compared to control.

Regarding urolithin B, data showed that this urolithin also reduced the percentage of cells in G0/G1 but was less effective than urolithin A, and its effect was more pronounced at 48 h of incubation (decreased 18.1% as compared to control). In addition, our data pointed out that urolithin B was the only urolithin that significantly increased the percentage of cells in the S phase (the percentage of cells increased 18.7% as compared to that in control cells) (Figure 4.3-B). These results are in agreement with those previously observed in colonic cell lines (González-Sarrías et al., 2014). Overall, we observed that different urolithins elicit dissimilar cellular response, suggesting that each urolithin triggers a specific signaling transduction profile.

4.3.3. APOPTOSIS/NECROSIS MODULATION BY UROLITHINS

Apoptosis induction is still considered a chemopreventive and chemotherapeutic strategy in cancer. In order to identify the type of cell death, specifically apoptosis and/or necrosis, UMUC3 cells were incubated with urolithins A, B or C, for 24 (Figure 4.4-A) and 48 h (Figure 4.4-B), and then stained with annexin V-FITC/PI. Data showed a statistically significant increase in early apoptotic, late apoptotic and necrotic cells after 48 h of UMUC3 treatment with urolithin A (Figure 4.4-B). In contrast, urolithins B and C induce neither apoptosis nor necrosis (Figure 4.4). This selective profile attributable to urolithin A was not observed in T24 cells, also derived from a transitional cell carcinoma, in which both urolithin A and B induced apoptotic cell death (Qiu et al., 2013). These differences are probably due to genetic and molecular differences between cell lines studied.

4.3.4. DETERMINATION OF UMUC3 CELLS VIABILITY AFTER UROLITHINS A, B AND C INCUBATION THROUGH TRYPAN BLUE EXCLUSION ASSAY

As previously described, the resazurin assay was used to evaluate the IC_{50} values for cell viability. The absence of significant effects on apoptotic/necrotic cell death and the magnitude of the outcomes on cell cycle distribution triggered by urolithins B and C led us to apply another viability test, the trypan blue exclusion assay that measures the integrity of plasmatic membrane (Strober, 2001). Therefore, cells were treated, for 48 h, with the urolithins' concentrations corresponding to IC_{50} values, as determined by the resazurin assay.

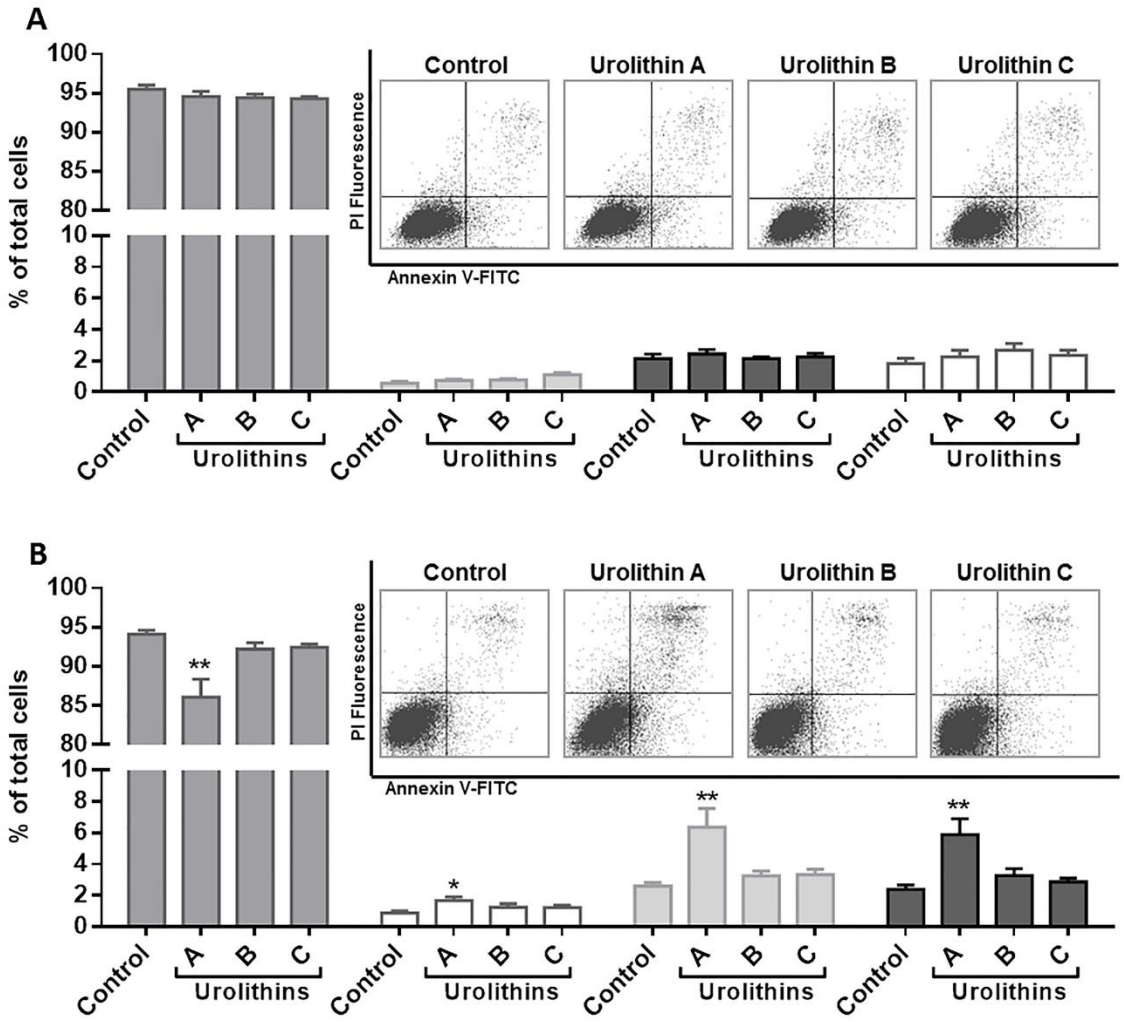

Figure 4.4 - Detection of Apoptosis/Necrosis after urolithins treatment. Cells were incubated with urolithins A, B and C for 24 (A) and 48 h (B). Annexin V-FITC/PI labelling was detected by FACSCalibur flow cytometer. The populations of early apoptotic cells (annexin V-positive/PI negative), late apoptotic cells (annexin V positve/PI positive), necrotic cells (annexin V negative/PI positive) and viable cells (annexin V negative/PI negative) were evaluated as a percentage of total cells and were given as the means ± SEM of at least three independent experiments. * $p<0.05$, ** $p<0.01$ when compared to control.

The results showed a slight statistically significant decrease of cell viability after incubation with urolithins B (20%) and C (22%), while for urolithin A the results were consistent with those obtained using the resazurin assay, with a decrease of 48% in cell viability (Figure 4.5). The resazurin based assay has been broadly used as indicator of metabolically active mitochondria, but might over/under estimate the number of viable cells. Considering these results, we may conclude that cells treated with urolithins B and C are probably metabolic defective, which for the time periods studied do not directly reflect the number of cells. Therefore, this study reinforces the concept that it may be more suitable to apply more than one viability test, allowing the evaluation of different parameters, to exclude false positive/negative results (Stoddart, 2011). Importantly, we may also

conclude that urolithin A is the most active molecule inUMUC3 cells, strongly suggesting its exploitation in *in vivo* models of transitional bladder cancer.

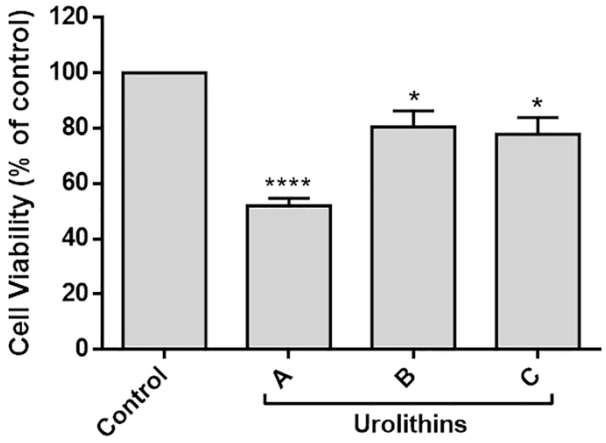

Figure 4.5 - Trypan blue exclusion test of cell viability. Cells were incubated with urolithins A, B and C for 48 h and then assayed for cell viability. Data are presented as mean ± SEM of, at least, 3 independent experiments and are expressed as percentage of control * $p<0.05$, **** $p<0.0001$ when compared to control.

4.3.5. EFFECT OF UROLITHINS ON THE INTRACELLULAR SIGNALING PATHWAYS PI3K/AKT AND MAPKS

We also evaluated the effects of the urolithins on the activation status of PI3K/Akt and MAPKs signaling pathways, which are implicated in cell survival and proliferation. This analysis was performed by measuring the levels of phosphorylated kinases by western blot at different time-points. The PI3K/Akt pathway promotes cellular survival by allowing defective cells to overcome cell cycle checkpoints and suppress apoptosis (Chang et al., 2003). Indeed, the aberrant activation of this pathway is characteristic of a wide range of cancers, including bladder cancer (Wu et al., 2004). Accordingly, pharmacological inhibition of PI3K/Akt pathway has been referred to reduce the invasive capacity of the UMUC3 cell line (Knowles et al., 2009). Based on these findings, we evaluated the effect of urolithins A, B and C on Akt phosphorylation status in bladder cancer UMUC3 cells (Figure 4.6-A-C). Our data showed that urolithin A decreased the levels of p-Akt at short times (Figure 4.6-A), suggesting the potential of urolithin A as chemopreventive/chemotherapeutic agent.

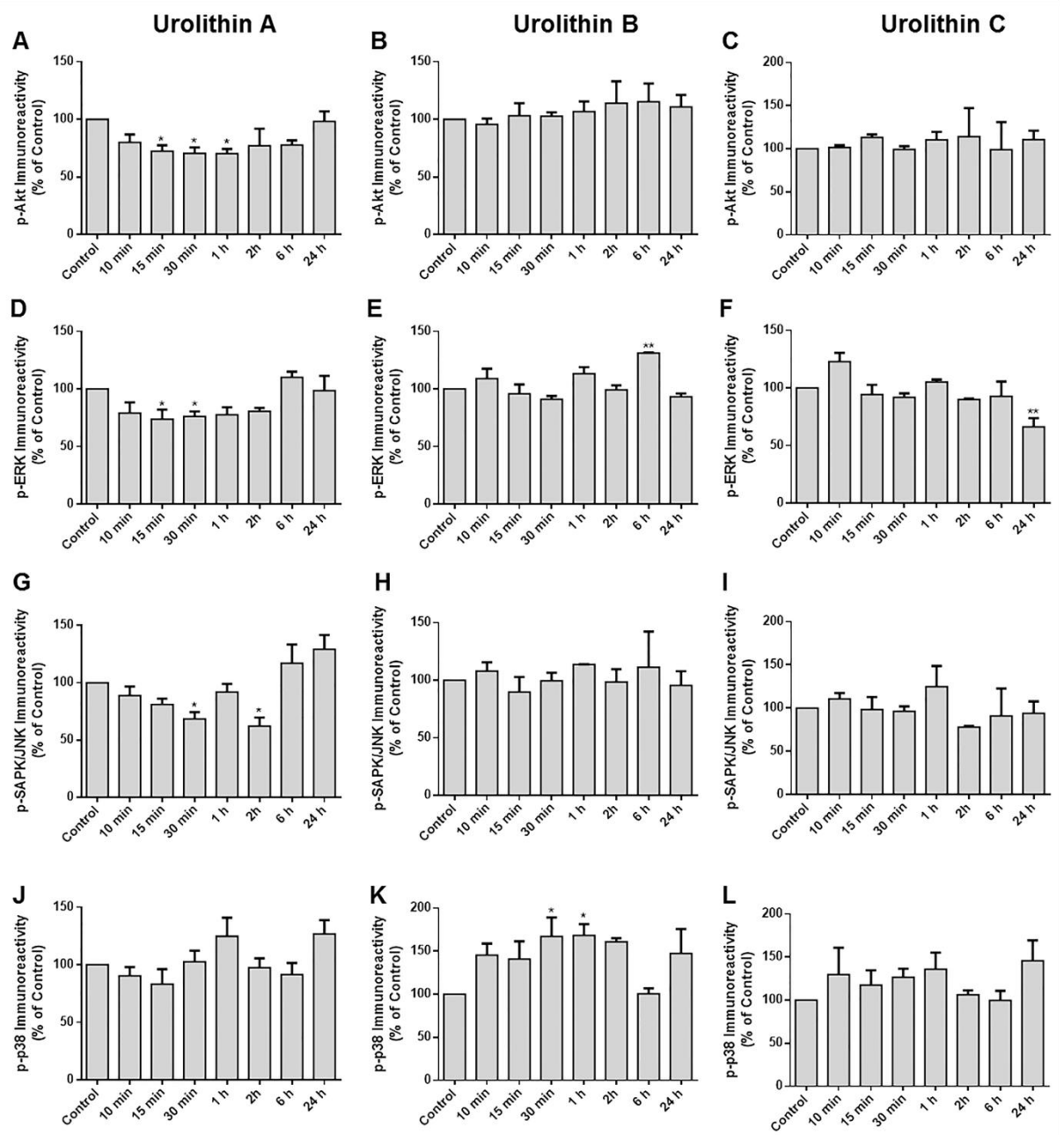

Figure 4.6 - Effect of urolithins on PI3K/AKT and MAPKs signaling pathways. UMUC3 cells were incubated with urolithins A, B and C for different time points. The levels of Akt, ERK1/2, SAPK/JNK and p38 phosphorylated proteins were evaluated by western blot. Representative immunoblots are presented in Supplementary Figure 4-I. Data are presented as mean ± SEM of, at least, 3 independent experiments and are expressed as percentage of control. *p<0.05, **p<0.01 when compared to control.

ERKs regulate several cellular processes such as proliferation, survival and prevention of apoptosis, while JNKs and p38 MAPKs usually positively regulate apoptosis and cell differentiation (Wada and Penninger, 2004). The majority of bladder cancers are highly dependent on ERK activation (Knowles and Hurst, 2014). Interestingly, our results demonstrated that urolithin A decreased the phosphorylation of ERK 1/2 (Figure 4.6-D) and SAPK/JNK (Figure 4.6-G) at short time periods of incubation. We may therefore suggest that the antiproliferative effects of urolithin A could be related to ERK 1/2 inhibition. However, the concomitant and intermittent decrease of SAPK/JNK phosphorylation could negatively regulate apoptosis. In fact, the effect of urolithin A in apoptotic cell death was only detected 48 h after cells treatment. Studies using specific MAPKs inhibitors should be addressed to further disclose the mechanisms behind apoptosis activation evoked by urolithin A. Furthermore, cells treated with urolithins B and C demonstrated sporadic differences, for instance urolithin C decreases the expression of p-ERK 1/2 after 24 h of treatment (Figure 4.6-F), while urolithin B increases the expression of p-ERK 1/2 at 6 h (Figure 4.6-E). Urolithin B also increases the expression of p-p38 at different time points (Figure 4.6-K).

These results showed clear differences in the activity among the different urolithins tested, highlighting the potential therapeutic value of urolithin A. These differences appear to be related with the number/position of hydroxyl groups (Figure 4.1). Indeed, in comparison with urolithin B, the presence of a hydroxyl group at position 8 in urolithin A determined an increase in biological activity. Conversely, the additional hydroxyl group in urolithin C at position 9 seems to have an opposite effect.

Even though urolithins A and B had been identified in human plasma and urine after ingestion of food containing ellagitannins, the more abundant metabolites found in these samples were their glucuronide conjugates (Truchado et al., 2012). Although in other cell lines the glucuronidation led to a decrease in the biological activity of urolithins (González-Sarrías et al., 2014) it would be interesting to evaluate the antiproliferative effects of these metabolites in bladder cancer cells. Furthermore, and since different ellagitannins' metabolites are present in biological samples, the effects of the combination of those molecules should also be addressed.

4.4. CONCLUDING REMARKS

The increasing occurrence of human malignancies and the side effects of conventional therapies highlight the importance to uncover alternative drugs. Bladder cancer is the most common malignancy of the urinary system with higher incidence in men and more than 90% of all bladder cancers are transitional cell carcinomas (Jemal et al., 2011). The treatment of metastatic bladder cancer still remains one of the main challenges in urologic oncology (Nicholson et al., 2004). The resistance of this carcinoma to a wide range of chemotherapeutic agents is the main reason for treatment failure (Knievel et al., 2014), emphasizing the urgency of discovering new therapeutic strategies. In the last years, the therapeutic potential of dietary ellagitannins has been investigated, however, it has also been demonstrated that the bioavailability of ellagitannins is very low, in contrast to their metabolites, the urolithins. This knowledge aroused the interest of the scientific community for this group of compounds that have been proposed as responsible for the anticancer activity and for the systemic health effects related to the intake of ellagitannins. Herein, we evidenced that urolithins A, B and C have antiproliferative effects in several human cancer cell lines. In particular, urolithin A induced cell cycle arrest, increased apoptosis and modulated the intracellular pathways PI3K/Akt and MAPKs signaling in UMUC3 cells. Of utmost importance we have also shown the selective effect of urolithins to tumor cells and established a structure-activity relationship, which constitutes valuable information in the future design of urolithins derivatives.

Overall, this paper is a first step in proof-of-principal work that generated important insights in the therapeutic value of urolithins, strongly supporting and encouraging further work on urolithins as potential chemopreventive/chemotherapeutic drugs for transitional bladder cancer.

ACKNOWLEDGEMENTS

We acknowledge FEDER/COMPETE (FCOMP-01-0124-FEDER-011096), Fundação para a Ciência e a Tecnologia (FCT, Portugal), European Union and QREN for funding the projects PTDC/SAU-FCF/105429/2008, PEst-C/SAU/LA0001/2013-2014, PEst-C/QUI/UI0062/2013, the Ph.D. fellowship SFRH/BD/72918/2010 and the QOPNA research unit (project PEst-C/QUI/UI0062/2013; FCOMP-01-0124-FEDER-037296).

We also thank Professor Conceição Pedroso Lima and Doctor Eugénia Carvalho (Center for Neurosciences and Cell Biology, University of Coimbra) for kindly supplied HepG2 and BJ cell lines, respectively.

SUPPLEMENTARY DATA

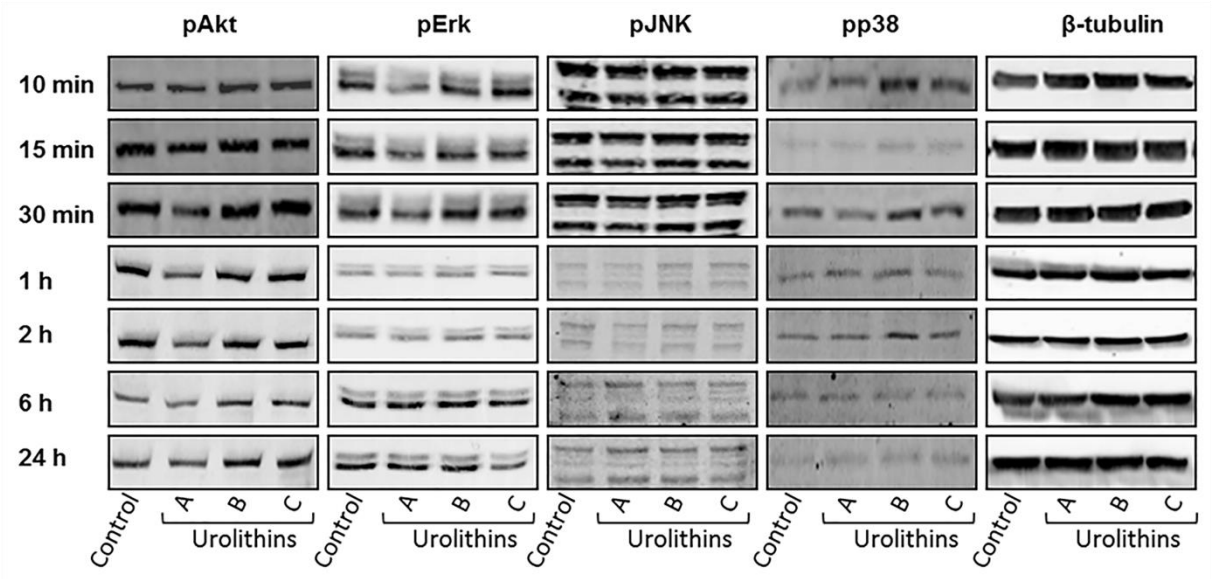

Supplementary Figure 4.I - Representative immunoblots of the data from Figure 4.6

Chapter 5

In vitro antiproliferative effects of urolithins on human osteosarcoma cells

Joana Liberal, Anália Carmo, Célia Gomes, Maria Teresa Cruz, Maria Teresa Batista

Manuscript in preparation

ABSTRACT

Osteosarcoma is the most common malignant primary bone tumor, with a higher incidence in children and adolescents. Despite the therapeutic advances, the prognosis of patients with metastatic disease is still poor. Therefore, the identification of novel anticancer molecules able to improve patients' outcome is of utmost importance.

Several studies have demonstrated that gut microbiota-derived ellagitannins' metabolites, urolithins, have chemotherapeutic potential. Therefore, in this study we aimed to evaluate the anticancer properties of urolithins A, B and C in the osteosarcoma cell line MNNG-HOS.

The evaluation of cell viability demonstrated that urolithins A and C were the most active, having the lowest IC_{50} values. Urolithins A and C also promoted an arrest of cell cycle at G2/M and S checkpoints, respectively. Furthermore, urolithin A slightly increased apoptotic and necrotic MNNG-HOS cell death. Overall, among the compounds tested, urolithin B was the less active molecule.

This data obtained highlights the antiproliferative effects of urolithins on a human osteosarcoma cell line and underlines the potential of urolithins A and C as chemopreventive/chemotherapeutic agents.

5.1. INTRODUCTION

Osteosarcoma is the most common malignant primary bone tumor in humans with a higher incidence in children and adolescents (Ottaviani and Jaffe, 2009). Current therapies include surgical resection and chemotherapy (methotrexate, doxorubicin, cisplatin, and ifosfamide) (Luetke et al., 2014), which have improved patient survival rates. However, approximately one third of patients with localized disease will relapse (Link et al., 1986) and the prognosis of patients with metastasis or recurrence is still poor (5-year survival is only about 20%) (Niswander and Kim, 2010). Therefore it is of utmost importance to identify novel compounds that alone or in combination with conventional chemotherapeutics could further improve patient outcome.

Polyphenols are a group of secondary metabolites of plants that have attracted widespread attention as cancer chemopreventive and chemotherapeutic agents (Asensi et al., 2011). Among them, ellagitannins (hydrolysable tannins) have shown potential as anticancer, antioxidant and anti-inflammatory compounds in both *in vitro* an *in vivo* studies (Ascacio-Valdes et al., 2011). Ellagitannins are frequently found in some fruits as pomegranates and berries and are characterized by the presence of one or more hexahydroxydiphenoyl (HHDP) moieties on a glucopyranose core (Lipińska et al., 2014). It is now well established that dietary ellagitannins undergo substantial metabolism after oral intake. They are first hydrolyzed in ellagic acid, which in turn is converted by colonic microflora into urolithins, which are much better absorbed (Cerdá et al., 2004; Espín et al., 2007). Urolithins are dibenzopyran-6-one derivatives with different hydroxyl substitutions (Larrosa et al., 2010b; Selma et al., 2014). Importantly, these metabolites, and not ellagitannins, were identified in plasma samples (González-Barrio et al., 2010; Larrosa et al., 2010b). Due to high concentrations of urolithins in plasma and the long time remaining in the body, they have been proposed as responsible for the biological activity and for the systemic health effects related to the intake of ellagitannins. Accordingly, recent studies evidenced the antiproliferative role of ellagitannins' metabolites (Kasimsetty et al., 2009; Qiu et al., 2013; Seeram et al., 2007; Vicinanza et al., 2013). We previously demonstrated that urolithins C (tri-hydroxylated), A (di-hydroxylated) and B (mono-hydroxylated) present antiproliferative activities in four human epithelial cancer cell lines and were less active in non-tumoral human fibroblasts, thus highlighting the selective effect of urolithins to tumor cells. In addition we observed that specifically urolithin A induced apoptosis in UMUC3 cell line and changed cell cycle distribution, increasing cells at G2/M phases (Chapter 4).

Hence, we aim to evaluate the antiproliferative effect of urolithins A, B, C and ellagic acid in the osteosarcoma cell line MNNG-HOS and further explore the cellular and molecular events behind the antiproliferative activities of each compound.

5.2. MATERIAL AND METHODS

5.2.1. CELL CULTURE

Human osteosarcoma cell line (MNNG/HOS - ATCC® CRL-1547™) was cultured in RPMI-1640 medium with L-glutamine (Sigma–Aldrich), containing 10% (v/v) heat-inactivated fetal bovine serum (Gibco), 100 U/mL penicillin, and 100 µg/mL streptomycin. Cells were maintained at 37ºC and 5% CO_2 in a humidifier incubator.

5.2.2. CHEMICALS

Urolithins A (3,8-dyhydroxy-urolithin; 98.3% purity), B (3-hydroxy-urolithin; 99.4% purity) and C (3,8,9-dyhydroxy-urolithin; 98.3% purity) (Dalton Pharma Services) were diluted in dimethylsulfoxide (DMSO) and stored at -20 ºC. Ellagic acid (Sigma–Aldrich) was diluted in 1 M NaOH, as described by the supplier.

5.2.3. ASSESSMENT OF CELL VIABILITY

Cell viability was firstly evaluated by resazurin assay (O'Brien et al., 2000). Metabolic active cells reduce resazurin (blue) into resorufin (pink) and therefore the magnitude of dye reduction is correlated with the number of viable cells. After plating in 48-well plates for 12 h, cells were treated for 48 h with serial concentrations of urolithins A, B and C (0.25 - 200 µM) and ellagic acid (0.5 - 75 µM). Resazurin (50 µM) (Sigma–Aldrich) was added to the cells 1 hour before recording fluorescence. Absorbance was read using a standard spectrophotometer (SLT, Austria) at 570 nm, with a reference wavelength of 620 nm. Treated cells were compared with the respective controls and the IC_{50} value, representing the concentration required to inhibit 50% of cell viability, was calculated by nonlinear regression.

The integrity of the cytoplasmic membrane was evaluated by trypan blue exclusion assay. Briefly, after 48 h of incubation with the urolithins, MNNG-HOS cells were trypsinized and resuspended in the cell culture medium. This suspension was diluted with equal volume of trypan blue dye (Sigma–Aldrich) and cells were counted in a hemocytometer.

In both experiments, control cells were incubated with the same amount of DMSO or NaOH of urolithins or ellagic acid-treated cells, respectively.

5.2.4. CELL CYCLE AND CELL DEATH ANALYSIS

MNNG-HOS cells were plated in 12-well plates and treated with urolithins for 24 or 48 h. Cell cycle and cell death were analyzed by flow cytometry as described previously (Chapter 4). The some concentration of DMSO was used in control condition.

5.2.5. PREPARATION OF UMUC3 CELLS EXTRACTS AND WESTERN BLOT ANALYSIS

MNNG/HOS cells were treated with the A, B and C urolithins for different time-points (10, 15 and 30 min and 1, 2, 6 and 24 h). On each time point the same concentration of DMSO presented in urolithin-treated cells was added to cultures. Whole cell lysates, protein concentration determination and western blot analysis of phosphorylated proteins Erk1/2, SAPK/JNK and Akt were performed as previously described in Chapter 4.

5.2.6. STATISTICAL ANALYSIS

Data are expressed as mean ± standard error of the mean (SEM). Statistical significance was determined using one-way analysis of variance (ANOVA), followed by Dunnett's post-hoc test. The statistical analysis was performed using Prism 5.0 Software (GraphPad Software). Differences were considered significant for $p < 0.05$.

5.3. RESULTS

5.3.1. DOSE-DEPENDENT EFFECT OF UROLITHINS ON MNNG-HOS CELLS

We started to evaluate the effects of urolithins on osteosarcoma cell line MNNG-HOS viability. Accordingly, cells were treated with different concentrations of urolithins A, B and C for 48 h and cell viability was measured with resazurin reduction colorimetric assay. For determination of IC_{50}, data points of the dose-response curves were fitted with a sigmoid function. All urolithins tested reduced cell viability in a dose dependent manner (Figure 5.1-A). However, urolithin C, that presented the lowest IC_{50} (16 μM), followed by urolithin A (28 μM) were much more active than urolithin B (60 μM) (Figure 5.1-A). Regarding ellagic acid, none of the concentrations tested affected cell viability (Figure 5.1-B). For that reason, it was not possible to determine the ellagic acid IC_{50} on MNNG-HOS cells.

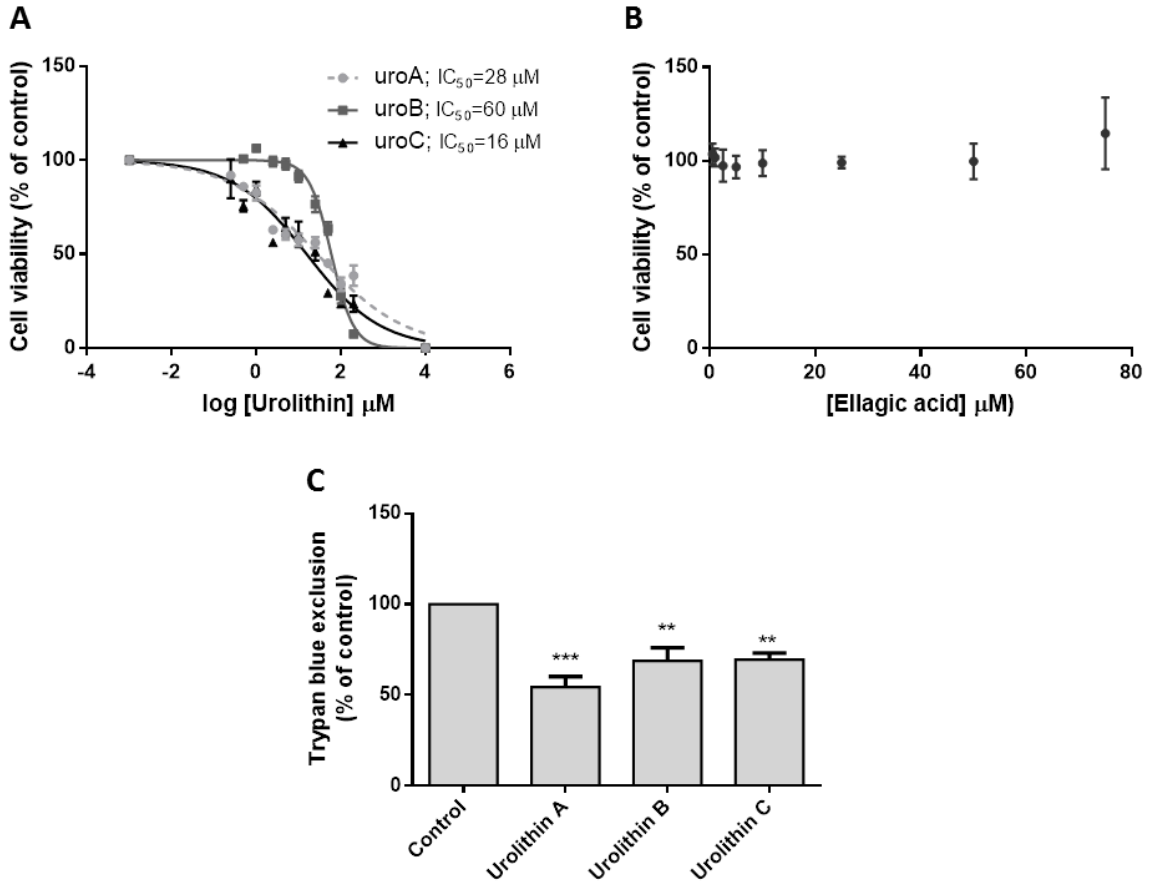

Figure 5.1 - Effect of urolithins on MNNG-HOS cells viability. (A) Cells were treated with different concentrations of urolithins A, B or C for 48 h. Data-points correspond to the mean ± standard deviation of the mean (SEM) of at least three independent assays. The IC_{50} values were fitted to a sigmoidal function from the dose-response curves of urolithins compounds; (B) Cells were treated with different concentrations of ellagic acid for 48 h. Data-points correspond to the mean ± SEM of at least three independent assays and are expressed as percentage of control; (C) Cells were incubated with urolithins A, B and C for 48 h and then assayed for cell viability through trypan blue exclusion test; ** p<0.01, ***p<0.001 when compared to control.

Previously, we observed that the results for cell viability after incubation with urolithins varied among different assays (Chapter 4). Therefore, to validate these results we performed the trypan blue exclusion test that evaluates the integrity of the cytoplasmic membrane, using the concentrations of the IC_{50} previously obtained. Similarly, urolithin A reduced cell viability to 54.5 ± 5.7% of the control. However, urolithins B and C only decreased cell viability to 68.8 ± 7.3% and 69.6 ± 3.6% of the control, respectively (Figure 5.1-C).

5.3.2. UROLITHINS A AND C INDUCED CELL CYCLE ARREST OF MNNG-HOS CELLS

Analysis of cell cycle distribution were performed after 24 and 48 h (Figure 5.2-A and 5.2-B, respectively) of MNNG-HOS cells incubation with urolithins A, B and C. Data showed that urolithin A induces an accumulation of cells at G2/M checkpoint after 24 and 48 h of treatment (the percentage of cells increased 9.5% and 8.6%, respectively, as compared to control cells). Similarly, and although not statistically significant, the incubation with urolithin C during 48 h increased the percentage of cells in G2 phase (the percentage of cells increased 8.6% as compared to control cells). Our data also showed that urolithin C increased the percentage of cells in the S phase at both time-points tested (increase of 10.9% and 12.44% after 24 and 48 h, respectively, as compared to control cells). Urolithin B addition to MNNG/HOS cells did not alter cell cycle distribution.

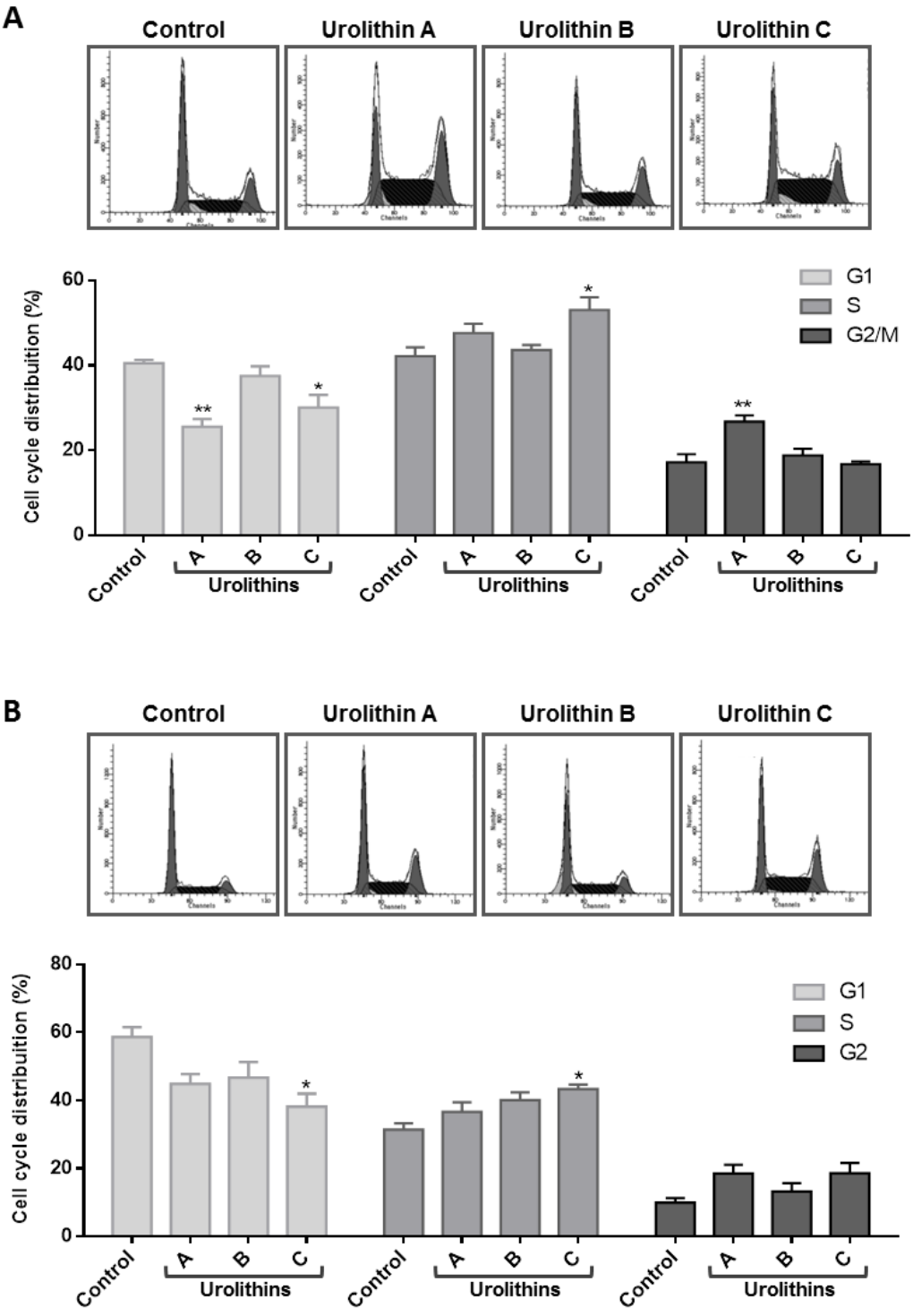

Figure 5.2 - Effect of Urolithins on MNNG-HOS cell cycle. Cells were incubated with urolithins A, B and C for 24 (A) and 48 (B) h. Data are expressed as percentages of PI-positive cells and were given as the means ± SEM of at least three independent experiments. * $p<0.05$, ** $p<0.01$ when compared to control.

5.3.3. UROLITHIN A INCREASES APOPTOTIC AND NECROTIC CELL DEATH

In order to evaluate the type of cell death evoked by urolithins in the MNNG-HOS cell line, cells were further incubated with urolithins A, B or C for 48 h and then stained with annexin V-FITC/PI. Data showed a slightly but statistically significant increase (2.5%, as compared to control) of early apoptotic cells after 48 h of MNNG-HOS treatment with urolithin A. The other urolithins studied induce neither apoptotic nor necrotic cell death (Figure 5.3).

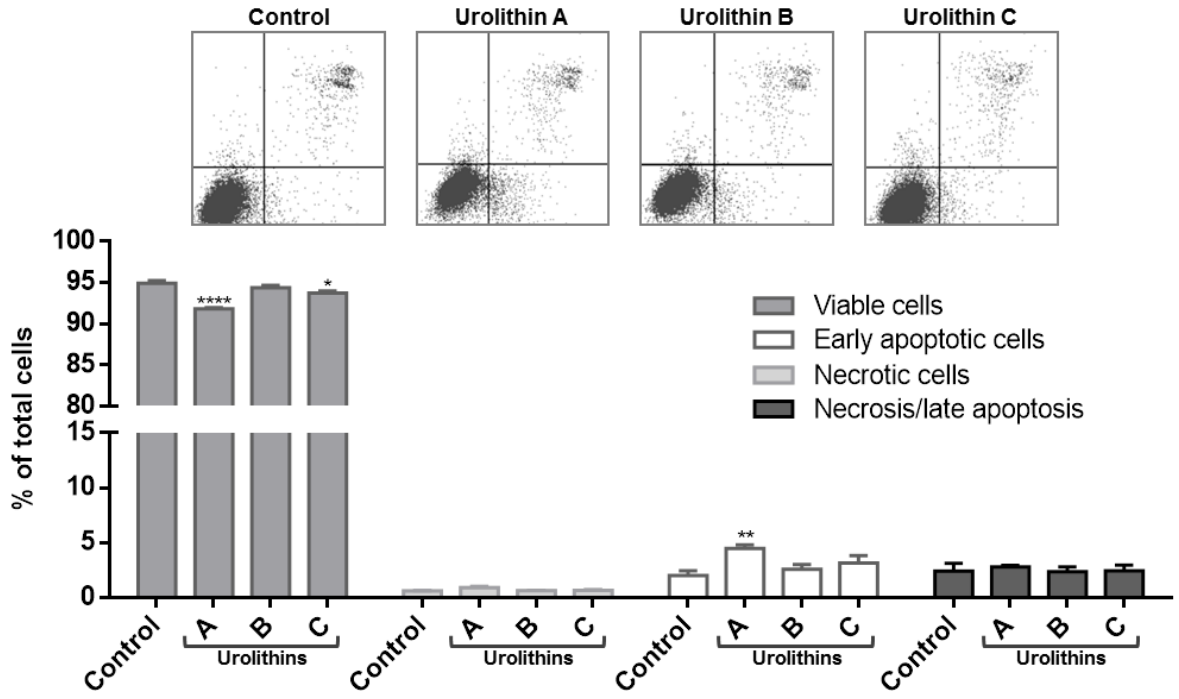

Figure 5.3 - Detection of Apoptosis/Necrosis induced by urolithins. MNNG-HOS cells were incubated with urolithins A, B and C for 48 h. Annexin V-FITC/PI labelling was detected by FACSCalibur flow cytometer. The populations of early apoptotic cells (annexin V-positive/PI negative), late apoptotic cells (annexin V positve/PI positive), necrotic cells (annexin V negative/PI positive) and viable cells (annexin V negative/PI negative) were evaluated as a percentage of total cells and were given as the means ± SEM of at least three independent experiments. * $p<0.05$, ** $p<0.01$, **** $p<0.0001$ when compared to control.

5.3.4. EFFECT OF UROLITHINS ON PHOSPHORYLATION OF AKT AND MAPKS

Previous studies performed in other cancer cell lines have shown that urolithins modulate PI3K/Akt and MAPK signalling pathways, which are implicated in cell survival and cell proliferation processes. Hence, we evaluated by western blot the total levels of phosphorylated (activated) Akt, ERK ½ and SAPK/JNK. We found sporadic differences in kinases phosphorylation, but we could not found a clear tendency in the modulation of these proteins (Figure 5.4). For instance, urolithin A decreases p-Akt (63.5 ± 4.9 % of the control) after 30 min of treatment (Figure 5.4-A) and urolithin C

decreases the phosphorylation of ERK ½ (63.3 ± 8.3 % of the control) after 24 h of cells treatment (Figure 5.4-F). Urolithin B, in turn, increases phosphorylation of ERK at 30 min (146.1 ± 7.6 % of the control) (Figure 5.4-E) and increases p-SAPK/JNK after 10 min (129.6 ± 6.0 % of the control) and 1 h (133.8 ± 6.42 % of the control) (Figure 5.4-H) of cells incubation.

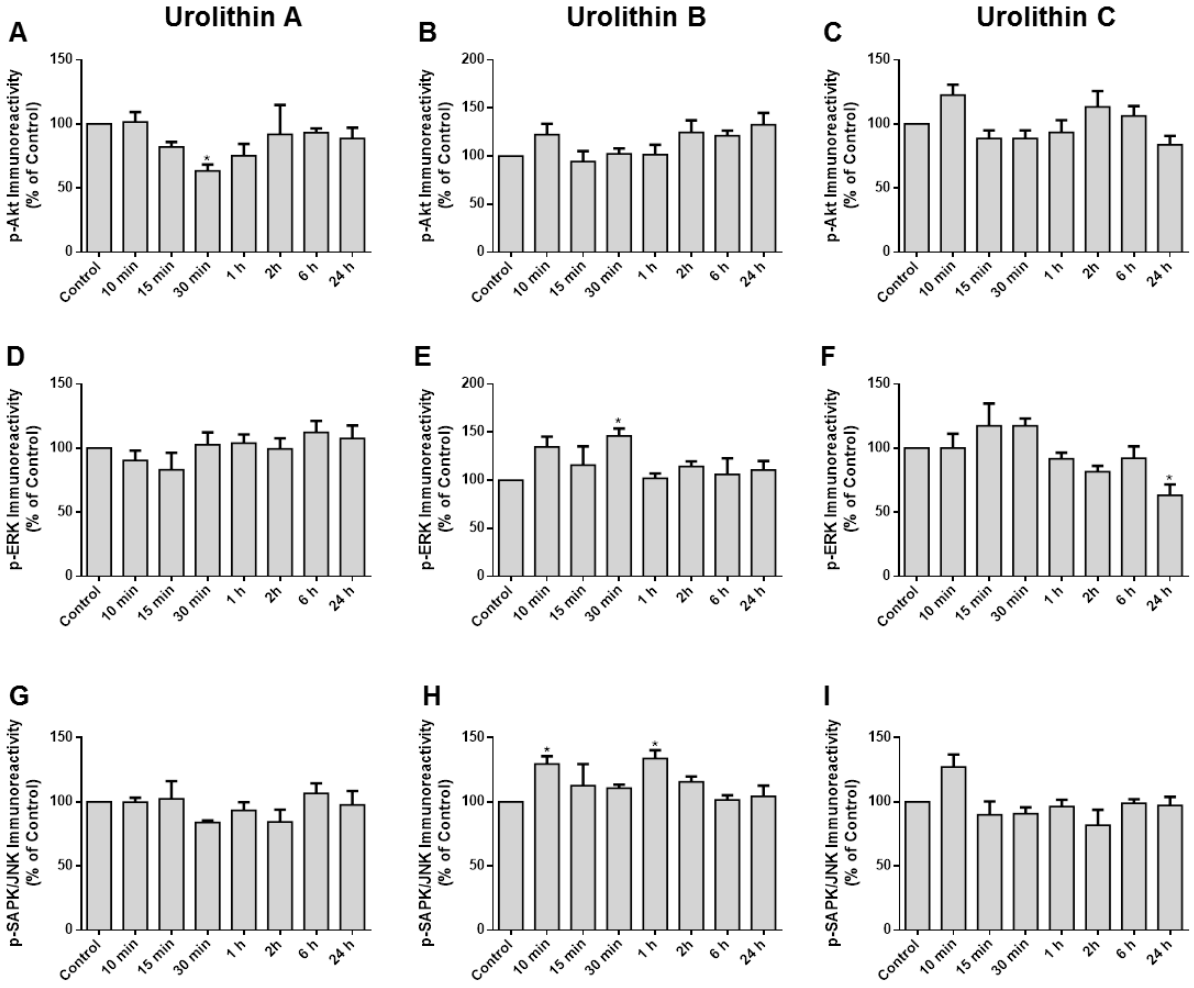

Figure 5.4 - Effect of urolithins on PI3K/AKT and MAPKs signaling pathways. MNNG-HOS cells were incubated with urolithins A, B and C for different time points. The levels of Akt, ERK1/2 and SAPK/JNK phosphorylated proteins were evaluated by western blot. Representative immunoblots are presented in Supplementary Figure 5.I. Data are presented as mean ± SEM of, at least, 3 independent experiments and are expressed as percentages of control. *p<0.05 when compared to control

5.4. DISCUSSION AND CONCLUSION

This study aimed to investigate the antiproliferative effect of ellagitannins' metabolites, urolithins and ellagic acid, on human osteosarcoma cells. We aimed to further evaluate their role in the cellular and molecular mechanisms implicated in cell proliferation in order to unveil the most promising molecule(s) to target this neoplasia.

Urolithins inhibited cell growth in a dose-dependent manner and the IC_{50} values achieved for this cell line were at the same range of the values achieved for UMUC3 cells, as previously described by our group (Chapter 4). In contrast, ellagic acid did not decrease cell viability. These results are somewhat contradictory with others previously performed with this molecule. In fact, Han et al. (2006) investigated the antiproliferative and pro-apoptotic activities of ellagic acid on human osteogenic carcinoma (HOS) cell line. Indeed, they found that ellagic acid inhibited the growth and induced HOS cells apoptosis, but the concentrations used were much more higher (more than 1000 times) than the concentrations used in this study.

In order to confirm the IC_{50} values, we also evaluated cell viability through the trypan blue exclusion assay. Consistent with our previous results (Chapter 4), the decrease of MNNG-HOS cell viability triggered by urolithins B and C did not reach the value of 50%, indicating a failure in cell metabolism that is not correlated with a complete membrane integrity loss. The results of annexinV-FITC/PI for the evaluation of cell death demonstrated that urolithin A promoted a slighter but significant increase of early apoptotic cells and even a smaller increase in necrotic cells. The lower magnitude of these effects and the lack of differences achieved for urolithins B and C suggest that the effect on cell viability/cell number relies on an inhibition of cell proliferation rather than cell death.

We previously showed in bladder cancer cells that urolithin A induced cell cycle arrest at G2/M phases (Chapter 4). In this study we observed the same pattern after 24 hours of cells treatment and, although not statistical significant, this effect was sustained until 48 hours. These results corroborate the studies of González-Sarrías et al. (2014) and Cho et al. (2015) that also verified an increase in cells arrested at G2/M in several colonic cancer cell lines. Therefore, these evidences suggest that the effect of urolithin A is not cell type dependent. Regarding urolithin C, we demonstrated, for the first time, that this compound increases the percentage of cells in S phase in osteosarcoma cells.

Lastly, we evaluated the effect of urolithins on cellular signaling pathways implicated in cell survival and proliferation. However, the sporadic differences in the levels of phosphorylated Akt and MAPKs did not allow to establish a relation between the activation/deactivation of kinases and cellular proliferation.

The increasing interest in urolithins in oncologic research is supported by their high bioavailability compared to ellagitannins and ellagic acid (Cerdá et al., 2004; Larrosa et al., 2010b)(Bialonska et al., 2010; González-Barrio et al., 2010), and their effects on crucial mechanisms associated to the control of cell proliferation and cell death (Qiu et al., 2013; Seeram et al., 2007; Vicinanza et al., 2013). In the present study, the most noticeable effect was related to cell cycle control. Urolithins A and C were able to induce cell cycle arrest in different phases, thus acting in different cell cycle checkpoints, and urolithin B was, once more, the less active molecule. Importantly, these results also highlight the significance of the hydroxyl groups in urolithins' activity, which constitutes valuable information in the design of urolithin-based molecules presenting potent bioactivity.

Further research will be needed to address the questions raised in this work, specifically regarding the effect of urolithins on cell cycle. However, overall, our findings suggest that the urolithins, especially urolithin A and C, may be potential chemopreventive/chemotherapeutic agents for osteosarcoma cells.

SUPPLEMENTARY DATA

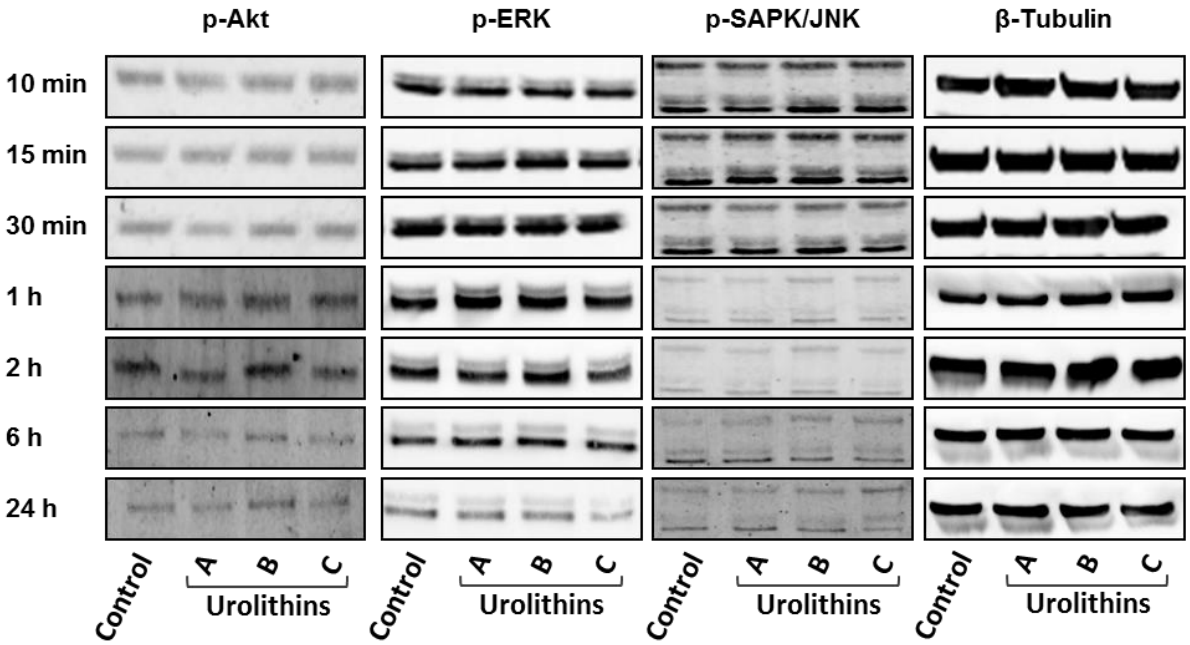

Supplementary Figure 5.I - Representative immunoblots of the data from Figure 5.4.

Chapter 6

GENERAL DISCUSSION

GENERAL DISCUSSION

Fragaria vesca is a wild growing plant that has long been used in ethnomedicine but whose benefits are not scientifically validated. Therefore, the first part of this work (Chapter 2) aimed to evaluate the biological effects of the leaf that, in traditional medicine, has been considered the most valued part of the plant. Given the wide applications of *Fragaria vesca* leaves found in ethnobotanical surveys, it was difficult to found a defined therapeutic purpose for their use. Nevertheless, as the pathophysiology of many of the described pathologies shared a strong inflammatory component we started to evaluate the anti-inflammatory properties of a hydroalcoholic extract from *Fragaria vesca* leaves, and we verified that the extract was able to decrease nitric oxide (NO) levels, one of the most important inflammatory mediators.

The evaluation of different pro-inflammatory mediators and the use of a NO-donor, led us to hypothesize that the NO reduction was probably due to a direct scavenging effect, rather than a consequence of the inhibition of inflammatory signaling pathways/mediators. It is well described that NO scavenging may have a protective role in the cells, because excessive amounts of NO can react with superoxide radical (O2•−) and form peroxynitrite (ONOO−) that could lead to cell damage (Radi, 2013). Although not being the main goal of this work, the NO scavenging potential emphasizes the antioxidant properties already described for the leaves of the plants from the genus *Fragaria* (Raudoniūtė et al., 2011; Wang and Lin, 2000). A previous study performed by our group also showed that the antioxidant capacity of the extract was related with its polyphenol content (Batista and Amaral, 2000). Here, we detailed the polyphenolic composition of the extract, being ellagitannins, proanthocyanidins, and quercetin and kaempferol glucuronide derivatives identified as the main compounds. Despite some differences in the extract preparation, these results are in accordance with a recent study that identifies the same polyphenolic classes in the leaves of wild growing and commercial samples of *Fragaria vesca* (Dias et al., 2015a); however, in the different preparations studied in that work the main compound present in our hydroalcoholic extract and ellagitannin-enriched fraction (EEF), the sanguiin H-6/agrimoniin/lambertianin A isomer, was not identified. In fact, we cannot assure that in our work this main peak comprises only one compound or if different isomers are co-eluted, since these molecules have similar fragmentation patterns and UV spectra, and are frequently found together in some plants (Gasperotti et al., 2013; Simirgiotis and Schmeda-Hirschmann, 2010; Vrhovsek et al., 2012).

In another set of experiences, we observed an accumulation of the anti-inflammatory mediator inhibitory kBα (IκBα), a protein degraded in the proteasome (Skaug et al., 2009), after cells

treatment with the hydroalcoholic extract. Thus, this data lead us to evaluate the effect of the extract in the ubiquitin-proteasome system UPS and autophagy, and we observed that the extract decreased proteasomal degradation and modulated autophagy. In fact, the modulation of the clearance mechanisms of the cell were the starting point for the work developed in Chapter 3; and because these mechanisms are currently considered promising molecular targets in cancer therapy, the cellular *in vitro* model was adjusted and other cellular and molecular events were considered. Furthermore, in order to investigate which compounds present in the extract were the responsible for the bioactivities previously observed a bioguided fractionation of *Fragaria vesca* leaves extract was performed and the fraction containing the ellagitannins (EEF), one of the most representative classes in the total extract, was selected.

Using human hepatocellular carcinoma cells (HepG2), in Chapter 3 we demonstrated that EEF induced cell cycle arrest at G2/M checkpoint, decreased cell proliferation and inhibited both autophagic and proteasomal degradation. Several studies have addressed the anticancer properties of ellagitannins but this was the first report demonstrating that ellagitannins could inhibit the proteolytic mechanisms of the cell. Furthermore, through a proteomic approach, proteins and pathways modulated by EEF were identified. Those proteins and processes should be deeply investigated in the future, namely the metabolic pathways of the cell, using this fraction or the ellagitannins identified in this study.

Regarding the proteolytic mechanisms, both total extract and EEF inhibited the chymotrypsin-like activity of the proteasome and induced the accumulation of ubiquitinated proteins, suggesting that ellagitannins are responsible for those effects. Concerning autophagy, in the first work (Chapter 2) we only investigated the effect of the extract on the conversion of microtubule-associated protein light chain 3 (LC3)-I to LC3-II proteins, which only allowed us to conclude that this sample modulated autophagy. Although, in Chapter 3, the concomitant use of the EEF and the pharmacological inhibitor of autophagy, chloroquine, suggests that the increase of LC3-II is not due to an increase of autophagy but to a blockage of autophagic flux. Therefore, giving the similar results on LC3 expression in both works, we may hypothesize that probably the crude extract of *Fragaria vesca* leaves also decreased autophagy, but clearly, this supposition must be confirmed. In a first approach and to complement these results, p62 protein expression was evaluated. The p62 protein, also called sequestosome 1, is used to monitor autophagic activity and it was shown to be increased after autophagy inhibition. However, it is also well known that p62 participates in proteasomal degradation and its protein levels may also be increased after proteasome inhibition (Bardag-Gorce et al., 2005; Klionsky et al., 2012). For that reason p62 is not a good autophagic marker for this work and for that reason it was excluded from this study.

Overall, all these findings raise several questions about the molecular and cellular mechanisms underlining the modulated processes that should be further clarified. The isolation and purification of the ellagitannins is presumably an advantage to study the anticancer properties of *Fragaria vesca* leaves. However, we cannot discard the possibility that different compounds of EEF or even of the extract, may act in synergy or in antagonism to modulate their overall activity.

Despite the notable ellagitannins' bioactivity *in vitro*, their activity *in vivo* is limited, which is due to their low lipophilicity, their large molecular weight and, if taken orally, their biodegradation into ellagic acid and urolithins. Hence, in order to increase the bioavailability, different pharmaceutical formulations containing ellagitannins or herbal extracts have been proposed (Ajazuddin and Saraf, 2010; Li et al., 2011). For instance, a standardized pomegranate extract (30% punicalagins) was complexed with phospholipid to formulate standardized pomegranate extract-phospholipid complex with an entrapment efficiency of 99.7% w/w of punicalagins. Furthermore, using the everted gut sac technique the investigators observed that the permeability across the intestinal membrane of the pomegranate extract increased almost two times after the complexation (Vora et al., 2015). Moreover, in a functional food and/or nutraceutical perspective, an extract of the vegetative parts of *Fragaria vesca* (leaves and stems) was encapsulated in alginate microspheres with encapsulation efficiency close to 95%, and incorporated in κ-carrageenan gelatin. This technique could protect and stabilize the molecules of the extract in the gastrointestinal tract (Dias et al., 2015a); however, it still did not allow the ellagitannins to overcome the intestinal barrier. The drug delivery and targeting for plant actives and extracts is an area of increasing interest (Ting et al., 2014). However, concerning ellagitannins, there is still much to explore and, as far as we know, *in vivo* studies have not yet been carried out for drug delivery with these bioactive molecules.

It has been shown that dietary ellagitannins are degraded in the upper gastrointestinal tract into ellagic acid. Thereafter, the also poorly absorbed ellagic acid (Seeram et al., 2004; Whitley et al., 2006) is metabolized by gut microbiota into urolithins (Cerdá et al., 2004; Espín et al., 2007). Considering the very low bioavailability of ellagitannins and ellagic acid, urolithins have been proposed to be the main responsible for the systemic health effects associated to the ingestion of ellagitannin-containing foods (Cerdá et al., 2004; González-Barrio et al., 2010; Larrosa et al., 2010b).

In the last few years there has been a growing interest in urolithins bioactivities. As outlined in Chapter 1, current research mostly supported by *in vitro* studies, has shown preliminary evidence for the anti-inflammatory, anticancer, antioxidant and antimicrobial activities of urolithins. However, mechanistic studies are still required to clarify the health effects of these metabolites. In line with the antiproliferative effects of EEF fraction in Chapter 3 and since urolithins have been pointed out as potential chemopreventive/chemotherapeutic agents (Cho et al., 2015; Sánchez-González et al., 2014), in Chapters 4 and 5 we investigated the antiproliferative effects of the urolithins most

produced in humans, urolithins A (dihydroxylated) and B (monohydroxylated), their trihydroxylated precursor, urolithin C, and ellagic acid in a panel of human cell lines representing different types of cancers.

Hence, the determination of IC_{50} for cell viability showed that human bladder transitional carcinoma UMUC3 (Chapter 4) and human osteosarcoma MNNG-HOS cell lines (Chapter 5) were the most sensitive to urolithins treatment, while these compounds were less toxic for non-tumoral human fibroblasts, thus highlighting the selective effect of urolithins in tumor cells. Another important point observed in both chapters, is that ellagic acid, an *in vivo* precursor of urolithins that is easily obtained by ellagitannins hydrolysis, is much less active than urolithins. In fact, the higher concentration tested (75 μM) was not enough to decrease cell viability in 50%, which did not allow to determinate the IC_{50} for ellagic acid. Actually, these data are in contrast to other reports evidencing the anticarcinogenic effects of ellagic acid, for instance by inhibiting tumor cell proliferation (Zhang et al., 2014); however, those studies used higher concentrations of ellagic acid or different tumor cells, pointing out some specificity of this molecule over distinct types of cells. On the other hand, our results are in agreement with other studies demonstrating that urolithin A and C (González-Sarrías et al., 2014; Larrosa et al., 2006a), but mostly urolithin A, are the most active antiproliferative molecules. Besides the effects on cell proliferation, urolithin A also disturbed cell cycle, induced apoptotic cell death and modulated the intracellular signaling pathway phosphatidylinositol 3-kinase (PI3K)/Akt, in both UMUC3 and MNNG-HOS cell lines, suggesting that the effect of urolithin A is not cell type dependent. Importantly, these results also highlight the significance of the hydroxyl groups in the urolithins activity, which constitutes valuable information in the rational design of urolithin-based molecules presenting potent bioactivity.

Several other questions remain to be addressed, namely the effect of phase-II metabolism of urolithins on the observed effects. In fact, urolithins are mainly reported in the plasma and peripheral tissues as glucuronides (Cerdá et al., 2004). Urolithins undergo glucuronidation and sulfation that typically make them significantly more hydrophilic molecules, which is required for their removal from the body. Since this biotransformation typically changes the bioactivities in comparison with the aglycone (González-Sarrías et al., 2014), *in vitro* studies with specific cell models and urolithins conjugates (glucuronides or sulfates) are needed to unravel the real anticancer potential of these molecules.

Furthermore, in this study we used concentrations close to or in the range of the plasma concentrations achievable *in vivo* (mainly as glucuronides), considering putative ellagitannin oral intake. Therefore, to extend our knowledge on ellagitannins health benefits and since different ellagitannins metabolites are present in biological samples, future studies should also investigate the effects of the combination of those molecules.

Summing up the results, *Fragaria vesca* leaf is a source of molecules with therapeutic potential and with a remarkably effect on autophagy and proteasome. Furthermore, EEF markedly inhibited these proteolytic systems and modulated several cellular and molecular targets implicated in carcinogenesis, being these effects most probably attributed to ellagitannins. Moreover, this work generated important insights in the therapeutic value of ellagitannins' metabolites, the urolithins, strongly supporting and encouraging further work on ellagitannins and urolithins in order to unveil their potential as chemopreventive/chemotherapeutic drugs.

Chapter 7

Main Conclusions

MAIN CONCLUSIONS

The results presented in this thesis allowed to elaborate the following main conclusions (Figure 7.1):

- The hydroalcoholic extract prepared from *Fragaria vesca* leaves contained proanthocyanidins, flavonols, and ellagic acid and its derivatives, and the major compound of the extract was identified as an isomeric form of the ellagitannin sanguiin H-6/agrimoniin. The hydroalcoholic extract decreased NO levels produced by macrophages treated with LPS, which was possibly due to a direct scavenging effect. Furthermore, *Fragaria vesca* extract inhibited the chymotrypsin-like activity of the proteasome leading to an accumulation of ubiquitinated proteins, and modulated autophagy.

- EEF was obtained from the hydroalcoholic crude extract of *Fragaria vesca* leaves and 12 ellagitannins were detected. Sanguiin H-6/agrimoniin isomer, main component of the crude extract, was also the major compound of this fraction. Moreover, in HepG2 cells EEF decreased cell proliferation, promoted cell cycle arrest at G2/M and induced cell death mainly through necrosis. EEF also promoted the accumulation of ubiquitinated proteins, inhibited chymotrypsin-like activity of 26S proteasome and decreased the expression of several proteasome subunits, indicating an impairment of UPS degradation. Along with the inhibition of proteasome, EEF inhibited autophagy through the blockage of autophagic flux. Furthermore, after treating the cells with EEF, 133 differentially expressed proteins were identified. In addition, the proteomic analysis allowed the identification of several functional clusters, primarily affecting metabolic processes.

- The main metabolites of ellagitannins, urolithins A, B and C, decreased cell viability in a dose-dependent way, in several human cancer cell lines and, in comparison with ellagic acid, their precursor, urolithins were much more active. Furthermore, clear differences among the compounds tested were shown, and, overall, urolithin A was the most promising molecule. In UMUC3 cells, urolithin A induced cell cycle arrest, increased apoptosis and modulated the intracellular pathways PI3K/Akt and MAPKs signaling. In MNNG-HOS cells, although not so pronounced, the effects of urolithin A on cell death and cell cycle were similar, indicating that those effects are not cell type-specific. Furthermore, urolithin B was, in both cell lines, the less active molecule. Therefore, these results highlight the significance of the

number/position of hydroxyl groups for urolithins' activity, which constitutes valuable information in the design of urolithin-based molecules presenting potent bioactivity.

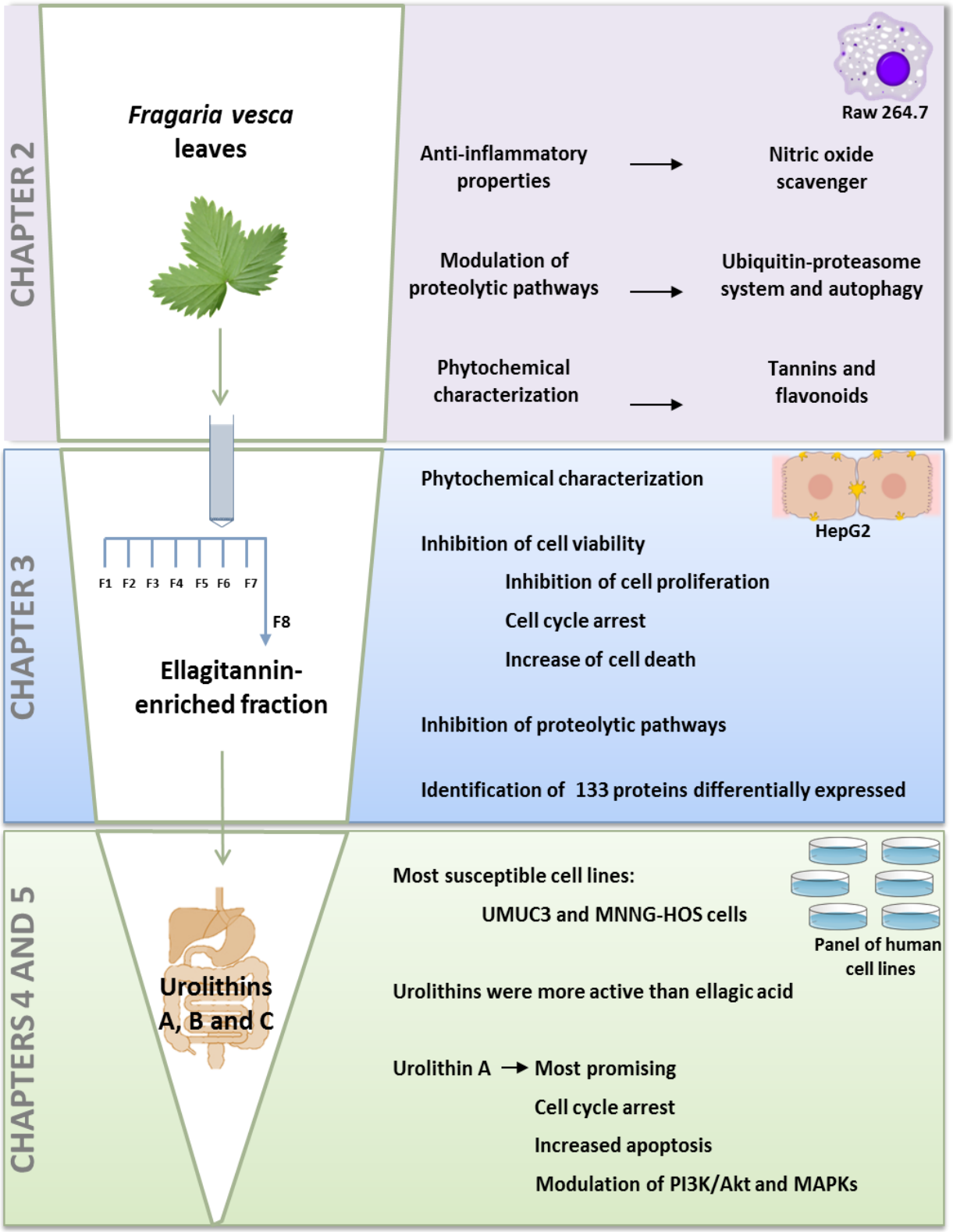

Figure 7.1 - Overview of the main conclusions of this work.

Chapter 8

References

REFERENCES

Aaby, K., Ekeberg, D., Skrede, G., 2007. Characterization of phenolic compounds in strawberry (Fragaria x ananassa) fruits by different HPLC detectors and contribution of individual compounds to total antioxidant capacity. J. Agric. Food Chem. 55, 4395–406. doi:10.1021/jf0702592

Aaby, K., Skrede, G., Wrolstad, R.E., 2005. Phenolic composition and antioxidant activities in flesh and achenes of strawberries (Fragaria ananassa). J. Agric. Food Chem. 53, 4032–40. doi:10.1021/jf048001o

Abe, L.T., Lajolo, F.M., Genovese, M.I., 2012. Potential dietary sources of ellagic acid and other antioxidants among fruits consumed in Brazil: jabuticaba (Myrciaria jaboticaba (Vell.) Berg). J. Sci. Food Agric. 92, 1679–87. doi:10.1002/jsfa.5531

Adams, L.S., Zhang, Y., Seeram, N.P., Heber, D., Chen, S., 2010. Pomegranate ellagitannin-derived compounds exhibit antiproliferative and antiaromatase activity in breast cancer cells in vitro. Cancer Prev. Res. (Phila). 3, 108–13. doi:10.1158/1940-6207.CAPR-08-0225

Aguilera-Carbo, A., Augur, C., Prado-Barragan, L.A., Favela-Torres, E., Aguilar, C.N., 2008. Microbial production of ellagic acid and biodegradation of ellagitannins. Appl. Microbiol. Biotechnol. 78, 189–99. doi:10.1007/s00253-007-1276-2

Ajazuddin, Saraf, S., 2010. Applications of novel drug delivery system for herbal formulations. Fitoterapia 81, 680–9. doi:10.1016/j.fitote.2010.05.001

Almeida, D., Araújo, P.V., Lourenço, J., Clamote, F., Silva, A., Porto, M., Carapeto, A., Aguiar, C., 2015. Fragaria vesca L. subsp. vesca - mapa de distribuição [WWW Document]. Flora-On Flora Port. Interactiva, Soc. Port. Botânica. URL http://www.flora-on.pt/#wid2721 (accessed 10.9.15).

Al-Sayed, E., El-Naga, R.N., 2015. Protective role of ellagitannins from Eucalyptus citriodora against ethanol-induced gastric ulcer in rats: impact on oxidative stress, inflammation and calcitonin-gene related peptide. Phytomedicine 22, 5–15. doi:10.1016/j.phymed.2014.10.002

Amaravadi, R., 2009. Autophagy can contribute to cell death when combining targeted therapy. Cancer Biol. Ther. 8, 130–3.

Anderson, K.J., Teuber, S.S., Gobeille, A., Cremin, P., Waterhouse, A.L., Steinberg, F.M., 2001. Walnut polyphenolics inhibit in vitro human plasma and LDL oxidation. J. Nutr. 131, 2837–42.

Arapitsas, P., 2012. Hydrolyzable tannin analysis in food. Food Chem. 135, 1708–17. doi:10.1016/j.foodchem.2012.05.096

Arapitsas, P., Menichetti, S., Vincieri, F.F., Romani, A., 2007. Hydrolyzable tannins with the hexahydroxydiphenoyl unit and the m-depsidic link: HPLC-DAD-MS identification and model synthesis. J. Agric. Food Chem. 55, 48–55. doi:10.1021/jf0622329

Ascacio-Valdes, J.A., Buenrostro-Figueroa, J.J., Aguilera-Carbo, A., Prado-Barragan, A., Rodriguez-Herrera, R., Aguilar, C.N., 2011. Ellagitannins: Biosynthesis, biodegradation and biological properties. J. Med. Plants Res. 5, 4696–703.

Asensi, M., Ortega, A., Mena, S., Feddi, F., Estrela, J.M., 2011. Natural polyphenols in cancer therapy. Crit. Rev. Clin. Lab. Sci. 48, 197–216. doi:10.3109/10408363.2011.631268

Auzanneau, C., Montaudon, D., Jacquet, R., Puyo, S., Pouységu, L., Deffieux, D., Elkaoukabi-Chaibi, A., De Giorgi, F., Ichas, F., Quideau, S., Pourquier, P., 2012. The polyphenolic ellagitannin vescalagin acts as a preferential catalytic inhibitor of the α isoform of human DNA topoisomerase II. Mol. Pharmacol. 82, 134–141. doi:10.1124/mol.111.077537

Bate-Smith, E., Swain, T., 1962. Flavonoid compounds. Comp. Biochem. 3, 705–809.

Batista, M.T., Amaral, M.T., 2000. Relationship between phenolic composition, radical scavenger and antioxidant activities from “Fragaria vesca” leaves, in: Eds. Martens, S. et al. G.P. (Ed.), In Polyphenols Communications. Freising-Weihenstephan, pp. 341–2.

Bauhin, C., 1623. Pinax theatri botanici. Basel.

Bedoya, L.M., Abad, M.J., Sánchez-Palomino, S., Alcami, J., Bermejo, P., 2010. Ellagitannins from Tuberaria lignosa as entry inhibitors of HIV. Phytomedicine 17, 69–74. doi:10.1016/j.phymed.2009.08.008

Bialonska, D., Kasimsetty, S.G., Khan, S.I., Ferreira, D., 2009. Urolithins, intestinal microbial metabolites of Pomegranate ellagitannins, exhibit potent antioxidant activity in a cell-based assay. J. Agric. Food Chem. 57, 10181–6. doi:10.1021/jf9025794

Bialonska, D., Ramnani, P., Kasimsetty, S.G., Muntha, K.R., Gibson, G.R., Ferreira, D., 2010. The influence of pomegranate by-product and punicalagins on selected groups of human intestinal microbiota. Int. J. Food Microbiol. 140, 175–82. doi:10.1016/j.ijfoodmicro.2010.03.038

Bie, P., Ciechanover, A., 2011. Ubiquitination of E3 ligases: self-regulation of the ubiquitin system via proteolytic and non-proteolytic mechanisms. Cell Death Differ. 18, 1393–402. doi:10.1038/cdd.2011.16

Bonfili, L., Cuccioloni, M., Mozzicafreddo, M., Cecarini, V., Angeletti, M., Eleuteri, A.M., 2011. Identification of an EGCG oxidation derivative with proteasome modulatory activity. Biochimie 93, 931–40. doi:10.1016/j.biochi.2011.02.003

Borah, M., Ahmed, S., Das, S., 2012. A comparative study of the antibacterial activity of the ethanolic extracts of Vitex negundo L., Fragaria vesca L., Terminalia arjuna and Citrus maxima. Asian J. Pharm. Biol. Res. 2, 183.

Brüning, A., Jückstock, J., 2015. Misfolded Proteins: From Little Villains to Little Helpers in the Fight Against Cancer. Front. Oncol. 5, 1–12. doi:10.3389/fonc.2015.00047

Brusselmans, K., De Schrijver, E., Heyns, W., Verhoeven, G., Swinnen, J. V, 2003. Epigallocatechin-3-gallate is a potent natural inhibitor of fatty acid synthase in intact cells and selectively induces apoptosis in prostate cancer cells. Int. J. Cancer 106, 856–62. doi:10.1002/ijc.11317

Buricova, L., Andjelkovic, M., Cermakova, A., Reblova, Z., Jurcek, O., Kolehmainen, E., Verhe, R., Kvasnicka, F., 2011. Antioxidant capacities and antioxidants of strawberry, blackberry and raspberry leaves. Czech J. Food Sci. 29, 181–89.

Cabral, C., Pita, J.R., Salgueiro, L., 2014. Plantas Medicinais: entre o passado e o presente: a colecção de fármacos vegetais da Faculdade de Farmácia da Universidade de Coimbra (séculos xix-xx). Imprensa da Universidade de Coimbra, Coimbra. doi:10.14195/978-989-26-0875-4

Callaway, E., Cyranoski, D., 2015. Anti-parasite drugs sweep Nobel prize in medicine 2015. Nature 526, 174–75. doi:10.1038/nature.2015.18507

Camejo-Rodrigues, J., Ascensão, L., Bonet, M.A., Vallès, J., 2003. An ethnobotanical study of medicinal and aromatic plants in the Natural Park of “Serra de São Mamede” (Portugal). J. Ethnopharmacol. 89, 199–209. doi:10.1016/S0378-8741(03)00270-8

Cance, W.G., Harris, J.E., Iacocca, M. V, Roche, E., Yang, X., Chang, J., Simkins, S., Xu, L., 2000. Immunohistochemical analyses of focal adhesion kinase expression in benign and malignant human breast and colon tissues: correlation with preinvasive and invasive phenotypes. Clin. Cancer Res. 6, 2417–23.

Cao, Y., Himmeldirk, K.B., Qian, Y., Ren, Y., Malki, A., Chen, X., 2014. Biological and biomedical functions of Penta-O-galloyl-D-glucose and its derivatives. J. Nat. Med. 68, 465–72. doi:10.1007/s11418-014-0823-2

Cargnello, M., Roux, P.P., 2011. Activation and function of the MAPKs and their substrates, the MAPK-activated protein kinases. Microbiol. Mol. Biol. Rev. 75, 50–83. doi:10.1128/MMBR.00031-10

Castroviejo, S., 1998. Flora Iberica. Plantas vasculares de la Península Ibérica e Islas Baleares. Real Jardín Botánico, CSIC, Madrid.

Center, M.M., Jemal, A., 2011. International trends in liver cancer incidence rates. Cancer Epidemiol. Biomarkers Prev. 20, 2362–8. doi:10.1158/1055-9965.EPI-11-0643

Cerdá, B., Espín, J.C., Parra, S., Martínez, P., Tomás-Barberán, F.A., 2004. The potent in vitro antioxidant ellagitannins from pomegranate juice are metabolised into bioavailable but poor antioxidant hydroxy-6H-dibenzopyran-6-one derivatives by the colonic microflora of healthy humans. Eur. J. Nutr. 43, 205–20. doi:10.1007/s00394-004-0461-7

Cerdá, B., Llorach, R., Cerón, J.J., Espín, J.C., Tomás-Barberán, F.A., 2003. Evaluation of the bioavailability and metabolism in the rat of punicalagin, an antioxidant polyphenol from pomegranate juice. Eur. J. Nutr. 42, 18–28. doi:10.1007/s00394-003-0396-4

Cerdá, B., Soto, C., Albaladejo, M.D., Martínez, P., Sánchez-Gascón, F., Tomás-Barberán, F., Espín, J.C., 2006. Pomegranate juice supplementation in chronic obstructive pulmonary disease: a 5-week randomized, double-blind, placebo-controlled trial. Eur. J. Clin. Nutr. 60, 245–53. doi:10.1038/sj.ejcn.1602309

Chang, F., Lee, J.T., Navolanic, P.M., Steelman, L.S., Shelton, J.G., Blalock, W.L., Franklin, R.A., McCubrey, J.A., 2003. Involvement of PI3K/Akt pathway in cell cycle progression, apoptosis, and neoplastic transformation: a target for cancer chemotherapy. Leukemia 17, 590–603. doi:10.1038/sj.leu.2402824

Chang, T.-L., Lin, S.-W., Wu, S., Hong, C.-M., 2013. Regulation of ubiquitin and 26S proteasome mediated by phenolic compounds during oxidative stress. J. Nutr. Biochem. 24, 1970–81. doi:10.1016/j.jnutbio.2013.07.001

Chaumeton, F.-P., Poiret, Chamberet, 1830. Flore médicale, Volume 3. Paris.

Cheel, J., Theoduloz, C., Rodríguez, J.A., Caligari, P.D.S., Schmeda-Hirschmann, G., 2007. Free radical scavenging activity and phenolic content in achenes and thalamus from Fragaria chiloensis ssp. chiloensis, F. vesca and F. x ananassa cv. Chandler. Food Chem. 102, 36–44. doi:10.1016/j.foodchem.2006.04.036

Chen, D., Daniel, K.G., Chen, M.S., Kuhn, D.J., Landis-Piwowar, K.R., Dou, Q.P., 2005. Dietary flavonoids as proteasome inhibitors and apoptosis inducers in human leukemia cells. Biochem. Pharmacol. 69, 1421–32. doi:10.1016/j.bcp.2005.02.022

Chen, D., Frezza, M., Schmitt, S., Kanwar, J., P. Dou, Q., 2011. Bortezomib as the First Proteasome Inhibitor Anticancer Drug: Current Status and Future Perspectives. Curr. Cancer Drug Targets 11, 239–53. doi:10.2174/156800911794519752

Chen, H.-Y., White, E., 2011. Role of autophagy in cancer prevention. Cancer Prev. Res. (Phila). 4, 973–83. doi:10.1158/1940-6207.CAPR-10-0387

Chen, J.-S., Yu, D. a. n., Liu, Q., Dong, M., 2004. Clonal integration of the stoloniferous herb Fragaria vesca from different altitudes in Southwest China. Flora - Morphol. Distrib. Funct. Ecol. Plants 199, 342–50. doi:10.1078/0367-2530-00162

Chen, L.-G., Huang, W.-T., Lee, L.-T., Wang, C.-C., 2009. Ellagitannins from Terminalia calamansanai induced apoptosis in HL-60 cells. Toxicol. In Vitro 23, 603–9. doi:10.1016/j.tiv.2009.01.020

Chen, W., Lee, J., Cho, S.Y., Fine, H.A., 2004. Proteasome-mediated destruction of the cyclin a/cyclin-dependent kinase 2 complex suppresses tumor cell growth in vitro and in vivo. Cancer Res. 64, 3949–57. doi:10.1158/0008-5472.CAN-03-3906

Chen, W.-J., Lin, J.-K., 2004. Induction of G1 arrest and apoptosis in human jurkat T cells by pentagalloylglucose through inhibiting proteasome activity and elevating p27Kip1, p21Cip1/WAF1, and Bax proteins. J. Biol. Chem. 279, 13496–505. doi:10.1074/jbc.M212390200

Cheng, H.-Y., Lin, C.-C., Lin, T.-C., 2002. Antiherpes simplex virus type 2 activity of casuarinin from the bark of Terminalia arjuna Linn. Antiviral Res. 55, 447–55.

Cheynier, V., Comte, G., Davies, K.M., Lattanzio, V., Martens, S., 2013. Plant phenolics: recent advances on their biosynthesis, genetics, and ecophysiology. Plant Physiol. Biochem. 72, 1–20. doi:10.1016/j.plaphy.2013.05.009

Cho, H., Jung, H., Lee, H., Yi, H.C., Kwak, H.-K., Hwang, K.T., 2015. Chemopreventive activity of ellagitannins and their derivatives from black raspberry seeds on HT-29 colon cancer cells. Food Funct. 6, 1675–83. doi:10.1039/c5fo00274e

Chung, Y.-C., Lu, L.-C., Tsai, M.-H., Chen, Y.-J., Chen, Y.-Y., Yao, S.-P., Hsu, C.-P., 2013. The inhibitory effect of ellagic acid on cell growth of ovarian carcinoma cells. Evidence-Based Complement. Altern. Med. 2013, 306705. doi:10.1155/2013/306705

Clarke, P.G.H., Puyal, J., 2012. Autophagic cell death exists. Autophagy 8, 867–9. doi:10.4161/auto.20380

Clifford, M.N., Scalbert, A., 2000. Ellagitannins - nature, occurrence and dietary burden. J. Sci. Food Agric. 80, 1118–25. doi:10.1002/(SICI)1097-0010(20000515)80:7<1118::AID-JSFA570>3.0.CO;2-9

Cmielová, J., Rezáčová, M., 2011. p21Cip1/Waf1 protein and its function based on a subcellular localization [corrected]. J. Cell. Biochem. 112, 3502–6. doi:10.1002/jcb.23296

Correia, H.S., Batista, M.T., Dinis, T.C.P., 2007. The activity of an extract and fraction of Agrimonia eupatoria L. against reactive species. Biofactors 29, 91–104. doi:10.1002/biof.552029209

Costa, G., Francisco, V., C. Lopes, M., T. Cruz, M., T. Batista, M., 2012. Intracellular Signaling Pathways Modulated by Phenolic Compounds: Application for New Anti-Inflammatory Drugs Discovery. Curr. Med. Chem. 19, 2876–900. doi:10.2174/092986712800672049

Crespo, P., Bordonaba, J.G., Terry, L.A., Carlen, C., 2010. Characterisation of major taste and health-related compounds of four strawberry genotypes grown at different Swiss production sites. Food Chem. 122, 16–24. doi:10.1016/j.foodchem.2010.02.010

Cuervo, A.M., Wong, E., 2014. Chaperone-mediated autophagy: roles in disease and aging. Cell Res. 24, 92–104. doi:10.1038/cr.2013.153

Cunha, A. da, Batista, M.T., 2005. Farmacognosia e fitoquímica, in: Cunha, A. da, Graça, J. da (Eds.), Farmacognosia E Fitoquímica. Fundação Calouste Gulbenkian, Lisb, pp. 291–336.

Cunha, A.P. da, Silva, A.P. da, Roque, O.R., 2003. Plantas e produtos vegetais em fitoterapia, 3rd ed. Fundação Calouste Gulbenkian, Lisboa.

D'Archivio, M., Filesi, C., Di Benedetto, R., Gargiulo, R., Giovannini, C., Masella, R., 2007. Polyphenols, dietary sources and bioavailability. Ann. Ist. Super. Sanita 43, 348–61.

Daglia, M., 2012. Polyphenols as antimicrobial agents. Curr. Opin. Biotechnol. 23, 174–81. doi:10.1016/j.copbio.2011.08.007

Dai, J., Mumper, R.J., 2010. Plant phenolics: extraction, analysis and their antioxidant and anticancer properties. Molecules 15, 7313–52. doi:10.3390/molecules15107313

Daniel, E.M., Ratnayake, S., Kinstle, T., Stoner, G.D., 1991. The Effects of pH and Rat Intestinal Contents on the Liberation of Ellagic Acid from Purified and Crude Ellagitannins. J. Nat. Prod. 54, 946-52. doi:10.1021/np50076a004

Das, G., Shravage, B. V., Baehrecke, E.H., 2012. Regulation and Function of Autophagy during Cell Survival and Cell Death. Cold Spring Harb. Perspect. Biol. 4, a008813. doi:10.1101/cshperspect.a008813

De Bruin, E.C., Medema, J.P., 2008. Apoptosis and non-apoptotic deaths in cancer development and treatment response. Cancer Treat. Rev. 34, 737–49. doi:10.1016/j.ctrv.2008.07.001

De Luca, A., Maiello, M.R., D'Alessio, A., Pergameno, M., Normanno, N., 2012. The RAS/RAF/MEK/ERK and the PI3K/AKT signalling pathways: role in cancer pathogenesis and implications for therapeutic approaches. Expert Opin. Ther. Targets 16 Suppl 2, S17–27. doi:10.1517/14728222.2011.639361

DeBerardinis, R.J., Lum, J.J., Hatzivassiliou, G., Thompson, C.B., 2008. The biology of cancer: metabolic reprogramming fuels cell growth and proliferation. Cell Metab. 7, 11–20. doi:10.1016/j.cmet.2007.10.002

Degenhardt, K., Mathew, R., Beaudoin, B., Bray, K., Anderson, D., Chen, G., Mukherjee, C., Shi, Y., Gélinas, C., Fan, Y., Nelson, D.A., Jin, S., White, E., 2006. Autophagy promotes tumor cell survival and restricts necrosis, inflammation, and tumorigenesis. Cancer Cell 10, 51–64. doi:10.1016/j.ccr.2006.06.001

Degterev, A., Huang, Z., Boyce, M., Li, Y., Jagtap, P., Mizushima, N., Cuny, G.D., Mitchison, T.J., Moskowitz, M.A., Yuan, J., 2005. Chemical inhibitor of nonapoptotic cell death with therapeutic potential for ischemic brain injury. Nat. Chem. Biol. 1, 112–9. doi:10.1038/nchembio711

Del Bubba, M., Checchini, L., Chiuminatto, U., Doumett, S., Fibbi, D., Giordani, E., 2012. Liquid chromatographic/electrospray ionization tandem mass spectrometric study of polyphenolic composition of four cultivars of Fragaria vesca L. berries and their comparative evaluation. J. Mass Spectrom. 47, 1207–20. doi:10.1002/jms.3030

Dias, M.I., Barros, L., Fernandes, I.P., Ruphuy, G., Oliveira, M.B.P.P., Santos-Buelga, C., Barreiro, M.F., Ferreira, I.C.F.R., 2015a. A bioactive formulation based on Fragaria vesca L. vegetative parts: Chemical characterisation and application in κ-carrageenan gelatin. J. Funct. Foods 16, 243–55. doi:10.1016/j.jff.2015.04.044

Dias, M.I., Barros, L., Morales, P., Sánchez-Mata, M.C., Oliveira, M.B.P.P., Ferreira, I.C.F.R., 2015b. Nutritional parameters of infusions and decoctions obtained from Fragaria vesca L. roots and vegetative parts. LWT - Food Sci. Technol. 62, 32–38. doi:10.1016/j.lwt.2015.01.034

Dias, M.I., Barros, L., Oliveira, M.B.P.P., Santos-Buelga, C., Ferreira, I.C.F.R., 2015c. Phenolic profile and antioxidant properties of commercial and wild Fragaria vesca L. roots: A comparison between hydromethanolic and aqueous extracts. Ind. Crops Prod. 63, 125–32. doi:10.1016/j.indcrop.2014.10.021

Ding, W.-X., Ni, H.-M., Gao, W., Chen, X., Kang, J.H., Stolz, D.B., Liu, J., Yin, X.-M., 2009. Oncogenic transformation confers a selective susceptibility to the combined suppression of the proteasome and autophagy. Mol. Cancer Ther. 8, 2036–45. doi:10.1158/1535-7163.MCT-08-1169

Ding, W.-X., Ni, H.-M., Gao, W., Yoshimori, T., Stolz, D.B., Ron, D., Yin, X.-M., 2007. Linking of autophagy to ubiquitin-proteasome system is important for the regulation of endoplasmic reticulum stress and cell viability. Am. J. Pathol. 171, 513–24. doi:10.2353/ajpath.2007.070188

Doherty, S.C., McKeown, S.R., McKelvey-Martin, V., Downes, C.S., Atala, A., Yoo, J.J., Simpson, D.A., Kaufmann, W.K., 2003. Cell cycle checkpoint function in bladder cancer. J. Natl. Cancer Inst. 95, 1859–68.

Doumett, S., Fibbi, D., Cincinelli, A., Giordani, E., Nin, S., Del Bubba, M., 2011. Comparison of nutritional and nutraceutical properties in cultivated fruits of Fragaria vesca L. produced in Italy. Food Res. Int. 44, 1209–16. doi:10.1016/j.foodres.2010.10.044

Driscoll, J.J., Chowdhury, R. De, 2012. Molecular crosstalk between the proteasome, aggresomes and autophagy: translational potential and clinical implications. Cancer Lett. 325, 147–54. doi:10.1016/j.canlet.2012.06.016

Du, Y., Yang, D., Li, L., Luo, G., Li, T., Fan, X., Wang, Q., Zhang, X., Wang, Y., Le, W., 2009. An insight into the mechanistic role of p53-mediated autophagy induction in response to proteasomal inhibition-induced neurotoxicity. Autophagy 5, 663–76. doi:10.4161/auto.5.5.8377

Duarte, J., Francisco, V., Perez-Vizcaino, F., 2014. Modulation of nitric oxide by flavonoids. Food Funct. 5, 1653–68. doi:10.1039/c4fo00144c

Duchesne, A., 1766. Histoire naturelle des fraisiers. Paris.

El-Serag, H.B., Rudolph, K.L., 2007. Hepatocellular carcinoma: epidemiology and molecular carcinogenesis. Gastroenterology 132, 2557–76. doi:10.1053/j.gastro.2007.04.061

Endo, E.H., Cortez, D.A.G., Ueda-Nakamura, T., Nakamura, C.V., Dias Filho, B.P., 2010. Potent antifungal activity of extracts and pure compound isolated from pomegranate peels and synergism with fluconazole against Candida albicans. Res. Microbiol. 161, 534–40. doi:10.1016/j.resmic.2010.05.002

Espín, J.C., González-Barrio, R., Cerdá, B., López-Bote, C., Rey, A.I., Tomás-Barberán, F.A., 2007. Iberian pig as a model to clarify obscure points in the bioavailability and metabolism of ellagitannins in humans. J. Agric. Food Chem. 55, 10476–85. doi:10.1021/jf0723864

Espín, J.C., Larrosa, M., García-Conesa, M.T., Tomás-Barberán, F., 2013. Biological significance of urolithins, the gut microbial ellagic Acid-derived metabolites: the evidence so far. Evid. Based. Complement. Alternat. Med. 2013, 270418. doi:10.1155/2013/270418

Fan, H., Tian, W., Ma, X., 2014. Curcumin induces apoptosis of HepG2 cells via inhibiting fatty acid synthase. Target. Oncol. 9, 279–86. doi:10.1007/s11523-013-0286-5

Feitelson, M.A., Arzumanyan, A., Kulathinal, R.J., Blain, S.W., Holcombe, R.F., Mahajna, J., Marino, M., Martinez-Chantar, M.L., Nawroth, R., Sanchez-Garcia, I., Sharma, D., Saxena, N.K., Singh, N., Vlachostergios, P.J., Guo, S., Honoki, K., Fujii, H., Georgakilas, A.G., Amedei, A., Niccolai, E., Amin, A., Ashraf, S.S., Boosani, C.S., Guha, G., Ciriolo, M.R., Aquilano, K., Chen, S., Mohammed, S.I., Azmi, A.S., Bhakta, D., Halicka, D., Nowsheen, S., 2015. Sustained proliferation in cancer: Mechanisms and novel therapeutic targets. Semin. Cancer Biol. 1–30. doi:10.1016/j.semcancer.2015.02.006

Fesik, S.W., 2005. Promoting apoptosis as a strategy for cancer drug discovery. Nat. Rev. Cancer 5, 876–85. doi:10.1038/nrc1736

Festjens, N., Vanden Berghe, T., Vandenabeele, P., 2006. Necrosis, a well-orchestrated form of cell demise: signalling cascades, important mediators and concomitant immune response. Biochim. Biophys. Acta 1757, 1371–87. doi:10.1016/j.bbabio.2006.06.014

Fischer, U.A., Carle, R., Kammerer, D.R., 2011. Identification and quantification of phenolic compounds from pomegranate (Punica granatum L.) peel, mesocarp, aril and differently produced juices by HPLC-DAD-ESI/MS(n). Food Chem. 127, 807–21. doi:10.1016/j.foodchem.2010.12.156

Fleming, T., 2000. PDR for herbal medicines., 4th ed. Medical Economics Company, Montvale, NJ.

Flora-On: Flora de Portugal Interactiva [WWW Document], 2014. . Soc. Port. Botânica. URL http://www.flora-on.pt/#/1fragaria (accessed 10.9.15).

Folta, K.M., Gardiner, S.E. (Eds.), 2009. Genetics and Genomics of Rosaceae. Springer New York, New York, NY. doi:10.1007/978-0-387-77491-6

Förstermann, U., Sessa, W.C., 2012. Nitric oxide synthases: regulation and function. Eur. Heart J. 33, 829–37, 837a–837d. doi:10.1093/eurheartj/ehr304

Fresco, P., Borges, F., Marques, M.P.M., Diniz, C., 2010. The anticancer properties of dietary polyphenols and its relation with apoptosis. Curr. Pharm. Des. 16, 114–34. doi:10.2174/138161210789941856

Fuertes, G., Martín De Llano, J.J., Villarroya, A., Rivett, A.J., Knecht, E., 2003a. Changes in the proteolytic activities of proteasomes and lysosomes in human fibroblasts produced by serum withdrawal, amino-acid deprivation and confluent conditions. Biochem. J. 375, 75–86. doi:10.1042/BJ20030282

Fuertes, G., Villarroya, A., Knecht, E., 2003b. Role of proteasomes in the degradation of short-lived proteins in human fibroblasts under various growth conditions. Int. J. Biochem. Cell Biol. 35, 651–64.

Fukuda, T., Ito, H., Yoshida, T., 2003. Antioxidative polyphenols from walnuts (Juglans regia L.). Phytochemistry 63, 795–801.

Funatogawa, K., Hayashi, S., Shimomura, H., Yoshida, T., Hatano, T., Ito, H., Hirai, Y., 2004. Antibacterial activity of hydrolyzable tannins derived from medicinal plants against Helicobacter pylori. Microbiol. Immunol. 48, 251–61.

Galluzzi, L., Vitale, I., Abrams, J.M., Alnemri, E.S., Baehrecke, E.H., Blagosklonny, M. V, Dawson, T.M., Dawson, V.L., El-Deiry, W.S., Fulda, S., Gottlieb, E., Green, D.R., Hengartner, M.O., Kepp, O., Knight, R.A., Kumar, S., Lipton, S.A., Lu, X., Madeo, F., Malorni, W., Mehlen, P., Nuñez, G., Peter, M.E., Piacentini, M., Rubinsztein, D.C., Shi, Y., Simon, H.-U., Vandenabeele, P., White, E., Yuan, J., Zhivotovsky, B., Melino, G., Kroemer, G., 2012. Molecular definitions of cell death subroutines: recommendations of the Nomenclature Committee on Cell Death 2012. Cell Death Differ. 19, 107–20. doi:10.1038/cdd.2011.96

Gao, Y., 2010. The multiple actions of NO. Pflügers Arch. - Eur. J. Physiol. 459, 829–39. doi:10.1007/s00424-009-0773-9

Garcia-Muñoz, C., Vaillant, F., 2014. Metabolic fate of ellagitannins: implications for health, and research perspectives for innovative functional foods. Crit. Rev. Food Sci. Nutr. 54, 1584–98. doi:10.1080/10408398.2011.644643

Gasperotti, M., Masuero, D., Guella, G., Palmieri, L., Martinatti, P., Pojer, E., Mattivi, F., Vrhovsek, U., 2013. Evolution of ellagitannin content and profile during fruit ripening in Fragaria spp. J. Agric. Food Chem. 61, 8597–607. doi:10.1021/jf402706h

GBIF Backbone Taxonomy, 2013. Georeferenced data of Fragaria vesca L. [WWW Document]. Glob. Biodivers. Inf. Facil. URL http://www.gbif.org/species/3029817 (accessed 10.9.15).

Geetha, T., Seibenhener, M.L., Chen, L., Madura, K., Wooten, M.W., 2008. p62 serves as a shuttling factor for TrkA interaction with the proteasome. Biochem. Biophys. Res. Commun. 374, 33–7. doi:10.1016/j.bbrc.2008.06.082

Giada, M.L., 2013. Food Phenolic Compounds: Main Classes, Sources and Their Antioxidant Power, in: Morales-Gonzalez, J.A. (Ed.), Oxidative Stress and Chronic Degenerative Diseases - A Role for Antioxidants. InTech. doi:10.5772/51687

Giampieri, F., Forbes-Hernandez, T.Y., Gasparrini, M., Alvarez-Suarez, J.M., Afrin, S., Bompadre, S., Quiles, J.L., Mezzetti, B., Battino, M., 2015. Strawberry as a health promoter: an evidence based review. Food Funct. 6, 1386–98. doi:10.1039/c5fo00147a

Giampieri, F., Tulipani, S., Alvarez-Suarez, J.M., Quiles, J.L., Mezzetti, B., Battino, M., 2012. The strawberry: Composition, nutritional quality, and impact on human health. Nutrition 28, 9–19. doi:10.1016/j.nut.2011.08.009

Gil, M.I., Tomás-Barberán, F.A., Hess-Pierce, B., Holcroft, D.M., Kader, A.A., 2000. Antioxidant activity of pomegranate juice and its relationship with phenolic composition and processing. J. Agric. Food Chem. 48, 4581–9.

Giménez-Bastida, J.A., González-Sarrías, A., Larrosa, M., Tomás-Barberán, F., Espín, J.C., García-Conesa, M.-T., 2012a. Ellagitannin metabolites, urolithin A glucuronide and its aglycone urolithin A, ameliorate TNF-α-induced inflammation and associated molecular markers in human aortic endothelial cells. Mol. Nutr. Food Res. 56, 784–96. doi:10.1002/mnfr.201100677

Giménez-Bastida, J.A., Larrosa, M., González-Sarrías, A., Tomás-Barberán, F., Espín, J.C., García-Conesa, M.-T., 2012b. Intestinal ellagitannin metabolites ameliorate cytokine-induced inflammation and associated molecular markers in human colon fibroblasts. J. Agric. Food Chem. 60, 8866–76. doi:10.1021/jf300290f

Giovannini, C., Masella, R., 2012. Role of polyphenols in cell death control. Nutr. Neurosci. 15, 134–49. doi:10.1179/1476830512Y.0000000006

Glabasnia, A., Hofmann, T., 2006. Sensory-Directed Identification of Taste-Active Ellagitannins in American (Quercus alba L.) and European Oak Wood (Quercus robur L.) and Quantitative Analysis in Bourbon Whiskey and Oak-Matured Red Wines. J. Agric. Food Chem. 54, 3380–90. doi:10.1021/jf052617b

Gođevac, D., Tešević, V., Vajs, V., Milosavljević, S., Stanković, M., 2011. Blackberry Seed Extracts and Isolated Polyphenolic Compounds Showing Protective Effect on Human Lymphocytes DNA. J. Food Sci. 76, C1039–C1043. doi:10.1111/j.1750-3841.2011.02305.x

Gonçalves, B., Borges, O., Costa, H.S., Bennett, R., Santos, M., Silva, A.P., 2010. Metabolite composition of chestnut (Castanea sativa Mill.) upon cooking: Proximate analysis, fibre, organic acids and phenolics. Food Chem. 122, 154–60. doi:10.1016/j.foodchem.2010.02.032

González-Barrio, R., Borges, G., Mullen, W., Crozier, A., 2010. Bioavailability of anthocyanins and ellagitannins following consumption of raspberries by healthy humans and subjects with an ileostomy. J. Agric. Food Chem. 58, 3933–9. doi:10.1021/jf100315d

González-Barrio, R., Truchado, P., Ito, H., Espín, J.C., Tomás-Barberán, F.A., 2011. UV and MS identification of Urolithins and Nasutins, the bioavailable metabolites of ellagitannins and ellagic acid in different mammals. J. Agric. Food Chem. 59, 1152–62. doi:10.1021/jf103894m

González-Sarrías, A., Espín, J.-C., Tomás-Barberán, F.A., García-Conesa, M.-T., 2009. Gene expression, cell cycle arrest and MAPK signalling regulation in Caco-2 cells exposed to ellagic acid and its metabolites, urolithins. Mol. Nutr. Food Res. 53, 686–98. doi:10.1002/mnfr.200800150

González-Sarrías, A., Giménez-Bastida, J.A., García-Conesa, M.T., Gómez-Sánchez, M.B., García-Talavera, N. V, Gil-Izquierdo, A., Sánchez-Alvarez, C., Fontana-Compiano, L.O., Morga-Egea, J.P., Pastor-Quirante, F.A., Martínez-Díaz, F., Tomás-Barberán, F.A., Espín, J.C., 2010. Occurrence of urolithins, gut microbiota ellagic acid metabolites and proliferation markers expression response in the human prostate gland upon consumption of walnuts and pomegranate juice. Mol. Nutr. Food Res. 54, 311–22. doi:10.1002/mnfr.200900152

González-Sarrías, A., Giménez-Bastida, J.A., Núñez-Sánchez, M.Á., Larrosa, M., García-Conesa, M.T., Tomás-Barberán, F.A., Espín, J.C., 2014. Phase-II metabolism limits the antiproliferative activity of urolithins in human colon cancer cells. Eur. J. Nutr. 53, 853–64. doi:10.1007/s00394-013-0589-4

Gordon, P.B., Holen, I., Seglen, P.O., 1995. Protection by naringin and some other flavonoids of hepatocytic autophagy and endocytosis against inhibition by okadaic acid. J. Biol. Chem. 270, 5830–8.

Goronzy, J.J., Weyand, C.M., 2009. Developments in the scientific understanding of rheumatoid arthritis. Arthritis Res. Ther. 11, 249. doi:10.1186/ar2758

Gross, G., 2009. Biosynthesis of ellagitannins: old ideas and new solutions, in: Quideau, S. (Ed.), Chemistry and Biology of Ellagitannins: An Underestimated Class of Bioactive Plant Polyphenols. WORLD SCIENTIFIC, pp. 94–118.

Gu, L., Kelm, M.A., Hammerstone, J.F., Beecher, G., Holden, J., Haytowitz, D., Gebhardt, S., Prior, R.L., 2004. Concentrations of proanthocyanidins in common foods and estimations of normal consumption. J. Nutr. 134, 613–7.

Hager, T.J., Howard, L.R., Liyanage, R., Lay, J.O., Prior, R.L., 2008. Ellagitannin composition of blackberry as determined by HPLC-ESI-MS and MALDI-TOF-MS. J. Agric. Food Chem. 56, 661–9. doi:10.1021/jf071990b

Hagerman, A.E., Riedl, K.M., Jones, G.A., Sovik, K.N., Ritchard, N.T., Hartzfeld, P.W., Riechel, T.L., 1998. High Molecular Weight Plant Polyphenolics (Tannins) as Biological Antioxidants. J. Agric. Food Chem. 46, 1887–92. doi:10.1021/jf970975b

Han, D.H., Lee, M.J., Kim, J.H., 2006. Antioxidant and apoptosis-inducing activities of ellagic acid. Anticancer Res. 26, 3601–6.

Hanhineva, K., Rogachev, I., Kokko, H., Mintz-Oron, S., Venger, I., Kärenlampi, S., Aharoni, A., 2008. Non-targeted analysis of spatial metabolite composition in strawberry (Fragaria×ananassa) flowers. Phytochemistry 69, 2463–81. doi:10.1016/j.phytochem.2008.07.009

Hao, Q., Li, T., Zhang, X., Gao, P., Qiao, P., Li, S., Geng, Z., 2014. Expression and roles of fatty acid synthase in hepatocellular carcinoma. Oncol. Rep. 32, 2471–6. doi:10.3892/or.2014.3484

Harborne, J.B., 1999. Classes and functions of secondary products from plants, in: Walton, N.J., Brown, D.E. (Eds.), Chemicals from Plants: Perspectives on Plant Secondary Products. Imperal College Press, London, pp. 1–25.

Hasima, N., Ozpolat, B., 2014. Regulation of autophagy by polyphenolic compounds as a potential therapeutic strategy for cancer. Cell Death Dis. 5, e1509. doi:10.1038/cddis.2014.467

Heim, K.E., Tagliaferro, A.R., Bobilya, D.J., 2002. Flavonoid antioxidants: chemistry, metabolism and structure-activity relationships. J. Nutr. Biochem. 13, 572–84.

Hershko, A., Heller, H., Elias, S., Ciechanover, A., 1983. Components of ubiquitin-protein ligase system. Resolution, affinity purification, and role in protein breakdown. J. Biol. Chem. 258, 8206–14.

Hoeller, D., Dikic, I., 2009. Targeting the ubiquitin system in cancer therapy. Nature 458, 438–44. doi:nature07960 [pii] 10.1038/nature07960

Hofseth, L.J., 2008. Nitric oxide as a target of complementary and alternative medicines to prevent and treat inflammation and cancer. Cancer Lett. 268, 10–30. doi:10.1016/j.canlet.2008.03.024

Hollebeeck, S., Winand, J., Hérent, M.-F., During, A., Leclercq, J., Larondelle, Y., Schneider, Y.-J., 2012. Anti-inflammatory effects of pomegranate (Punica granatum L.) husk ellagitannins in Caco-2 cells, an in vitro model of human intestine. Food Funct. 3, 875–85. doi:10.1039/c2fo10258g

Hummer, K.E., Bassil, N., Njuguna, W., 2011. Fragaria, in: Wild Crop Relatives: Genomic and Breeding Resources. Springer Berlin Heidelberg, Berlin, Heidelberg, pp. 17–44. doi:10.1007/978-3-642-16057-8_2

Ishii, R., Saito, K., Horie, M., Shibano, T., Kitanaka, S., Amano, F., 1999. Inhibitory effects of hydrolyzable tannins from Melastoma dodecandrum Lour. on nitric oxide production by a murine macrophage-like cell line, RAW264.7, activated with lipopolysaccharide and interferon-gamma. Biol. Pharm. Bull. 22, 647–53.

Ishimoto, H., Shibata, M., Myojin, Y., Ito, H., Sugimoto, Y., Tai, A., Hatano, T., 2011. In vivo anti-inflammatory and antioxidant properties of ellagitannin metabolite urolithin A. Bioorg. Med. Chem. Lett. 21, 5901–4. doi:10.1016/j.bmcl.2011.07.086

Israël, A., 2010. The IKK complex, a central regulator of NF-kappaB activation. Cold Spring Harb. Perspect. Biol. 2, a000158. doi:10.1101/cshperspect.a000158

Ivanov, I., Petkova, N., Denev, P., Pavlov, A., 2015. Polyphenols content and antioxidant activities in infusion and decoction extracts obtained from Fragaria vesca L. leaves. Sci. Bull. Ser. F. Biotechnol. 19, 145–8.

Jarić, S., Popović, Z., Macukanović-Jocić, M., Djurdjević, L., Mijatović, M., Karadzić, B., Mitrović, M., Pavlović, P., 2007. An ethnobotanical study on the usage of wild medicinal herbs from Kopaonik Mountain (Central Serbia). J. Ethnopharmacol. 111, 160–75. doi:10.1016/j.jep.2006.11.007

Jemal, A., Bray, F., Center, M.M., Ferlay, J., Ward, E., Forman, D., 2011. Global cancer statistics. CA. Cancer J. Clin. 61, 69–90. doi:10.3322/caac.20107

Jin, Z., El-Deiry, W.S., 2005. Overview of cell death signaling pathways. Cancer Biol. Ther. 4, 139–63.

Kähkönen, M., Kylli, P., Ollilainen, V., Salminen, J.-P., Heinonen, M., 2012. Antioxidant activity of isolated ellagitannins from red raspberries and cloudberries. J. Agric. Food Chem. 60, 1167–74. doi:10.1021/jf203431g

Kallio, T., Kallio, J., Jaakkola, M., Mäki, M., Kilpeläinen, P., Virtanen, V., 2013. Urolithins display both antioxidant and pro-oxidant activities depending on assay system and conditions. J. Agric. Food Chem. 61, 10720–9. doi:10.1021/jf403208d

Kampa, M., Nifli, A.-P., Notas, G., Castanas, E., 2007. Polyphenols and cancer cell growth. Rev. Physiol. Biochem. Pharmacol. 159, 79–113. doi:10.1007/112_2006_0702

Kanodia, L., Borgohain, M., Das, S., 2011. Effect of fruit extract of Fragaria vesca L. on experimentally induced inflammatory bowel disease in albino rats. Indian J. Pharmacol. 43, 18–21. doi:10.4103/0253-7613.75660

Kanodia, L., Das, S., 2008. A comparative study of analgesic property of whole plant and fruit extracts of Fragaria vesca in experimental animal models. Bangladesh J. Pharmacol. 4, 35–8. doi:10.3329/bjp.v4i1.1049

Kasimsetty, S.G., Bialonska, D., Reddy, M.K., Ma, G., Khan, S.I., Ferreira, D., 2010. Colon cancer chemopreventive activities of pomegranate ellagitannins and urolithins. J. Agric. Food Chem. 58, 2180–7. doi:10.1021/jf903762h

Kasimsetty, S.G., Bialonska, D., Reddy, M.K., Thornton, C., Willett, K.L., Ferreira, D., 2009. Effects of pomegranate chemical constituents/intestinal microbial metabolites on CYP1B1 in 22Rv1 prostate cancer cells. J. Agric. Food Chem. 57, 10636–44. doi:10.1021/jf902716r

Kastan, M.B., Bartek, J., 2004. Cell-cycle checkpoints and cancer. Nature 432, 316–23. doi:10.1038/nature03097

Kerr, J.F., Wyllie, A.H., Currie, A.R., 1972. Apoptosis: a basic biological phenomenon with wide-ranging implications in tissue kinetics. Br. J. Cancer 26, 239–57.

Khanbabaee, K., van Ree, T., 2001. Tannins: classification and definition. Nat. Prod. Rep. 18, 641–9.

Kiselova, Y., Ivanova, D., Chervenkov, T., Gerova, D., Galunska, B., Yankova, T., 2006. Correlation between the in vitro antioxidant activity and polyphenol content of aqueous extracts from Bulgarian herbs. Phytother. Res. 20, 961–5. doi:10.1002/ptr.1985

Klionsky, D.J. et al., Guidelines for the use and interpretation of assays for monitoring autophagy. Autophagy 8, 445–544.

Knievel, J., Schulz, W.A., Greife, A., Hader, C., Lübke, T., Schmitz, I., Albers, P., Niegisch, G., 2014. Multiple mechanisms mediate resistance to sorafenib in urothelial cancer. Int. J. Mol. Sci. 15, 20500–17. doi:10.3390/ijms151120500

Knowles, M.A., Hurst, C.D., 2014. Molecular biology of bladder cancer: new insights into pathogenesis and clinical diversity. Nat. Rev. Cancer 15, 25–41. doi:10.1038/nrc3817

Knowles, M.A., Platt, F.M., Ross, R.L., Hurst, C.D., 2009. Phosphatidylinositol 3-kinase (PI3K) pathway activation in bladder cancer. Cancer Metastasis Rev. 28, 305–16. doi:10.1007/s10555-009-9198-3

Kool, M.M., Comeskey, D.J., Cooney, J.M., McGhie, T.K., 2010. Structural identification of the main ellagitannins of a boysenberry (Rubus loganbaccus×baileyanus Britt.) extract by LC–ESI-MS/MS, MALDI-TOF-MS and NMR spectroscopy. Food Chem. 119, 1535–43. doi:10.1016/j.foodchem.2009.09.039

Koponen, J.M., Happonen, A.M., Mattila, P.H., Törrönen, A.R., 2007. Contents of anthocyanins and ellagitannins in selected foods consumed in Finland. J. Agric. Food Chem. 55, 1612–9. doi:10.1021/jf062897a

Korolchuk, V.I., Mansilla, A., Menzies, F.M., Rubinsztein, D.C., 2009. Autophagy inhibition compromises degradation of ubiquitin-proteasome pathway substrates. Mol. Cell 33, 517–27. doi:10.1016/j.molcel.2009.01.021

Korolchuk, V.I., Menzies, F.M., Rubinsztein, D.C., 2010. Mechanisms of cross-talk between the ubiquitin-proteasome and autophagy-lysosome systems. FEBS Lett. 584, 1393–8. doi:10.1016/j.febslet.2009.12.047

Kouroukis, T.C., Baldassarre, F.G., Haynes, A.E., Imrie, K., Reece, D.E., Cheung, M.C., 2014. Bortezomib in multiple myeloma: systematic review and clinical considerations. Curr. Oncol. 21, e573–603. doi:10.3747/co.21.1798

Koyama, S., Cobb, L.J., Mehta, H.H., Seeram, N.P., Heber, D., Pantuck, A.J., Cohen, P., 2010. Pomegranate extract induces apoptosis in human prostate cancer cells by modulation of the IGF–IGFBP axis. Growth Horm. IGF Res. 20, 55–62. doi:10.1016/j.ghir.2009.09.003

Kresty, L.A., Howell, A.B., Baird, M., 2011. Cranberry proanthocyanidins mediate growth arrest of lung cancer cells through modulation of gene expression and rapid induction of apoptosis. Molecules 16, 2375–90. doi:10.3390/molecules16032375

Kumar, S., Pandey, A.K., 2013. Chemistry and biological activities of flavonoids: an overview. ScientificWorldJournal. 2013, 162750. doi:10.1155/2013/162750

Kumatori, A., Tanaka, K., Inamura, N., Sone, S., Ogura, T., Matsumoto, T., Tachikawa, T., Shin, S., Ichihara, A., 1990. Abnormally high expression of proteasomes in human leukemic cells. Proc. Natl. Acad. Sci. U. S. A. 87, 7071–5.

Kuo, P.-L., Hsu, Y.-L., Lin, T.-C., Chang, J.-K., Lin, C.-C., 2005a. Induction of cell cycle arrest and apoptosis in human non-small cell lung cancer A549 cells by casuarinin from the bark of Terminalia arjuna Linn. Anticancer. Drugs 16, 409–15.

Kuo, P.-L., Hsu, Y.-L., Lin, T.-C., Lin, L.-T., Chang, J.-K., Lin, C.-C., 2005b. Casuarinin from the Bark of Terminalia arjuna Induces Apoptosis and Cell Cycle Arrest in Human Breast Adenocarcinoma MCF-7 Cells. Planta Med. 71, 237–43. doi:10.1055/s-2005-837823

Kuo, P.-L., Hsu, Y.-L., Lin, T.-C., Tzeng, W.-S., Chen, Y.-Y., Lin, C.-C., 2007. Rugosin E, an ellagitannin, inhibits MDA-MB-231 human breast cancer cell proliferation and induces apoptosis by inhibiting nuclear factor-κB signaling pathway. Cancer Lett. 248, 280–91. doi:10.1016/j.canlet.2006.08.006

Kuo, P.-T., Lin, T.-P., Liu, L.-C., Huang, C.-H., Lin, J.-K., Kao, J.-Y., Way, T.-D., 2009. Penta- O -galloyl-β-d -glucose Suppresses Prostate Cancer Bone Metastasis by Transcriptionally Repressing EGF-Induced MMP-9 Expression. J. Agric. Food Chem. 57, 3331–9. doi:10.1021/jf803725h

Küpeli, E., Tatli, I.I., Akdemir, Z.S., Yesilada, E., 2007. Estimation of antinociceptive and anti-inflammatory activity on Geranium pratense subsp. finitimum and its phenolic compounds. J. Ethnopharmacol. 114, 234–40. doi:10.1016/j.jep.2007.08.005

Kurokawa, M., Hozumi, T., Tsurita, M., Kadota, S., Namba, T., Shiraki, K., 2001. Biological characterization of eugeniin as an anti-herpes simplex virus type 1 compound in vitro and in vivo. J. Pharmacol. Exp. Ther. 297, 372–9.

Kwon, D.-J., Bae, Y.-S., Ju, S.M., Goh, A.R., Choi, S.Y., Park, J., 2011. Casuarinin suppresses TNF-α-induced ICAM-1 expression via blockade of NF-κB activation in HaCaT cells. Biochem. Biophys. Res. Commun. 409, 780–5. doi:10.1016/j.bbrc.2011.05.088

Lam, Y.A., Lawson, T.G., Velayutham, M., Zweier, J.L., Pickart, C.M., 2002. A proteasomal ATPase subunit recognizes the polyubiquitin degradation signal. Nature 416, 763–7. doi:10.1038/416763a

Lamari, Z., Landsberger, S., Braisted, J., Neggache, H., Larbi, R., 2007. Trace element content of medicinal plants from Algeria. J. Radioanal. Nucl. Chem. 276, 95–9. doi:10.1007/s10967-007-0415-7

Larrosa, M., García-Conesa, M.T., Espín, J.C., Tomás-Barberán, F.A., 2010a. Ellagitannins, ellagic acid and vascular health. Mol. Aspects Med. 31, 513–39. doi:10.1016/j.mam.2010.09.005

Larrosa, M., González-Sarrías, A., García-Conesa, M.T., Tomás-Barberán, F.A., Espín, J.C., 2006a. Urolithins, ellagic acid-derived metabolites produced by human colonic microflora, exhibit estrogenic and antiestrogenic activities. J. Agric. Food Chem. 54, 1611–20. doi:10.1021/jf0527403

Larrosa, M., González-Sarrías, A., Yáñez-Gascón, M.J., Selma, M. V, Azorín-Ortuño, M., Toti, S., Tomás-Barberán, F., Dolara, P., Espín, J.C., 2010b. Anti-inflammatory properties of a pomegranate extract and its metabolite urolithin-A in a colitis rat model and the effect of colon inflammation on phenolic metabolism. J. Nutr. Biochem. 21, 717–25. doi:10.1016/j.jnutbio.2009.04.012

Larrosa, M., Tomás-Barberán, F.A., Espín, J.C., 2006b. The dietary hydrolysable tannin punicalagin releases ellagic acid that induces apoptosis in human colon adenocarcinoma Caco-2 cells by using the mitochondrial pathway. J. Nutr. Biochem. 17, 611–25. doi:10.1016/j.jnutbio.2005.09.004

Lattanzio, V., 2013. Phenolic Compounds: Introduction, in: Ramawat, K.G., Mérillon, J.-M. (Eds.), Natural Products. Springer Berlin Heidelberg, Berlin, Heidelberg, pp. 1543–80. doi:10.1007/978-3-642-22144-6_57

Lee, J.-C., Tsai, C.-Y., Kao, J.-Y., Kao, M.-C., Tsai, S.-C., Chang, C.-S., Huang, L.-J., Kuo, S.-C., Lin, J.-K., Way, T.-D., 2008. Geraniin-mediated apoptosis by cleavage of focal adhesion kinase through up-regulation of Fas ligand expression in human melanoma cells. Mol. Nutr. Food Res. 52, 655–63. doi:10.1002/mnfr.200700381

Lee, J.H., Talcott, S.T., 2002. Ellagic acid and ellagitannins affect on sedimentation in muscadine juice and wine. J. Agric. Food Chem. 50, 3971–6. doi:10.1021/jf011587j

Lee, S.H., Soyoola, E., Chanmugam, P., Hart, S., Sun, W., Zhong, H., Liou, S., Simmons, D., Hwang, D., 1992. Selective expression of mitogen-inducible cyclooxygenase in macrophages stimulated with lipopolysaccharide. J. Biol. Chem. 267, 25934–8.

Levine, B., Kroemer, G., 2008. Autophagy in the pathogenesis of disease. Cell 132, 27–42. doi:10.1016/j.cell.2007.12.018

Li, B., Dou, Q.P., 2000. Bax degradation by the ubiquitin/proteasome-dependent pathway: involvement in tumor survival and progression. Proc. Natl. Acad. Sci. U. S. A. 97, 3850–5. doi:10.1073/pnas.070047997

Li, J., Huang, H., Zhou, W., Feng, M., Zhou, P., 2008. Anti-hepatitis B virus activities of Geranium carolinianum L. extracts and identification of the active components. Biol. Pharm. Bull. 31, 743–7.

Li, J., Wang, S., Yin, J., Pan, L., 2013. Geraniin induces apoptotic cell death in human lung adenocarcinoma A549 cells in vitro and in vivo. Can. J. Physiol. Pharmacol. 91, 1016–24. doi:10.1139/cjpp-2013-0140

Li, W., Li, J., Bao, J., 2012. Microautophagy: lesser-known self-eating. Cell. Mol. Life Sci. 69, 1125–36. doi:10.1007/s00018-011-0865-5

Li, Z., Percival, S.S., Bonard, S., Gu, L., 2011. Fabrication of nanoparticles using partially purified pomegranate ellagitannins and gelatin and their apoptotic effects. Mol. Nutr. Food Res. 55, 1096–103. doi:10.1002/mnfr.201000528

Liberal, J., Costa, G., Carmo, A., Vitorino, R., Marques, C., Domingues, M.R., Domingues, P., Gonçalves, A.C., Alves, R., Sarmento-Ribeiro, A.B., Girão, H., Cruz, M.T., Batista, M.T., 2015. Chemical characterization and cytotoxic potential of an ellagitannin-enriched fraction from Fragaria vesca leaves. Arab. J. Chem. doi:10.1016/j.arabjc.2015.11.014

Liberal, J., Francisco, V., Costa, G., Figueirinha, A., Amaral, M.T., Marques, C., Girão, H., Lopes, M.C., Cruz, M.T., Batista, M.T., 2014. Bioactivity of Fragaria vesca leaves through inflammation, proteasome and autophagy modulation. J. Ethnopharmacol. 158PA, 113–22. doi:10.1016/j.jep.2014.09.043

Lightfoot, H.M., Lark, A., Livasy, C.A., Moore, D.T., Cowan, D., Dressler, L., Craven, R.J., Cance, W.G., 2004. Upregulation of focal adhesion kinase (FAK) expression in ductal carcinoma in situ (DCIS) is an early event in breast tumorigenesis. Breast Cancer Res. Treat. 88, 109–16. doi:10.1007/s10549-004-1022-8

Lin, C.C., Hsu, Y.F., Lin, T.C., 1999. Effects of punicalagin and punicalin on carrageenan-induced inflammation in rats. Am. J. Chin. Med. 27, 371–6. doi:10.1142/S0192415X99000422

Lin, L.-T., Chen, T.-Y., Chung, C.-Y., Noyce, R.S., Grindley, T.B., McCormick, C., Lin, T.-C., Wang, G.-H., Lin, C.-C., Richardson, C.D., 2011. Hydrolyzable tannins (chebulagic acid and punicalagin) target viral glycoprotein-glycosaminoglycan interactions to inhibit herpes simplex virus 1 entry and cell-to-cell spread. J. Virol. 85, 4386–98. doi:10.1128/JVI.01492-10

Lin, S., Hoffmann, K., Schemmer, P., 2012. Treatment of Hepatocellular Carcinoma: A Systematic Review. Liver cancer 1, 144–58. doi:10.1159/000343828

Link, M.P., Goorin, A.M., Miser, A.W., Green, A.A., Pratt, C.B., Belasco, J.B., Pritchard, J., Malpas, J.S., Baker, A.R., Kirkpatrick, J.A., 1986. The effect of adjuvant chemotherapy on relapse-free survival in patients with osteosarcoma of the extremity. N. Engl. J. Med. 314, 1600–6. doi:10.1056/NEJM198606193142502

Linkermann, A., Green, D.R., 2014. Necroptosis. N. Engl. J. Med. 370, 455–65. doi:10.1056/NEJMra1310050

Linnaeus, C., 1738. Hortus cliffortianus, Salomonem Schouten, Amstelaedami.

Linnaeus, C., 1753. Species plantarum, 1st ed, Laurentii Salvii, Stockholm.

Lipińska, L., Klewicka, E., Sójka, M., 2014. The structure, occurrence and biological activity of ellagitannins: a general review. Acta Sci. Pol. Technol. Aliment. 13, 289–99.

Liston, A., Cronn, R., Ashman, T.-L., 2014. Fragaria: a genus with deep historical roots and ripe for evolutionary and ecological insights. Am. J. Bot. 101, 1686–99. doi:10.3732/ajb.1400140

Liu, C.-W., Jacobson, A.D., 2013. Functions of the 19S complex in proteasomal degradation. Trends Biochem. Sci. 38, 103–10. doi:10.1016/j.tibs.2012.11.009

Liu, H., Li, J., Zhao, W., Bao, L., Song, X., Xia, Y., Wang, X., Zhang, C., Wang, X., Yao, X., Li, M., 2009. Fatty Acid Synthase Inhibitors from Geum japonicum Thunb. var. chinense. Chem. Biodivers. 6, 402–10. doi:10.1002/cbdv.200700462

Liu, M.-J., Wang, Z., Li, H.-X., Wu, R.-C., Liu, Y.-Z., Wu, Q.-Y., 2004. Mitochondrial dysfunction as an early event in the process of apoptosis induced by woodfordin I in human leukemia K562 cells. Toxicol. Appl. Pharmacol. 194, 141–55.

Liu, S., Chen, Z.J., 2011. Expanding role of ubiquitination in NF-κB signaling. Cell Res. 21, 6–21. doi:10.1038/cr.2010.170

Lobo, V., Patil, A., Phatak, A., Chandra, N., 2010. Free radicals, antioxidants and functional foods: Impact on human health. Pharmacogn. Rev. 4, 118–26. doi:10.4103/0973-7847.70902

Loda, M., Cukor, B., Tam, S.W., Lavin, P., Fiorentino, M., Draetta, G.F., Jessup, J.M., Pagano, M., 1997. Increased proteasome-dependent degradation of the cyclin-dependent kinase inhibitor p27 in aggressive colorectal carcinomas. Nat. Med. 3, 231–4.

Luetke, A., Meyers, P.A., Lewis, I., Juergens, H., 2014. Osteosarcoma treatment - where do we stand? A state of the art review. Cancer Treat. Rev. 40, 523–32. doi:10.1016/j.ctrv.2013.11.006

Maldonado, P.D., Rivero-Cruz, I., Mata, R., Pedraza-Chaverrí, J., 2005. Antioxidant activity of A-type proanthocyanidins from Geranium niveum (Geraniaceae). J. Agric. Food Chem. 53, 1996–2001. doi:10.1021/jf0483725

Malik, N.S., Perez, J.L., Lombardini, L., Cornacchia, R., Cisneros-Zevallos, L., Braford, J., 2009. Phenolic compounds and fatty acid composition of organic and conventional grown pecan kernels. J. Sci. Food Agric. 89, 2207–13. doi:10.1002/jsfa.3708

Manolova, L., 2003. Natural Pharmacy, 1st ed. Dorrance Publishing Co., Inc., Pittsburgh.

Mantovani, A., 2010. Molecular pathways linking inflammation and cancer. Curr. Mol. Med. 10, 369–73.

Marín, M., María Giner, R., Ríos, J.-L., Recio, M.C., 2013. Intestinal anti-inflammatory activity of ellagic acid in the acute and chronic dextrane sulfate sodium models of mice colitis. J. Ethnopharmacol. 150, 925–34. doi:10.1016/j.jep.2013.09.030

Martinez-Perez, C., Ward, C., Cook, G., Mullen, P., McPhail, D., Harrison, D.J., Langdon, S.P., 2014. Novel flavonoids as anti-cancer agents: mechanisms of action and promise for their potential application in breast cancer. Biochem. Soc. Trans. 42, 1017–23. doi:10.1042/BST20140073

Martino, V., Morales, J., Martínez-Irujo, J.J., Font, M., Monge, A., Coussio, J., 2004. Two ellagitannins from the leaves of Terminalia triflora with inhibitory activity on HIV-1 reverse transcriptase. Phytother. Res. 18, 667–9. doi:10.1002/ptr.1504

Mathew, R., Karantza-Wadsworth, V., White, E., 2007. Role of autophagy in cancer. Nat. Rev. Cancer 7, 961–7. doi:10.1038/nrc2254

McCord, J.M., 2000. The evolution of free radicals and oxidative stress. Am. J. Med. 108, 652–9.

Mehrpour, M., Esclatine, A., Beau, I., Codogno, P., 2010. Overview of macroautophagy regulation in mammalian cells. Cell Res. 20, 748–62. doi:10.1038/cr.2010.82

Menković, N., Savikin, K., Tasić, S., Zdunić, G., Stesević, D., Milosavljević, S., Vincek, D., 2011. Ethnobotanical study on traditional uses of wild medicinal plants in Prokletije Mountains (Montenegro). J. Ethnopharmacol. 133, 97–107. doi:10.1016/j.jep.2010.09.008

Milacic, V., Banerjee, S., Landis-Piwowar, K.R., Sarkar, F.H., Majumdar, A.P.N., Dou, Q.P., 2008. Curcumin inhibits the proteasome activity in human colon cancer cells in vitro and in vivo. Cancer Res. 68, 7283–92. doi:10.1158/0008-5472.CAN-07-6246

Moilanen, J., Koskinen, P., Salminen, J.-P., 2015. Distribution and content of ellagitannins in Finnish plant species. Phytochemistry 116, 188–97. doi:10.1016/j.phytochem.2015.03.002

Mouradov, A., Spangenberg, G., 2014. Flavonoids: a metabolic network mediating plants adaptation to their real estate. Front. Plant Sci. 5, 620. doi:10.3389/fpls.2014.00620

Mudnic, I., Modun, D., Brizic, I., Vukovic, J., Generalic, I., Katalinic, V., Bilusic, T., Ljubenkov, I., Boban, M., 2009. Cardiovascular effects in vitro of aqueous extract of wild strawberry (Fragaria vesca, L.) leaves. Phytomedicine 16, 462–9. doi:10.1016/j.phymed.2008.11.004

Mullen, W., Yokota, T., Lean, M.E.J., Crozier, A., 2003. Analysis of ellagitannins and conjugates of ellagic acid and quercetin in raspberry fruits by LC–MSn. Phytochemistry 64, 617–24. doi:10.1016/S0031-9422(03)00281-4

Murdoch, J.R., Lloyd, C.M., 2010. Chronic inflammation and asthma. Mutat. Res. 690, 24–39. doi:10.1016/j.mrfmmm.2009.09.005

Nam, S., Smith, D.M., Dou, Q.P., 2001. Ester bond-containing tea polyphenols potently inhibit proteasome activity in vitro and in vivo. J. Biol. Chem. 276, 13322–30. doi:10.1074/jbc.M004209200

Neves, J.M., Matos, C., Moutinho, C., Queiroz, G., Gomes, L.R., 2009. Ethnopharmacological notes about ancient uses of medicinal plants in Trás-os-Montes (northern of Portugal). J. Ethnopharmacol. 124, 270–83. doi:10.1016/j.jep.2009.04.041

Newman, D.J., Cragg, G.M., 2012. Natural Products As Sources of New Drugs over the 30 Years from 1981 to 2010. J. Nat. Prod. 75, 311–35. doi:10.1021/np200906s

Nicholson, B.E., Frierson, H.F., Conaway, M.R., Seraj, J.M., Harding, M.A., Hampton, G.M., Theodorescu, D., 2004. Profiling the evolution of human metastatic bladder cancer. Cancer Res. 64, 7813–21. doi:10.1158/0008-5472.CAN-04-0826

Niemetz, R., Gross, G.G., 2005. Enzymology of gallotannin and ellagitannin biosynthesis. Phytochemistry 66, 2001–11. doi:10.1016/j.phytochem.2005.01.009

Niswander, L.M., Kim, S.Y., 2010. Stratifying osteosarcoma: minimizing and maximizing therapy. Curr. Oncol. Rep. 12, 266–70. doi:10.1007/s11912-010-0106-3

Nuñez-Sánchez, M.A., García-Villalba, R., Monedero-Saiz, T., García-Talavera, N. V, Gómez-Sánchez, M.B., Sánchez-Álvarez, C., García-Albert, A.M., Rodríguez-Gil, F.J., Ruiz-Marín, M., Pastor-Quirante, F.A., Martínez-Díaz, F., Yáñez-Gascón, M.J., González-Sarrías, A., Tomás-Barberán, F.A., Espín, J.C., 2014. Targeted metabolic profiling of pomegranate polyphenols and urolithins in plasma, urine and colon tissues from colorectal cancer patients. Mol. Nutr. Food Res. 58, 1199–211. doi:10.1002/mnfr.201300931

O'Brien, J., Wilson, I., Orton, T., Pognan, F., 2000. Investigation of the Alamar Blue (resazurin) fluorescent dye for the assessment of mammalian cell cytotoxicity. Eur. J. Biochem. 267, 5421–26. doi:10.1046/j.1432-1327.2000.01606.x

O'Connor, P.M., Lapointe, T.K., Beck, P.L., Buret, A.G., 2010. Mechanisms by which inflammation may increase intestinal cancer risk in inflammatory bowel disease. Inflamm. Bowel Dis. 16, 1411–20. doi:10.1002/ibd.21217

Okada, H., Mak, T.W., 2004. Pathways of apoptotic and non-apoptotic death in tumour cells. Nat. Rev. Cancer 4, 592–603. doi:10.1038/nrc1412

Okuda, T., Yoshida, T., Hatano, T., 1993. Classification of oligomeric hydrolysable tannins and specificity of their occurrence in plants. Phytochemistry 32, 507–21. doi:10.1016/S0031-9422(00)95129-X

Okuda, T., Yoshida, T., Hatano, T., Ito, H., 2009. Ellagitannins Renewed the Concept of Tannins, in: Quideau, S. (Ed.), Chemistry and Biology of Ellagitannins: An Underestimated Class of Bioactive Plant Polyphenols. WORLD SCIENTIFIC, pp. 1–54. doi:10.1142/9789812797414_0001

Olajide, O.A., Kumar, A., Velagapudi, R., Okorji, U.P., Fiebich, B.L., 2014. Punicalagin inhibits neuroinflammation in LPS-activated rat primary microglia. Mol. Nutr. Food Res. 58, 1843–51. doi:10.1002/mnfr.201400163

Orlowski, M., Wilk, S., 2000. Catalytic activities of the 20 S proteasome, a multicatalytic proteinase complex. Arch. Biochem. Biophys. 383, 1–16. doi:10.1006/abbi.2000.2036

Ottaviani, G., Jaffe, N., 2009. The epidemiology of osteosarcoma. Cancer Treat. Res. 152, 3–13. doi:10.1007/978-1-4419-0284-9_1

Ovaskainen, M.-L., Törrönen, R., Koponen, J.M., Sinkko, H., Hellström, J., Reinivuo, H., Mattila, P., 2008. Dietary intake and major food sources of polyphenols in Finnish adults. J. Nutr. 138, 562–6.

Ozpolat, B., Benbrook, D.M., 2015. Targeting autophagy in cancer management - strategies and developments. Cancer Manag. Res. 7, 291–9. doi:10.2147/CMAR.S34859

Ozüdoğru, B., Akaydın, G., Erik, S., Yesilada, E., 2011. Inferences from an ethnobotanical field expedition in the selected locations of Sivas and Yozgat provinces (Turkey). J. Ethnopharmacol. 137, 85–98. doi:10.1016/j.jep.2011.04.050

Pallauf, K., Rimbach, G., 2013. Autophagy, polyphenols and healthy ageing. Ageing Res. Rev. 12, 237–252. doi:10.1016/j.arr.2012.03.008

Patil, M.V.K., Kandhare, A.D., Ghosh, P., Bhise, S.D., 2012. Determination of role of GABA and nitric oxide in anticonvulsant activity of Fragaria vesca L. ethanolic extract in chemically induced epilepsy in laboratory animals. Orient. Pharm. Exp. Med. 12, 255–264. doi:10.1007/s13596-012-0072-4

Patil, S.D., 2013. A recent review on anticancer herbal drugs. J. drug Discov. Ther. 1.

Pattingre, S., Espert, L., Biard-Piechaczyk, M., Codogno, P., 2008. Regulation of macroautophagy by mTOR and Beclin 1 complexes. Biochimie 90, 313–23. doi:10.1016/j.biochi.2007.08.014

Pawlaczyk, I., Lewik-Tsirigotis, M., Capek, P., Matulová, M., Sasinková, V., Dąbrowski, P., Witkiewicz, W., Gancarz, R., 2013. Effects of extraction condition on structural features and anticoagulant activity of F. vesca L. conjugates. Carbohydr. Polym. 92, 741–50. doi:10.1016/j.carbpol.2012.10.011

Piwowarski, J.P., Granica, S., Kiss, A.K., 2014a. Influence of gut microbiota-derived ellagitannins' metabolites urolithins on pro-inflammatory activities of human neutrophils. Planta Med. 80, 887–95. doi:10.1055/s-0034-1368615

Piwowarski, J.P., Granica, S., Zwierzyńska, M., Stefańska, J., Schopohl, P., Melzig, M.F., Kiss, A.K., 2014b. Role of human gut microbiota metabolism in the anti-inflammatory effect of traditionally used ellagitannin-rich plant materials. J. Ethnopharmacol. 155, 801–9. doi:10.1016/j.jep.2014.06.032

Piwowarski, J.P., Kiss, A.K., Granica, S., Moeslinger, T., 2015. Urolithins, gut microbiota-derived metabolites of ellagitannins, inhibit LPS-induced inflammation in RAW 264.7 murine macrophages. Mol. Nutr. Food Res. doi:10.1002/mnfr.201500264

Pizer, E.S., Jackisch, C., Wood, F.D., Pasternack, G.R., Davidson, N.E., Kuhajda, F.P., 1996. Inhibition of fatty acid synthesis induces programmed cell death in human breast cancer cells. Cancer Res. 56, 2745–7.

Polivka, J., Janku, F., 2014. Molecular targets for cancer therapy in the PI3K/AKT/mTOR pathway. Pharmacol. Ther. 142, 164–75. doi:10.1016/j.pharmthera.2013.12.004

Popović, Z., Smiljanić, M., Kostić, M., Nikić, P., Janković, S., 2014. Wild flora and its usage in traditional phytotherapy (Deliblato Sands, Serbia, South East Europe). Indian J. Tradit. Knowl. 13, 9–35.

Popović, Z., Smiljanić, M., Matić, R., 2012. Phytotherapeutical plants from the Deliblato Sands (Serbia): Traditional pharmacopoeia and implications for conservation. Indian J. Tradit. Knowl. 11, 385-400.

Porto, M., 2014. Flora-On | Flora de Portugal interactiva [WWW Document]. Soc. Port. Botânica. URL http://www.flora-on.pt/#/hiLC3 (accessed 12.21.15).

Pouységu, L., Deffieux, D., Malik, G., Natangelo, A., Quideau, S., 2011. Synthesis of ellagitannin natural products. Nat. Prod. Rep. 28, 853–74. doi:10.1039/c0np00058b

Pradelli, L.A., Bénéteau, M., Ricci, J.-E., 2010. Mitochondrial control of caspase-dependent and -independent cell death. Cell. Mol. Life Sci. 67, 1589–97. doi:10.1007/s00018-010-0285-y

Proskuryakov, S., Gabai, V., 2010. Mechanisms of Tumor Cell Necrosis. Curr. Pharm. Des. 16, 56–68. doi:10.2174/138161210789941793

Qian, H., Yang, Y., Wang, X., 2011. Curcumin enhanced adriamycin-induced human liver-derived Hepatoma G2 cell death through activation of mitochondria-mediated apoptosis and autophagy. Eur. J. Pharm. Sci. 43, 125–31. doi:10.1016/j.ejps.2011.04.002

Qiu, Z., Zhou, B., Jin, L., Yu, H., Liu, L., Liu, Y., Qin, C., Xie, S., Zhu, F., 2013. In vitro antioxidant and antiproliferative effects of ellagic acid and its colonic metabolite, urolithins, on human bladder cancer T24 cells. Food Chem. Toxicol. 59, 428–37. doi:10.1016/j.fct.2013.06.025

Quideau, S., 2009. Chemistry and Biology of Ellagitannins. WORLD SCIENTIFIC. doi:10.1142/6795

Quideau, S., Deffieux, D., Douat-Casassus, C., Pouységu, L., 2011. Plant polyphenols: chemical properties, biological activities, and synthesis. Angew. Chem. Int. Ed. Engl. 50, 586–621. doi:10.1002/anie.201000044

Quideau, S., Jourdes, M., Lefeuvre, D., Pardon, P., Saucier, C., Teissedre, P.-L., Glories, Y., 2010. Ellagitannins—an underestimated class of plant polyphenols: chemical reactivity of C-Glucosidic ellagitannins in relation to wine chemistry and biological activity, in: Santos-Buelga, C., Escribano-Bailon, T., Lattanzio, V. (Eds.), Recent Advances in in Polyphenol Research. Blackwell Publishing Ltd., pp. 81–137. doi:10.1002/9781444323375.ch4

Radi, R., 2013. Peroxynitrite, a stealthy biological oxidant. J. Biol. Chem. 288, 26464–72. doi:10.1074/jbc.R113.472936

Radtke, J., Linseisen, J., Wolfram, G., 1998. Phenolic acid intake of adults in a Bavarian subgroup of the national food consumption survey. Z. Ernahrungswiss. 37, 190–7.

Ramos, S., 2008. Cancer chemoprevention and chemotherapy: Dietary polyphenols and signalling pathways. Mol. Nutr. Food Res. 52, 507–26. doi:10.1002/mnfr.200700326

Raudoniūtė, I., Rovira, J., Venskutonis, P.R., Damašius, J., Rivero-Pérez, M.D., González-SanJosé, M.L., 2011. Antioxidant properties of garden strawberry leaf extract and its effect on fish oil oxidation. Int. J. Food Sci. Technol. 46, 935–43. doi:10.1111/j.1365-2621.2011.02582.x

Reddy, B.U., Mullick, R., Kumar, A., Sudha, G., Srinivasan, N., Das, S., 2014. Small molecule inhibitors of HCV replication from Pomegranate. Sci. Rep. 4, 5411. doi:10.1038/srep05411

Romo-Vaquero, M., García-Villalba, R., González-Sarrías, A., Beltrán, D., Tomás-Barberán, F.A., Espín, J.C., Selma, M. V., 2015. Interindividual variability in the human metabolism of ellagic acid:

Contribution of Gordonibacter to urolithin production. J. Funct. Foods 17, 785–91. doi:10.1016/j.jff.2015.06.040

Ross, H.A., McDougall, G.J., Stewart, D., 2007. Antiproliferative activity is predominantly associated with ellagitannins in raspberry extracts. Phytochemistry 68, 218–28. doi:10.1016/j.phytochem.2006.10.014

Rouzer, C.A., Marnett, L.J., 2009. Cyclooxygenases: structural and functional insights. J. Lipid Res. 50 Suppl, S29–34. doi:10.1194/jlr.R800042-JLR200

Sakagami, H., Jiang, Y., Kusama, K., Atsumi, T., Ueha, T., Toguchi, M., Iwakura, I., Satoh, K., Ito, H., Hatano, T., Yoshida, T., 2000. Cytotoxic activity of hydrolyzable tannins against human oral tumor cell lines--a possible mechanism. Phytomedicine 7, 39–47. doi:10.1016/S0944-7113(00)80020-3

Salminen, A., Kauppinen, A., Kaarniranta, K., 2012. Phytochemicals suppress nuclear factor-κB signaling: impact on health span and the aging process. Curr. Opin. Clin. Nutr. Metab. Care 15, 23–8. doi:10.1097/MCO.0b013e32834d3ae7

Sánchez-González, C., Ciudad, C.J., Izquierdo-Pulido, M., Noé, V., 2015. Urolithin A causes p21 up-regulation in prostate cancer cells. Eur. J. Nutr. doi:10.1007/s00394-015-0924-z

Sánchez-González, C., Ciudad, C.J., Noé, V., Izquierdo-Pulido, M., 2014. Walnut polyphenol metabolites, urolithins A and B, inhibit the expression of the prostate-specific antigen and the androgen receptor in prostate cancer cells. Food Funct. 5, 2922–30. doi:10.1039/c4fo00542b

Sangiovanni, E., Vrhovsek, U., Rossoni, G., Colombo, E., Brunelli, C., Brembati, L., Trivulzio, S., Gasperotti, M., Mattivi, F., Bosisio, E., Dell'Agli, M., 2013. Ellagitannins from Rubus berries for the control of gastric inflammation: in vitro and in vivo studies. PLoS One 8, e71762. doi:10.1371/journal.pone.0071762

Santos, M.J., Fonseca, J.E., 2009. Metabolic syndrome, inflammation and atherosclerosis - the role of adipokines in health and in systemic inflammatory rheumatic diseases. Acta Reum. Port 34, 590–8.

Santos-Buelga, C., Gonzalez-Manzano, S., Dueñas, M., Gonzalez-Paramas, A.M., 2012. Extraction and isolation of phenolic compounds. Methods Mol. Biol., Methods in Molecular Biology 864, 427–64. doi:10.1007/978-1-61779-624-1_17

Sarić-Kundalić, B., Dobes, C., Klatte-Asselmeyer, V., Saukel, J., 2010. Ethnobotanical study on medicinal use of wild and cultivated plants in middle, south and west Bosnia and Herzegovina. J. Ethnopharmacol. 131, 33–55. doi:10.1016/j.jep.2010.05.061

Sarić-Kundalić, B., Dobeš, C., Klatte-Asselmeyer, V., Saukel, J., 2011. Ethnobotanical survey of traditionally used plants in human therapy of east, north and north-east Bosnia and Herzegovina. J. Ethnopharmacol. 133, 1051–76. doi:10.1016/j.jep.2010.11.033

Sartippour, M.R., Seeram, N.P., Rao, J.Y., Moro, A., Harris, D.M., Henning, S.M., Firouzi, A., Rettig, M.B., Aronson, W.J., Pantuck, A.J., Heber, D., 2008. Ellagitannin-rich pomegranate extract inhibits angiogenesis in prostate cancer in vitro and in vivo. Int. J. Oncol. 32, 475–80.

Savo, V., Giulia, C., Maria, G.P., David, R., 2011. Folk phytotherapy of the Amalfi Coast (Campania, Southern Italy). J. Ethnopharmacol. 135, 376–92. doi:10.1016/j.jep.2011.03.027

Scalzo, J., Politi, A., Pellegrini, N., Mezzetti, B., Battino, M., 2005. Plant genotype affects total antioxidant capacity and phenolic contents in fruit. Nutrition 21, 207–13. doi:10.1016/j.nut.2004.03.025

Schmid, D., Gruber, M., Piskaty, C., Woehs, F., Renner, A., Nagy, Z., Kaltenboeck, A., Wasserscheid, T., Bazylko, A., Kiss, A.K., Moeslinger, T., 2012. Inhibition of NF-κB-Dependent Cytokine and Inducible Nitric Oxide Synthesis by the Macrocyclic Ellagitannin Oenothein B in TLR-Stimulated RAW 264.7 Macrophages. J. Nat. Prod. 75, 870–75. doi:10.1021/np200756f

Schmidt, M., Finley, D., 2014. Regulation of proteasome activity in health and disease. Biochim. Biophys. Acta 1843, 13–25. doi:10.1016/j.bbamcr.2013.08.012

Schwartz, A.L., Ciechanover, A., 2009. Targeting proteins for destruction by the ubiquitin system: implications for human pathobiology. Annu. Rev. Pharmacol. Toxicol. 49, 73–96. doi:10.1146/annurev.pharmtox.051208.165340

Seeram, N.P., Adams, L.S., Henning, S.M., Niu, Y., Zhang, Y., Nair, M.G., Heber, D., 2005. In vitro antiproliferative, apoptotic and antioxidant activities of punicalagin, ellagic acid and a total pomegranate tannin extract are enhanced in combination with other polyphenols as found in pomegranate juice. J. Nutr. Biochem. 16, 360–7. doi:10.1016/j.jnutbio.2005.01.006

Seeram, N.P., Aronson, W.J., Zhang, Y., Henning, S.M., Moro, A., Lee, R.-P., Sartippour, M., Harris, D.M., Rettig, M., Suchard, M.A., Pantuck, A.J., Belldegrun, A., Heber, D., 2007. Pomegranate ellagitannin-derived metabolites inhibit prostate cancer growth and localize to the mouse prostate gland. J. Agric. Food Chem. 55, 7732–7. doi:10.1021/jf071303g

Seeram, N.P., Henning, S.M., Zhang, Y., Suchard, M., Li, Z., Heber, D., 2006. Pomegranate juice ellagitannin metabolites are present in human plasma and some persist in urine for up to 48 hours. J. Nutr. 136, 2481–5.

Seeram, N.P., Lee, R., Heber, D., 2004. Bioavailability of ellagic acid in human plasma after consumption of ellagitannins from pomegranate (Punica granatum L.) juice. Clin. Chim. Acta. 348, 63–8. doi:10.1016/j.cccn.2004.04.029

Seeram, N.P., Lee, R., Scheuller, H.S., Heber, D., 2006. Identification of phenolic compounds in strawberries by liquid chromatography electrospray ionization mass spectroscopy. Food Chem. 97, 1–11. doi:10.1016/j.foodchem.2005.02.047

Seeram, N.P., Zhang, Y., McKeever, R., Henning, S.M., Lee, R., Suchard, M.A., Li, Z., Chen, S., Thames, G., Zerlin, A., Nguyen, M., Wang, D., Dreher, M., Heber, D., 2008. Pomegranate juice and extracts provide similar levels of plasma and urinary ellagitannin metabolites in human subjects. J. Med. Food 11, 390–4. doi:10.1089/jmf.2007.650

Selma, M. V, Beltrán, D., García-Villalba, R., Espín, J.C., Tomás-Barberán, F.A., 2014. Description of urolithin production capacity from ellagic acid of two human intestinal Gordonibacter species. Food Funct. 5, 1779–84. doi:10.1039/c4fo00092g

Sequeira, M., Espírito-Santo, D., Aguiar, C., Capelo, J., Honrado, J.J., 2011. Checklist da Flora de Portugal Continental, Açores e Madeira.

Serrano, J., Puupponen-Pimiä, R., Dauer, A., Aura, A.-M., Saura-Calixto, F., 2009. Tannins: current knowledge of food sources, intake, bioavailability and biological effects. Mol. Nutr. Food Res. 53 Suppl 2, S310–29. doi:10.1002/mnfr.200900039

Shaid, S., Brandts, C.H., Serve, H., Dikic, I., 2013. Ubiquitination and selective autophagy. Cell Death Differ. 20, 21–30. doi:10.1038/cdd.2012.72

Shen, H.-M., Tergaonkar, V., 2009. NFkappaB signaling in carcinogenesis and as a potential molecular target for cancer therapy. Apoptosis 14, 348–63. doi:10.1007/s10495-009-0315-0

Shen, M., Chan, T.H., Dou, Q.P., 2012. Targeting tumor ubiquitin-proteasome pathway with polyphenols for chemosensitization. Anticancer. Agents Med. Chem. 12, 891–901.

Shen, S., Kepp, O., Kroemer, G., 2012. The end of autophagic cell death? Autophagy 8, 1–3. doi:10.4161/auto.8.1.16618

Shi, L., Gao, X., Li, X., Jiang, N., Luo, F., Gu, C., Chen, M., Cheng, H., Liu, P., 2015. Ellagic Acid Enhances the Efficacy of PI3K Inhibitor GDC-0941 in Breast Cancer Cells. Curr. Mol. Med. 15, 478–86.

Shin, M.S., Kang, E.H., Lee, Y.I., 2005. A flavonoid from medicinal plants blocks hepatitis B virus-e antigen secretion in HBV-infected hepatocytes. Antiviral Res. 67, 163–8. doi:10.1016/j.antiviral.2005.06.005

Simirgiotis, M.J., Schmeda-Hirschmann, G., 2010. Determination of phenolic composition and antioxidant activity in fruits, rhizomes and leaves of the white strawberry (Fragaria chiloensis spp. chiloensis form chiloensis) using HPLC-DAD–ESI-MS and free radical quenching techniques. J. Food Compos. Anal. 23, 545–53. doi:10.1016/j.jfca.2009.08.020

Singh, K.N., Lal, B., 2008. Ethnomedicines used against four common ailments by the tribal communities of Lahaul-Spiti in western Himalaya. J. Ethnopharmacol. 115, 147–59. doi:10.1016/j.jep.2007.09.017

Skaug, B., Jiang, X., Chen, Z.J., 2009. The role of ubiquitin in NF-kappaB regulatory pathways. Annu. Rev. Biochem. 78, 769–96. doi:10.1146/annurev.biochem.78.070907.102750

Sonoda, Y., Matsumoto, Y., Funakoshi, M., Yamamoto, D., Hanks, S.K., Kasahara, T., 2000. Anti-apoptotic role of focal adhesion kinase (FAK). Induction of inhibitor-of-apoptosis proteins and apoptosis suppression by the overexpression of FAK in a human leukemic cell line, HL-60. J. Biol. Chem. 275, 16309–15.

Sõukand, R., Kalle, R., 2013. Where does the border lie: locally grown plants used for making tea for recreation and/or healing, 1970s-1990s Estonia. J. Ethnopharmacol. 150, 162–74. doi:10.1016/j.jep.2013.08.031

Souza-Moreira, T., Severi, J., Lee, K., Preechasuth, K., Santos, E., Gow, N., Munro, C., Vilegas, W., Pietro, R., 2013. Anti-Candida Targets and Cytotoxicity of Casuarinin Isolated from Plinia cauliflora Leaves in a Bioactivity-Guided Study. Molecules 18, 8095–108. doi:10.3390/molecules18078095

Spiridonov, N., 2008. Botanical Medicine in Clinical Practice, in: Watson, R.R., Preedy, V.R. (Eds.), . Cromwell Press, Cambridge, pp. 421–29.

Srubar-Vernon, A., 2014. Analysis of the potential for Rubus fruit ellagitannins to induce anti-inflammatory effects in in vitro models. Massey University, Manawatu.

Stoddart, M.J., 2011. Cell viability assays: introduction. Methods Mol. Biol. 740, 1–6. doi:10.1007/978-1-61779-108-6_1

Strober, W., 2001. Trypan blue exclusion test of cell viability. Curr. Protoc. Immunol. Appendix 3, Appendix 3B. doi:10.1002/0471142735.ima03bs21

Sun, J., Chen, P., 2012. Ultra high-performance liquid chromatography with high-resolution mass spectrometry analysis of African mango (Irvingia gabonensis) seeds, extract, and related dietary supplements. J. Agric. Food Chem. 60, 8703–9. doi:10.1021/jf302703u

Surh, Y.-J., 2003. Cancer chemoprevention with dietary phytochemicals. Nat. Rev. Cancer 3, 768–80. doi:10.1038/nrc1189

Taguri, T., Tanaka, T., Kouno, I., 2004. Antimicrobial activity of 10 different plant polyphenols against bacteria causing food-borne disease. Biol. Pharm. Bull. 27, 1965–9.

Tait, S.W.G., Ichim, G., Green, D.R., 2014. Die another way--non-apoptotic mechanisms of cell death. J. Cell Sci. 127, 2135–44. doi:10.1242/jcs.093575

Tatsuno, T., Jinno, M., Arima, Y., Kawabata, T., Hasegawa, T., Yahagi, N., Takano, F., Ohta, T., 2012. Anti-inflammatory and anti-melanogenic proanthocyanidin oligomers from peanut skin. Biol. Pharm. Bull. 35, 909–16.

Ting, Y., Jiang, Y., Ho, C.-T., Huang, Q., 2014. Common delivery systems for enhancing in vivo bioavailability and biological efficacy of nutraceuticals. J. Funct. Foods 7, 112–28. doi:10.1016/j.jff.2013.12.010

Tiţă, I., Mogoşanu, G.., Tiţă, M.G., 2009. Ethnobotanical inventory of medicinal plants from the South-West of Romania. Farmacia 57, 141–56.

Tomás-Barberan, F., Espín, J., García-Conesa, M., 2009. Bioavailability and metabolism of ellagic acid and ellagitannins, in: Quideau, S. (Ed.), Chemistry and Biology of Ellagitannins: An Underestimated Class of Bioactive Polyphenols. World Scientific Singapure, pp. 293–97.

Tomás-Barberán, F.A., García-Villalba, R., González-Sarrías, A., Selma, M. V, Espín, J.C., 2014. Ellagic acid metabolism by human gut microbiota: consistent observation of three urolithin phenotypes in intervention trials, independent of food source, age, and health status. J. Agric. Food Chem. 62, 6535–8. doi:10.1021/jf5024615

Tomczyk, M., Latté, K.P., 2009. Potentilla--a review of its phytochemical and pharmacological profile. J. Ethnopharmacol. 122, 184–204. doi:10.1016/j.jep.2008.12.022

Törrönen, R., 2009. Sources and health effects of dietary ellagitannins, in: Quideau, S. (Ed.), Chemistry and Biology of Ellagitannins: An Underestimated Class of Bioactive Polyphenols. World Scientific Singapure, pp. 298–319.

Truchado, P., Larrosa, M., García-Conesa, M.T., Cerdá, B., Vidal-Guevara, M.L., Tomás-Barberán, F.A., Espín, J.C., 2012. Strawberry processing does not affect the production and urinary excretion of urolithins, ellagic acid metabolites, in humans. J. Agric. Food Chem. 60, 5749–54. doi:10.1021/jf203641r

Tsao, R., 2010. Chemistry and biochemistry of dietary polyphenols. Nutrients 2, 1231–46. doi:10.3390/nu2121231

Umesalma, S., Nagendraprabhu, P., Sudhandiran, G., 2015. Ellagic acid inhibits proliferation and induced apoptosis via the Akt signaling pathway in HCT-15 colon adenocarcinoma cells. Mol. Cell. Biochem. 399, 303–13. doi:10.1007/s11010-014-2257-2

Umesalma, S., Sudhandiran, G., 2011. Ellagic acid prevents rat colon carcinogenesis induced by 1, 2 dimethyl hydrazine through inhibition of AKT-phosphoinositide-3 kinase pathway. Eur. J. Pharmacol. 660, 249–58. doi:10.1016/j.ejphar.2011.03.036

Vassallo, A., Vaccaro, M.C., De Tommasi, N., Dal Piaz, F., Leone, A., 2013. Identification of the Plant Compound Geraniin as a Novel Hsp90 Inhibitor. PLoS One 8, e74266. doi:10.1371/journal.pone.0074266

Vermerris, W., Nicholson, R., 2007. Families of Phenolic Compounds and Means of Classification, in: Phenolic Compound Biochemistry. Springer Netherlands, Dordrecht, pp. 1–34. doi:10.1007/978-1-4020-5164-7_1

Vicinanza, R., Zhang, Y., Henning, S.M., Heber, D., 2013. Pomegranate Juice Metabolites, Ellagic Acid and Urolithin A, Synergistically Inhibit Androgen-Independent Prostate Cancer Cell Growth via Distinct Effects on Cell Cycle Control and Apoptosis. Evid. Based. Complement. Alternat. Med. 2013, 247504. doi:10.1155/2013/247504

Vilchez, D., Saez, I., Dillin, A., 2014. The role of protein clearance mechanisms in organismal ageing and age-related diseases. Nat. Commun. 5, 5659. doi:10.1038/ncomms6659

Vilhelmova, N., Jacquet, R., Quideau, S., Stoyanova, A., Galabov, A.S., 2011. Three-dimensional analysis of combination effect of ellagitannins and acyclovir on herpes simplex virus types 1 and 2. Antiviral Res. 89, 174–81. doi:10.1016/j.antiviral.2010.11.014

Vilhelmova-Ilieva, N., Jacquet, R., Quideau, S., Galabov, A.S., 2014. Ellagitannins as synergists of ACV on the replication of ACV-resistant strains of HSV 1 and 2. Antiviral Res. 110, 104–14. doi:10.1016/j.antiviral.2014.07.017

Vitorino, R., Guedes, S., Manadas, B., Ferreira, R., Amado, F., 2012. Toward a standardized saliva proteome analysis methodology. J. Proteomics 75, 5140–165. doi:10.1016/j.jprot.2012.05.045

Vogl, D.T., Stadtmauer, E.A., Tan, K.-S., Heitjan, D.F., Davis, L.E., Pontiggia, L., Rangwala, R., Piao, S., Chang, Y.C., Scott, E.C., Paul, T.M., Nichols, C.W., Porter, D.L., Kaplan, J., Mallon, G., Bradner, J.E., Amaravadi, R.K., 2014. Combined autophagy and proteasome inhibition: a phase 1 trial of

hydroxychloroquine and bortezomib in patients with relapsed/refractory myeloma. Autophagy 10, 1380–90. doi:10.4161/auto.29264

Vogl, S., Picker, P., Mihaly-Bison, J., Fakhrudin, N., Atanasov, A.G., Heiss, E.H., Wawrosch, C., Reznicek, G., Dirsch, V.M., Saukel, J., Kopp, B., 2013. Ethnopharmacological in vitro studies on Austria's folk medicine--an unexplored lore in vitro anti-inflammatory activities of 71 Austrian traditional herbal drugs. J. Ethnopharmacol. 149, 750–71. doi:10.1016/j.jep.2013.06.007

Vora, A.K., Londhe, V.Y., Pandita, N.S., 2015. Preparation and characterization of standardized pomegranate extract-phospholipid complex as an effective drug delivery tool. J. Adv. Pharm. Technol. Res. doi:10.4103/2231-4040.154542

Vrhovsek, U., Guella, G., Gasperotti, M., Pojer, E., Zancato, M., Mattivi, F., 2012. Clarifying the Identity of the Main Ellagitannin in the Fruit of the Strawberry, Fragaria vesca and Fragaria ananassa Duch. J. Agric. Food Chem. 60, 2507–516. doi:10.1021/jf2052256

Wada, L., Ou, B., 2002. Antioxidant Activity and Phenolic Content of Oregon Caneberries. J. Agric. Food Chem. 50, 3495–500. doi:10.1021/jf011405l

Wada, T., Penninger, J.M., 2004. Mitogen-activated protein kinases in apoptosis regulation. Oncogene 23, 2838–49. doi:10.1038/sj.onc.1207556

Wang, B., Jin, Z., 2011. Agrimoniin induced SGC7901 cell apoptosis associated mitochondrial transmembrane potential and intracellular calcium concentration. J. Med. Plants Res. 5, 3512–19.

Wang, C.C., Chen, L.G., Yang, L.L., 2000. Cuphiin D1, the macrocyclic hydrolyzable tannin induced apoptosis in HL-60 cell line. Cancer Lett. 149, 77–83.

Wang, C.C., Chen, L.G., Yang, L.L., 2001. Camelliin B induced apoptosis in HeLa cell line. Toxicology 168, 231–40.

Wang, J., Maldonado, M.A., 2006. The ubiquitin-proteasome system and its role in inflammatory and autoimmune diseases. Cell. Mol. Immunol. 3, 255–61.

Wang, S., Huang, M., Li, J., Lai, F., Lee, H., Hsu, Y., 2013. Punicalagin induces apoptotic and autophagic cell death in human U87MG glioma cells. Acta Pharmacol. Sin. 34, 1411–9. doi:10.1038/aps.2013.98

Wang, S.Y., Lin, H.-S., 2000. Antioxidant Activity in Fruits and Leaves of Blackberry, Raspberry, and Strawberry Varies with Cultivar and Developmental Stage. J. Agric. Food Chem. 48, 140–46. doi:10.1021/jf9908345

Wang, Y., Ma, J., Chow, S.C., Li, C.H., Xiao, Z., Feng, R., Fu, J., Chen, Y., 2014. A potential antitumor ellagitannin, davidiin, inhibited hepatocellular tumor growth by targeting EZH2. Tumor Biol. 35, 205–12. doi:10.1007/s13277-013-1025-3

Wang, Y., Qiu, Z., Zhou, B., Liu, C., Ruan, J., Yan, Q., Liao, J., Zhu, F., 2015. In vitro antiproliferative and antioxidant effects of urolithin A, the colonic metabolite of ellagic acid, on hepatocellular carcinomas HepG2 cells. Toxicol. In Vitro 29, 1107–15. doi:10.1016/j.tiv.2015.04.008

Whitley, A.C., Sweet, D.H., Walle, T., 2006. Site-specific accumulation of the cancer preventive dietary polyphenol ellagic acid in epithelial cells of the aerodigestive tract. J. Pharm. Pharmacol. 58, 1201–9. doi:10.1211/jpp.58.9.0006

Wink, M., 2010. Introduction: biochemistry, physiology and ecological functions of secondary metabolites, in: Wink, M. (Ed.), Annual Plant Reviews, Biochemistry of Plant Secondary Metabolism. Blackwell Publishing Ltd., pp. 1–19.

Wong, E., Cuervo, A.M., 2010. Integration of clearance mechanisms: the proteasome and autophagy. Cold Spring Harb. Perspect. Biol. 2, a006734. doi:10.1101/cshperspect.a006734

Wu, X., Obata, T., Khan, Q., Highshaw, R.A., De Vere White, R., Sweeney, C., 2004. The phosphatidylinositol-3 kinase pathway regulates bladder cancer cell invasion. BJU Int. 93, 143–50.

Xavier, C.P.R., 2010. The anticarcinogenic potential of dietary natural compounds on colorectal carcinoma: Effects on signalling pathways related to proliferation and cell death. University of Minho.

Xiao, F., Zhai, Z., Jiang, C., Liu, X., Li, H., Qu, X., Ouyang, Z., Fan, Q., Tang, T., Qin, A., Gu, D., 2015. Geraniin suppresses RANKL-induced osteoclastogenesis in vitro and ameliorates wear particle-induced osteolysis in mouse model. Exp. Cell Res. 330, 91–101. doi:10.1016/j.yexcr.2014.07.005

Xu, X., Yin, P., Wan, C., Chong, X., Liu, M., Cheng, P., Chen, J., Liu, F., Xu, J., 2014. Punicalagin Inhibits Inflammation in LPS-Induced RAW264.7 Macrophages via the Suppression of TLR4-Mediated MAPKs and NF-κB Activation. Inflammation 37, 956–65. doi:10.1007/s10753-014-9816-2

Yamaguchi, M.U., Garcia, F.P., Cortez, D.A.G., Ueda-Nakamura, T., Filho, B.P.D., Nakamura, C.V., 2010. Antifungal effects of Ellagitannin isolated from leaves of Ocotea odorifera (Lauraceae). Antonie Van Leeuwenhoek 99, 507–14. doi:10.1007/s10482-010-9516-3

Yang, C.-M., Cheng, H.-Y., Lin, T.-C., Chiang, L.-C., Lin, C.-C., 2007a. The in vitro activity of geraniin and 1,3,4,6-tetra-O-galloyl-beta-D-glucose isolated from Phyllanthus urinaria against herpes simplex virus type 1 and type 2 infection. J. Ethnopharmacol. 110, 555–8. doi:10.1016/j.jep.2006.09.039

Yang, C.-M., Cheng, H.-Y., Lin, T.-C., Chiang, L.-C., Lin, C.-C., 2007b. Hippomanin A from acetone extract of Phyllanthus urinaria inhibited HSV-2 but not HSV-1 infection in vitro. Phytother. Res. 21, 1182–6. doi:10.1002/ptr.2232

Yang, P.-M., Tseng, H.-H., Peng, C.-W., Chen, W.-S., Chiu, S.-J., 2012. Dietary flavonoid fisetin targets caspase-3-deficient human breast cancer MCF-7 cells by induction of caspase-7-associated apoptosis and inhibition of autophagy. Int. J. Oncol. 40, 469–78. doi:10.3892/ijo.2011.1203

Yokozawa, T., Chen, C.P., Tanaka, T., Kitani, K., 2002. Effects of sanguiin H-6, a component of Sanguisorbae Radix, on lipopolysaccharide-stimulated nitric oxide production. Biochem. Pharmacol. 63, 853–8. doi:10.1016/S0006-2952(01)00930-3

Yu, H., 2000. Role of the Insulin-Like Growth Factor Family in Cancer Development and Progression. J. Natl. Cancer Inst. 92, 1472–89. doi:10.1093/jnci/92.18.1472

Zaurov, D.E., Belolipov, I. V., Kurmukov, A.G., Akimaliev, Ishenbay S. Sodombekov, A.A., Eisenman, S.W., 2013. Medicinal Plants of Central Asia: Uzbekistan and Kyrgyzstan. Springer New York, New York, NY. doi:10.1007/978-1-4614-3912-7

Zhang, H.-M., Zhao, L., Li, H., Xu, H., Chen, W.-W., Tao, L., 2014. Research progress on the anticarcinogenic actions and mechanisms of ellagic acid. Cancer Biol. Med. 11, 92–100. doi:10.7497/j.issn.2095-3941.2014.02.004

Zhao, M., Tang, S.-N., Marsh, J.L., Shankar, S., Srivastava, R.K., 2013. Ellagic acid inhibits human pancreatic cancer growth in Balb c nude mice. Cancer Lett. 337, 210–7. doi:10.1016/j.canlet.2013.05.009

Zlatković, B.K., Bogosavljević, S.S., Radivojević, A.R., Pavlović, M.A., 2014. Traditional use of the native medicinal plant resource of Mt. Rtanj (Eastern Serbia): ethnobotanical evaluation and comparison. J. Ethnopharmacol. 151, 704–13. doi:10.1016/j.jep.2013.11.037